TABLE OF CONTENTS

	PAGE
ABSTRACT	ii
FOREWORD	iv
DISCLAIMER	v
LIST OF FIGURES	vii
INTRODUCTION	1
1.0 SITE SELECTION	3
2.0 IMPACT OF SALT CREEP ON THE DESIGN APPROACH	6
3.0 RETRIEVABILITY	9
4.0 THERMOMECHANICAL ANALYSES	10
5.0 COMPUTER CODE VERIFICATION AND VALIDATION	12
6.0 CONCLUDING REMARKS	14
REFERENCES	15

LIST OF FIGURES

FIGURE	TITLE	PAGE
1	Complex Geology	4
2	Simple Geology	5
3	Repository Layout	7
4	Waste Emplacement Package	8

INTRODUCTION

The discussion in this paper is based on eight years of experience on three different nuclear waste repository projects, two in bedded salt and the other in densely welded tuff. The bedded salt projects are the Waste Isolation Pilot Plant (WIPP) Project in New Mexico and the Salt Repository Project (SRP) in Texas. The densely welded tuff is the potential host rock being studied by the Nevada Nuclear Waste Storage Investigations Project. All activities on these projects were associated with designs from the concepts or conceptual level to designs released for construction. In the last 20 years of my professional experience, all major projects have proceeded through construction except the last two repositories. As a result, my current participation in review or development of a repository design comes from the practical design engineer's perspective. This includes being intimately concerned about safety in the underground environment, proper interpretation and application of codes and regulations, adequacy of the design, licensability, application of quality assurance requirements, constructibility and operational considerations, and economics. The design engineer knows the day will always come when one must be able to state the design is good, it meets all of the requirements, and now let's build it. It is from this perspective that the following discussion is provided on the impact of thermomechanical behavior of salt on repository design and analysis.

Rock salt was identified 30 years ago by the National Academy of Science as being a potentially suitable host rock for the disposal of nuclear waste. Salt has a number of characteristics that make it attractive for disposing of nuclear waste:

- Salt deposits are available that are sufficiently deep, laterally extensive, and geologically stable.
- Many salt formations have remained water free for millions of years.
- Salt has adequate radiation-shielding properties.
- Fractures at repository depths will tend to close plastically and seal themselves.
- Salt has a high thermal conductivity compared to most other host rocks.

Heat is generated by the nuclear waste, and the thermomechanical response of the rock salt to this heat is a major design issue. Increased salt temperatures result in higher creep rates. Accelerated creep enhances the closing and sealing of fractures in the salt. On the other hand, the higher creep rates impact the retrievability and underground repository designs.

Understanding the nature and magnitude of the thermomechanical response of the host rock is important throughout the site selection and design process. It is imperative that the performance assessment specialist, geologist, hydrologist, and design engineers work closely together during the evolution of a repository design to be sure the performance and design requirements are integrated effectively. For a repository in salt, scoping calculations should be performed at the early stages of site selection to allow objective comparisons of any differences in the thermomechanical behavior of salt at different sites or in different salt formations at the same site.

This paper is organized into six sections that discuss considerations of the influence of salt creep on geology, repository design, retrieval, and thermomechanical analyses. The first section includes a discussion on site selection and the role of thermomechanical analyses in this process. The second section covers the impact of salt creep on some of the design features of the repository. Section three contains a discussion of the retrievability issue. The fourth section discusses thermomechanical analyses and associated uncertainties. Section 5 discusses verification and validation of computer codes, and Section 6 provides concluding remarks.

1.0 SITE SELECTION

Selecting a nuclear waste repository site is a long and involved process in the United States. The thermomechanical response of the host rock is only one of a multitude of issues that must be considered in the site selection process. It is not the purpose of this paper to discuss this involved process; however, it is important to emphasize the significance of thermomechanical analyses in the site selection process for a nuclear waste repository in bedded salt. As the site screening process narrows from regions to areas and finally to sites, the thermomechanical calculations become more important.

Because uncertainty in thermomechanical calculations already exists (as will be discussed later), sites should be selected with simple geology, when possible, to keep the thermomechanical calculations as simple as possible. Within the repository area, the geology should be uniform and predictable. Depositional features such as barrier reefs, river channels, solutioning fronts, etc., should be avoided. In selecting a good repository site, one should strive for cleaner salt, salt thickness of hundreds of feet, minimum number of interbeds, low formation dips, low in situ rock temperatures, and a minimum depth consistent with performance assessment and regulatory requirements. In general, the purer the salt, the higher the strength and thermal conductivity. Salt is the material that forms the cocoon around the nuclear waste and forms one of the barriers that isolates waste from the accessible environment. The number of interbeds should be minimized to reduce the complexity of the thermomechanical model and increase the confidence of thermomechanical calculations. It is more desirable to have a repository site with in situ temperatures of 25°C than to have a site with 50°C. Since significant quantities of heat must be accommodated in the disposal of high-level nuclear waste, lower in situ rock salt temperatures will result in a smaller nuclear waste repository with lower creep rates.

This can be summarized in two examples, a complex geology and a simple geology. Figure 1 is an example of the type of geology that should be avoided for a nuclear waste repository in salt. The geology shown is complex. Formation thicknesses vary significantly and there are a large number of interbeds and clay seams occurring on a regular basis. The formations have a significant dip, the in situ rock temperature is relatively high (example is 50°C), and the salt beds are thin. Independent of the other implications associated with the geology shown in Figure 1, developing an accurate thermomechanical model of the formation shown would be, at best, difficult and expensive.

Figure 2 is an example of a simple geology for a nuclear waste repository. The formations are uniform with salt beds that are very thick. The dip is low, and there are only a few clay seams. The in situ rock temperature is low (example is 25°C), and the purity of the salt is higher. The thermomechanical model in this formation will be less complex, and the confidence in the results will be higher.

The simplified situation of a complex or simple geology is, of course, not the real world. For most sites, the geology is somewhere between the two geologies described. The point is, for thermomechanical analyses, a site tending toward the simple geology is more desirable. It is also obvious that this is not, and cannot, be made an absolute requirement.

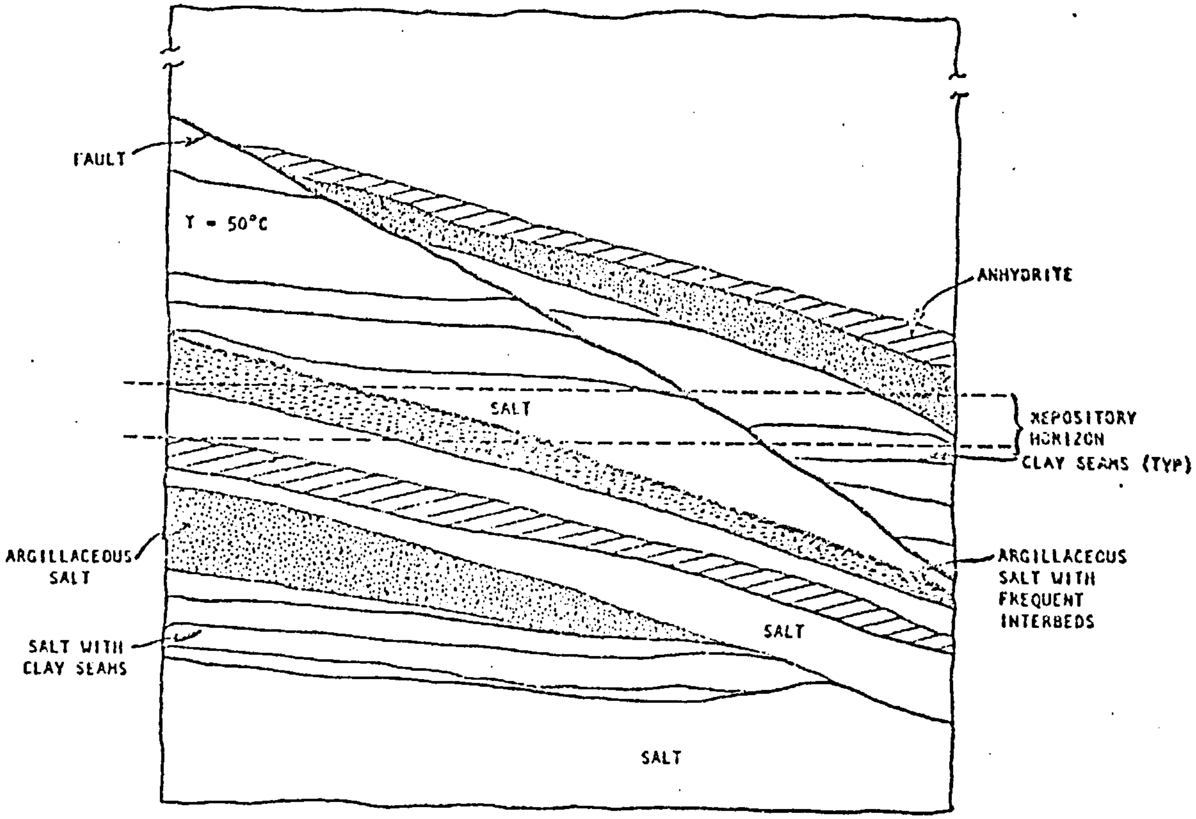
FAULT
T = 50°C
ANHYDRITE
SALT
REPOSITORY
HORIZON
CLAY SEAMS (TYP)
ARGILLACEOUS
SALT
ARGILLACEOUS
SALT WITH
FREQUENT
INTERBEDS
SALT
SALT WITH
CLAY SEAMS
SALT

Figure 1. Complex Geology

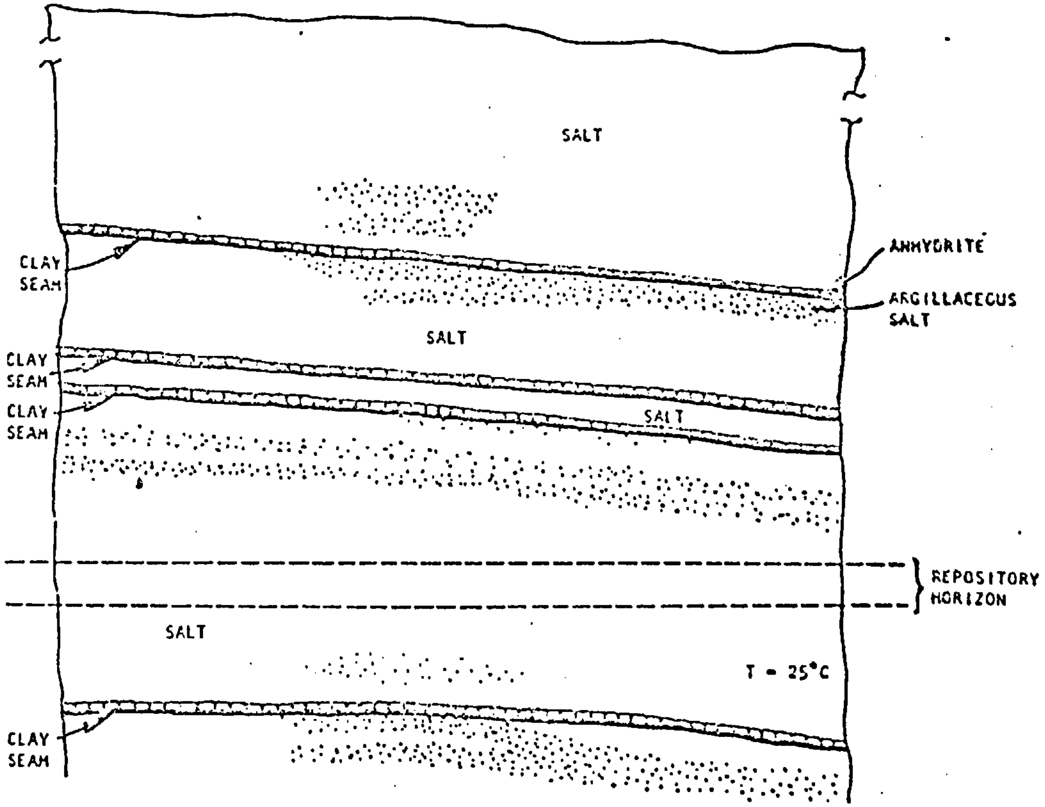
SALT
CLAY SEAM
ANHYDRITE
ARGILLACEOUS SALT
SALT
CLAY SEAM
CLAY SEAM
SALT
REPOSITORY HORIZON
SALT
T = 25°C
CLAY SEAM

Figure 2. Simple Geology

2.0 IMPACT OF SALT CREEP ON THE DESIGN APPROACH

Salt creep is one of the major design issues that is ever present with the design engineer, and the importance of accurate thermomechanical calculations to the design approach cannot be overemphasized. The thermomechanical response of the salt to the underground excavations and emplacement of nuclear waste has an impact on many aspects of repository design such as the overall underground repository layout, underground ventilation, room and pillar design, and the waste package.

Ideally, one would like to stop salt creep during the operational and retrievability time periods. Then after operational and retrieval requirements have been fulfilled, start, and perhaps even accelerate, creep. Several things can be done in developing the underground repository layout so that this ideal condition can be approached. First, the extraction ratios should be kept low, preferably 20% or less. Low extraction ratios keep the deviatoric stresses lower and result in reduced creep rates. Next, the waste-generated heat per unit of disposal area should be kept low. The Salt Repository Project is presently using an areal heat load of 10 W/M^2. This areal heat load results in lower host rock temperatures and in reduced creep rates. In addition, excavation of emplacement rooms should not be completed far in advance, but only immediately before the waste is emplaced. Finally, the waste emplacement rooms should be backfilled with a crushed salt or reconstituted (brick) salt to reduce the total creep and to enhance final closure of the room.

An underground conceptual layout for the SRP is shown in Figure 3. This figure is based upon current work being performed by the SRP repository architect engineer. The shop area, main entries, and ventilation return drifts should have an operating life of about 100 years. The rooms will continue to close during this time period as a result of creep. The amount of creep closure must be known so the ventilation system can be designed for the higher pressure drops associated with smaller and rougher underground drifts. Eventually the creep closure will be large enough to require remining of the ventilation drifts to maintain adequate cross sectional areas and smoothness. The amount and frequency of the remining will be estimated from the thermomechanical analyses for many areas under varying conditions. The drifts that contain operating equipment will also have to be remined periodically to maintain adequate clearances.

On the Salt Repository Project, the conceptual design of the waste package for consolidated spent fuel is about 35 cm in diameter, and about 450 cm long. Figure 4 shows a cross section of the emplacement package with an outer container (ASTM 216 steel) designed for the temperature, pressures, and corrosion conditions. In salt, the container must be designed for lithostatic pressures; however, higher pressures can be induced by the local thermal expansion of salt around the container if inadequate void space around the container is provided. Also, the corrosion of the container is sensitive to temperatures at the salt/container interface. It is important that analytical methods are available to accurately predict the waste package container design environments of pressure and temperature. Accordingly, salt creep strongly affects the design conditions in the vicinity of the waste package. These design conditions must be accurately bounded.

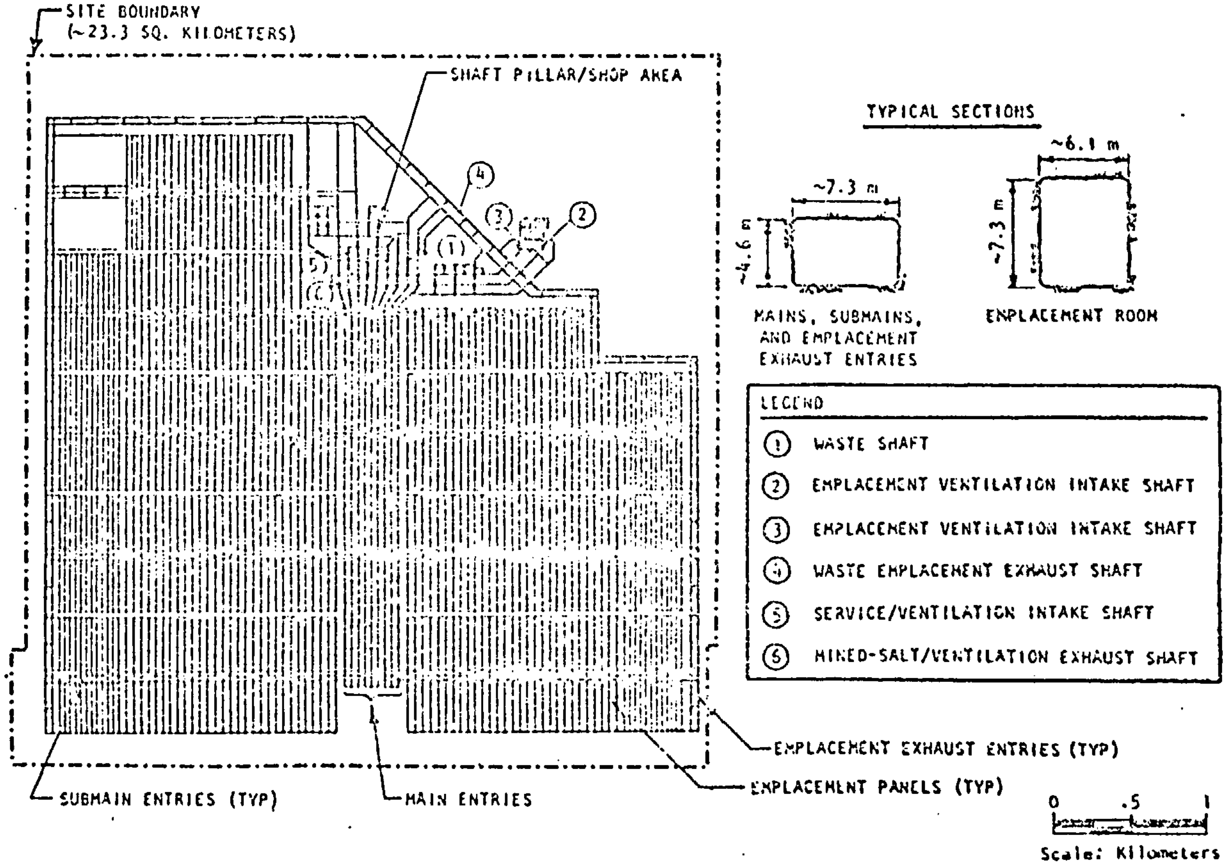
SITE BOUNDARY
(~23.3 SQ. KILOMETERS)
SHAFT PILLAR/SHOP AREA
④
③
②
①
⑤
TYPICAL SECTIONS
~7.3 m
~4.6 m
MAINS, SUBMAINS, AND EMPLACEMENT EXHAUST ENTRIES
~6.1 m
~7.3 m
EMPLACEMENT ROOM
LEGEND
① WASTE SHAFT
② EMPLACEMENT VENTILATION INTAKE SHAFT
③ EMPLACEMENT VENTILATION INTAKE SHAFT
④ WASTE EMPLACEMENT EXHAUST SHAFT
⑤ SERVICE/VENTILATION INTAKE SHAFT
⑥ MINED-SALT/VENTILATION EXHAUST SHAFT
EMPLACEMENT EXHAUST ENTRIES (TYP)
EMPLACEMENT PANELS (TYP)
SUBMAIN ENTRIES (TYP)
MAIN ENTRIES
0
.5
1
Scale: Kilometers

Figure 3. Repository Layout

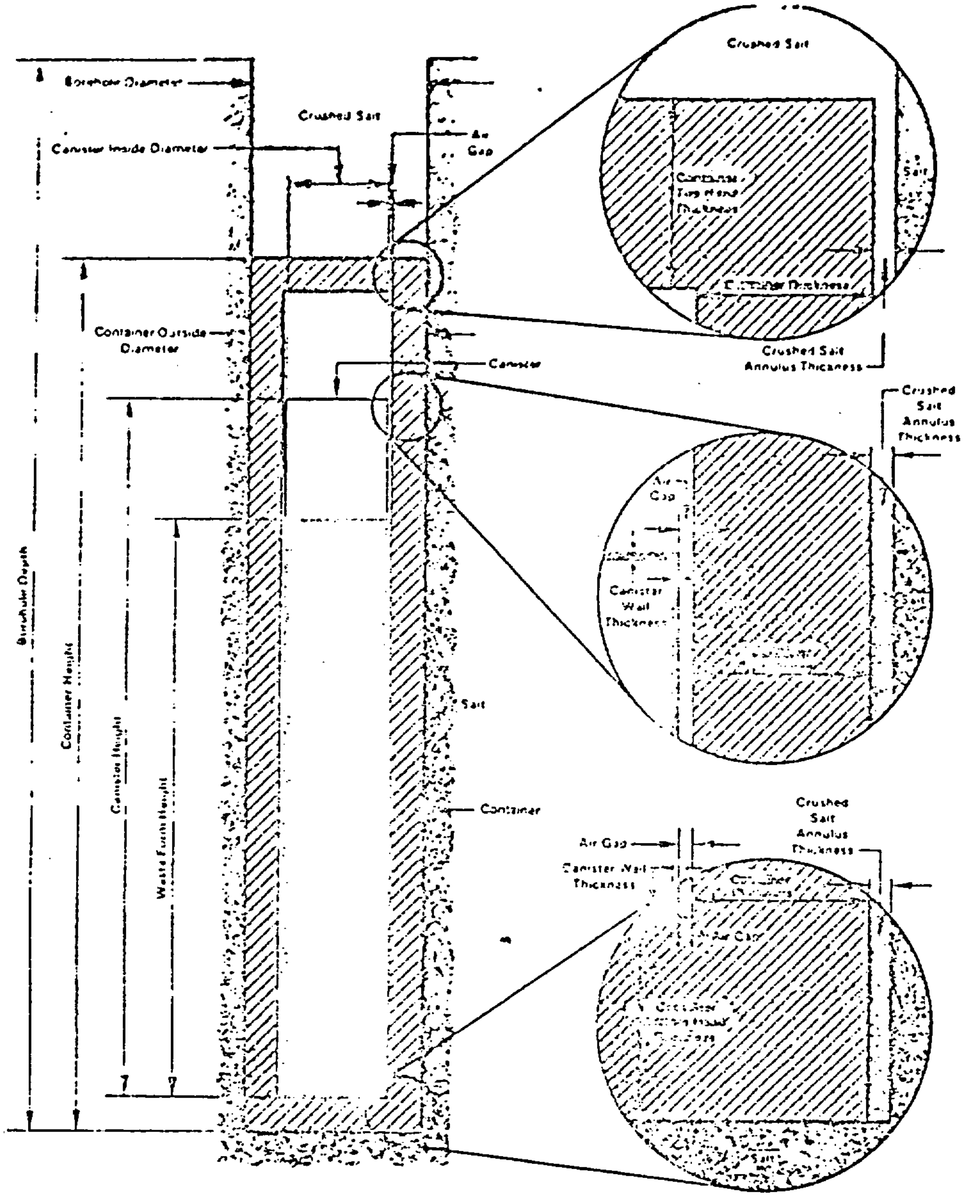
Crushed Salt
Borehole Diameter
Crushed Salt
Air Gap
Canister Inside Diameter
Container Top Head Thickness
Salt
Container Thickness
Container Outside Diameter
Crushed Salt Annulus Thickness
Canister
Crushed Salt Annulus Thickness
Air Gap
Canister Wall Thickness
Salt
Borehole Depth
Container Height
Canister Height
Waste Form Height
Salt
Container
Crushed Salt Annulus Thickness
Air Gap
Canister Wall Thickness
Container Thickness
Air Gap
Canister Bottom Head Thickness
Salt

FIGURE 4

WASTE EMPLACEMENT PACKAGE

12

3.0 RETRIEVABILITY

In the United States, retrievability is an important requirement that increases the importance of thermomechanical modeling and analyses for nuclear waste repositories disposing of high-level nuclear waste. In the Code of Federal Regulations, the U.S. Nuclear Regulatory Commission (NRC) requires that any or all of the emplaced waste be retrievable for up to 50 years. The emplaced nuclear waste must also be retrieved in approximately the same time period as it took to emplace it. Since the operational time period to emplace all of the 70,000 MTU of nuclear waste is estimated at about 25 years, all of the nuclear waste will be emplaced before the 50-year retrievability requirement expires. Reasonable assurance must be provided to the NRC that retrieval of any or all of the waste will be possible during the 50 years. Retrieval must be conducted in a safe working environment using state-of-the-art equipment and technology. However, this requirement does not preclude new engineering development or designs to meet the requirements.

And so, salt creep, one of the major advantages of salt as a host rock, becomes a major design issue with respect to long-term retrievability. Battelle, in support of the Salt Repository Project, started a retrieval compliance study a few months ago. This study will establish a plan which will ultimately provide the retrieval and proof-of-principle details necessary to support repository advanced conceptual design and facility licensing. The objectives of this study are as follows:

- Develop an interpretation of the retrievability/retrieval issue.
- Define key circumstances that may ultimately call for retrieval.
- Define the approach to retrieval system design.
- Establish an approach to licensing as it applies to retrieval.
- Develop and define the SRP interpretation and approach to testing for prototype equipment and retrieval demonstrations.

In most of these objectives, the thermomechanical response of salt to the excavated opening and emplaced waste will be very important. Thermomechanical models will be developed, and calculations will cover time periods of up to 100 years. These models must include accurate representations of the geologic formations and the response of these formations to varying room and pillar designs and thermal environments. In addition, the emplacement rooms will be backfilled with crushed salt. Over time, this salt will be reconsolidated as a result of room closure pressures and increased temperatures from the emplaced waste. Hence, the thermomechanical codes will need to have the capability to analyze rooms backfilled with crushed salt.

Long-term retrievability is, therefore, a requirement that places new demands upon the geotechnical and design engineers. The challenges are complicated and multiple. As the design requirements and designs become more sophisticated, the associated thermomechanical analytical methods must be expanded to meet these challenges.

4.0 THERMOMECHANICAL ANALYSIS

Thermomechanical analyses, therefore, play an important role in the design of a nuclear waste repository. The Salt Repository Project must comply with the requirements defined by the Nuclear Regulatory Commission in 10 CFR Part 60, and those systems and components important to safety or waste isolation will be reviewed by the Nuclear Regulatory Commission. To meet the requirements for a licensed facility, one must be able to analyze and predict the behavior of the host rock, and the analyses must provide reasonable assurance to the NRC that the repository will perform as designed.

In addition, work on a nuclear waste repository is performed under constant public scrutiny; public confidence and trust are very important to such projects. All project work is available to the public, and it is subject to multiple internal and external reviews by the U. S. Department of Energy, other project participants, other Federal agencies, state and local governments, and other interested organizations and citizens. As a result, the thermomechanical analyses will be reviewed thoroughly by many organizations.

Analyses of the repository host rock usually fall into one of three categories. First are the thermal calculations of increased temperatures of the host rock resulting from the heat being produced by the nuclear waste package. These temperatures are used to help establish the local waste package environment, the spacing of the nuclear waste packages, and the thermal environment of waste disposal rooms during retrieval.

Next are the mechanical calculations (isothermal) of the host rock at ambient temperatures. These calculations are used in establishing the underground design of drifts not subject to heat from the waste packages. Shaft pillar areas, where the shops and warehouses are located, are in this category. Also included are the main entries and ventilation return drifts.

In the third category are the thermomechanical analyses of emplacement rooms which are heated by nuclear waste packages which act as transient heat sources. These calculations are used to evaluate the response of the waste disposal rooms to the emplaced waste and to evaluate the creep response of the heated salt during waste retrieval.

Initial indications are that the thermal calculations and associated codes of the first category are relatively straightforward, and the comparison of results between different codes is quite good. Specifically, thermal calculations on the same problem have been compared at Battelle using HEATING6 and SPECTROM41 (Ref. McNulty, Scott, 1985). Results from these codes for the same problem usually are within 10%-20%. In the second Waste Isolation Pilot Plant (WIPP) benchmark problem (Morgan, 1981), the calculated salt temperature histories at the three locations were quite similar for seven of the nine codes tested. In addition, test results reported by Molecke and Beraun (1986) showed good correlation with the calculated temperatures, except for the first few days after the heater startup.

The salt creep phenomenon of the second category has been studied for many years. The last eight years have provided many opportunities for addressing and resolving design issues associated with the repository underground designs. At the start of the WIPP preliminary design, salt creep and the associated room and pillar designs were identified as major design issues. Since most of the nuclear waste scheduled for disposal at WIPP is non-heat producing, the WIPP salt creep design issue is not nearly as involved as the salt creep issue for a repository disposing of spent fuel. Eight years ago, it seemed obvious that the salt creep phenomenon would be solved, but data to date from WIPP indicates a solution has not been found. The WIPP quarterly geotechnical field data report (WIPP-DOE, 1984) indicates the measured vertical closure is almost twice that predicted. Other investigators (Morgan et al. 1985) analyzing WIPP data, indicate that measured closure data are 2 to 4 times larger than calculated. Numerous calculations were performed to try to understand the difference between the calculated and measured closures. The results of this work are summarized in the following quote from the work by Morgan, et al. 1985:

> "In fact, even when the most promising salt property variations are combined with the most promising non-salt parameter variations, the computed and measured closures are still significantly different. This seems to imply that some important phenomenon or phenomena, yet to be identified, are missing from the model."

In a series of reports on the pretest reference calculations for various heated room tests at WIPP, Morgan and Stone expect the unresolved discrepancies observed in the south drift to also appear in the measured data from the heated room tests.

With test data to date indicating calculated closure rates may be low by a factor of 2 to 4 or more, it seems our ability to perform thermomechanical calculations on bedded salt exceeds our ability to accurately predict actual in situ room response. This doesn't mean we should stop performing these calculations. However, design engineers should use the results with caution and with an understanding of the associated uncertainties. The codes are still a valuable tool for performing tradeoff studies and for making comparisons of alternate designs. Likewise, they should not take closure rates as absolutes, but use them only as relative indicators.

A new generation of thermomechanical codes is needed to support the design engineer. How the codes should be modified is not necessarily obvious, nor will it be easy. Several areas look promising for improving code accuracy. Consideration should be given to modifying the constitutive equations to account for multiple load paths. Additionally, large strain codes need to be developed to handle large deformations in salt.

5.0 COMPUTER CODE VERIFICATION AND VALIDATION

The SRP is also required to meet the quality assurance requirements as defined in 10 CFR Part 50, Appendix B, NQA-1, and other DOE orders. These requirements result in a series of formal rigorous procedures, some of which place specific procedural requirements on the design and on verifying and validating computer codes. Verification is required for all codes, whereas validation is only required for codes used in support of a license application.

Verification is the process which assures that the mathematical calculations are performed correctly in the numerical model. Verification can be accomplished by comparing the results with hand calculations, with other analytical solutions or approximations, or with the results of a verified code that performs the same type of analysis (benchmarking).

Computer code validation is the process which assures that the results of the computer code are a correct representation of the actual process or system. Validation is usually achieved by comparing the computer code results with physical data or with the results from another validated computer code that performs the same type of analysis (validation benchmarking). In addition, code validation can be achieved with a peer review when it is the only means available for validating the code.

At Battelle, for code verification, a verification plan is prepared. Included in the verification plan is the computer code version number, a description of the verification process, and a definition of the documentation required in the verification report to assure that the verification has been completed. The plan is subject to an internal review, and all comments to the plan are resolved. At least one of the individuals involved in the details of the verification process must be independent of the code development effort.

The results of the verification process are included in a verification report. If the verification is unsuccessful, recommended modifications to the code are described for correcting the error(s). If the verification is successful, the conditions under which the verification was completed are described. This includes the ranges, options, and any appropriate restrictions. In either case, the verification report is subjected to an internal review, and the review comments are resolved. The approved verification plan and verification report become part of the permanent record for that particular code.

A similar process is used for computer code validation with one possible exception: a validation panel may be established which includes one or more members who are independent of the code development effort. The validation panel participates in the review of the validation plan and validation report. Again, the approved validation plan and validation report become part of the permanent record for that particular code.

The thermal and thermomechanical codes being used by Battelle have been verified. When the codes are transferred to Battelle's computer, they are reverified by comparing the results of verification problems obtained on the new system to the results obtained during the external verification process. Again, this process is documented in the verification plan and report.

G. Kenton Beall

The Salt Repository Project is in the site characterization phase. Part of the work to be accomplished during this phase is the construction of the Exploratory Shaft Facility (ESF). The ESF will consist of two 3.66 M diameter shafts constructed to the repository depth and approximately 1500 meters of test rooms. Data obtained from these test rooms will be used as part of the validation process, if required. Also, peer reviews may be used for validation of the long-term (100 years) thermomechanical response of the repository rooms.

6.0 CONCLUDING REMARKS

An overview from a design engineer's perspective has been provided on the need and importance of thermomechanical analyses in repository site selection and design in bedded salt. Computer codes are available that accurately calculate temperature distributions around emplaced nuclear waste. Initial in situ test results have confirmed the accuracy of these analytical methods. However, the actual thermomechanical response (creep) of excavated rooms has been significantly higher than the calculated creep rates.

With the published differences between calculated and measured creep data, more emphasis should be placed on the importance of early site characterization and in situ testing. Early creep data from the actual repository host rock formation will be valuable to both the geotechnical and design engineer. In addition, efforts should continue on developing analytical methods that correctly describe the creep response of excavated rooms in salt.

While this work is continuing, the design engineer should use the results of thermomechanical calculations cautiously. Thermomechanical calculations can and should be used for comparing relative differences between sites and design options. However, the calculated closures and creep rates cannot be used as yet to set absolute values. In fact, actual closures and creeps may be significantly higher. So where does this leave the design engineer who must develop a design?

If possible sites should be selected where the geology is simple, uniform, and predictable. The repository horizon at a given site should be selected where the geology near the underground openings has minimal bedding and discontinuities. Simple designs should be developed with reasonable flexibility for adjusting the design for unforseen circumstances. Extraction ratios for the underground excavations should be kept below 20%, and the initial areal heat load should be kept low to accommodate retrievability requirements.

Even if the uncertainties in the thermomechanical calculations are not resolved in the near future, repository designs in bedded salt can and will be generated. These uncertainties can be accommodated by including reasonable conservatism in the repository design. This will provide flexibility, if required, to adjust the designs in the future.

REFERENCES

Ashworth, E. 1985. "Research & Engineering Applications in Rock Masses," *Proceedings of the 25th U.S. Symposium on Rock Mechanics*, Vol. 2 (June 26-28, Rapid City, South Dakota).

McNulty, E. Gregory and Leslie A. Scott, 1985. "Evaluation of Temperatures for a Nuclear Waste Repository in Salt," *High-Level Nuclear Waste Disposal*, Battelle Press, Edited by Harry C. Burkholder.

Miller, J. D., C. M. Stone, and L. J. Branstetter, 1982. *Reference Calculations for Underground Rooms of the WIPP*, SAND82-1176, prepared for the U.S. Department of Energy by Sandia National Laboratories, Albuquerque, NM.

Molecke, M. A., and R. Beraun, 1986. "WIPP Simulated DHLW Tests: Status and Initial In Situ Backfill Thermal Conductivities," SAND86-0489C, *Proceedings of the Waste Management '86 Meeting* (March 3-6, Tucson, Arizona).

Morgan, H. S., C. M. Stone, R. D. Krieg, and D. E. Munson, 1986. "Thermal/Structural Modeling of a Large Scale In Situ Overtest Experiment for Defense High Level Waste at the Waste Isolation Pilot Plant," SAND85-1925C, *Proceedings of the 2nd International Symposium on Numerical Models in Geomechanics* (March 31-April 4, Ghent, Belgium).

Morgan, H. S., and C. M. Stone, 1985. *Pretest Reference Calculation for the 18-W/m^2 Mockup for Defense High-Level Waste (WIPP Room A In Situ Experiment)*, SAND85-0207, prepared for the U.S. Department of Energy by Sandia National Laboratories, Albuquerque, NM.

Morgan, H. S., R. D. Krieg, and R. V. Matalucci, 1981. *Comparative Analysis of Nine Structural Codes Used in the Second WIPP Benchmark Problem*, SAND81-1389, prepared for the U.S. Department of Energy by Sandia National Laboratories, Albuquerque, NM.

Quarterly Geotechnical Field Data Report, 1984, prepared for the Waste Isolation Pilot Plant, WIPP-DOE-206, Carlsbad, NM.

U.S. Department of Energy, 1986. *Environmental Assessment, Deaf Smith County Site, Texas*, Vol. 1, DOE/RW-0069, prepared for the Office of Civilian Radioactive Waste Management, Washington, D.C.

Westinghouse Electric Corporation, 1985. *Waste Package Reference Conceptual Designs for a Repository in Salt*, BMI/ONWI-517, prepared for Office of Nuclear Waste Isolation, Battelle Memorial Institute, Columbus, OH.

HYDROGEOLOGIC MODELLING OF FRACTURED ROCK

Bernard FEUGA

Bureau de Recherches Géologiques et Minières
B.P. 6009 - 45060 ORLEANS CEDEX 02 - FRANCE

ABSTRACT

The hydrologic modelling of fractured rocks is necessarily based on knowledge of the real distribution of the fractures and their characteristics. Recent studies, using a geostatistical approach, show that the distribution of natural fractures is organised in space to form nested structures.

While the hypothesis of an equivalent continuous medium is satisfactory in some cases, modelling of the natural fracture network is necessary in others. In these cases we may prefer a geostatistically equivalent network model to an exact copy of the natural fracture network. Numerical codes have been developed to generate simulated fracture systems with statistically equivalent characteristics to those of natural fractured rock (fracture orientation, length, aperture, etc.). The final model is achieved by attributing an hydraulic connectivity coefficient to each fracture of the network. Recent studies show that the flow in narrow fractures is concentrated in certain channels representing only a very small part of the fracture surface. The hypothesis introduced for the hydraulic behaviour of the fractures requires verification by appropriate in situ testing.

This modelling of flow in tractured rocks is a step in the construction of models of radioelement migration beneath the earth's surface.

For the near field, it is necessary to couple the hydraulic and thermo-mechanical behaviour of the fractured rock. Thermo-mechanical coupling requires the introduction of mechanical characteristics measured directly on the natural fractured rock field.

INTRODUCTION

Projects for the underground storage or burial of radioactive waste materials are confronted with a major problem, namely, the transport towards the biosphere, through the intermediary of circulating groundwater, of radionuclides that may be released from the deposit after a shorter or longer time underground. The resolution of this problem requires the possibility of modelling the underground flows and the mechanisms of transport by the fluid, or of retention in the surrounding medium, of the substances in solution. This paper deals only with the first of these aspects.

In the case of hard fractured rocks such as granite, subsurface flow occurs through the fracture system, and the study of flow cannot be separated from that of the fractures. A knowledge of the fracturing and the subsurface circulation is important at various stages in a project for the disposal of radioactive waste. Selection of a site will be made in an area of low fracture density, and whose natural hydraulic gradient induces downward flow. At the planning stage, a forecast must be made of the anticipated inflow during the construction and exploitation of the deposit in order to be able to control or possibly limit it. It can be noted in passing that a good knowledge of the fracturing is also important for the geotechnical aspect, proper of the project - dimensioning and orientation of the underground spaces and specifications for their support.

Finally, an important part of the analysis of safety factors, which is based on a forecast of the long-term evolution of the repository and its environment, uses modelling of the flows and of their variation in time.

THE INFLUENCE OF VARIATIONS IN STRESS AND TEMPERATURE ON FLOW IN A FRACTURED MEDIUM

The fractured medium is theoretically distinguished from the porous (continuous) medium by a basic difference in properties, in that the state of hydrodynamic characteristics of the former are a function of the state of stress, since they are related to the fracture network that cuts the medium and which, as will be seen, becomes deformed under the effect of stress variations. (In reality, it has been shown experimentally that the hydrodynamic characteristics of certain natural porous media also vary with the state of stress, but this is nevertheless much less marked than in the case of fractured rocks). This has two consequences. The first is that, with constant fracture density, the permeability of fractured terrain decreases with depth, due to the closing up of the fractures caused by the increase of stress brought on by the increasing weight of overlying rock. The second consequence is that, at a given point, the hydrodynamic characteristics of the terrain can vary if the stresses themselves vary. Such stress variations may be due essentially either to the excavation of the underground spaces or to variations of temperature. The various hydraulic, mechanical and thermal phenomena mutually influence each other as shown diagrammatically in fig. 1.

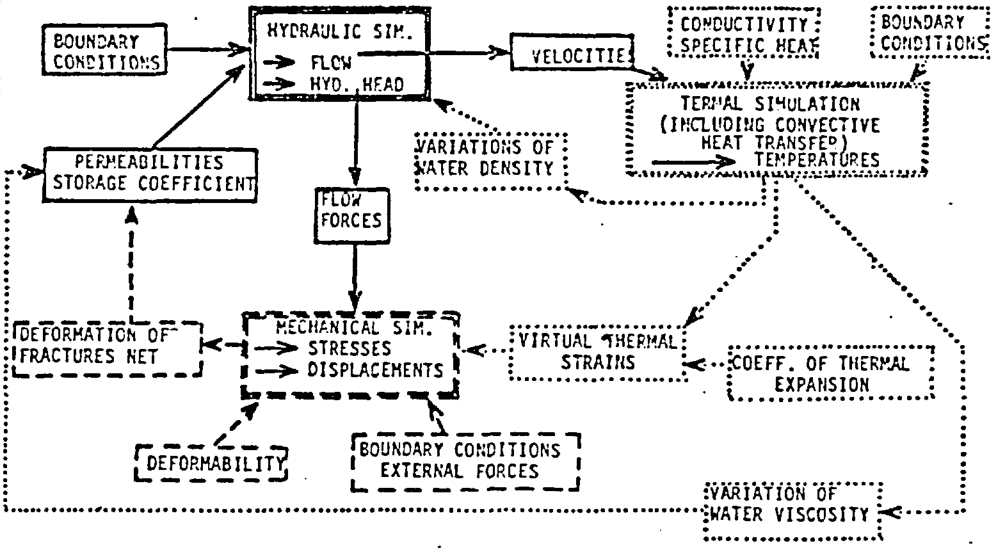
BOUNDARY CONDITIONS
HYDRAULIC SIM.
→ FLOW
→ HYD. HEAD
VELOCITIES
CONDUCTIVITY SPECIFIC HEAT
BOUNDARY CONDITIONS
TERMAL SIMULATION (INCLUDING CONVECTIVE HEAT TRANSFER)
→ TEMPERATURES
VARIATIONS OF WATER DENSITY
PERMEABILITIES STORAGE COEFFICIENT
FLOW FORCES
DEFORMATION OF FRACTURES NET
MECHANICAL SIM.
→ STRESSES
→ DISPLACEMENTS
VIRTUAL THERMAL STRAINS
COEFF. OF THERMAL EXPANSION
DEFORMABILITY
BOUNDARY CONDITIONS EXTERNAL FORCES
VARIATION OF WATER VISCOSITY

Fig. 1 - Diagram showing the relationships between hydraulic, thermal and mechanical phenomena in a fractured rock mass.

If only the flows are being considered, their characteristics (flowrate or velocity, and head) can be calculated, for a given field, if the hydrodynamic properties of the medium (permeability, coefficient of storage, field boundary conditions (flow and head)) and, in the case of an unsteady state regime, the initial conditions are known.

If only the thermal aspect of the problem is being considered, in the absence of any flow, heat propagation is effected solely through solid conduction and the distribution of temperature can be calculated, given the thermal conductivity and specific heat of the medium, the field boundary conditions (temperature or heatflow) and if necessary the initial conditions.

However, it is very often impossible to ignore flow in the study of thermal problems, since flowing water in fact transports heat, and such "convective" flow is often far from negligible. Furthermore, variations in the density related to variations in temperature (the density of water at 0°C is 999.87 kg/m^3, at 20°C it is 998.23 and at 100°C it is 958.38 kg/m^3) of the water may cause the appearance of convection cells (this is "natural convection", as opposed to "forced convection" in the preceding case). Finally, the viscosity of water is strongly temperature dependent (at 0°C its kinematic viscosity is 1.8×10^{-6} m^2/s, at 20°C it is 1.0×10^{-6} m^2/s, and at 100°C it is 0.3×10^{-6} m^2/s). This means that the permeability of the rock medium, which is inversely proportional to the kinematic viscosity, increases considerably as temperature increases (all other things being equal, it increases by a factor of six between 0°C and 100°C)

In the case which concerns us, only the last of these need be taken into account. In effect, the permeability of fractured rock media is in general sufficiently low that heat transported by flow is negligible compared with that transported by conduction. As far as natural convection is concerned, calculations show that it only becomes effective above a certain size of space available for the circulation of water, which is much greater than that offered by a low-permeability, fractured medium [1]. Thus the thermal can be dissociated from the hydraulic calculation. The values of viscosity derived from temperature distribution are required for the latter, but temperature calculations can be made without taking flow into account.

The object of mechanical modelling is to calculate the distribution of stresses and displacements in the medium. The parameters required here are the deformability of the rock (given by the elastic modulis, the Poisson coefficient and the shear modulis, for anisotropic elastic behaviour, which is a reasonable assumption for the rock matrix in the case of crystalline rocks, and the laws of behaviour of discontinuities), the applied exterior forces (in particular gravity) and the boundary conditions, expressed in terms of stress or of displacements (zero in most cases).

As mentioned above, the deformations of fractures due to stress variations, which can be determined by the mechanical calculation, cause important variations in the permeability of the terrain, which in general cannot be ignored in the hydraulic calculation.

Conversely, the circulation of water generates flow forces (specific forces equal, in a continuous medium, to $-\gamma_w . \overrightarrow{\text{grad}}\phi$, where γ_w is the specific mass of the fluid and ϕ the head of water in metres) that can play a very important mechanical role. Obviously these forces are added to buoyancy, and are a way of expressing the pressures exerted on the lips of the fractures, which tend to reduce the effective normal stresses acting upon them.

If these flow forces are weak, they can be neglected and the mechanical calculation can be dissociated from the hydraulic calculation. In this case only the variations in permeability due to variations in stress are taken into account, the latter being calculated without taking into account the flow forces influences (but without forgetting buoyancy).

The influence of temperature upon stress, and therefore indirectly upon permeability can never be ignored. While it is possible, at a first approximation to ignore the variations in the mechanical characteristics of the rock, the same cannot be done for thermal expansion, which being restricted within a confined elastic medium, results in a increase in stress equal to $E\alpha\Delta T/(1-2\nu)$ (where E is Young's modulus, ν is the Poisson coefficient, α is the coefficient of linear thermal expansion and ΔT is the increase in temperature)

For a granite with average characteristics ($E = 60{,}000$ MPa, $\nu = 0.2$, $\alpha = 8 \times 10^{-6} K^{-1}$) a 1° increase in temperature results in a stress increase of 0.8 MPa ! This demonstrates the importance of the phenomenon, which more and more is leading specialists in underground works to look for the cause of certain ruptures in variations of temperature.

In real discontinuous media, the presence of fractures, much more deformable than the rock matrix, at least for low stresses, has the effect of diminishing this increase of stress of thermal origin, but does not eliminate it.

Taking temperature into account in the mechanical calculation presents no problem as long as no mechanical phenomena influence the distribution of temperature which is a perfectly justified assumption in the case under consideration.

In short, it can be said that, in a fractured rock medium subjected to the type of hydraulic, thermal and mechanical influences that are likely to exist in the vicinity of a subsurface radioactive waste repository, the only interactions that need, in a first approximation, be taken into account in the calculations are the following :

a. Thermal/mechanical - thermal stresses
b. Thermal/hydraulic - variations in the viscosity of water
c. Mechanical/hydraulic - deformation of a fracture network resulting in modification of its hydrodynamic characteristics.

MODELLING THE FRACTURED ROCK MEDIUM - EQUIVALENT CONTINUOUS MEDIUM OR MEDIUM WITH DISCRETE FRACTURES ?

It is a natural tendency, when confronted with the problem of modelling a medium or a complex phenomenon to simplify it in order to reduce it to a form that one is able to deal with. It was in this way that the notion of an "equivalent continuous medium" was conceived in dealing with fractured rock media, a concept to which we shall return later. It soon became clear that this approach had certain limitations that prevented its application in certain cases, and this led to the development of "discrete fracture" models.

Although they have appeared more recently, these are what we shall speak about first, for the very good reason that before speaking of an "equivalent continuous medium" it is a good idea to define what it is that the medium is equivalent to, which is of course the real fracture field. It is clear that only a good knowledge of the fracture field and of the properties of the individual fractures that constitute the field will enable eventual definition of the "equivalent continuous medium".

DISCRETE FRACTURE MODELS

The very idea of a discrete fracture model, that is to say, a model in which each individual fracture is taken into account, comes up against the problem of scale - how to describe the medium, which is accessible only through outcrops, galleries or drillholes? Where are the fractures? What is their orientation, their shape, etc.? These are known only along a small number of lines and surfaces of observation. Short of taking the rock body apart block by block, the idea that it is possible to design models that will exactly represent the real medium must be abandoned from the beginning.

People therefore naturally turner towards models giving a statistically exact model of the real medium*. Among the most recent work in this direction, particular mention must be made of that of Jane Long [2] and Daniel Billaux [3] and that of Hamid Massoud and Jean-Paul Chiles [4]. The work of Long and Billaux is the subject of another talk to be given at this symposium.

GEOSTATISTICAL MODELLING OF A FRACTURE FIELD

The work of Massoud and Chilès, whose point of departure was the geologists' observation that fractures are not randomly distributed but on the contrary possess a certain spatial organization, aimed first at investigating the structure of the phenomenon of "fracturing", so as then to develop techniques for generating simulated fracture fields with features statistically and geostatistically analogous to those of real fracture fields.

The geostatistical study of a phenomenon is in general made in two stages. The first consists in an approach to the structure of the phenomenon, utilizing a first sampling. Once the main features of the structure are known a second sampling can be defined that is adapted to the particular case in question and will be able to serve as a basis for modelling.

The first sample used by Massoud and Chiles resulted from detailed fracture surveys carried out in the Saint Sylvestre granite north of Limoges, in the Massif Central. The surveys were made at four stations on surface and in the galleries of the Fanay-Augères mine, at depths down to 200 m. 2 940 fractures longer than 0.20m were recorded along a total length of gallery and quarry wall of 260m, and a height of 2m. Each fracture was precisely located and its strike and dip were recorded, as well as fifteen or so other parameters relating to its dimensions, width, morphology, relations to other fractures, etc.

Fracturing is a complex phenomenon that cannot be defined simply by values along a scale at all points in space, as is the case for example for metal content values in an ore. Fractures form directional families, within which a greater or lesser amount of dispersion occurs. It quickly became evident that, in order to be efficient, a geostatistical approach must distinguish the various families, preferably according to the episodes of brittle deformation that caused them. Within a given family certain parameters can be recorded at points, but others can only be recorded over an area. Massoud and Chilès, in their study, took the following variables into account for each family : the number of fracture centres on a given wall area (in general a 5m x 2m rectangle), the cumulative length of fracture traces on the same wall area, the strike and dip (in fact, the variable recorded was the angle between the poles to two adjacent fractures), and the interfracture distance along a horizontal line.

Variographic study of these parameters showed a random component in the structure that was more or less important in different families, and which was manifested in a "nugget" effect. This effect can in part however be explained by errors in measurement or by the existence of a structure smaller than the survey unit area.

The experimental variograms brought out clearly, for most of the families and parameters studied, two levels of nested structures, respectively of 5 to 7m and 20 to 40m (figs 2 and 3). The

---

* This does not mean that research into methods, direct or indirect, for locating and precisely characterizing fractures should be abandoned, quite the contrary. This information is essential to establish good statistical models. It will, in particular, always be essential to precisely identify the major fractures, which play a dominant part with respect to flow in the neighbourhood of a waste repository.

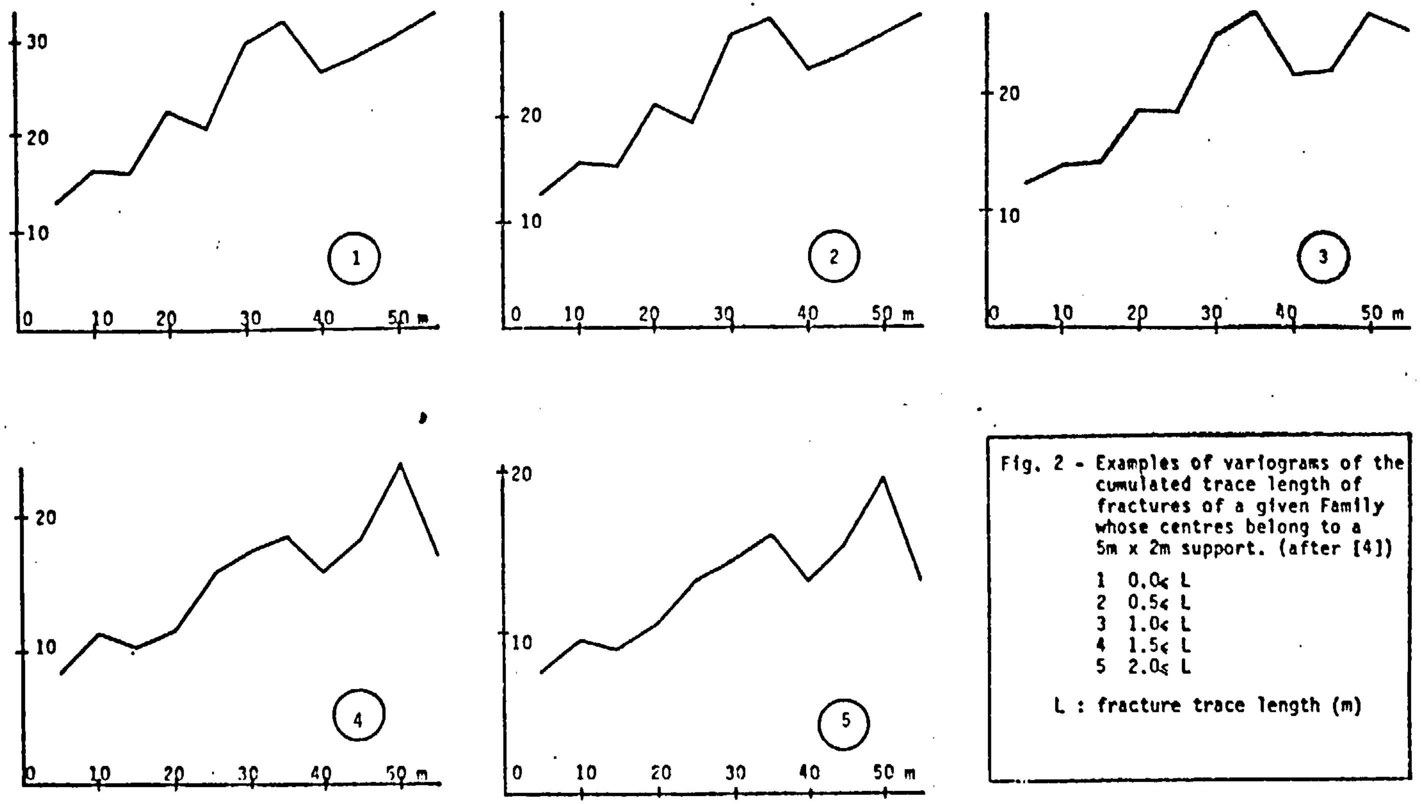

Fig. 2 - Examples of variograms of the cumulated trace length of fractures of a given Family whose centres belong to a 5m x 2m support. (after [4])

1 0.0≤ L
2 0.5≤ L
3 1.0≤ L
4 1.5≤ L
5 2.0≤ L

L : fracture trace length (m)

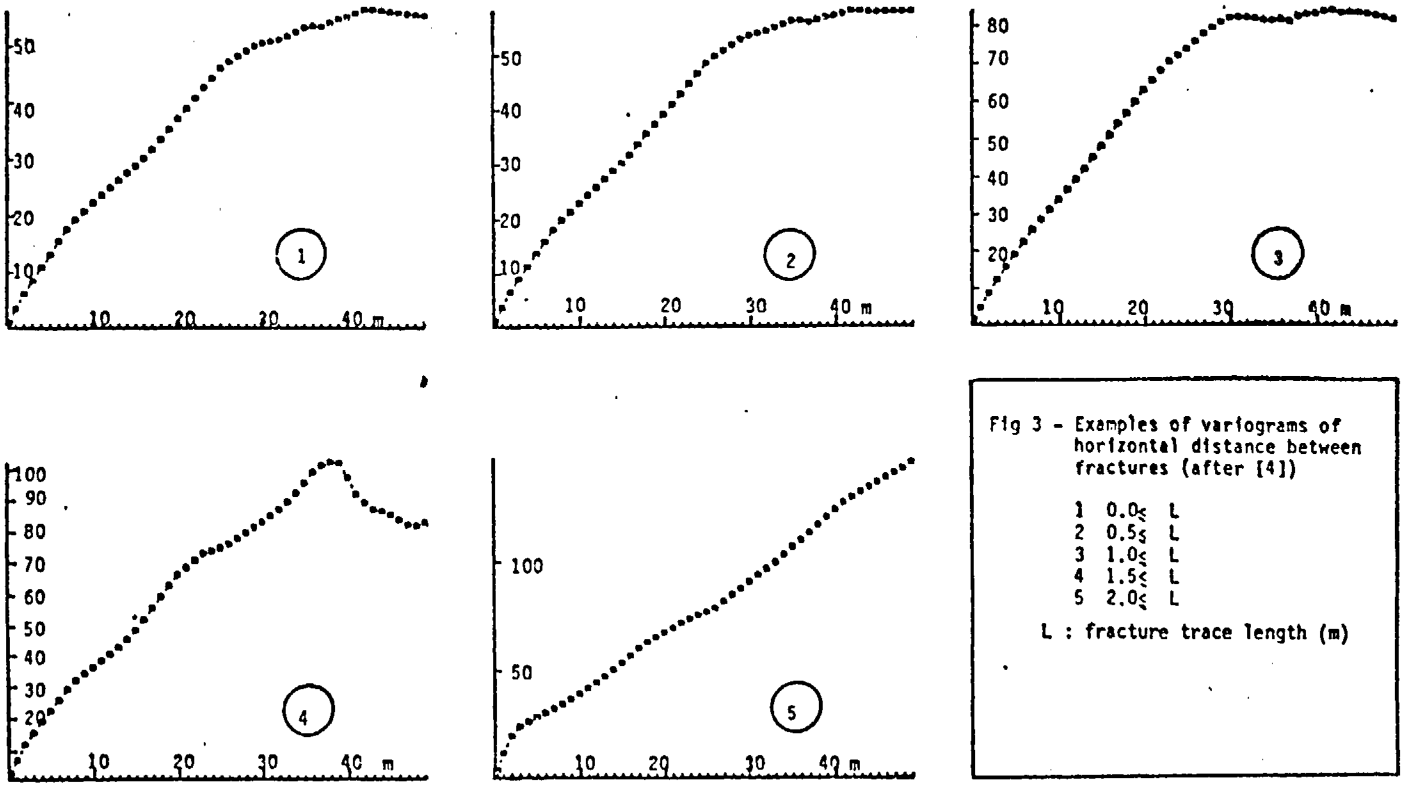

Fig 3 - Examples of variograms of horizontal distance between fractures (after [4])

1 0.0 ≤ L
2 0.5 ≤ L
3 1.0 ≤ L
4 1.5 ≤ L
5 2.0 ≤ L

L : fracture trace length (m)

Bernard FEUGA

larger of these corresponds to the organization of the fractures in the "packets" or fracture zones observed so many times by geologists, while the smaller grouping characterizes the organization of the fractures within these packets.

This first stage made possible satisfactory characterization of the structure of the fracture system over short distances (up to 100 m), leaving the question of estimation of the variogram over greater distances (100-1000 m) to be resolved.

Since such an estimation would have required further surveys at widely spaced stations, representating a considerable amount of additional work, Massoud and Chilès wondered if it would be possible to reduce the amount of work required by taking into account only those fractures that exceeded a certain size. This in turn led to consideration of the role of the small fractures in the overall structure. To resolve this problem, the variographic analysis was made again, eliminating in successive phases all fractures whose trace was shorter than 0.5m, 1.0m, 1.5m and finally 2.0m. This showed that the critical dimension, beyond which the structure of the fracture field began to change, was 1.5 (figs 2 and 3). Thus, from this approach, the following sampling procedure can be deduced :

1 - Survey systematically all the fractures whose trace is longer than 0.20m at several stations on the order of 100m long.
2 - Determine the critical trace length.
3 - Carry out surveys at stations from 100 to 1000 m apart, discounting all fractures shorter than the critical length.

At Fanay-Augères the elimination of fractures shorter than the critical length reduced by a factor of five the number of fractures to be recorded and by half the total cumulative length of the surveyed fractures.

Having determined and characterized the structural organization of the fracturing in a given domain it becomes possible to proceed to modelling, that is to say, the creation of a simulated fracture field representative of reality.

Massoud and Chilès, as a basis for this work, used the first two moments (average and variance) of distribution of the parameters studied, and the shape of their variograms to assist the choice of a family of random processes. More precisely, the procedure falls into two stages, the generation of a swarm of points, each representing the centre of a fracture, followed by the allocation to each point of the characteristics of the fracture that it represents.

The first phase itself comprises three steps - choice of a type of model, search for a method of estimating its parameters from the data, and confirmation of the suitability of the model for representing reality. The Poissonian model is commonly used, but here does not allow correct modelling fo the location of the centres of the fractures. The work of Massoud and Chilès brings out the particular interest of two more general models.

The "parent-daughter" process (or the Poissonian swarm) attributes a random swarm of points to each point or seed of a Poisson process. The number of points in each swarm is indefinite (random), and the position of each point relative to the seed is independent of those of the other points but obeys a certain law of distribution (Massoud and Chilès used a Gaussian law as an *a priori* model). The first two moments of this model are compatible with the experimental moments calculated for all the fractures of a family, but it does not take into account the regionalization of the fractures satisfactorily for all the families.

The regionalized density Poissonian process takes into account not only the random aspect but also the regionalization of the density of fracturing. In this process, the density of the seeds $\theta(x)$, depends upon the point x. It is a random function that is characterized by a variogram, and whose average is assumed to be constant. This model seems to be particularly well suited to the representation of large fractures. A substantial amount of work remains to be done to fully validate these two models, but, in view of their simplicity, this line of research can be considered very promising.

The attribution of the characteristics of individual fractures to the swarm of points generated by one or other of these methods requires further research, undertaken, as far as the density of the fractures is concerned, by Massoud and Chilès, who have devised a method by which the distribution of the real length of the fractures can be determined from field surveys, without the aid of a model based on an *a priori* law.

Figure 4 shows examples of histograms of the reconstructed real lengths of fractures for four stations at the Fanay-Augères mine. It can be seen that they are appreciably different from one another, which cannot be explained only by the fact that the surveys were made by different people, and that they cannot be represented by a single law of distribution. The entire modelling can be done in two dimensions or directly in three dimensions, if for example, the fractures can be considered as discs.

Research is obviously not complete, and work continues to be done on a number of questions, such as the variability over great distances or in a vertical direction.

The possibility of generating a field of fractures representative of reality and on which it would be possible to carry out hydrogeologic modelling, by geostatistical or any other method, assumes good sampling, not only of the geometrical characteristics of the real fracture field, but also of its hydraulic characteristics. We shall see later the problems that are posed by definition of these characteristics. Nevertheless, in a simplified approach, one can simply use the notion of

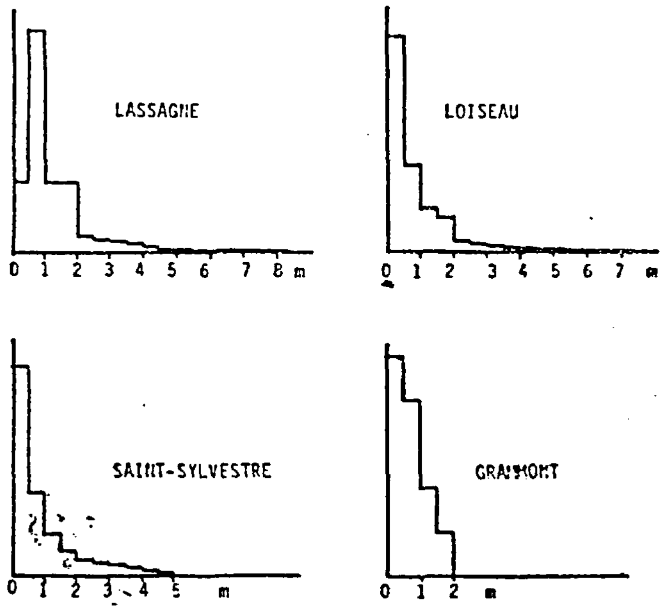

Fig. 4 - Histograms of true fracture length at 4 places of the Fanay-Augères mine (after [4])

an "equivalent hydraulic opening", defined as the opening of an imaginary fracture plane with smooth walls, whose degree of separation is equal to 1 (i.e. without connecting bridges), and whose flow/gradient relation is identical to that determined *in situ* on a real fracture.

A knowledge of the significant distributions of such "equivalent hydraulic fractures" can only be acquired through programmes of hydraulic testing in boreholes, on fractures isolated between packers. These programmes are costly, which is why there is as yet so little information available in this field. Figure 5 represents the distributions of the equivalent hydraulic openings of the five principal fracture families identified in the Fanay-Augères granite, determined by injection tests between packers, in the context of work carried out by the BRGM and financed by the French Atomic Energy Commission. More than two hundred tests have been carried out, and were interpreted in the steady state, a method which assumes a number of simplifying hypotheses that are unnecessary when using the unsteady state. It should be pointed out that the average equivalent opening of the fractures of 30µm, determined by the tests, is ten times smaller than the apparent opening deduced form the examination of cores.

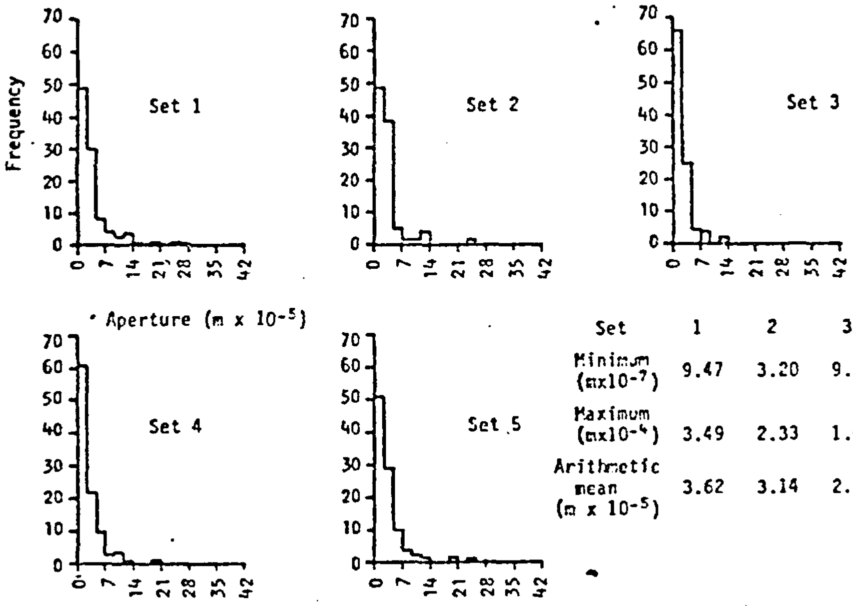

Set	1	2	3	4	5
Minimum (mx10^{-7})	9.47	3.20	9.47	9.47	9.47
Maximum (mx10^{-4})	3.49	2.33	1.40	2.01	4.67
Arithmetic mean (m x 10^{-5})	3.62	3.14	2.40	2.85	3.40

Fig. 5 - Examples of histograms of hydraulic aperture derived from water tests in boreholes for each set of fractures in the Fanay-Augères mine (after [3])

Once the problem of the generation of fracture fields has been resolved, that of their utilization arises. A cube-shaped mass of granite measuring 100m a side contains several million fractures. The manipulation of such models is clearly beyond the capacity of computers, even the most powerful ones. It will therefore be necessary to simplify these models in order to apply them to large masses of rock. At least two approaches can be envisaged to achieve this. The first consists in searching for a critical fracture dimension such that ignoring fractures below this threshold will have no significant effect on the hydraulic calculations. The second is to use mixed models, in which only large fractures are treated individually, the smaller ones being incorporated into an equivalent continuous medium.

MODELLING THE HYDROMECHANICAL BEHAVIOUR OF A FRACTURE

The effect of stress variations on the hydraulic behaviour of a fracture has been mentionned earlier. Taking this phenomenon into consideration in the calculations assumes that it can be modeled in a fairly simple way. The influence of the variations in normal stress upon the opening and the hydraulic conductivity of a natural fracture in granite has been studied by Gentier [5], in the Gueret granite, in the French Massif Central.

Since the classical laws of flow in a fracture (see, for example, Louis [6]) use a certain number of morphological parameters (opening and degree of separation, height of asperities) that may also govern the mechanical behaviour of the fracture, Gentier's basic idea was to quantify these parameters by a fine morphologic study of the fracture, to be able to introduce them first of all into a model relating opening and normal stress, and then into a model relating hydraulic conductivity and normal stress. Using fracture profiles such as that shown in fig. 6 she was able to establish theoretical curves giving the relation between the degree of separation (ratio of open surface of the fracture to its total surface) and the opening of the fracture (distance between its lips), given in fig. 7. These curves are derived directly from the widths of the space in the fracture.

A series of simple compression tests on test blocks containing a fracture perpendicular to the direction of application of the force enabled curves of stress/normal displacement to be established (fig. 8) which show that virtually all the deformation of the fracture has been acquired by 15 MPa.

Different behaviour models were tested in order to reproduce the results of these experiments b calculation. A model called the "confined teeth model" was found to be the most suitable for this purpose. In this model, one of the walls of the fracture is assumed to be plane, the other consisting of "teeth" whose distribution and elevations are the complement of the space-widths previously determined. Each tooth, confined by its neighbours, is assumed to have perfect elasto-plastic behaviour, the rupture criterion used being the empirical criterion defined by Hoek and Brown [7].

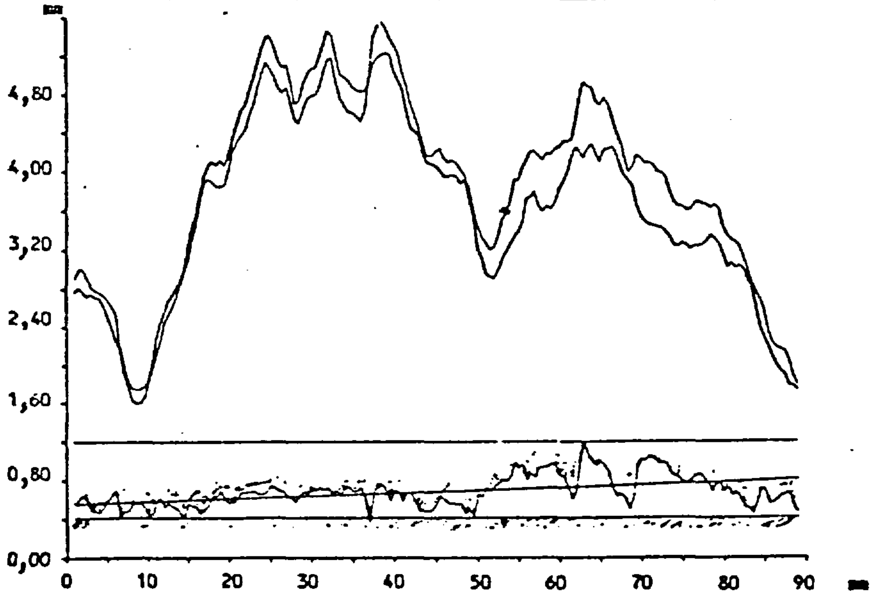

Fig. 6 - Example of fracture profile (below : representation of the fracture by a rough surface in contact with a plane). Guéret granite. After [5]

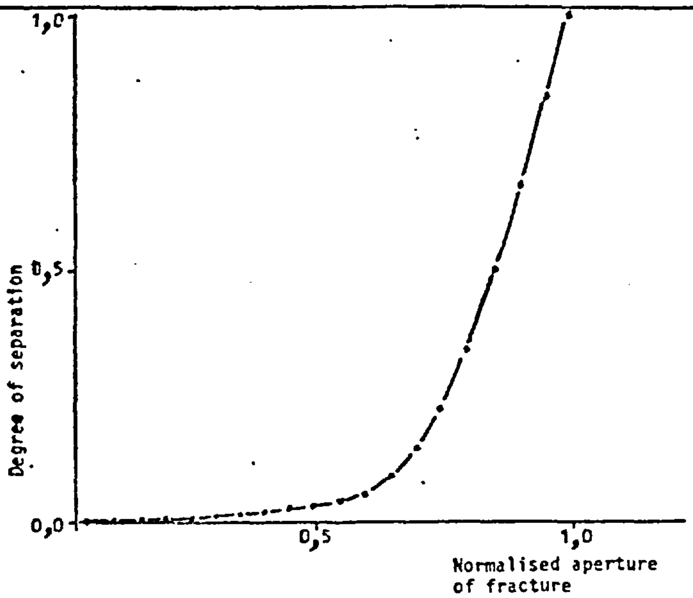

Fig. 7 - Example of the relationship between the aperture of a fracture in a granite and its degree of separation (ratio of open surface over total surface) After [5]

Imprints of the fracture taken during the tests at different loads were processed by image analyser, giving curves of surface-of-contact/applied stress that were completely in agreement with what would have been expected from the stress/displacement relations and the distributions of space-widths.

Tests of percolation under pressure in the fracture were made on different test-blocks, with divergent radial flow and in the steady state. The results obtained varied considerably from one test-block to another, even though they had all been taken on the same fracture (fig. 10). They show large deviations with respect to the cubic law of flow, which signifies that consideration of the variations of opening alone is inadequate to describe the hydromechanical behaviour of a fracture under normal stress. The reduction of the surface available for flow due to the closing up of the walls of the fracture and the creation of new contacts must be taken into account, not only as such (reduction of the degree of separation) but also and especially because of the phenomenon of "channeling" that it entrains.

This channeling, which can have effect even at low levels of stress, is illustrated by fig. 11. This represents the points of emission of the coloured fluid used in this experiment at the edge of the fracture on the surface of the test block (its trace is 38 cm long) for various stresses. It can be seen that flow, essentially generalized within the fracture at low pressures, tends to become concentrated in a gradually decreasing number of channels as the pressure increases. Above 15 MPa, the threshold already found in the study of deformability of the fracture, the number of channels stops decreasing, and remains constant.

This phenomenon was evidently not taken into account by the experimenters to whom we owe the classical laws of flow in fractures, that were established for relative roughnesses (ratio of the maximum of heights of the asperities to the hydraulic diameter) not exceeding 0.5. In fractures that, because of the pressures applied to them, are very narrow, relative roughness can be much above this value, which can explain the phenomenon of channeling.

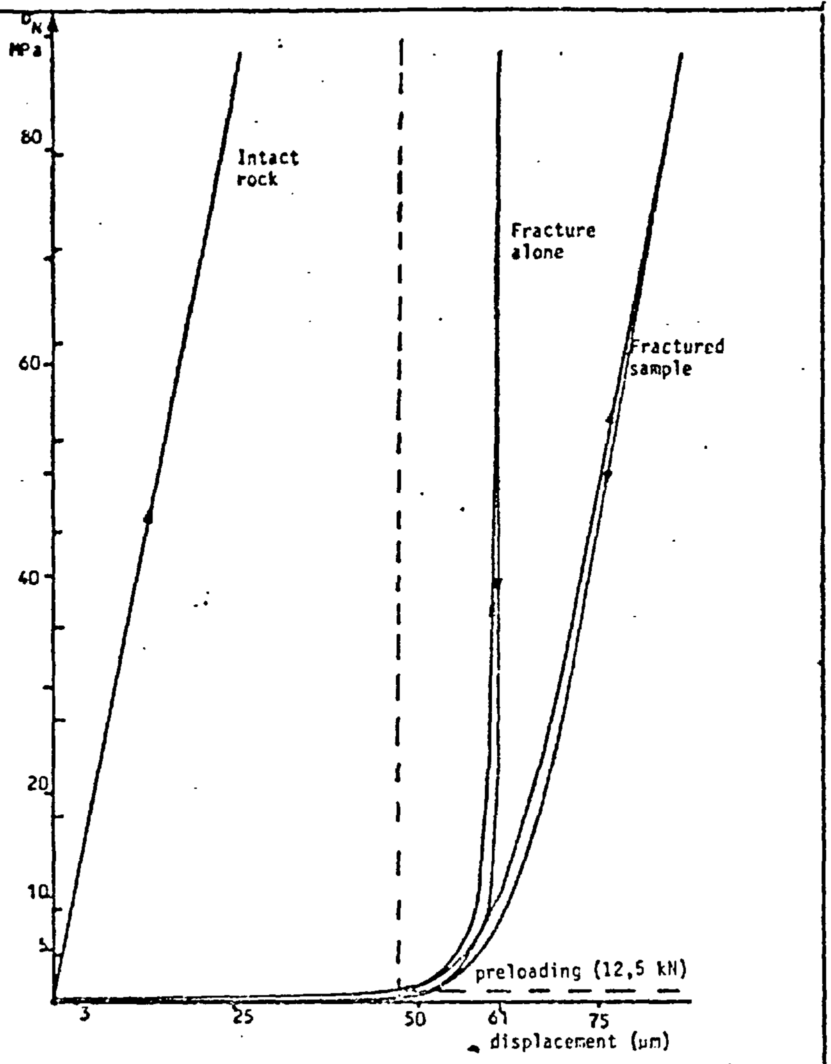

Fig. 8 : Example of a stress-displacement curve for a fracture under normal loading. Guéret granite. After [5]

It can be understood that the introduction of the cubic law into the "confined teeth" model did not make it possible to reproduce by calculation the results of the experiments on percolation under stress that were carried out by Gentier. It is nevertheless still possible that a more detailed analysis of fracture morphology would lead to the proposal of laws of flow that take into account the phenomenon of channeling.

Before leaving this subject, an important observation must be made. It has been seen that above a certain threshold, the fracture no longer closes up and its hydraulic conductivity stops decreasing. For the fracture studied this threshold was situated at about 15 MPa, which corresponds to the lithostatic pressure at about 600 m depth. This means that open fractures can be expected down to great depths in granites.

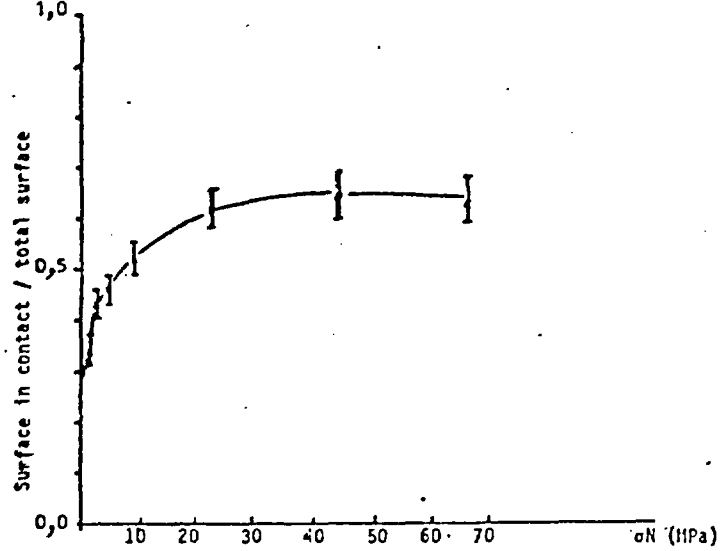

Fig. 9 - Example of the relationship between normal stress and the proportion of contact area in a fracture plane. Guéret granite. After [5]

IMPORTANCE OF THE EFFECT OF SHEAR ON THE HYDRODYNAMIC BEHAVIOUR OF FRACTURES

The consideration of normal stresses alone is not sufficient to account for the variations in permeability of these fractured rock media. Fig. 12 gives the results of calculations of flow at 1000 m depth around a geothermal doublet of the "hot dry rock type". The hydraulic conductivity of fractures cutting this medium is in one instance constant, and in the other varies simply with the effective normal stress (total pressure minus water pressure), according to a law of the type :

$$k_f.e = \beta.\sigma^\alpha,$$

where k_f = hydraulic conductivity
e = aperture
σ = normal stress

A law of this kind, as proposed by Gale [9], takes into account quite satisfactorily the results of laboratory tests. Calibrated against the results of Gentier it gives the following values for his two parameters :

α = -0.9
β = 1.43 x 10^{-8} m^2/s

It can be seen on fig. 12 that the equipotential curves calculated on the assumption that hydraulic conductivity varies with the normal stress differ very little from those obtained with constant conductivity. The calculated variations of permeability, which do not exceed a ratio of 2, appear to be too low in view of the measurements made in the Carnmenellis granite in England by the Camborne School of Mines, which showed that locally, permeability can be multiplied by more than 10 at a depth of 2000 m, under the effect of a 5 MPa overpressure.

The same tests also showed the importance of shear along the fracture planes, induced by injection. It may be that this shearing is the cause of the important observed variations in permeability, due to the dilatancy that accompanies it. Fig. 13, taken from Tsang and Witherspoon [10], illustrates this phenomenon qualitatively. Considerable experimental work remains to be done to quantify it, however. The morphological analysis of fractures will undoubtedly be of great utility in this respect.

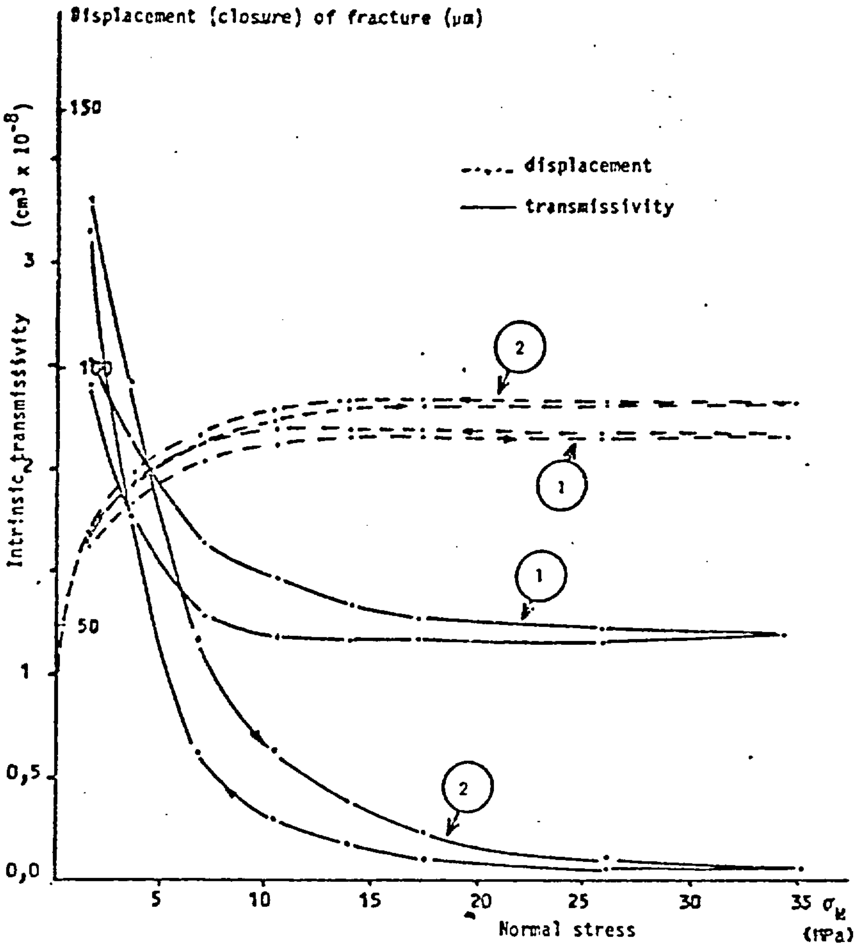

Fig. 10 - Examples of normal stress-displacement and normal stress-intrinsic transmissivity relationship for two samples (1 and 2) taken from the same fracture in granite. Guérit granite. After [5]

(Intrinsic transmissivity : hydraulic conductivity x hydraulic aperture)

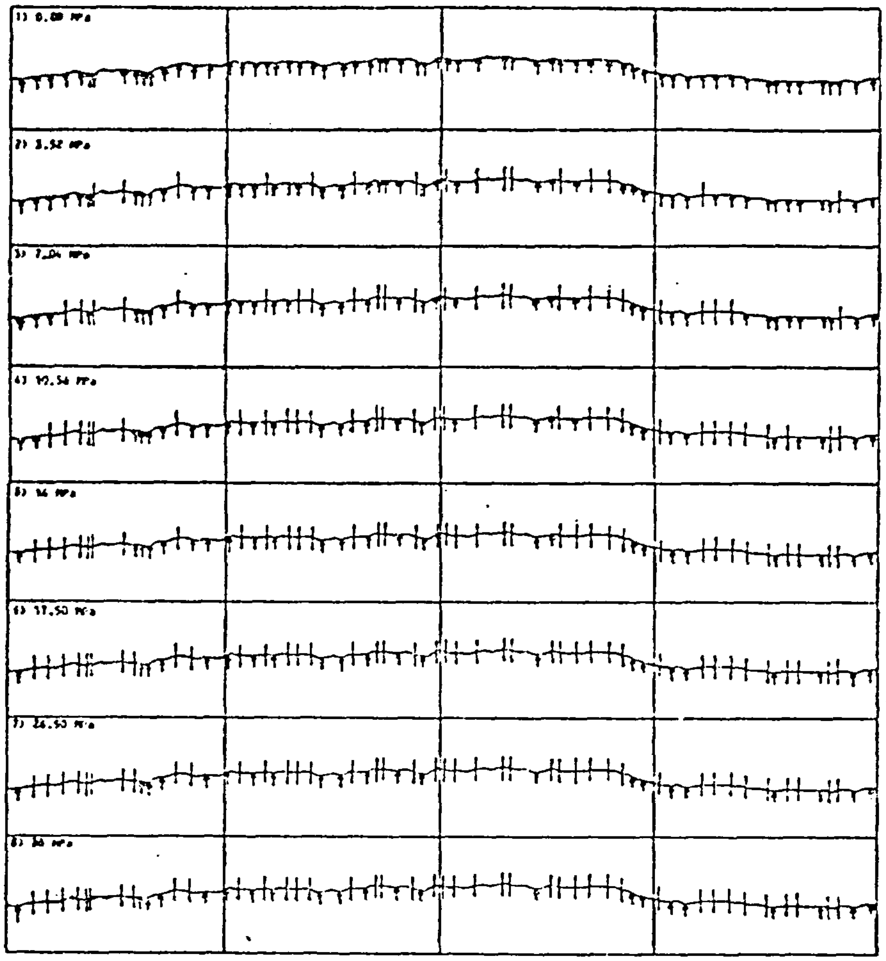

Fig. 11 - Distribution of fluid emission points along edge of fracture submitted to radial percolation, under increasing normal load. Guéret granite. After [5]

—→ emission point
—— emission point vanished

THE EQUIVALENT CONTINUOUS MEDIUM

Consideration of the real fractured medium as an equivalent continuous medium for the purpose of calculating flow is not new. It raises two problems, that of the very existence of the equivalent continuous medium (or of the possibility of defining it) and that of determining its characteristics. While the second of these problems, by the nature of things, has from the outset held the attention of researchers, it is only recently that attention has been paid to the first (Feuga [11]).

Definition of the equivalent continuous medium assumes the notion of a physical basis, known in this case as the representative volume. The smallest basis allowing the equivalent continuous medium to be defined is called the "representative elementary volume". This must contain a sufficiently large number of fractures for such a formalization to be possible, a requirement that determines its size, for the size will be greater as the density of fractures is lower and as the size of the fractures is smaller (note that these two factors both imply poorer connectivity).

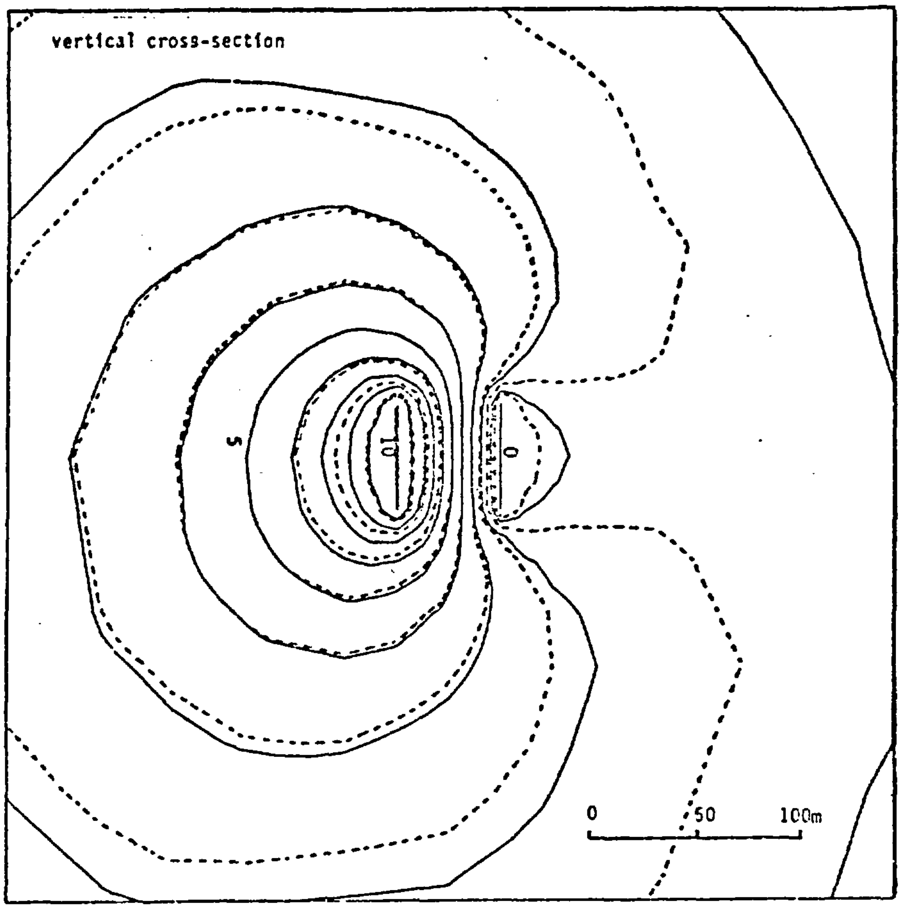

Fig. 12 - Equipotential lines in the vicinity of "Hot dry rock" exploitation wells (10 MPa overpressure in injection well).

—— Constant permeability
- - - Permeability varies with effective stress

After [8]

But, and this has not always been clearly perceived, there is also an upper limit to the size of the representative elementary volume. This results from the nested character of the fracture structure, for if, in order to contain a sufficiently large number of fractures, the size of the representative elementary volume, which is assumed to contain fractures only of the first structural order, has to be so large that it includes one or more fractures of a higher structural order, it is no longer possible to define an equivalent continuous medium.

One approach to the notion of the equivalent continuous medium is that developed by Jane Long (cf. her talk in the present symposium). In this approach, the question of the existence of this medium and of the size of the representative elementary volume is treated at the same time as that of the determination of its characteristics.

The first attempts to determine the hydraulic characteristics of the equivalent continuous medium from the characteristics of the fracture field and of the individual fractures assumed that all the fractures were of infinite extension and were therefore perfectly connected to one another (see for example Bertrand et al. [12]). Howewer, this approach gave calculated permeabilities several

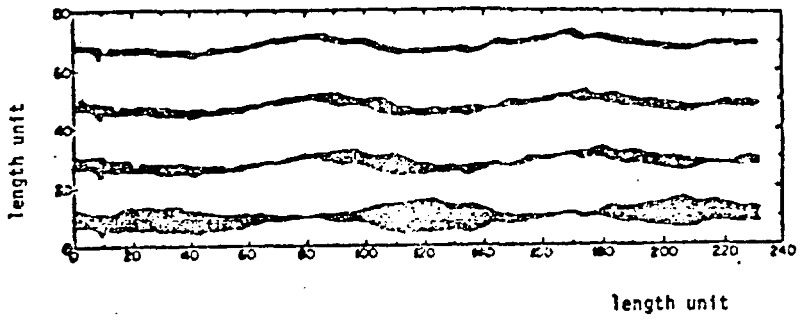

Fig. 13 - Diagram showing the variations of a fracture aperture due to shear displacements. After [10]

orders of magnitude greater than those evaluated from in-situ tests. It was first of all considered whether this considerable difference could be due to overestimation of the opening of the fractures used in the calculation, but it appeared that this was not sufficient to explain all of the observed difference.

The difference is in fact largely due to limited extension of the fractures. It was realised that it was not enough that a medium should contain fractures, however wide their opening, for it to *be permeable on the large scale ; it is also necessary that they intersect each other, and this occurs* the more as the fractures are longer and more numerous.

A completely original approach to this problem of the connectivity of fractures in a field was made by heterogeneous material physicists. Charlaix et al. [13], using considerations based on the theory of percolation, showed that it was possible to define a certain threshold of size, simply as a function of the density and length of fractures, below which the fracture network is not interconnected ; it is at best composed of finite permeable masses that are not connected to one another, and its permeability is zero. Above this threshold, however, the network is interconnected and it becomes possible to envisage the existence of a continuous medium that is equivalent to the network.

This approach does not enable quantification of the permeability of the equivalent continuous medium, but it does make it possible to see very quickly whether or not a given fracture field can have large-scale permeability.

The considerations developed above are based on regarding the fractures as thin slices totally available to flow, whereas we have seen that very commonly, and in particular when the fractures are subjected to increasing normal stress, flow becomes concentrated in channels in the plane of the fracture. This further complicates the problem of interconnectivity, which must be posed in terms of the intersection not only of portions of planes, but also of conduits within these planes. An important consideration, dictated by field observations, is that the intersections of fractures themselves very commonly constitute channels of preferential flow. If this were not so, one would come across very few deep fractured rock masses with large-scale permeability, since the probability of channelways anarchically distributed in space intersecting one another is extremely small (fig.14).

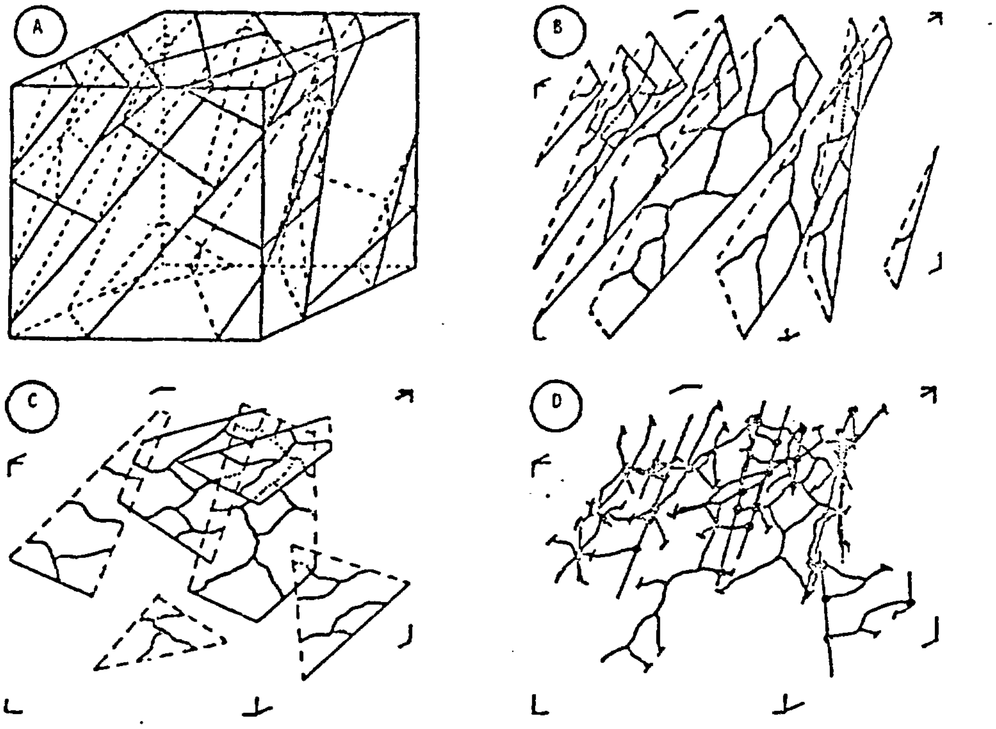

Diagram illustrating flow paths in a fractured rock mass

Fig. 14 - A. Fractured rock block with two sets of fractures
B. Conducting channels on set 1
C. Conducting channels on set 2
D. Fractures intersections and inter-connected channels

The problem of the determination of the hydrodynamic characteristics of the equivelent continuous medium, which is not simple and is still very far from being solved in a practical manner in the case where it is assumed that flow occurs throughout the plane of the fracture, is still further complicated if chanelling is taken into account.

The problem of the variation of hydrodynamic characteristics under the influence of variations of stress is also very poorly resolved, to the extent that the problem of the hydraulic conductivity of an individual fracture is itself, as we have seen, poorly resolved.

All that has been said so far concerns the continuous medium equivalent to a real fractured medium from the purely hydraulic point of view. In so far as mechanical and/or thermal phenomena also intervene in the problem, it is also necessary to define the medium equivalent to the real medium relative to these two aspects.

While, as far as temperature is concerned, non-consideration of the presence of fractures still allows calculations to be made that have been shown by *in situ* experiments to represent a satisfactory approximation to reality, as far as the mechanical aspect of the problem is concerned, the question of the equivalent continuous medium is not on the way to being solved, its complexity being even greater than that of the hydraulic domain.

An important observation must be made here, which is that researches into continuous media equivalent to real fractured media cannot be made independently of one another without the risk of incompatibilities arising, removing any physical sense from the modellings carried out. As an example, the work of Gentier showed the complexity of the notion of the opening of a fracture ; the models she established have led to the consideration of three types of opening - geometrical, mechanical and hydraulic. These three types of opening should clearly be related to a single, quantifiable, morphological reality in order to reduce the models to the same basis so that they can be used in coupled calculations.

CONCLUSION

This talk in no way pretends to presents a body of doctrine on the hydrogeological modelling of fractured rock media. This is a field that is in full development, and in which, although spectacular progress has been made in recent years, a great deal still remains to be done, as we have attempted to show.

Considering the very high cost of *in situ* tests in deep fractured media, and the difficulty of characterizing large masses of these media, due to their very low permeability, the author would tend to favour an approach based on synthetic models of fracture fields, constructed upon data (fracture surveys and measurements of conductivity of individual fractures) whose cost of acquisition is well below that of data relating to the large-scale hydraulic characterization of rock masses. These models should of course be validated by *in situ* tests designed specifically for this purpose.

In view of the complexity of these models, both in terms of their generation and of their application, their preferred utilization might be in the determination of the validity of the notion of equivalent continuous medium, and determination of the characteristics of this medium, on a given site.

As far as practical applications are concerned, at least in the field of radioactive waste repositories, we shall probably see the development of the mixed models mentioned above (some of which already exist, under the name "double porosity models"), in which only the large fractures are taken individually into account, all the smaller fractures being incorporated into an equivalent continuous medium.

BIBLIOGRAPHY

[1] BEREST P. (1986) - Thermomécanique des roches. Ecole d'été, Alès. Comité français de mécanique des roches. To be publishen in "Manuels et méthodes", BRGM éd.

[2] LONG J.C.S. (1983) - Investigation of equivalent porous medium permeability in networks of discontinuous fractures. Ph. D. Thesis. Univ. of California, Berkeley.

[3] LONG J.C.S., BILLAUX D. (1986) - The use of geostatistics to incorporate spatial variability in the modelling of flow through fracture networks. Report of Lawrence Berkeley Laboratory n° 21439

[4] MASSOUD H., CHILES J.P. (1986) - La modélisation de la petite fracturation par les techniques de la géostatistique. Rapport Ecole des Mines d' Alès-BRGM - Mai 1986.
The information contained in this report will appear in the thesis of H. MASSOUD, which will be defended, at the Ecole des Mines de Paris, at the end of 1986.

[5] GENTIER S. (1986) - Morphologie et comportement hydromécanique d'une fracture naturelle dans un granite sous contrainte normale. Thèse Université d'Orléans.

[6] LOUIS C. (1976) - Introduction à l'hydraulique des roches. Thèse Université Pierre et Marie Curie. Paris.

[7] HOEK E., BROWN E.T. (1980) - Underground excavation in rock. Institution of Mining and Metallurgy. London.

[8] RECAN M. (1986) - Simulation des écoulements dans un milieu a perméabilité variable en fonction de la pression du fluide. Rapport BRGM n° 86 SGN 327 GEG.

[9] GALE J.E. (1982) - The effects of fracture type (induced versus natural) on stress-fracture closure-fracture permeability relationships. Proc. 23 rd US Rock Mech. Symp., Berkeley, Calif.

[10] TSANG Y.W., WITHERSPOON P.A. (1983) - The dependence of fracture mechanical and fluid flow properties on fracture roughness and sample size. J. of Geophys. Res., vol. 88, n° 83, p. 2359-2366.

[11] FEUGA B. (1983) - Caracterisation du milieu poreux équivalent à un milieu rocheux fracturé par essais à l'eau in situ. Bull. IAEG n° 23-27.

[12] BERTRAND L., DURAND E., FEUGA B. (1982) - Détermination en sondages de la perméabilité d'un milieu rocheux fracturé : aspects théoriques et pratiques. Revue française de géotechnique, n° 20.

[13] CHARLAIX E., GUYON E., RIVIER N. (1984) - A criterion for percolation threshold in a random array of plates. Solid state communications, vol 50, n° 11, p. 999-1002.

Coupled Processes in Single Fracture, Double Fractures and Fractured Porous Media

Chin-Fu Tsang

Earth Sciences Division
Lawrence Berkeley Laboratory
University of California
Berkeley, California 94720

ABSTRACT

The emplacement of a nuclear waste repository in a fractured porous medium provides a heat source of large dimensions over an extended period of time. It also creates a large cavity in the rock mass, changing significantly the stress field. Such major changes induce various coupled thermohydraulic, hydromechanic and hydrochemical transport processes in the environment around a nuclear waste repository.

The present paper gives, first, a general overview of the coupled processes involving thermal, mechanical, hydrological and chemical effects. Then investigations of a number of specific coupled processes are described in the context of fluid flow and transport in a single fracture, two intersecting fractures and a fractured porous medium near a nuclear waste repository. The results are presented and discussed.

Introduction to Coupled Processes

The assessment of the long-term performance of a nuclear waste repository involves the evaluation of the travel time and rate of transport of radioactive elements from the repository to the accessible environment. This evaluation involves understanding the combined effects of many different processes that may affect such transport. These combined or coupled processes are initiated or induced by the large perturbations to the rock mass due to the emplacement of a nuclear waste repository. The rock mass is perturbed in two ways. First, the nuclear waste repository represents a heat source of large dimensions over an extended period of time. Thermally induced buoyancy and rock expansion effects do not depend directly on the value of temperature rise, but on the integrated heat input into the system. Thus, a relatively low temperature rise over a large volume and a long period of time could cause major buoyancy effects. Second, the repository represents a large cavity constructed out of the rock mass, changing significantly the original stress distribution.

The coupled processes induced by these drastic changes involve mainly four different effects, namely, thermal (T), hydrological (H), mechanical (M) and chemical (C). Among these four, there can be only 11 (i.e., 2^4-5) types of couplings of various levels of importance. These are listed in Table I, which also indicates one example for each of these couplings. It may be useful to draw definite distinctions between different degrees of coupling in order to clarify what we mean by coupled processes. Table II displays schematically several possible connections between processes. The fully uncoupled processes conceptually have negligible influence or effect on one another, so that they can be evaluated independently. The sequential case implies that one process depends on the final state of another so that the order in which they are evaluated becomes important.

The one-way coupled processes demonstrate a continuing effect of one or more processes on the others, so that their mutual influences change over time. The two-way coupling (or feedback coupling) reveals a continuing reciprocal interaction among different processes, and represents in general the most complex form of coupling. In this study, the term coupled processes refers to either the one-way or the two (or more) way couplings among the physical processes considered.

In many studies for the performance assessment of a nuclear waste repository, some of these coupled processes, such as buoyancy flow in a porous medium, have been addressed. However the value of considering these coupled processes in an overall way as suggested by Tsang (1980, 1985) and Tsang and coworkers (1982) lies in the comprehensiveness in the consideration of all possible coupled processes that may occur.

Table I

Types of Coupled Processes
(T = Thermal, M = Mechanical, H = Hydrological, C = Chemical;
single line indicates weak coupling, double line, strong coupling)

Type	Examples
T = C	e.g. phase changes
T = H	e.g. buoyancy flow
T = M	e.g. thermally induced fractures
H = C	e.g. solution and precipitation
H = M	e.g. hydraulic fracturing
C — M	e.g. stress corrosion
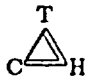	e.g. chemical reactions and transport in hydrothermal systems
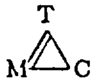	e.g. thermomechanical effects with change of mechanical strengths due to thermochemical transformation
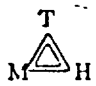	e.g. thermally induced hydromechanical behavior of fractured rocks
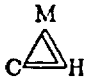	e.g. hydromechanical effects in fractures that may influence chemical transport
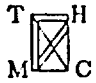	e.g. chemical reactions and transport in fractures under thermal and hydraulic loading

Thus one hopes that all significant coupled processes will be properly evaluated in the performance assessment. The safety of a nuclear waste repository presents a problem of unusual requirements to the scientific and engineering communities. One is required to make predictions thousands of years into the future and one is also required to predict not just the mean arrival time of radionuclides which may have escaped from the repository, but also the early arrival times at low concentrations. With these extraordinary requirements, coupled processes that may usually be neglected may become of significance. In a panel report devoted to this discussion (LBL, 1984), a few of the often ignored coupled processes were pointed out. One example is the piping effect, i.e., the formation of fluid flow tubes due to pressure induced chemical dissolution and other processes. Such an effect is known in the fields of mining and soil mechanics, but is not much addressed in the nuclear waste storage problem. Another example is the osmotic effects (thermal osmosis and chemical osmosis), which may have significant control of radionuclide transport through clay backfill materials, thus having important impact on the source term for the geosphere transport modeling. A recent international symposium (LBL, 1985) surveyed many of the coupled processes and discussed their significance. Many of the papers in this symposium have been updated and will be a good source of information on this subject (Tsang, 1987).

Table II

Diagrams of Uncoupled and Coupled Processes
(T = Thermal, M = Mechanical, H = Hydrological, C = Chemical)

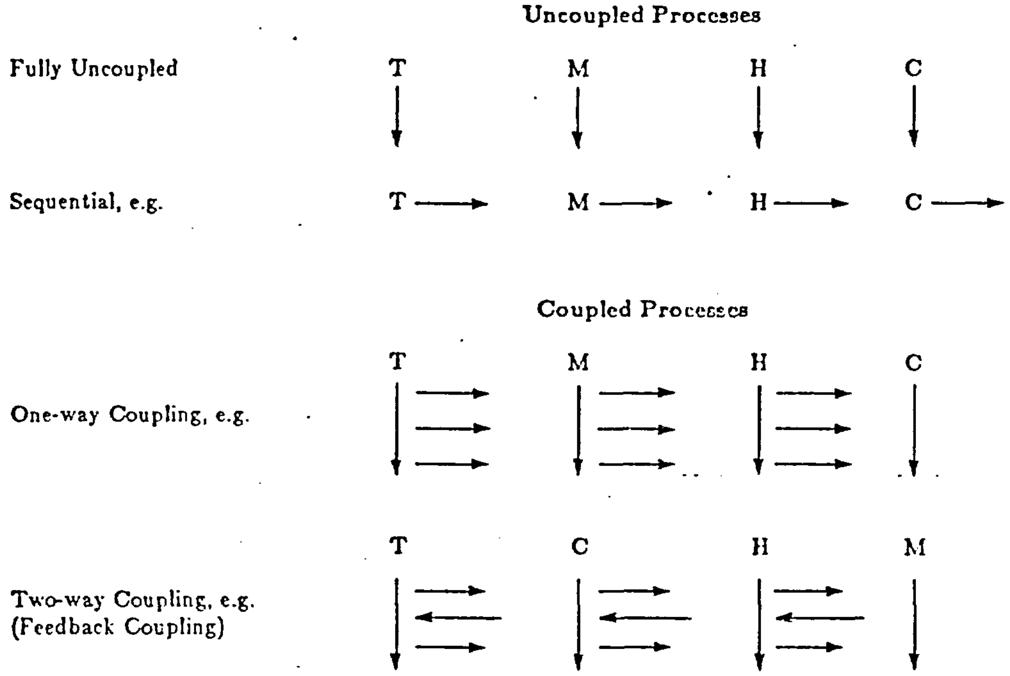

The present paper will describe results of investigations by the group at Berkeley on a number of coupled processes for the case of a single fracture, two intersecting fractures and fractured porous media. The topics are:

(1) Tracer transport in a single fracture under stress, based on the channel model.
(2) Hydrothermal buoyancy flow in two intersecting fractures.
(3) Modeling of non-isothermal hydrofracturing of a porous reservoir.
(4) Thermohydromechanical process in a fractured porous medium around a heat source.

After the discussion of these results, a few brief conclusions and comments will conclude the paper.

Solute Transport in a Single Fracture Under Stress Based on the Channel Model

In this first example, we shall consider the transport of chemical solute through a water-saturated single fracture under mechanical stress (Tsang and Tsang, 1986). The flow through each fracture is most commonly treated as the flow through a pair of smooth parallel plates separated by a constant aperture, and thus the fluid flowrate varies as the cube of the constant separation. However, a real fracture in rock masses has rough-walled surfaces, and, unlike parallel plates, portions of the fracture may be blocked by filling material or closed when subjected to normal stress. As a matter of fact, it is the blockages or contacts between upper and lower surfaces of a fracture that provide a correlation between normal mechanical stress variations and the fluid flow that is controlled by fracture aperture closure (Tsang and Witherspoon, 1981, 1983).

Table II

Diagrams of Uncoupled and Coupled Processes

(T = Thermal, M = Mechanical, H = Hydrological, C = Chemical)

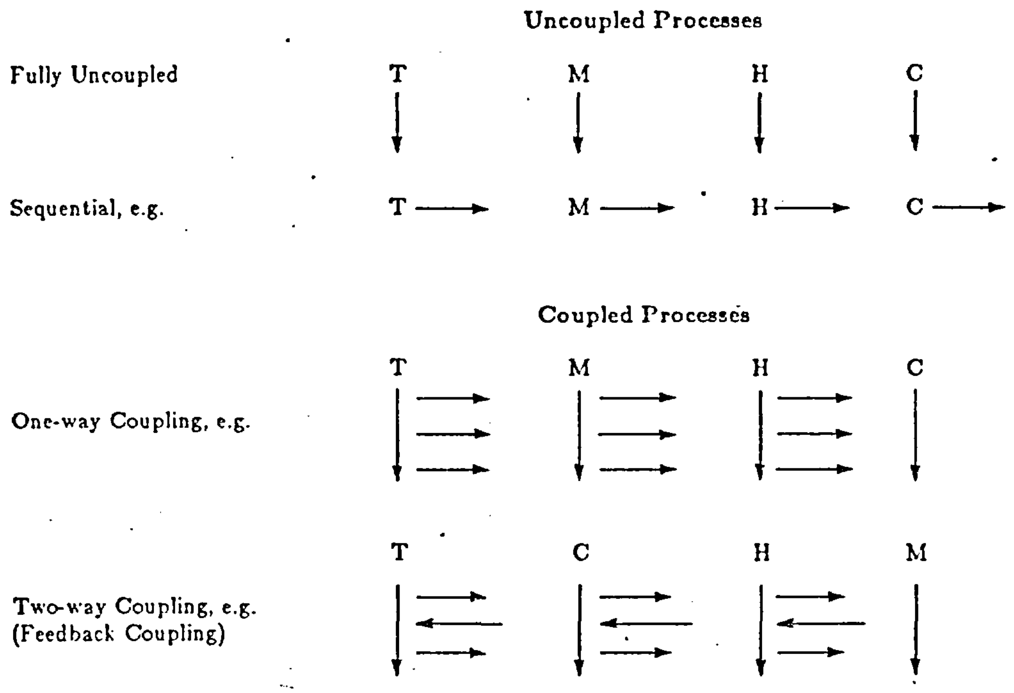

The present paper will describe results of investigations by the group at Berkeley on a number of coupled processes for the case of a single fracture, two intersecting fractures and fractured porous media. The topics are:

(1) Tracer transport in a single fracture under stress, based on the channel model.
(2) Hydrothermal buoyancy flow in two intersecting fractures.
(3) Modeling of non-isothermal hydrofracturing of a porous reservoir.
(4) Thermohydromechanical process in a fractured porous medium around a heat source.

After the discussion of these results, a few brief conclusions and comments will conclude the paper.

Solute Transport in a Single Fracture Under Stress Based on the Channel Model

In this first example, we shall consider the transport of chemical solute through a water-saturated single fracture under mechanical stress (Tsang and Tsang, 1986). The flow through each fracture is most commonly treated as the flow through a pair of smooth parallel plates separated by a constant aperture, and thus the fluid flowrate varies as the cube of the constant separation. However, a real fracture in rock masses has rough-walled surfaces, and, unlike parallel plates, portions of the fracture may be blocked by filling material or closed when subjected to normal stress. As a matter of fact, it is the blockages or contacts between upper and lower surfaces of a fracture that provide a correlation between normal mechanical stress variations and the fluid flow that is controlled by fracture aperture closure (Tsang and Witherspoon, 1981, 1983).

Theoretical studies (Tsang, 1984) have shown that only at low applied stress, when fracture is essentially open, does the parallel-plate idealization of a rock fracture adequately describe fluid flow. Because of the contact areas between fracture surfaces and constrictions of the fracture subject to stress, flow through a single fracture takes place in a few channels which are tortuous, have variable apertures along their lengths, and which may or may not intersect each other.

Evidence that flow takes place in channels also occurs in field and laboratory experiments. In the field experiments of solute migration in single fractures in the Stripa mine, Sweden (Abelin et al., 1985; Neretnieks, 1985), the observation that the amount and time of tracer returns at two near-by sampling points were very different, and that many of the neighboring collection holes registered no tracer (non-sorbing) return at all lends support to the channel nature of fluid flow within a single fracture.

The laboratory experiments of Pyrak et al., (1985) and the field experiment carried out in a single fracture in Cornwell (Bourke et al., 1985; P.J. Bourke, personal communication, 1986) also demonstrated that flow in a single fracture took place in a limited number of channels.

On the basis of theoretical and experimental observations referred to above, we have studied fluid flow and solute transport in a tight fractured medium in terms of flow through a limited number of tortuous and intersecting channels. These channels have variable apertures, b, along their lengths. Figure 1a shows schematically the channeling effect in a single fracture. Each channel in Figure 1a is represented schematically in Figure 1b. It is defined by the aperture density distribution n(b) along its length. The channel width is assumed to be constant, of the same order as the correlation length, λ, since, by definition, the correlation length is the spatial range within which the apertures have similar values. The channel length does not equal the linear length between two points, but is not expected to vary more than a factor of two to three from the actual linear length. For a given aperture density distribution and correlation length, different realizations of statistically equivalent channels may be generated (Tsang and Tsang, 1986) using geostatistical methods.

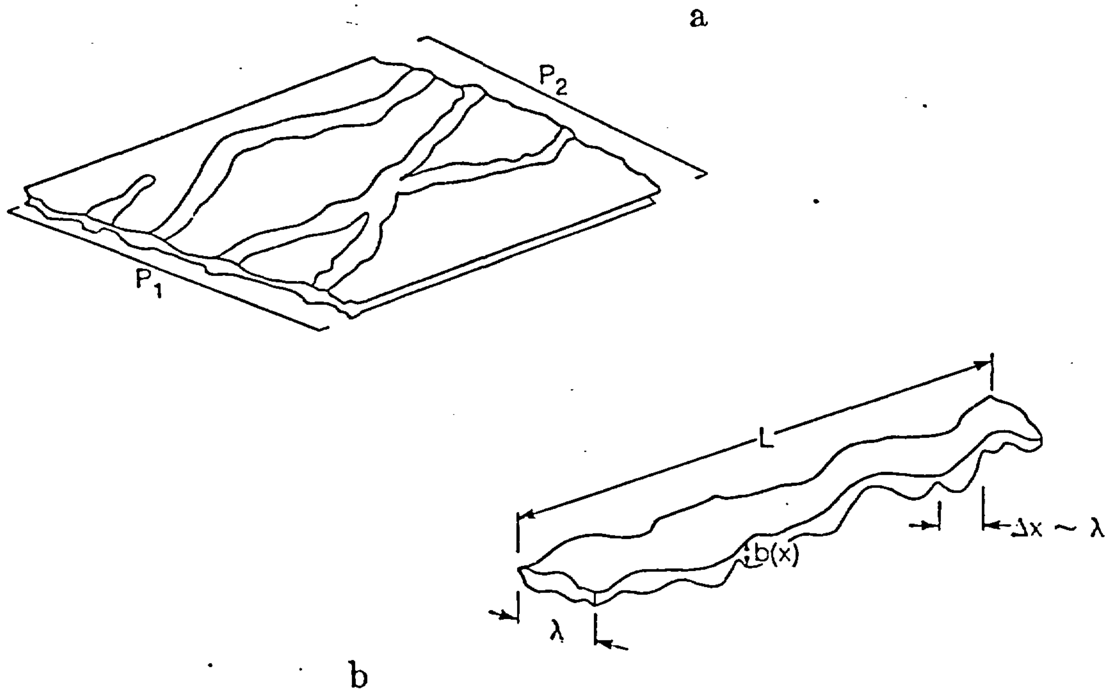

XBL 863-10710 A

Figure 1. (a) Schematic diagram of the channel representation of fluid flow in a single fracture.
(b) Schematic sketch for one channel.

When a pressure difference is applied between two ends of a single fracture, flow takes place along a number, M, of these channels in the fracture plane. If we assume that a step function input of chemical solute (tracer) at constant concentration be injected at the high pressure end, we can calculate the tracer concentration breakthrough curves at the exit end. Figures 2a through 2d show the tracer concentration breakthrough curves as a function of time for M = 32, 16, 11 and 8, respectively. We note a rather steep rise in the concentration curves in the early times, then some "stair-step" structure due to the finite delay for the solute carried in the next channel to breakthrough. The early arrivals correspond to flow in fast channels, those with few very small aperture constrictions. The steep rise therefore indicates that a large proportion of the total flow is in fast channels. In Figures 3a through 3d we reproduce the breakthrough curves from laboratory experiments (Moreno, et al., 1985) performed on a single fracture in a 18.5 cm core. Careful examination of Figures 2 and 3 indicates that the prominent features in the theoretical curve based on the channel model are also evident in the observed curves. These features (such as the steep rise in tracer returns and the stair-step structures) are not found in the conventional advection-dispersion curves. We are aware of the fact that there are data measurement errors in the laboratory breakthrough data, hence raising a question made over the claim that the stair-step structure in the experimental breakthrough curve arises from the channel nature of the flow. Discussions with Eriksen (private communication, 1986) who performed the experiments as shown in Figure 3 about the precision of the measurements led us to believe that the stair-step structures are not merely data scatter.

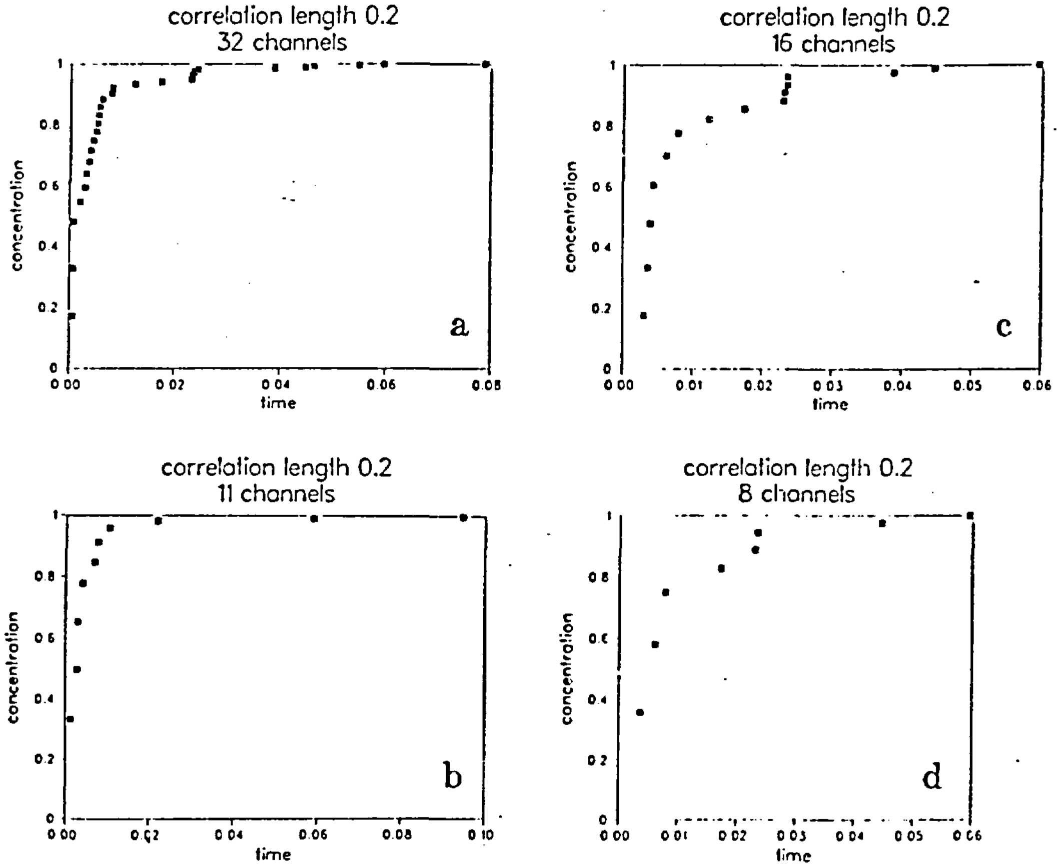

XBL 864-1244A

Figure 2. (a) - (d) Theoretical tracer concentration breakthrough curves for a set of M channels with common end point pressures P_1 and P_2, with M = 32, 16, 11 and 8 respectively.

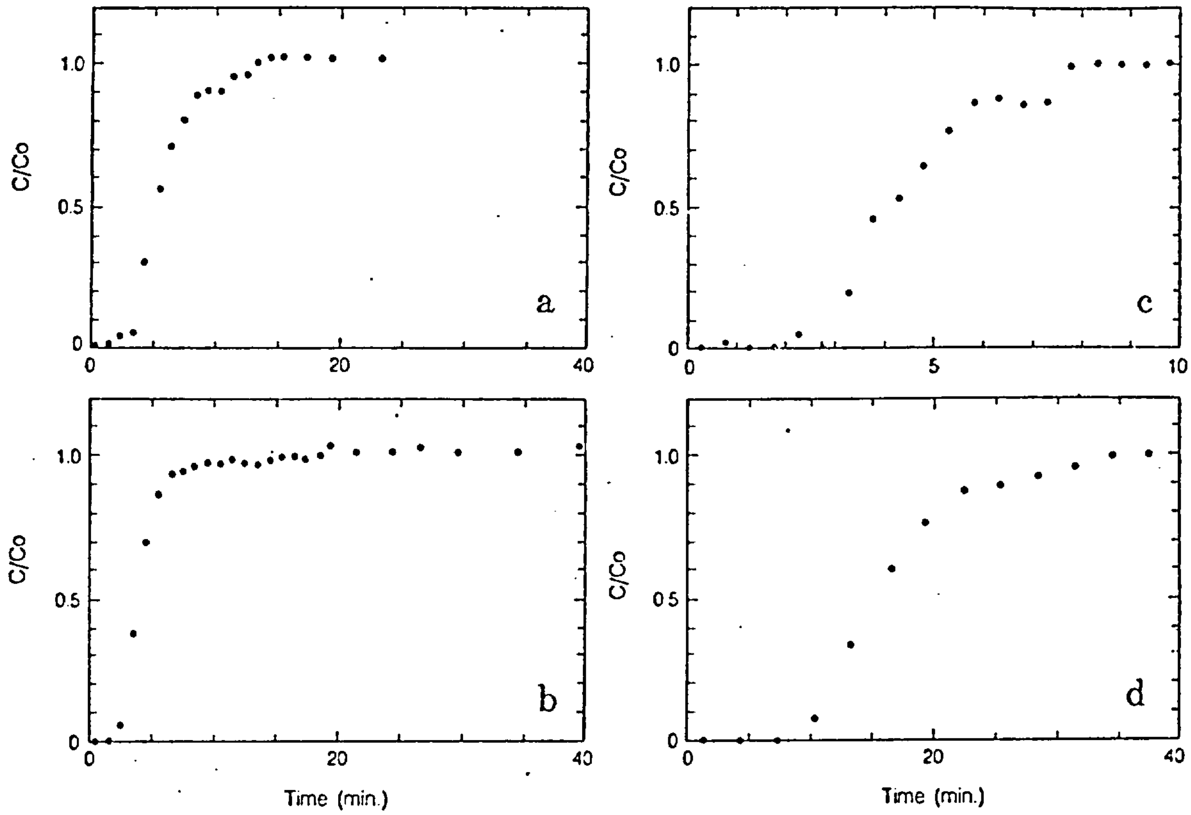

Figure 3. (a) - (d) Tracer concentration breakthrough data from laboratory measurements on a single fracture in a granitic core 18.5 cm in height and 10 cm in diameter (Moreno et al., 1985). The four curves correspond to different runs involving different injection flowrates and different tracers (NaLS or I).

When the normal stress across a fracture is increased, the reduction in channel apertures affects the tracer breakthrough curves. One may start with the experimental concentration breakthrough data such as in Figure 3a and interpret them in terms of our conceptual channel model. Making the assumption that all the apertures in the fracture are reduced by 6% due to the mechanical stress, a new tracer breakthrough curve may be derived (Fig. 4). This figure indicates that even with a small change in the mean fracture aperture (6% reduction), a large change in the breakthrough curve resulted. The reason is that the small change affects significantly the constricted part of the channels, which controls the flow rates. Thus the signature of channeling in fracture is in the stair-step structure of the breakthrough curves and their sensitivity to stress applied across the fracture. These suggested possible coupled hydromechanical laboratory experiments which may be performed in order to further investigate the channel nature of fluid flow in fractures. Note that these hydromechanical effects would not be expected if flow through fractures were approximated by flow between smooth parallel plates.

Buoyancy Flow in a Two-Fracture Model

The coupling of heat and fluid flow in porous media around a nuclear waste repository is studied by a number of authors. We made a study of such a coupled process in two intersecting fractures. These two fractures may be either one horizontal and one vertical (Wang et al., 1980; Wang et al., 1979) or both vertical (Wang and Tsang, 1980). Recent buoyancy flow studies (Tsang and Pruess, 1986; Pruess, et al., 1985) also considered two-phase flow in a highly fractured porous medium, in which water vapor and air may also

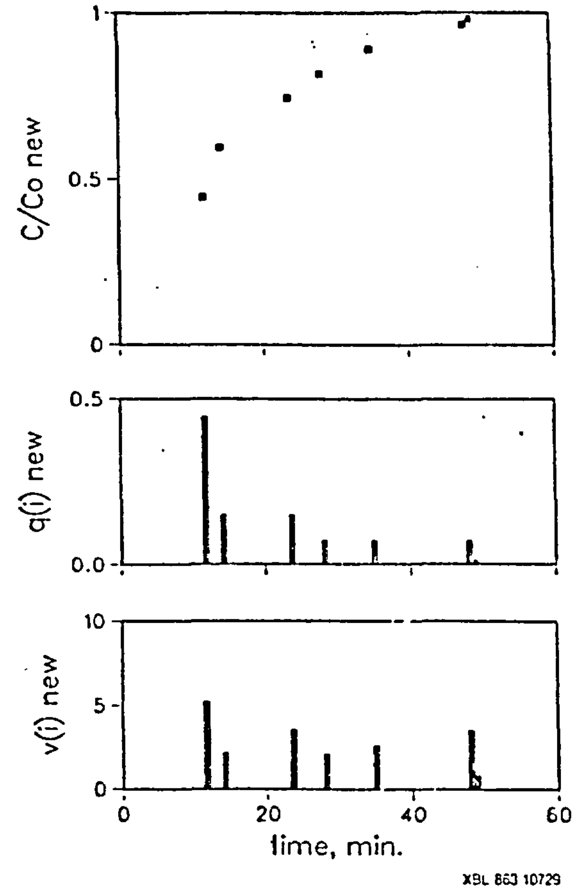

Figure 4. Predicted tracer concentration breakthrough curves for flow through a single fracture subject to normal stress, based on the laboratory data shown in Figure 3c.

be present. In this case, for example, water may evaporate into vapor near heat source at the repository and condense as the vapor moves up away from it. For our present illustration of coupled buoyancy flow we shall present the simple case of single phase flow in a system of one horizontal and one vertical fracture.

It is well known that variations in the temperature of the rock mass cause changes in the density and viscosity of water in the rock fracture system and induce buoyant flows. The permeability of many crystalline and argillaceous rocks arises mainly from the hydraulic conductivity of fractures. The concern on fracture flow is related to the important question of the possibility of waste components being carried by the fracture water from the repository to the surface. The model used is comprised of a horizontal fracture at the depth of repository connecting a recharge zone to the repository, which is also connected to a discharge zone in the opposite direction, and the horizontal fracture is intercepted by a vertical fracture from the center of the repository to the surface as shown in Figure 5. Before the repository is loaded and the rock mass subjected to changes in temperature, it is assumed that the original groundwater flow is horizontal from recharge zone to discharge zone. As the rock temperature increases, the water initially at the depth of the repository will move upward in the vertical fracture by buoyancy forces.

The repository is assumed to have a radius, R, of 1500 m and is positioned at D = 500 m or 1000 m below the land surface. The temperature rise is calculated by a heat conduction model assuming an instant emplacement of nuclear waste with a heat output density of 10 W/m^2. The heat power output variations with time are assumed to be given by $P(t) \propto 10(t/to)^{-3/4}$ This corresponds approximately to the power output curve for spent fuel (Wang et al., 1979). The thermal diffusivity for the rock formation (granite) is assumed to be 15 x 10^{-6} m^2/sec and the thermal conductivity is 2.5 W/m/°C. The recharge and discharge zones are assumed to be far away from the repository and maintained at normal hydrostatic pressure and ambient temperature. Before the emplacement of wastes, an ambient temperature field of 20°C at ground surface and a normal geothermal gradient of 30°C/km is assumed. The buoyancy force is proportional to the density contrast between the heated water in the vertical fracture and the cooled water in the recharge and discharge zones. In Figure 6, the upward movement of water initially at the depth of the repository is plotted as a function of time. The results in two cases, one with the repository at a depth of 500 m and the other at a depth of 1000 m are compared. There is little difference due to the change in depth. Essentially, the flow of water as a result of buoyancy depends upon the average temperature of the water throughout the length of the vertical fracture. The more important factor affecting the buoyant flow of groundwater is the ratio between the distance L from repository to the recharge zone and the depth D of the repository. For the particular case illustrated in Figure 6, the repository is assumed to be located a distance, L = 5000 m, midway between the recharge and distance zone. The vertical and horizontal fractures are assume to have the same aperture $b_z = b_x = 1 \mu m$.

In addition to the temperature change and hydrologic connecting distances L and D, the buoyant flow depends sensitively on the apertures and permeabilities of the fractures. For a fracture with aperture b, the permeability $k = b^2/12$ for laminar fracture flow (Lamb, 1932; Witherspoon et al., 1980) is assumed in the calculation. If the horizontal fracture representing the recharge path from the surrounding formation has a given finite aperture, the dependence of the buoyant flow on the vertical aperture is of great interest. In Figure 7, the results of a constant horizontal aperture $b_x = 1 \mu m$ and with a range of vertical apertures $b_z = 10 \mu m$, $1 \mu m$ and $0.1 \mu m$ are shown. The movement of the groundwater in the vertical fracture is significantly slower both for the case of $b_z = 10\, b_x$ and of $b_z = 0.1\, b_x$ than with $b_z = b_x$. For nonzero distance L and a finite horizontal aperture b_x, the buoyant flow does not become infinite as the vertical fracture aperture b_z increases. On the contrary, the buoyancy flow decreases as b_z increases. This can be easily explained by the fact that a large vertical fracture with large storage capacity reduces fluid flow velocity. Thus, the buoyant flow in the vertical fracture is controlled by the finite recharge capacity through the horizontal fracture.

Although the thermohydrological model used for the analysis above is very simple, it possesses the same physical behavior as that of the more complex repository systems. Accordingly, it should provide a good insight into the dynamics of the thermally-induced groundwater flow, and illustrate the sensitivity of this flow to various parameters. The actual numerical results should be considered as no more than an order of magnitude estimation. It must be pointed out also that the transport of nuclides does not take place at the same rate as that of the groundwater. Nuclide transport is retarded in a certain degree by various physical and chemical processes, such as sorption.

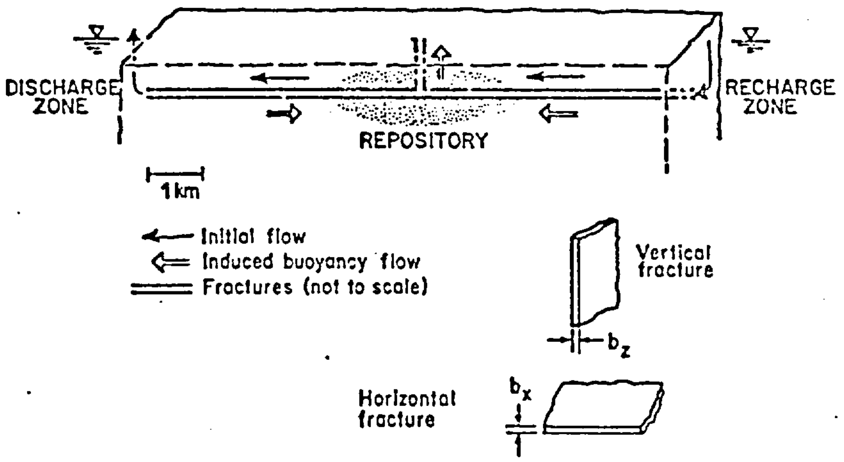

XBL 7810-11678

Figure 5. Two-fracture model for simulating buoyant flow.

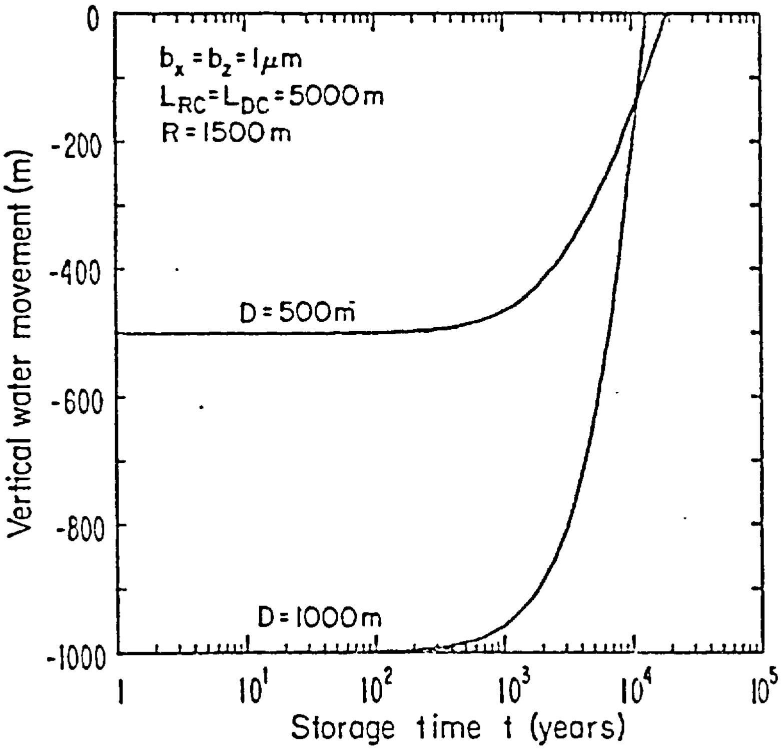

XBL 7810-11960

Figure 6. Effects of repository depths on the water movement along the vertical fracture.

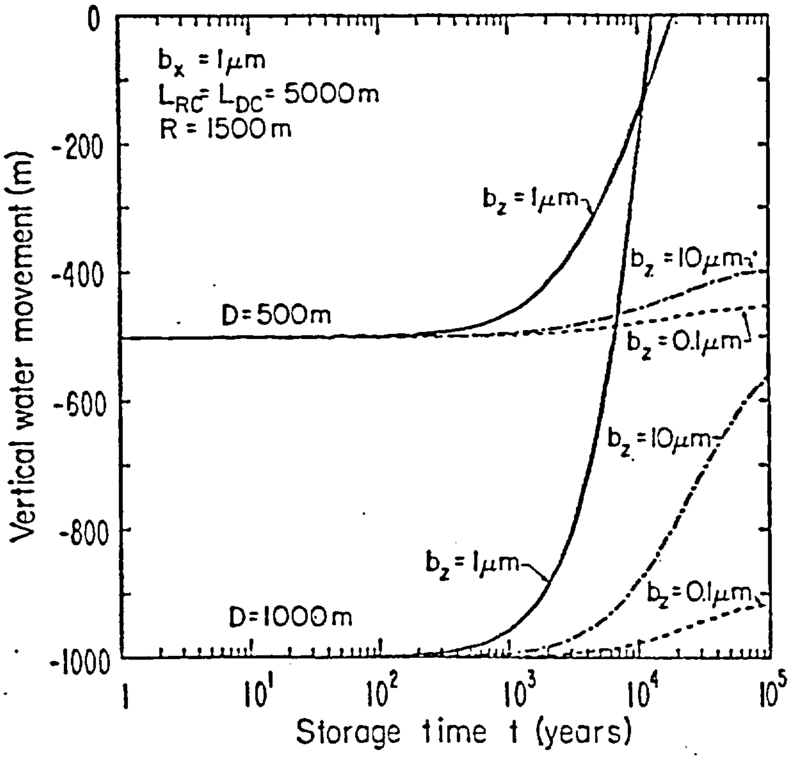

XBL 7810-11961

Figure 7. Effects of vertical fracture apertures on the water movement along the vertical fracture.

Non-isothermal Hydrofracturing of a Porous Medium

In this example of coupled process, we consider fluid injection into a fracture embedded in a permeable porous medium (Noorishad and Tsang, 1987). In general, the deformation of fractured rocks in response to fluid pressurization (e.g., by fluid injection) is a well-known phenomenon. Repressurization of hydraulically induced fractures in hydrofracturing experiments is commonly used to obtain better estimates of in situ stresses. In this procedure the compressive stress in the fracture is neutralized by the pressure of the injected fluid, resulting in an increase in fracture aperture. The deformation process, both in the rock as a whole and in the fracture specifically, is a coupled phenomenon. Thus far, realistic simulation of fluid injection has not been possible because of the lack of data and the complexity of analysis. These limitations are even greater if one considers nonisothermal injection, which is used in hot-dry-rock experiments or cold-water flooding of oil reservoirs. Cold-water flooding entails a triply coupled thermohydromechanical (THM) process among the flow of heat, the flow of fluid, and the host medium deformability. Theoretical developments of Nowacki (1962) and other observations (e.g., Stephens and Voight, 1982) have pointed to the important role of thermal stress in the process of fracture deformation. Even though the scarcity of data and complexity of the processes prevent the realistic simulation of THM phenomena, the availability of numerical procedures (Noorishad et al., 1984) does allow a scoping analysis of some observations to be made. This calculation is intended to explain the observations made for the case of cold-water flooding of an oil reservoir.

Field equations of THM phenomena, the general setup of a THM initial boundary value problem, and a numerical solution approach are given in Noorishad et al. (1984). That work also provides a basis for an understanding of the role of the thermal stresses in the THM phenomena through inspection of the stress-strain relationships. To investigate the role of thermal stresses in circumstances where transport of energy is enhanced by fluid flow, as well as in conjunction with the mechanical aspect of the flow of fluids, numerical techniques such as the code ROCMAS (Noorishad et al., 1984) must be used.

The numerical simulation in this work is based on semi-quantitative data on cold-water flooding experiments provided by an oil company. In these experiments, it was noticed that hydrofracturing and/or reopening of existing fractures in the warm reservoir consistently took place at pressure gradients that were about 1.5×10^{-3} MPa/m less than the expected values. For a reservoir at a depth of about 3000 m, the above reduction in gradient implies a shut-in pressure reduction of about 5 MPa. Using the code ROCMAS we constructed a hypothetical two-dimensional (x-y) model of the reservoir to study this problem. Figure 8 shows a sketch of the geometry and the initial and boundary data. In the field experiments, water is injected at constant rates until well pressure stabilizes; the rate is then increased by a constant amount, and the procedure continues for a period of a day or more, during which one or two hydrofacturing episodes is observed. A realistic simulation of the experiment is not possible; instead we seek a crude approximation. We do this by

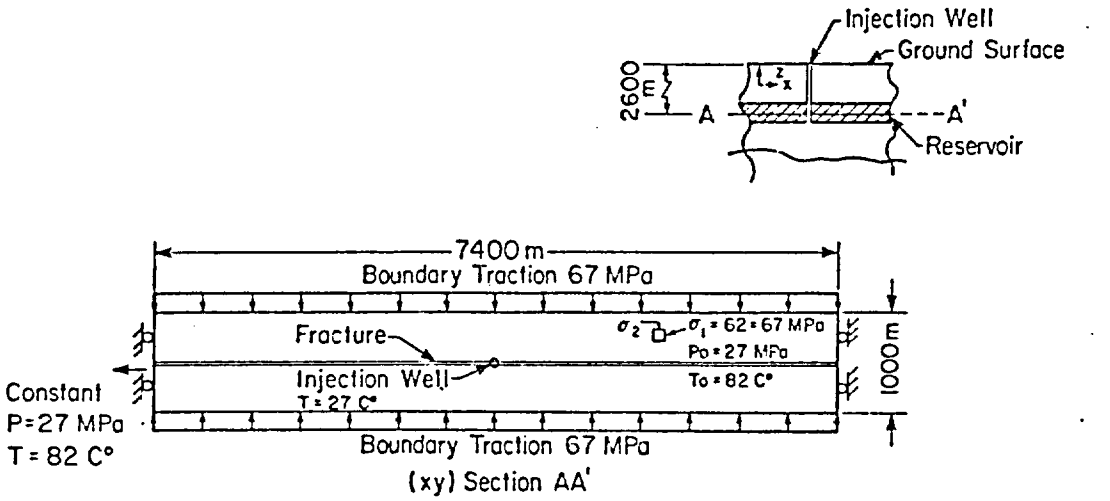

Figure 8. Schematic geometry of the non-isothermal fracturing model and initial and boundary conditions.

obtaining a THM response of the model though a series of steady-state HM calculations that use the results of a coupled transient thermal analysis. The approximation is justified because of the large difference between the time constants for fluid flow and heat flow. The fracture in the model is regarded to be closed initially (with aperture 10^{-7} m). Pressurization of the reservoir opens the fracture elastically against sustained compressive stresses. This increase in the aperture allows further penetration of the pressure front until the fracture goes into a tension state and hydrofracturing takes place. In the simulations, the occurrence of hydrofracturing is marked by instability of the system in the numerical solution. The presence of thermal stresses accelerates this phenomenon. Figure 9 show the results of an isothermal (HM) calculation and nonisothermal (THM) calculation of the model. As can be observed in the figure, the system become unstable at an injection pressure close to one order of magnitude less than that of isothermal injection calculations. Figure 10 depicts the advancement of the thermal front in the fracture, and Figure 11 displays the calculated TH and THM pressure distributions in the fracture as they separate from each other with the advancement of time.

Thermohydromechanical Process in a Fractured Porous Medium Around a Heat Source

In this last example, we present the results, based on the numerical code ROCMAS used for the problem in the last section, of thermohydromechanical behavior of a fractured porous medium around a nuclear waste canister hole (Noorishad et al., 1984). The nuclear waste canister is represented by a 5-kW heater located at a depth of 350 m in granite. A horizontal fracture is assumed to lie 3 m below the heater mid-plane and to extend from the heater borehole to a hydrostatic boundary at a radial distance of 20 m from the borehole. The properties of rock and fractures are given in Noorishad et al. (1984) and the two-dimensional axisymmetric (r,z) finite-element grid is shown in Figure 12. The heater drift, approximated by cylinderical hatched

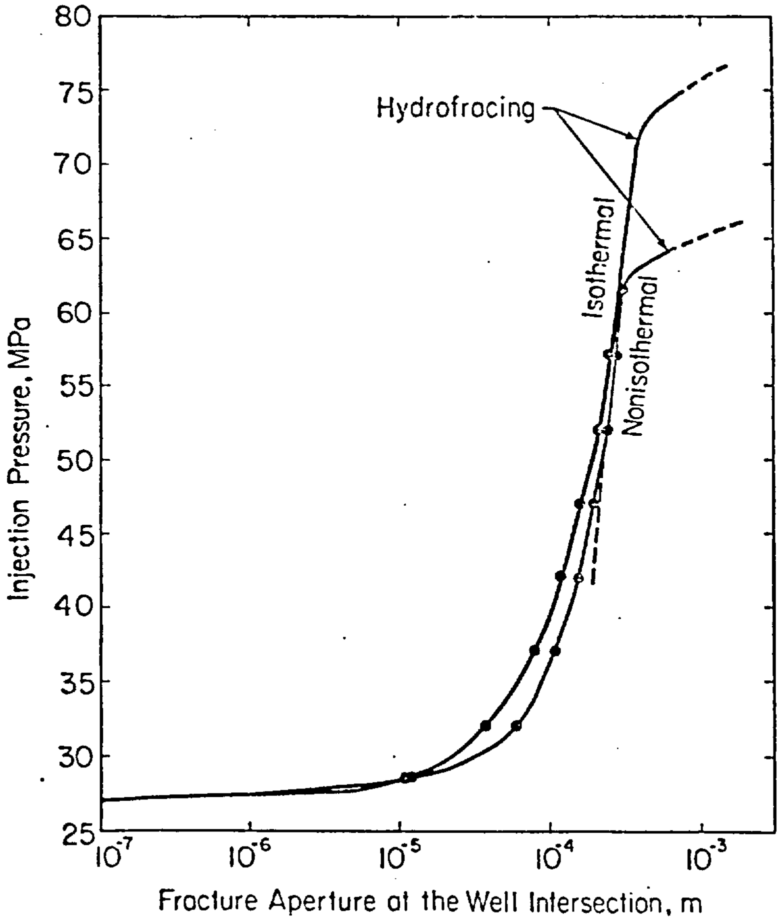

Figure 9. Variation of fracture aperture in response to pressurization.

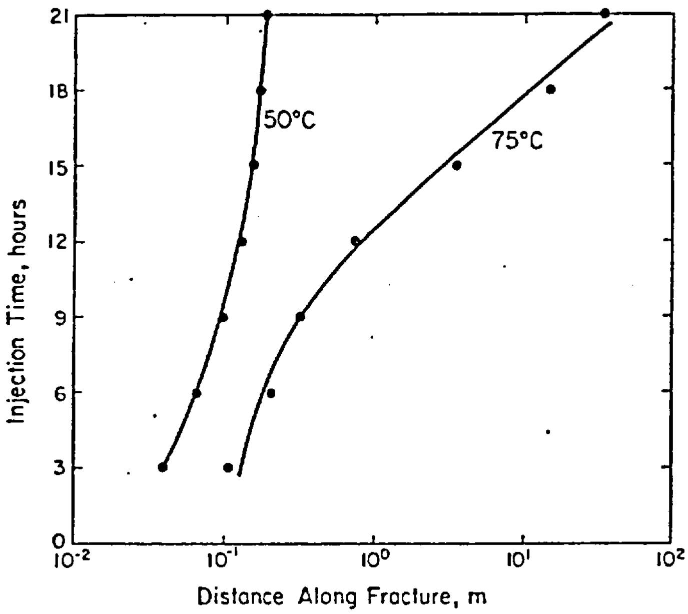

Figure 10. Thermal front advancement in the fracture.

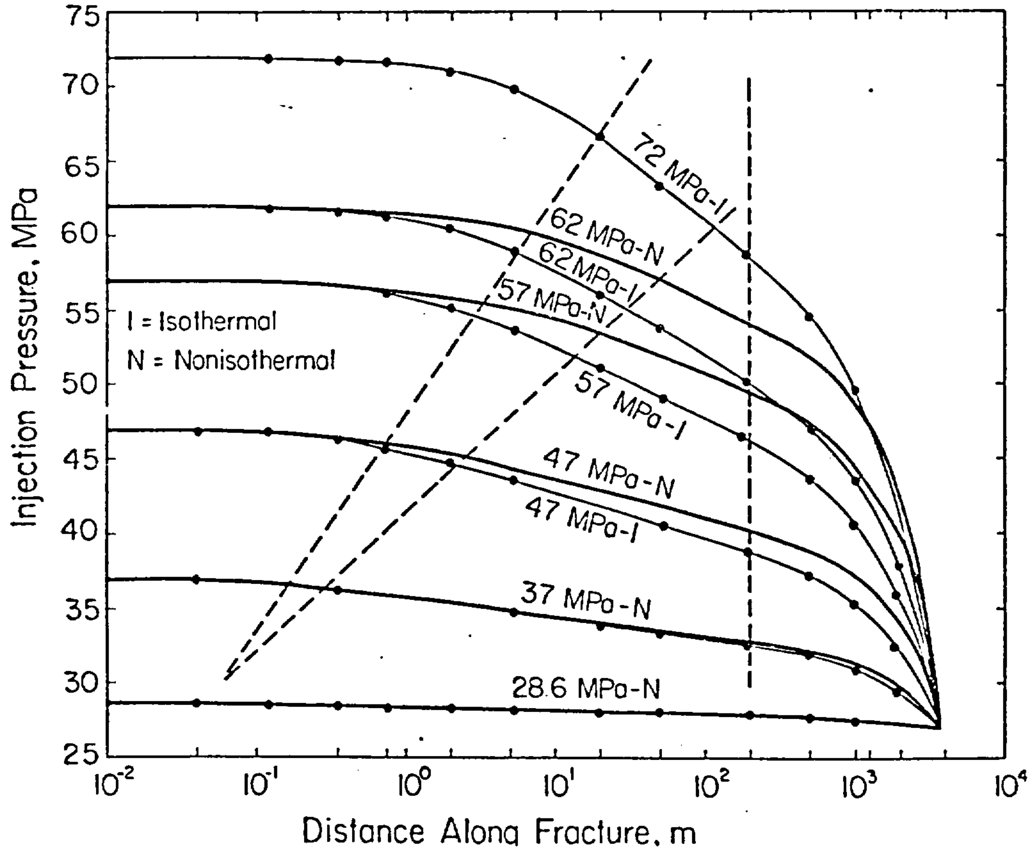

Figure 11. Pressure profile in the fracture for isothermal and nonisothermal injection episodes.

area, is simulated by assigning a very low value of Young's modulus to the elements. Before the heater raises the temperature of a large volume of rock, the flow from the hydrostatic outer boundary to the atmospheric ("zero" hydraulic pressure) borehole is high. Later in time, with the heated rock above the fracture expanding and the fracture aperture near the heater borehole closing, the flow decreases sharply, as shown in Figure 13. The evolution of the fracture aperture profile, together with the variations of the pressure and temperature distributions, are shown in Figure 14. As may be seen in the pressure-distance graph of this figure, before the tapping of the fracture at 0-day, full hydrostatic pressure prevails in the fracture. This pressure diminishes rapidly at 0.25-day before a major development of the thermal front. However, as thermal stresses are established, the fracture starts closing. As a result the pressure inside the fracture starts rising, thus leading to the establishment of full pressure in the fracture at 14-day, similar to the situation at 0-day. These results may provide a better understanding of some of the observations made in the in situ heater experiments in the Stripa granite. The delayed responses of the extensometers in these experiments (Witherspoon et al., 1981) may be explained by the closing of the fracture. Similarly, gradual stoppage of the water inflow into the heater borehole (Nelson et al., 1981) can be explained by the same phenomena.

The above example indicates a case ("one-way coupling," Table I) where thermo-hydro-mechanical changes take place in the field near a heat source. Such changes are hard to calculate if one considers the three phenomena T, H, M independently.

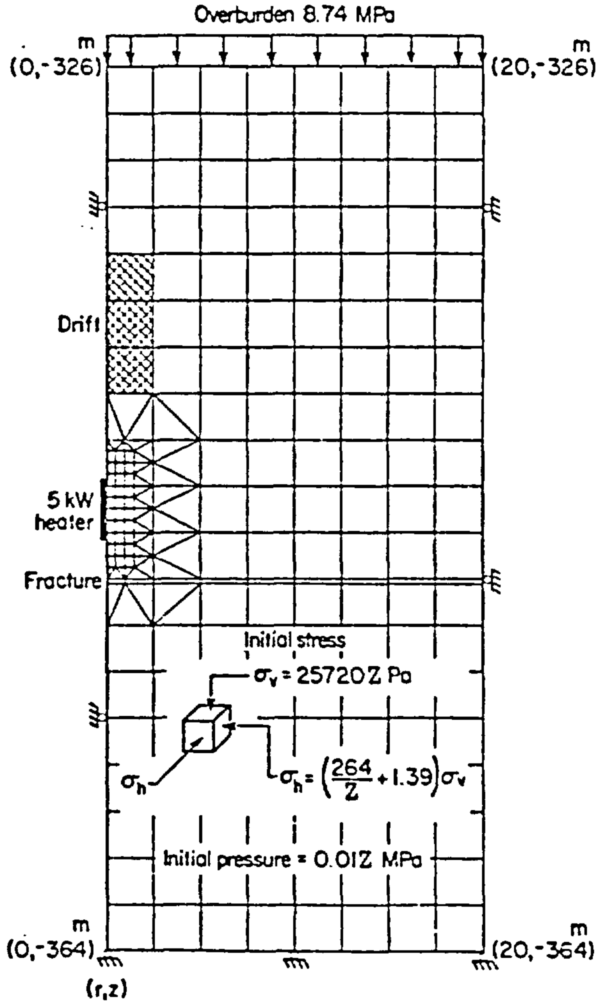

XBL 8210-4847

Figure 12. Finite-element model of an heat source environment.

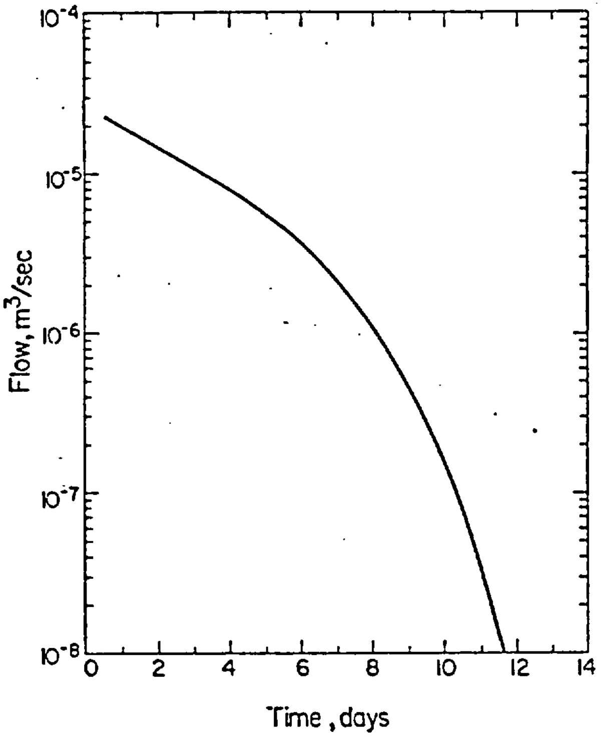

Figure 13. Variation of fluid inflow to the heater borehole as a function of time.

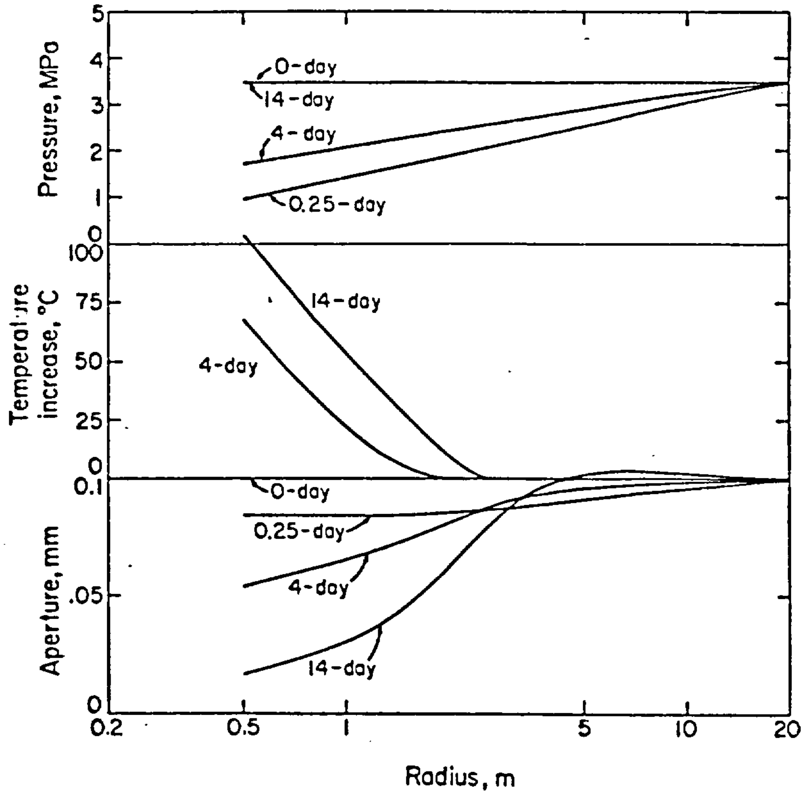

Figure 14. Pressure and aperture profiles in the fracture for various durations and temperature profiles along the heater midplane.

CONCLUDING COMMENTS

The performance assessment of a nuclear waste geologic repository requires a capability to make predictions of transport of low concentrations of radionuclides in the geologic formation for thousands of years. This represents a major challenge. The consideration of coupled processes provides a convenient framework to survey and address major elements that need to be evaluated or modelled in order to perform a proper safety assessment. Such a consideration has opened up new areas of research, such as combined effects of heat transfer, fluid pressure and mechanical stress-displacements in fractured rock masses. Chemical dissolution and precipitation accompanied with temperature gradients and steam-water flows are also new areas of research currently underway.

The present paper attempts to introduce the coupled processes framework, to describe four examples of specific coupled processes in fractured media and to provide references for further study.

ACKNOWLEDGEMENTS

This work was supported through U.S. Department of Energy Contract No. DE-AC03-76SF00098 by the Assistant Secretary for Energy Research, Office of Basic Energy Sciences. Part of the results presented in this paper are also based on work performed under the sponsorship of the U.S. Department of Energy, Office of Civilian Radioactive Waste Management and the U.S. Nuclear Regulatory Commission, Office of Nuclear Regulatory Research..

REFERENCES

Abelin, H., Neretnieks, I., Tunbrant, S., and Moreno, L. (1985), Final Report on the Migration in a Single Fracture, Experimental Results and Evaluation, SKB Technical Report 85-03.

Bourke, P. J., Dunance, E. M., and Heath, M. J., and Hodgkinson, D. P. (1985), Fracture Hydrology Relevant to Radionuclide Transport, AERE Harwell Report R11414, United Kingdom.

Lamb, H. (1932), *Hydrodynamics*, Cambridge University Press, New York, 6th Edition, pp. 583.

LBL (1984), Panel Report on Coupled Thermo-Mechanical-Hydro-Chemical Processes Associated with a Nuclear Waste Repository, Tsang, C. F., and Mangold, D. C., (ed.), Lawrence Berkeley Laboratory report LBL-18250.

LBL (1985), Proceedings of the International Symposium on Coupled Processes Affecting the Performance of a Nuclear Waste Repository, Berkeley, California, September 18-20, 1985, Lawrence Berkeley Laboratory report LBL-21850.

Moreno, L., Neretnieks, I., and Eriksen, T. (1985), Analysis of Some Laboratory Tracers Runs in Natural Fissures, *Water Resour. Res.*, Vol. 21, No. 7, pp. 951-958.

Nelson, P. H., Rachiele R., and Remer, J. S. (1981), Water Inflow into Borehole during Stripa Heater Experiments, Lawrence Berkeley Laboratory report LBL-12574, Berkeley, California.

Neretnieks, I. (1985), Transport in Fractured Rocks, Proceedings, 17th International Congress of International Association of Hydrologists, Tuscon, Arizona, Vol. XVII, pp. 301-318.

Noorishad, J., and Tsang, C. F. (1987), Thermal-Hydraulic-Mechanical Behavior of Fractured Rocks Around a Cylindrical Cavity, in *Coupled Thermomechanical-Hydrochemical Processes Associated with a Nuclear Waste Geologic Repository*, Academic Press, Orlando, Florida, to be published.

Noorishad, J., Tsang, C. F., and Witherspoon, P. A. (1984), Coupled Thermal-Hydraulic-Mechanical Phenomena in Saturated Fractured Porous Rocks: Numerical Approach, *J. Geophys. Res.*, Vol. 89, No. B12, pp. 10365-10373.

Nowacki, W. (1962), *Thermoelasticity*, Pergamon Press, New York.

Pruess, K., Tsang, Y. W., and Wang, J. S. Y. (1985), Modeling of Strongly Heat Driven Flow In Partially Saturated Fractured Porous Media, Proceedings, 17th International Congress of International Association of Hydrologists, Tuscon, Arizona, Vol. XVII, pp. 486-497.

Pyrak, L., Myer, L. R., and Cooke, N. G. W. (1985), Determination of Fracture Void Geometry and Contact Area at Different Effective Stress, *American Geophysical Union Transactions*, Vol. 66, No. 903.

Stephens, G., and Voight, B. (1982), Hydraulic Fracturing Theory for Conditions of Thermal Stress, *Int. J. Rock Mech. and Geomech.*, Abstract, Vol. 19, pp. 279-284.

Tsang, C. F. (ed.) (1987), *Coupled Thermomechanical-Hydrochemical Processes Associated with a Nuclear Waste Geologic Repository*, Academic Press, Orlando, Florida, to be published.

Tsang, C. F. (1985), Mass Transport in Low Permeability Rocks Under the Influence of Coupled Thermomechanical and Hydrochemical Effects - An Overview, Invited paper, 17th International Congress of the International Association of Hydrogeologists, Tucson, Arizona, January 7-12, 1985.

Tsang, C. F. (1980), A Review of the State-of-the-Art of Thermomechanical-Hydrochemical Modeling of a Hardrock Waste Repository, Proceedings, Workshop on Thermomechanical-Hydrochemical Modeling for a Hardrock Waste Repository, Berkeley, California, July 29-31, 1980; ONWI-164, LBL-11204.

Tsang, C. F., Noorishad, J., and Wang, J. S. Y. (1982), A Study of Coupled Thermomechanical, Thermohydrological, and Hydromechanical Processes Associated with a Nuclear Waste Repository in a Fractured Rock Medium, Proceedings, 1982 Annual Meeting of the Materials Research Society, Boston, Massachusetts, November 1-4, 1982, pp. 515-523.

Tsang, Y. W. (1984), The Effect of Tortuosity on Fluid Flow through a Single Fracture, *Water Resour. Res.*, Vol. 20, No. 9, pp. 1209-1215.

Tsang, Y. W., and Pruess, K. (1986), A Study of Thermally Induced Convection Near a High-Level Nuclear Waste Repository in Partially Saturated Fractured Tuff, Lawrence Berkeley Laboratory report LBL-21311, submitted to *Water Resour. Res.*

Tsang, Y. W., and Tsang, C. F. (1986), Channel Model of Flow Through Fractured Media, *Water Resour. Res.*, in press.

Tsang, Y. W., and Witherspoon, P. A. (1981), Hydromechanical Behavior of a Deformable Rock Fracture Subject to Normal Stress, *J. Geophys. Res.*, Vol. 86, No. B10, pp. 9287-9298.

Tsang, Y. W., and Witherspoon, P. A. (1983), The Dependence of Fracture Mechanical and Fluid Properties on Fracture Roughness and Sample Size, *J. Geophys. Res.*, Vol. 88, No. B3, pp. 2359-2366.

Wang, J. S. Y., and Tsang, C. F. (1980), Buoyancy Flow in Fractures Intersecting a Nuclear Waste Repository, in *Heat Transfer in Nuclear Waste Disposal*, Vol. HTD-II, American Society of Mechanical Engineers, pp. 105-112.

Wang, J. S. Y., Tsang, C. F., Cook, N. G. W., and Witherspoon, P. A. (1980), Long-Term Thermohydrologic Behavior of Nuclear Waste Repositories, in *Predictive Geology*, G. de Marsily and D. F. Merrian, editors, Pergamon Press, Oxford, United Kingdom.

Wang, J. S. Y., Tsang, C. F., Cook, N. G. W., and Witherspoon, P. A. (1979), A Study of Regional Temperature and Thermohydrological Effects of an Underground Repository for Nuclear Wastes in Hard Rock, *J. of Geophy. Res.*, Vol. 86, No. B5, pp. 3759-3770.

Witherspoon, P. A., Cook, N. G. W., and Gale, J. E. (1981), Geologic Storage of Radioactive Waste, Field Studies in Sweden, *Science*, Vol. 211, pp. 894-900.

Witherspoon, P. A., Wang, J. S. Y., and Iwai, K., and Gale, J. E. (1980), Validity of Cubic Law for Fluid Flow in a Deformable Rock Fracture, *Water Resour. Res.*, Vol. 16, No. 6, pp. 1016-1024.

Hydrogeological Modelling in High Level Radioactive Waste Disposal

Dr. Devraj Sharma

Principia Mathematica Inc.
110 Beaver Brook Drive
Evergreen, Colorado 80439
U. S. A.

The primary object of this paper is to present salient features of a mathematical model designed to predict fluid motions, and concomitant transport of heat ans mass, within variably-saturated porous media. Important features of modelling, which are often obscured in the literature, are discussed. Their relevance to the disposal of high level radioactive waste in underground repositories is also discussed. Special importance is given in this paper to mathematical formulation of problems and to the design of numerical solution algorithms.

1.0 INTRODUCTION

The primary purpose of this paper is to focus the reader's attention on features of formulation, mathematical representation and numerical solution of problems which involve fluid motions in porous media. Features associated with the transport of heat, and of mass, as a result of such motions are also presented. Descriptions are provided with special reference to hydrogeological problems concerning repositories for high level nuclear waste (HLW). Despite the attention this subject has received in recent years, and the burgeoning number of publications which purport to describe 'complete' prediction procedures or models, several important features remain curiously obscure. It is the author's intention in this paper to bring such features to the limelight.

The contents of this paper necessarily cover the mechanisms of fluid flow in porous media and the concomitant transport of mass, of dissolved chemical species, and of thermal energy. The latter are introduced, wherever appropriate, to demonstrate the inextricable linkage between the mechanisms. That such linkages require careful attention, in each of the problem features referred to above, is emphasized in this paper. The importance of unifications in mathematical representations, terminology and symbolism used, in devising of numerical solution algorithms and in computer program development are discussed. It is not the purpose of this paper to distract attention with long drawn out discussions of the limitations imposed by simplifications adopted in problem representations. Neither do approximations which may be made in imposing boundary conditions or in comparisons of a particular numerical method employed with others reported in the literature to solve ostensibly similar problems receive attention.

Last, but by no means least, the reader's attention is drawn to the implications of the computing system employed on the numerical solution algorithms adopted to solve fluid dynamical problems. Such implications and their relationship to computing coding practices are described.

2.0 MECHANISMS CONSIDERED

The mechanisms considered in this paper are: dynamics of fluid flows in variably saturated porous media; and, the concomitant transport of mass and heat. The media considered are heterogeneous and anisotropic rock which do not contain large amounts of dissolvable material; hence salt formations are excluded from consideration here, although application or the technique is reported elsewhere (Sharma et al., 1980). Within the media considered, a variety of man-made features associated with a host of possible repository designs may be present. Although the host medium will, in general, be variably saturated with water and contain complex fracture systems. The latter are also excluded from explicit consideration in this paper. Such features have received increasing attention in recent years (see for example, Huyakorn et al., 1983); in fact, elaborate treatment of such features are expected to be presented at the same workshop where this paper will be presented. The transport of mass and heat may be the result of either natural or man-made events; thus, water entry accidents into a HLW repository which cause the transport of radionuclides into the geosphere receive the same attention as thermal recirculatory motions of ground water due to temperature changes brought about by thermal energy releases from the repository. All such mechanisms are linked, and, under certain circumstances the linkage involves mathematical coupling; a feature which receives special attention in this paper.

The mechanisms of fluid motions, and those associated transport of mass and heat, which may be associated with a HLW repository necessarily occupy three dimensional space, and are strong functions of time. It is therefore quite important to represent such mechanisms, in scale and in magnitude, in adequate mathematical fashion. The test of adequacy is naturally associated with the particular solution algorithm devised to solve the representation, its verification and calibration to site conditions. These topics receive attention in the following sections.

3.0 MATHEMATICAL REPRESENTATIONS

In the following discussions, problem dimensionality will not be invoked as a restrictive assumption. Three dimensional space is considered and, in order to avoid distractions, a cartesian coordinate system is adopted with tensor notation for illustrative purposes. Within this framework, mathematical representations of the problem consist of applying four conservation principles. These are: conservation of fluid mass; conservation of fluid momentum; conservation of fluid thermal energy; and conservation of mass of conserved chemical species dissolved in the fluid.

The emphasis on fluid mass and not, as convention would dictate, fluid volume is deliberate; the implication is that variations in fluid density, whatever the root causes, are important to consider. The principle of fluid mass conservation for a variably-saturated porous medium is represented in the general form noted below. This form includes man-made features as well as natural changes of fluid mass within an elemental control volume.

$$\frac{\partial}{\partial t}\left\{\rho n S_+\right\} + \frac{\partial}{\partial x_i}\left\{\rho n S_+ U_i\right\} = \dot{m}''' \quad . (1)$$

where the symbols employed are described in the nomenclature list. It is nonetheless important to note that ρ denotes variable fluid density, n the porosity of the host medium, S_+ the local degree of saturation of this medium with the fluid considered, U_i the local fluid particle velocity vector and $\dot{m}'''$ the man-made sources and/or sinks of mass. The changes to fluid mass within a control volume encompassing the variably saturated porous medium thus may be wrought by changes to fluid density, to porosity and to the state of saturation. It is the changes to fluid density which, under the guise of the so-called Boussinesq approximation, is often neglected. Furthermore, account of changes to the degree of saturation is fraught with difficulties in obtaining solutions and requires special attention. Finally, account of man-made influences should consider the features of repository design such as shafts, galleries, methods devised for isolation sections of the repository, progressive character of repository construction, etc. Since most such features violate primary assumptions concerning the behaviour of fluids within porous media, special attention is necessary to accommodate them. In such cases, fluid inertia or momentum forces, and consequently, fluid turbulence may no longer be ignored.

A generalized form of the Darcy formulation made be adequately adopted to represent, in abbreviated form, the changes to fluid motions within the variably saturated porous medium. Much discussion is made in recent literature of the adequacy of such a representation; little satisfactory evidence is reported to rationally justify departures from it. For purposes of applications to problems associated with HLW repositories, the following representation is adopted:

$$\rho n S_+ U_i = -\rho K_+ \frac{k_{ij}}{\mu}\left\{\frac{\partial b}{\partial x_j} + \frac{\partial z_g}{\partial x_j}\rho g\right\} \quad , (2)$$

where the additional parameters introduced are: K_r which denotes relative permeability, k_{ij} the intrinsic permeability of the formation, μ the fluid viscosity, p the static pressure of the fluid, g the local acceleration due to gravitational forces and z_g the true direction of gravitational acceleration. The composite Darcy velocity is the product of the three variables on the left hand side of equation (2); this will be referred to as the generalized Darcy velocity.

It should be noted at this stage that equation (2) may be considered to be an abbreviation of the general principle of fluid momentum conservation. Such a principle, i.e. the set of Navier Stokes equations representing turbulent fluid motions, needs to be invoked when fluid motions within shafts, galleries and chambers of a HLW repository are to be represented. Just such a principle may be implemented by noting that the following algebraic adjustment may be simply made in such cases:

$$\rho U_i = \{\rho U_i\}^* - \rho \bar{K}_{ij} \left\{ \frac{\partial p}{\partial x_j} + \frac{\partial z_g}{\partial x_j} \rho g \right\} \quad ,(2a)$$

where the terms possessing an asterisk superscript denote inertial and diffusive influences of fluid momentum. Such implementations have been successfully applied in a number of cases (Sharma et al., 1978).

The combination of equations (1) and (2), or (2a), gives rise to the so-called fluid pressure equation; it is convenient to express this equation in terms of three normalized parameter groups. The convenience stems both from conceptual understanding of the coupling mechanisms as well as improvements to computational efficiency. The normalized groups are defined as follows. First of all, fluid pressure head is defined as:

$$\psi \equiv \frac{p}{\rho_0 g} \quad . (3)$$

Next, dimensionless forms of fluid viscosity and density, i.e. specific gravity, are defined as:

$$M \equiv \frac{\mu_0}{\mu} \quad ,(4a)$$

$$R \equiv \frac{\rho}{\rho_0} \qquad .(4b)$$

In the definitions presented above, fluid property variables employed with a subscript "o" denote values evaluated at a reference, i.e. known, thermodynamic state. It may be recognized even at this stage that significant computational advantages accrue from the use of dimensionless variables instead of their primitive forms. Such uses are considered part of the general concept of unification of the manner with which governing equations are expressed. In keeping with this same concept, the general definition of hydraulic conductivity is expressed in terms of the reference state fluid as:

$$K_{ij} \equiv \frac{k_{ij}\rho_0 g}{\mu_0} \qquad . (5)$$

Employing the above stated definitions in combining equations (1) and (2), or (2a), yields the so-called fluid pressure equation. First however, the time dependent term of equation (1) is recast (see Sharma, 1982) into a physically correct and computational efficient form thus:

$$\begin{aligned}\frac{\partial}{\partial t}\left\{\rho n S_+\right\} &= S_+\left\{n\frac{\partial\rho}{\partial p} + \rho\frac{\partial n}{\partial p}\right\}\frac{\partial p}{\partial t} \\ &\quad + \rho n\frac{\partial S_+}{\partial t} + nS_+\left\{\frac{\partial\rho}{\partial T}\frac{\partial T}{\partial t} + \cdots\right\}\end{aligned} \qquad , (6)$$

where, it may be observed that the dependence of fluid density upon other significant variables is taken into account. The first two terms may be grouped together in the conventional manner as follows:

$$S_+\left\{n\frac{\partial\rho}{\partial p} + \rho\frac{\partial n}{\partial p}\right\}\frac{\partial p}{\partial t} = S_+\left\{n\beta\rho + (1-n)\alpha\right\}\frac{\partial p}{\partial t} \qquad , (7)$$

with the additional definitions:

$$S_c \equiv \rho_0\left\{n\beta\rho + (1-n)\alpha\right\} \qquad , (8)$$

$$\alpha \equiv \frac{1}{1-n}\frac{\partial n}{\partial p}, \quad \beta \equiv \frac{1}{\rho}\frac{\partial\rho}{\partial p} \qquad . (9)$$

The third term represents the central cause of difficulties experienced in obtaining numerical solutions (see Sharma, 1981) and is, for the moment, left unaltered. The fourth term, which denotes the rate of change in fluid density with time, takes account of the dependence of density upon scalar properties such as temperature and concentration of dissolved chemical species. These terms constitute one component of linkage, and hence of mathematical coupling, between the equations of fluid motion and of scalar property transport in porous media.

The general form of the fluid pressure, or flow, equation is thence derived, after dividing throughout by reference fluid density, ρ_0, as:

$$R S_r S_c \frac{\partial \psi}{\partial t} = \frac{\partial}{\partial x_i}\left\{ R K_r K_{ij} M \left[\frac{\partial \psi}{\partial x_j} + R \frac{\partial z_g}{\partial x_j} \right] \right\}$$

$$+ \frac{\dot{m}'''}{\rho_0} - R n \frac{\partial S_r}{\partial t} - n S_r \left\{ \frac{\partial R}{\partial T} \frac{\partial T}{\partial t} + \cdots \right\} \qquad .(10)$$

Note that the general definitions presented previously have been employed in this derivation and that two of the time dependent terms have been grouped into the right hand side of equation (10). Furthermore, explicit algebraic relationships must be found to represent relative saturation and relative permeability as functions of fluid pressure. Such expressions have been reported elsewhere (Sharma et al., 1981) and are not repeated here. These actions are not merely accidents but the result of much research in obtaining physically plausible and accurate numerical solutions to the equation under strongly coupled conditions. Furthermore, simpler or more convenient forms of the governing equation may be obtained under the constraints of appropriate approximations.

The general form of the transport equation for thermal energy in variably saturated porous media may be expressed (see Sharma and Pralong, 1982 for details) as:

$$\frac{\partial}{\partial t}\left\{ R n S_r C_v T \right\} + \frac{\partial}{\partial x_i}\left\{ R n S_r U_i C_p T \right\} =$$

$$\frac{\partial}{\partial x_i}\left\{ n S_r K_{ij}^{T} \frac{\partial T}{\partial x_j} \right\} \quad + \quad \frac{\dot{m}'''}{\rho_0} \hat{C}_P \hat{T} \qquad ,(11)$$

where, additional variables such as specific heats and effective thermal conductivity have been introduced. The corresponding transport equation for concentration of dissolved chemical species "ℓ" is expressed (see Sharma, 1982) as:

$$\begin{aligned} &\frac{\partial}{\partial t}\left\{ R n S_r m_\ell \right\} + \frac{\partial}{\partial t}\left\{ R_S (1-n) m_{\ell,s} \right\} + \frac{\partial}{\partial x_i}\left\{ R n S_r U_i m_\ell \right\} \\ &= \quad \frac{\partial}{\partial x_i}\left\{ n S_r \bar{K}_{ij}^{m} \frac{\partial m_\ell}{\partial x_j} \right\} \quad + \quad \frac{\dot{m}'''}{\rho_0} \hat{m}_\ell \end{aligned} \qquad ,(12)$$

where, to complete the formulation for a liquid phase, the storage of such concentrations in the immobilized or solid phase is introduced. Note that each of the terms is expressed in mass rather than in volume units for it is the former which is conserved. Furthermore, the source/sink term is intended to represent both reactive contributions such as those caused by radioactive decay as well as man-made contributions. The concentration of the same chemical species in the immobilized phase is expressed through the general relation:

$$m_{\ell,s} \quad = \quad c_1 \quad + \quad c_2 \, m_\ell^{\,c_3} \qquad ,(13)$$

which in turn may be expressed according to particular convenience as any one of the linear, Fruendlich, Langmuir or other 'isotherms' (Sharma et al., 1981). Each such expression of equilibrium between phases, or time dependent expressions as in the case of kinetically controlled phase transformations of the chemical species, requires caution in the manner of its expression and hence of solution. For further discussions in this paper, the commonly employed linear isotherm will be presumed to be satisfactory. Finally, the effective dispersion coefficient introduced in equation (12) is expressed, according to convention (Bear, 1979), as:

$$K_{ij}^{m} \quad = \quad \alpha_T \, |U| \, \delta_{ij} \quad + \quad (\alpha_L - \alpha_T) \frac{U_i U_j}{|U|} \qquad .(14)$$

The object of a numerical solution algorithm is thus to seek efficient and accurate solutions to the primary equations (10), (11), (12) and (13) under appropriate initial and boundary conditions. Before proceeding to describe just such an algorithm, the important features of present mathematical representations are summarized as follows.

(a) Mass, rather volume, conservation principles have been employed. This implies that the significant influences of fluid density changes have been correctly represented.

(b) Fluid density changes resulting from temperature and concentration variations are accounted for in the fluid flow equation. Such account is referred to as mathematical coupling and requires simultaneous knowledge of the thermodynamic state of the fluid, i.e. the values of fluid temperature and chemical species concentrations within it.

(c) Rate of changes to fluid density, and state of saturation, with time are expressed in an unconventional manner by direct transposition to the right hand side as unknown terms to be evaluated iteratively. In order to evaluate such expressions, additional relationships connecting fluid density to temperature and concentrations as well as degree of saturation to fluid pressure are required.

(d) The nomenclature and representation of the governing equations of flow and scalar property transport are unified. Advantage is taken of the essential similarity between mechanisms to obtain similar expressions. Such similarity in expression possesses advantages both in deriving the numerical solution algorithm and in operational efficiency of the computer program which embodies it.

(e) In order to derive the discretized forms of the governing equations in a manner which is suitable for efficient solution, the equations are subjected to a transformation. In this transformation, each dependent variable is expressed as being composed of a 'guessed' or estimated value and a 'correction' value, thus:

$$\phi = \phi^{*} + \phi' \quad .(15)$$

Substituting this expression into the appropriate governing equations permits them to be cast into the so-called residual forms. It is such forms which are actually solved by the computational algorithm; a feature which in itself possesses several advantages.

4.0 NUMERICAL SOLUTION ALGORITHM

The purpose of this section is to identify significant features of the numerical solution algorithm devised to obtained the above referenced solutions. This algorithm has been reported elsewhere (see Sharma et al., 1981; Sharma, 1981; Sharma and Pralong, 1982; Sharma, 1982; etc.) and hence only salient features are summarized here.

(a) The numerical solution algorithm is of the implicit integrated finite difference (IFD) variety. Cartesian coordinate systems are generally employed and the numerical grid cells are rectangular but irregularly sized. All variables, with the exceptions of flow velocity components and effective dispersion coefficients, are presumed to be located at grid nodes identified at the geometric centers of grid cells. The exceptional variables are located at corresponding grid cell faces which will not, in general, lie midway between adjacent grid nodes.

(b) The use of rectangular grid cells is not as restrictive as confusingly referred to in the literature. The loss of flexibility is usage of non-rectangular grid cells in order to represent irregular geometric features of a problem, are more than compensated for by increases in computational efficiency. Such increases are contributed to by a number of features of the numerical algorithm.

(c) The discretized form of each governing differential equation is derived by integrating it over each grid cell which serves as the control volume for applying conservation principles. In conducting the integration, the assumption is made that variables progress linearly between adjacent grid nodes. Important exceptions to this rule are made in respect of: hydraulic conductivity; degree of saturation; and, fluid velocity components. Such exceptions do have quite important consequences, for, seemingly trivial adjustments can make all the difference between an otherwise unworkable algorithm and its efficient counterpart. Every term of each equation thus has to be expressed in a unique way which preserves its special differential character and yet interacts consistently with other terms.

(d) Each set of discretized equations is considered to be manifestation of the appropriate conservation principle in discrete form. This feature is often overlooked by otherwise 'elegant' algorithms. The methods of solving the discretized set of equations must hence preserve this principle throughout its application. This is also a feature which is sometimes ignored. A number of alternative methods are implemented into the algorithm for solving discretized equation sets; they range from point-by-point techniques such as Gauss-Seidel elimination to slab-wise simultaneous techniques. Their application is dependent upon the type of dependent variable and the type of boundary conditions which require to be accounted for.

(e) The sequence of numerical operations in the algorithm plays an important role in obtaining convergent solutions. This is especially true of mathematically coupled problems wherein fluid density, for example, links the flow equation with that of thermal energy transport. In natural convection dominated systems, it has been found to be of vital importance that discrete forms of the flow and thermal energy transport equations are solved simultaneously for each grid cell. It is only in this way that satisfaction of the conservation principle can be rigorously ensured.

(f) Nonlinear features of problems associated with HLW repositories such as fluid motions within open spaces rather than porous media, flows which are strongly dependent upon natural convection forces arising from density differences, etc. are all accounted for in an efficient manner.

Important facets of the numerical algorithm will be presented and discussed at the workshop.

5.0 COMPUTER SYSTEM USE

The use of computational procedures to solve hydrogeological problems associated with HLW repositories involves the coding of numerical solution algorithms and the running of computer programs, together with site specific data, on computing systems. Both these features receive relatively little attention in the reported literature; perhaps they are considered to be comparatively minor importance. It has been the author's experience however, that they play an important role in the efficiency and accuracy with which reliable solutions are obtained. The following points summarize the important features of computing system use.

(a) A variety of computing systems, ranging from powerful main frame computers such as the CRAY-XMP2 to microcomputers such as the IBM PC/AT, are being used to solve hydrogeological problems connected with HLW repositories. Each possesses different numerical truncation, numerical roundoff, disk storage space and disk access speed, main memory allocation per user, and arithmetic operations characteristics. It is often important to recognize such characteristics and take them into account when devising the numerical solution algorithm as well as the computer program structure and coding practices.

(b) In analyzing problems which involve large variations in material properties such as hydraulic conductivities, great care is needed in preserving consistency of fluid mass fluxes and in minimizing the effects of roundoff errors. Those sub-regions which are associated with large values of hydraulic conductivities will, in general, respond with small gradients in fluid pressure heads. If care is not taken, such gradients can often be masked by the buildup of roundoff errors during iterative solutions. Performing large numbers of iterative computations in such cases does not yield better solutions! The "guess-and-correct" numerical algorithm described previously is one efficient way to overcome such difficulties whatever the type of computer being employed. It does so by requiring that, any any given step in an iterative process, only those numbers of significant digits which are required to be preserved are indeed retained.

(c) Judicious choices of model domain sizes, numerical grid cell sizes and shapes as well as sizes of time steps to suit the features of a given problem remain important assets in obtaining reliable solutions. With the exception of current generation of microcomputers, most computers nowadays permit extraordinarily large numbers of grid cells to be employed in representing hydrogeological problems. For instance, a single 32-bit computer workstation such as the Apollo Domain 3000 can permit the user to employ as many as 100,000 grid cells to represent a three-dimensional near field hydrogeological problem in HLW repository performance evaluation. With such facilities becoming accessible to many, a new look has to be taken at the nature of computational difficulties which used to be faced in their absence. Certain issues such as numerical dispersion difficulties can now be simply resolved.

(d) Much, by way of efficiency and accuracy, can be gained by paying close attention to computer coding practices and especially those practices which are designed to take advantage of the special characteristics of the particular computer intended to be employed. The use of double precision arithmetic for specific numerical operations, the use of structured programming, modifications to algebra in order to suit array processing machines, etc. are all examples.

6.0 REFERENCES

Bear, J. (1979)
"Hydraulics of Groundwater"

McGraw-Hill Publ. Co.

Huyakorn, P.S., B.H. Lester and C.R. Faust (1983)
"Finite Element Techniques for Modeling Groundwater Flow in Fractured Aquifers"
Water Res. Research J., 19, (4), pp 1019-1035.

Sharma, D. (1981)
"Applications of an Efficient Computational Procedure for the Prediction of Momentum, Heat and Mass Transfers in Variably Saturated Porous Media"
Invited Pap., AGU Semi-Centennial Session: Impact of the Richard's Equation, San Francisco, California, Dec. 17-21.

Sharma, D. (1982)
"Fluid Dynamics and Mass Transfer in Variably Saturated Porous Media: Formulation and Application of a Mathematical Model"
Invited Pap., Symp. on Unsat. Flow and Mass Transport, Battelle-NRC, Seattle, Washington, Mar. 23-24.

Sharma, D., R.J. Hopkirk and P-J. Pralong (1978)
"Practical Developments in the Modelling of Turbulent Heat and Mass Transfer"
Int. Conf. on Num. Methods in Laminar & Turbulent Flow, Swansea, Wales, Jul. 18-21.

Sharma, D., R.J. Hopkirk and P-J. Pralong (1980)
"Nuclear Waste Storage in Excavated Cavities Within Salt Domes: Postulated Problems and Theoretical Analyses"
Pres. Fall Meeting, Solution Mining Research Institute, Minneapolis, Minnesota, October 13-14.

Sharma, D., J.L. Moreno and M.I. Asgian (1981)
"A Novel Computational Procedure for the Prediction of Momentum, Heat and Mass Transfers in Variably Saturated Porous Media"

Pres. Joint ASME/ASCE Mechanics Conference, Boulder, Colorado, Jun. 22-24.

Sharma, D. and P-J. Pralong (1982)
"Transient Freezing and Thawing Around Buried Pipelines"
Int. Symp. on Numerical Methods in Geomechanics, Zurich, Switzerland, Sep. 13-17.

7.0 NOMRNCLATURE LIST

C_V, C_P	Specific heats at constant volume and constant pressure.
C_1, C_2, C_3	Coefficients in the immobilization relationship.
k_{ij}	Tensorial form of intrinsic permeability.
K_{ij}	Tensorial form of hydraulic conductivity.
K^T_{ij}	Tensorial form of effective thermal conductivity.
K^m_{ij}	Tensorial form of the effecive dispersion coefficient.
K_r	Relative permeability.
$\dot{m}'''$	Man-made sources and/or sinks of mass.
M	Viscosity Ratio.
n	Porosity.
p	Fluid static pressure.
R	Fluid density ratio, or specific gravity.
R_S	Soil density ratio, or specific gravity.
S_r	Degree of saturation.
t	Time.
T	Temperature.
U_i	Local particle velocity vector.
x_i	Cartesian coordinate direction
ψ	General fluid static pressure head.
ϕ	General dependent variable.
ρ	Fluid density.
ρ_0	Fluid density at a reference state.
μ	Fluid viscosity.
μ_0	Fluid viscosity at a reference state.

VERIFICATION AND VALIDATION OF GEOSPHERE ASSESSMENT MODELS. SUMMARY OF THE INTRACOIN AND HYDROCOIN STUDIES

Bertil Grundfelt*, Kjell Andersson**, Alf Larsson**

* KEMAKTA Consultants Co, Stockholm, Sweden
** Swedish Nuclear Power Inspectorate, Stockholm, Sweden

Abstract

In this paper two international studies managed by the Swedish Nuclear Power Inspectorate are summarised. The first study, INTRACOIN, which is now finalised, has dealt with the evaluation of radionuclide transport models. The second study, HYDROCOIN, is still running and addresses the issue of verifying and validating the models used for groundwater flow calculations. This summary comprises the major conclusions of the INTRACOIN study and the current status of the HYDROCOIN study.

1. BACKGROUND AND ORGANISATION

The performance assessment of geological repositories typically involves the evaluation of the groundwater flow, the calculation of radionuclide release from the repository (near-field), the modelling of radionuclide transport through the geosphere (far-field) and the assessment of ecological transfer and bioaccumulation of radionuclides including an estimation of the resulting radiation dose to man (Figure 1). In all these steps mathematical models play an important role.

As the Swedish waste management programme developed during the second half of the 1970:s the Swedish Nuclear Power Inspectorate (SKI) realised an increasing need to evaluate the models used in the performance assessment both with respect to the reliability of the numerical algorithms used and the validity of the conceptual models. After having investigated the interest among organisations in different countries the

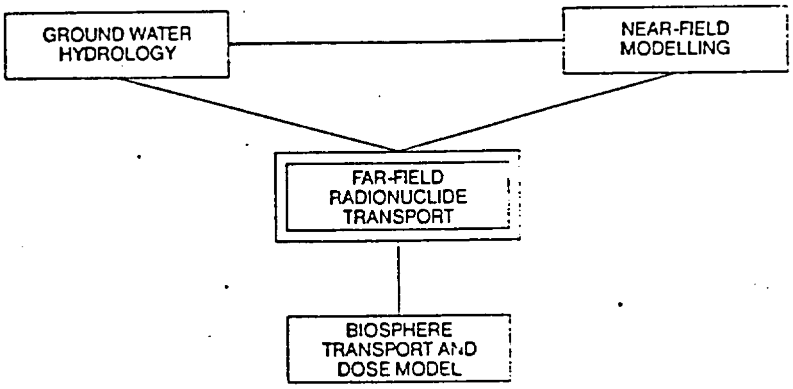
GROUND WATER HYDROLOGY
NEAR-FIELD MODELLING
FAR-FIELD RADIONUCLIDE TRANSPORT
BIOSPHERE TRANSPORT AND DOSE MODEL

Figure 1 Major modelling areas in performance assessment of repositories for radioactive waste.

INTRACOIN study (INTernational RAdionuclide transport COde INter-comparison) was initilised in 1981 with the participation of 11 organisations in eight countries (see Appendix 1). The project work of the INTRACOIN study was finalised in 1984 and has been published in two reports /1,2/.

In order to broaden the model evaluation to cover not only the far-field radionuclide transport but also the groundwater flow a second study, HYDROCOIN (HYDROlogical COde INtercomparison study), was initiated in 1984. This study is scheduled to be finalised during 1987. In HYDROCOIN, 13 organisations in 10 countries participate (see Appendix 2). In addition the Nuclear Energy Agency of the OECD and the Nordic Liaison Committee for Atomic Energy Matters participate in the project secreteriat.

Both projects have been organised in the same way (Figure 2). The study is set up by Parties. Each party has a representative in the Coordinating Group which takes the decisions necessary for the progress of the project. SKI acts as Managing Participant and appoints the chairman of the Coordinating Group.

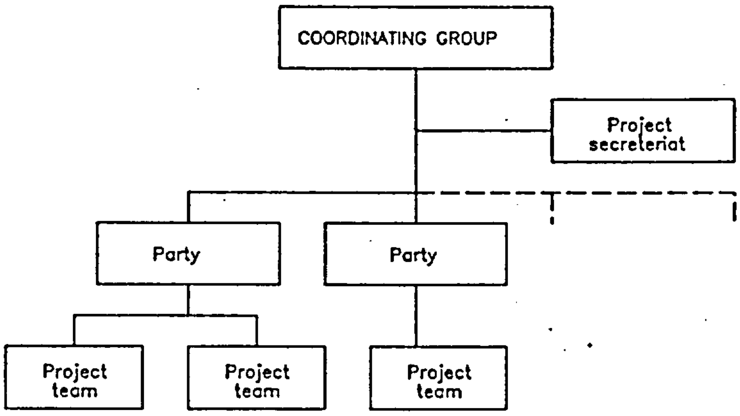

Figure 2 Project organisation used for INTRACOIN and HYDROCOIN.

Each party is responsible for the organisation of one or more Project Teams that carry out the calculations and other work within the project. A Project Secreteriat is set up to act as an executive body, e.g. for defining test cases, compiling results, preparing reports and carrying out all sorts of administrative work. KEMAKTA Consultants Co acts as Principal Investigator and is responsible for the technical work within the secreteriat.

The Parties cover the costs for their own participation including the work of their Project Teams. The Project Secreteriat is set up by SKI with some support from other organisations (see Appendices 1 and 2 for details). This organisation means that no money is transferred over the national borders. This has proven to greatly facilitate the set up and management of the studies.

2. TECHNICAL STRUCTURE

The technical structure has been the same for both INTRACOIN and HYDROCOIN. The studies have consisted of three parts, called levels, with the following principal objectives:

Level 1 Verification and benchmarking of computer codes.

Level 2 Study of the capabilities of mathematical models to describe experiments in order to partially validate the models.

Level 3 Sensitivity and uncertainty analysis.

At level 1 the numerical accuracy of the codes is tested by comparing numerical solutions with analytical solutions and by intercomparing numerical solutions of well defined test cases. The test cases have been selected on the basis that they should form adequate tests for the codes rather than being realistic scenarios for the radionuclide waste management problem. The number of test problems formulated for level 1 is seven for both INTRACOIN and HYDROCOIN. The results of INTRACOIN level 1 has been published /1/ whereas a final draft of the level 1 report for HYDROCOIN is currently being reviewed by the participants.

Level 2 addresses the difficult issue of model validation, i.e. building confidence that the model describes the reality reasonably well. In the studies presented in this paper this is done by selecting carefully designed and performed experiments out of the litterature and formulating test cases with the aim to simulate these experiments with models.

In INTRACOIN two experiments, one for a porous medium and one for a fractured medium were selected. In addition a hypothetical test case involving two media with different permeabilities and transport properties was defined /2/. Level 2 of the HYDROCOIN study is currently running and only preliminary results have been presented in workshops. Five test cases have been defined for level 2 of HYDROCOIN.

The design of level 3 is slightly different for the two studies. Level 3 of the INTRACOIN study was a rather limited exercise aiming at studying the sensitivity with respect to physical phenomena of a given scenario /2/. This was done by either including or excluding the different phenomena (dispersion, sorption, matrix diffusion, etc.) in the model. In the HYDROCOIN study level 3 is more oriented towards studying different methodologies for sensitivity and uncertainty analysis. This exercise is presently on going and preliminary results for the seven test cases defined have been presented in workshops.

3. SUMMARY OF INTRACOIN RESULTS

3.1 Verfication of codes for radionuclide transport

Level 1 of the INTRACOIN study comprised seven test cases designed to test the various types of models used for radionuclide transport in the context of repository performance assessment. The cases can briefly be described as:

1. One-dimensional advection-dispersion, constant migration parameters (ground water velocity, retention factors and dispersivity), and constant leach rate.
2. One-dimensional advection-dispersion in a layered medium (piece-wise constant migration parameters).
3. One-dimensional advection-dispersion with continously varying parameters.
4. Two-dimensional advection-dispersion with constant retention factors and dispersivity.
    a) Parallel flow field and radial dispersion
    b) Two-dimensional flow field and radial dispersion
5. One-dimensional advection-dispersion with diffusion into the rock matrix.
6. Two-dimensional advection-dispersion with matrix diffusion.
    a) Parallel flow field and radial dispersion
    b) Two-dimensional flow field and radial dispersion
7. One-dimensional advection-dispersion with linear mass transfer kinetics and constant migration parameters.

When the test cases were defined the boundary conditions to be used were only loosely stated. As a consequence much of the result evaluation in the final report /1/ was focused on the influence of boundary conditions. Figure 3 shows the maximum concentrations for one of the parameter variations of test case 1 (advection and dispersion along a 500 m long path with constant retardation factors) as calculated by different codes. The three frames of the figure corresponds to the three radionuclides in the decay chain ^{234}U - ^{230}Th - ^{226}Ra. It can be seen in the figure that the agreement for the parent nuclide of the decay chain is good between most of the codes when the same boundary condition is used. This is further illustrated in Figure 4 showing the outlet concentration versus time. The results in Figure 4 show four distinct bands representing different combinations of boundary conditions.

For the daughter nuclides there is some scatter in Figure 3 (within approximately a factor of 2). For some of the codes the scatter stems from an approximative treatment of the transport with chain decay (GETOUTO and NUTRAN) whereas for some of the codes the dispersive character of the test case (Peclet number is 10) has caused some difficulties to obtain a convergent solution. In particular this is so for the codes in which the dispersion is simulated by giving particles a velocity distribution using random numbers (NWFT/DVM, MMT1DPNL, MMTIVTT and DRAMA).

The relative magnitude of the advective and dispersive terms of the transport equation has an effect on the sensitivity of a bench-marking exercise like level 1 of the INTRACOIN study. As shown in Figure 5 the scatter of maximum concentrations is greater at lower Peclet numbers (high dispersion).

The character of the problem also has an impact on the solution algorithm to be chosen. Algorithms like Finite differences and Finite elements are well suited for problems with a high dispersion. For more advective problems, methods like Discrete Parcels or the Method of Characteristics can be more advantageous. Also many analytical solutions are better designed for advective cases since the highly dispersive situations often require numerical integretations.

The results of INTRACOIN level 1 show that there exist algorithms to solve the seven test cases in an adequate way. As mentioned above, a given algorithm may be better suited for some situations than for others. It is obvious from the level 1 results that when an algorithm is used outside the context for which it is best suited, the application needs a substantial amount of "finger tip feeling" to yield reliable results. In particular this seems to be true for discrete parcel-random walk algorithms when applied to predominantly dispersive problems.

Some of the test cases were not enough taxing for the codes to yield sensitive results. In future bench-marking studies care should be taken in the design of the test cases that they tax the codes in an appropriate way.

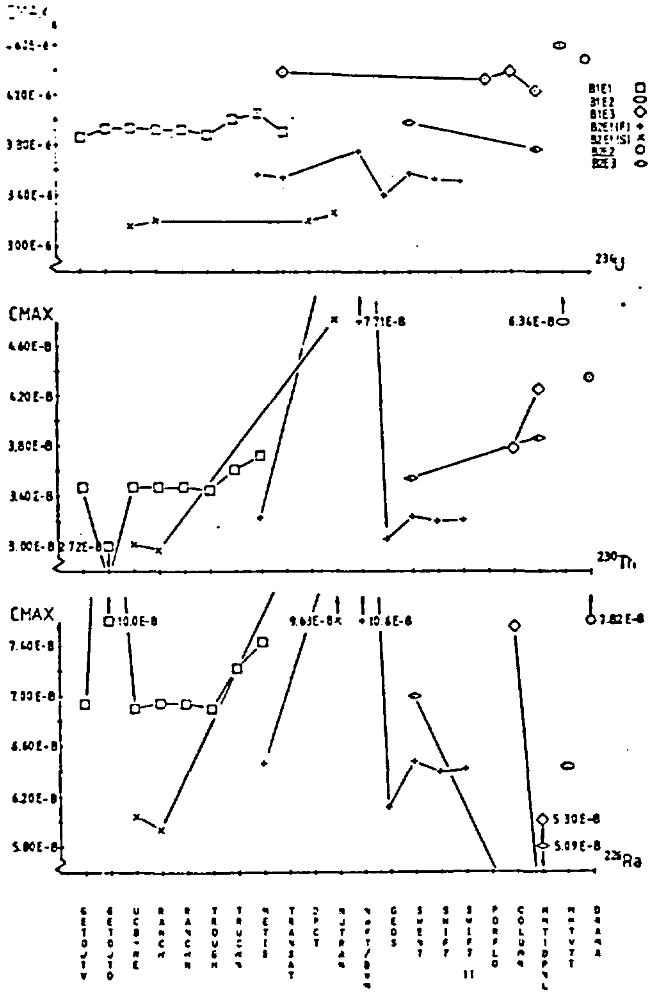

Figure 3 Maximum concentrations for ^{234}U (top), ^{230}Th (middle) and ^{226}Ra (bottom) at the outlet of the column in Case 1 of INTRACOIN level 1 as calculated with different computer codes. The results calculated with identical boundary conditions are connected with lines and use the same markers.

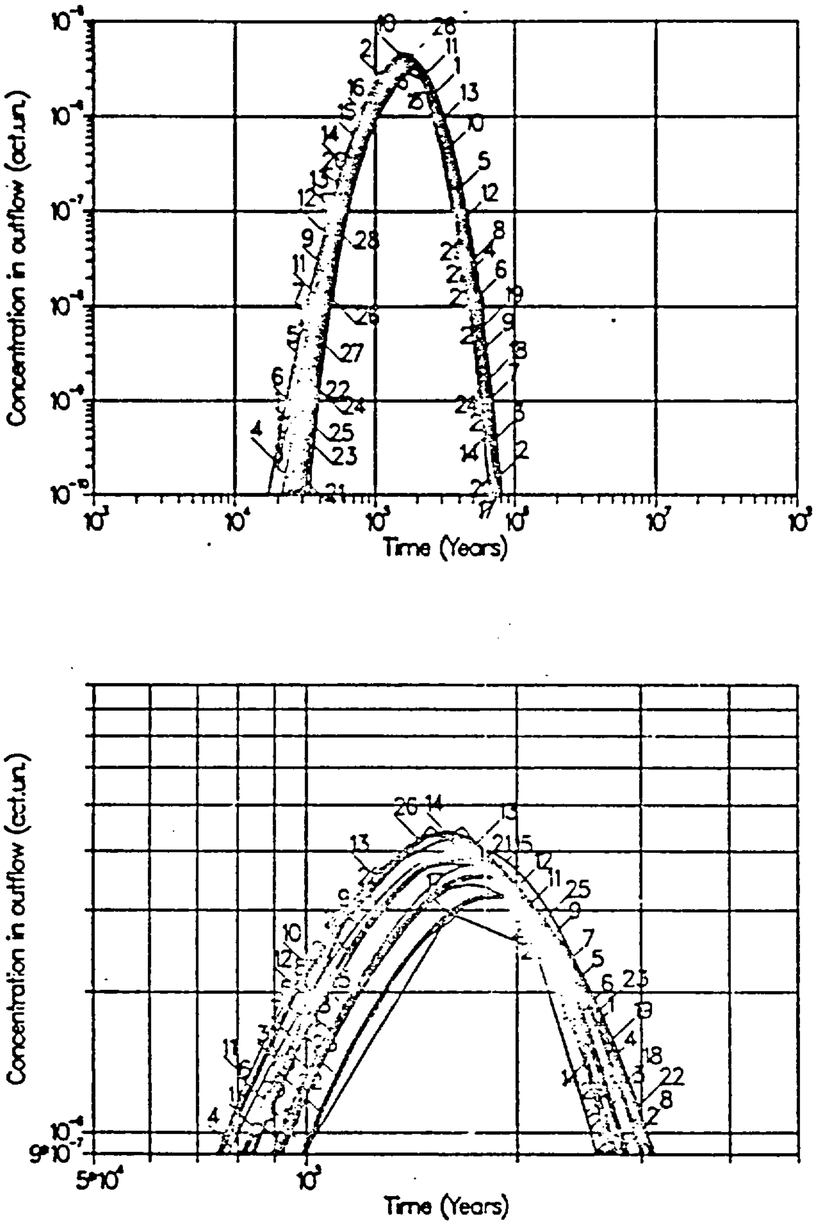

Figure 4 Concentration of ^{234}U versus time for Case 1 of INTRACOIN level 1. The bottom frame is a close-up of the region around the peak concentration.

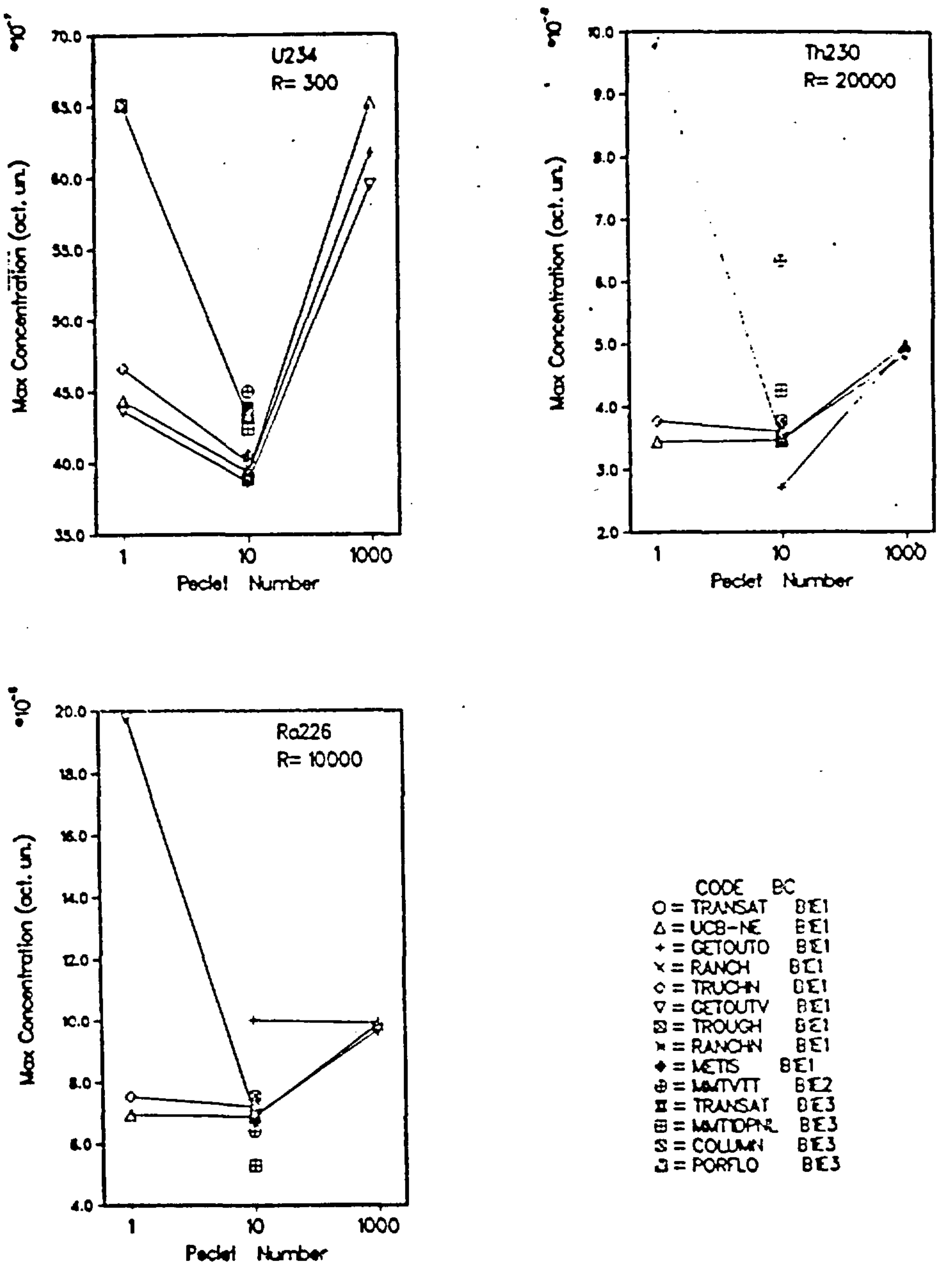

Figure 5 Maximum calculated concentrations versus the Peclet number for the decay chain $^{234}U-^{230}Th-^{226}Ra$ for Case 1 of INTRACOIN level 1.

3.2 Simulation of tracer tests in the field

Level 2 of the INTRACOIN study consisted of three test cases:

1. An idealised two-dimensional porous medium situation with a radionuclide source in a low permeable medium.
   This test case is purely theoretical and not based on experimental data.

2. A single well injection-withdrawal experiment in a shallow sandy aquifer in Canada using ^{131}I and ^{85}Sr as tracers /3/. The Project Teams were asked to simulate breakthrough curves for ^{85}Sr at several locations using the ^{131}I - breakthrough curves to characterise the hydraulics and K_d-values for Sr measured on sediment cores in the laboratory. Figure 6 gives an impression of the scale of the field experiment (approximately two metres radially).

3. A dual well tracer experiment performed in a granitic bedrock in Sweden /4/. The tracers I^-, Sr^{2+} and Blue Dextrance (a large molecule organic dye) were injected between two packers at 100 metres depth. Water was continuously pumped out of a 30 m distant borehole in order to assure a radial, mass conservative flow field (Figure 7). The breakthrough curves from the field were complemented by laboratory data on the sorption /5/ and the diffusivities in the rock matrix /6/. The Project Teams were asked to simulate the Sr^{2+} breakthrough curves using the breakthrough curves for I^- to characterise the hydraulics and the laboratory experiments as independent data sources for other transport parameters.

In the following only cases 2 and 3 will be treated since case 1 is a purely theoretical exercise that was used primarily for benchmarking and to study the possibilities to use for flow-tube approximations of the radionuclide transport in a two-dimensional flow field.

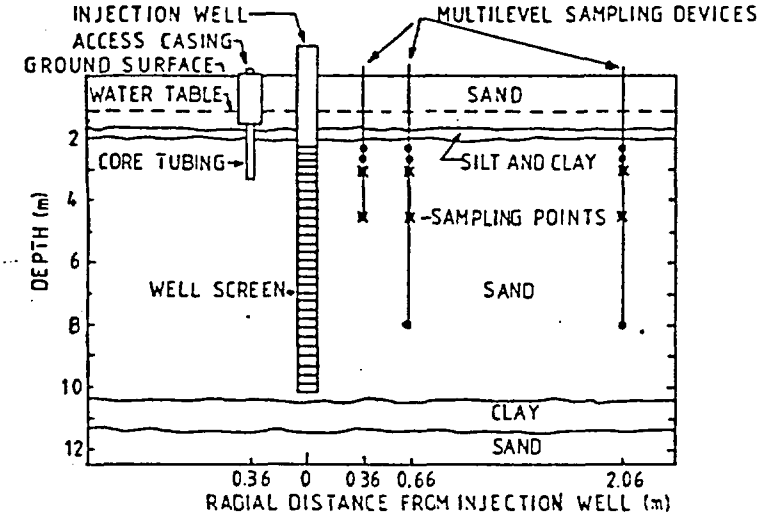
INJECTION WELL
ACCESS CASING
GROUND SURFACE
MULTILEVEL SAMPLING DEVICES
WATER TABLE
SAND
CORE TUBING
SILT AND CLAY
SAMPLING POINTS
WELL SCREEN
SAND
CLAY
SAND
DEPTH (m)
2
4
6
8
10
12
0.36
0
0.36
0.66
2.06
RADIAL DISTANCE FROM INJECTION WELL (m)

Figure 6 Schematic of the experiment used for Case 2 of INTRACOIN level 2. The sampling points for which the Project Teams were asked to simulate the breakthrough curves are marked with crosses.

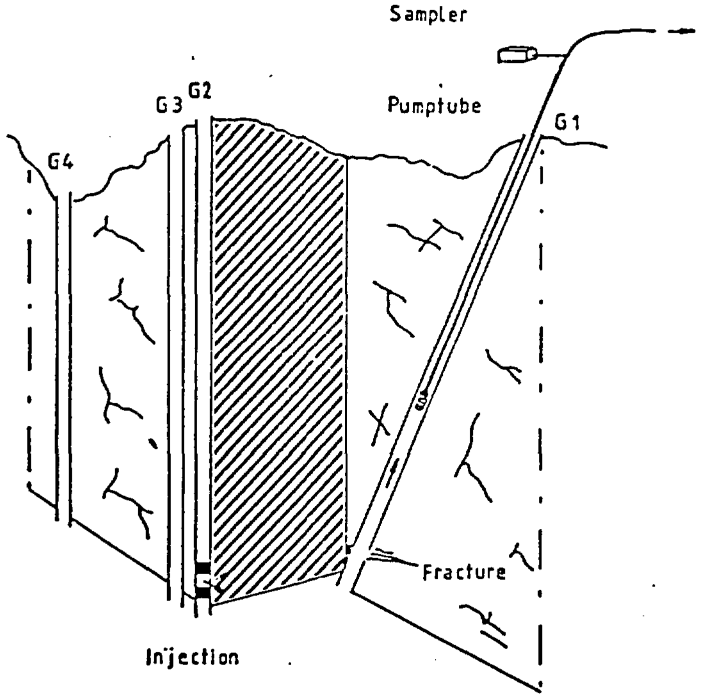
Sampler
Pumptube
G3
G2
G1
G4
Fracture
Injection

Figure 7 Cutaway view of the experiment used for Case 3 of INTRACOIN level 2.

Single well injection withdrawal experiment

The sandy aquifer where the experiment was performed was modelled as a stratified medium with five layers by both teams that tackled this test case. Reasonable fits between experimental data and the simulations could be obtained using the advective dispersive equation. However, the number of free parameters used in the fitting procedure was too large to allow for any conclusions that the models are validated. In particular, one of the teams showed that the best fit was obtained if the groundwater flow rate is allowed to increase with an increasing distance from the injection well. It was also shown that this apparant inconsistency in the flow conditions could not be explained by transfer of tracers between the layers by transverse dispersion unless a dispersivity value approximately 10 times higher than that obtained by fitting the breakthrough curves was used.

It was concluded that the scale of the single well injection withdrawal experiment was so small that heterogeneities could not be averaged in order to justify a homogeneous porous medium approach in the modelling. Possibly heterogeneties such as clay lenses, that were not identified during the experimental programme, should have been included explicitly in the models.

Dual well tracer experiment

The third test case was tackled by three teams. This case was subject to a rather broad analysis in terms of different model concepts tried for the dispersion phenomenon and for the transfer of radionuclides between different flow regimes in the rock. Figure 8 illustrates some of the concepts applied.

The focus of the discussion of the experiment interpretation came to lie on some specific features as described below.

The breakthrough curves for I^- has pronouncedly long tail. This could be explained by either different variants of multiple pathways (multiple fractures with different apertures, channeling within a fracture plane etc.) or by diffusion in and out of the rock matrix. It was not possible from the available information to distinguish between these two classes of explanations. Figure 9 illustrates the effect of the matrix diffusion.

The value of the diffusivity used for the fit in Figure 9 is in the order of 500 times larger than the value measured in the laboratory. A possible explanation is that the rock adjacent to the fracture might be more porous due to interaction with the ground water or porous fracture fillings chemical atterations of the rock surface.

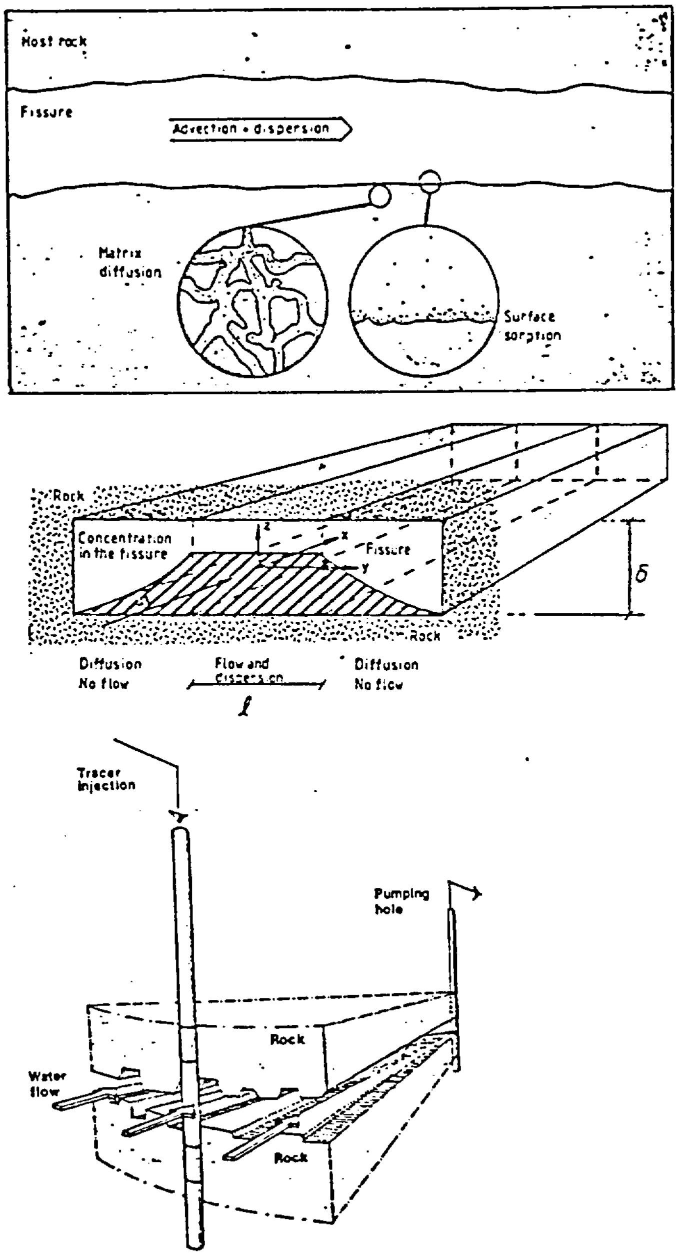
Host rock
Fissure
Advection + dispersion
Matrix diffusion
Surface sorption
Rock
Concentration in the fissure
z
x
Fissure
y
δ
Rock
Diffusion
No flow
Flow and dispersion
ℓ
Diffusion
No flow
Tracer injection
Pumping hole
Rock
Water flow
Rock

Figure 8 Schematic of some model concepts applied to Case 3 of INTRACOIN level 2. A: Matrix diffusion, B: Diffusion into stagnant water in a fracture, C: Channeling.

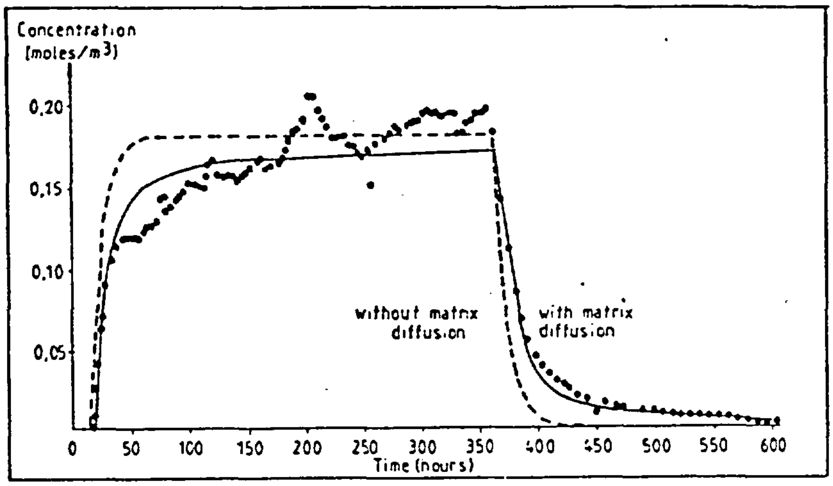

Figure 9 Illustration of the effect of matrix diffusion I$^-$ in Case 3 of INTRACOIN level 2.

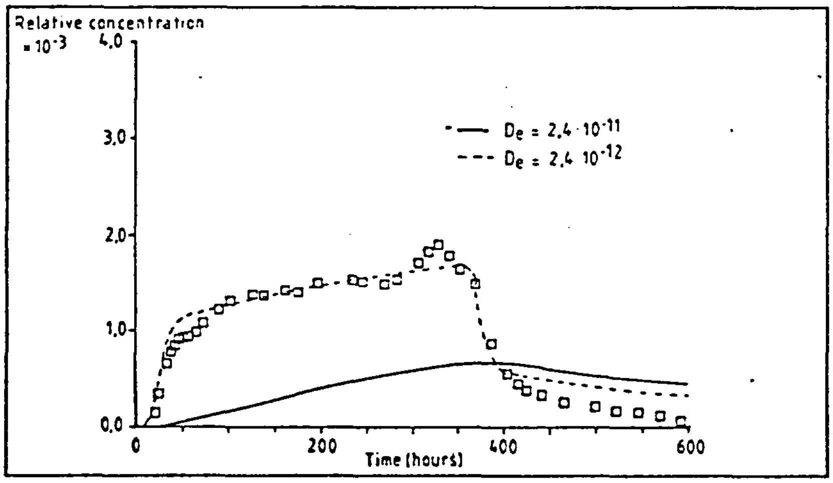

Figure 10 Fit between calculated and measured concentrations for Sr^{2+} with two diffusivities. The full line corresponds to the laboratory data and the dashed line to the best fit for the field experiment.

The diffusivity and sorption data that was determined in the laboratory for Sr^{2+} gave, when applied to the field experiment, a too strong interaction with the rock. The diffusivity value that gave the best fit was about an order for magnitude smaller than the value from the laboratory (Figure 10). The reasons for this can be that the sorption of Sr^{2+} is non-linear, i.e. the K_d-value decreases when the concentration increases, or that the laboratory data were derived from rock samples with much greater specific surface area that the in-situ rock since the samples had been crushed. The data available does not allow firm conclusions on this point.

A final important feature of the field experiment was that the Sr^{2+} recovery was only 60% while 98% of I^- was recovered. The Sr^{2+} concentration in the injected solution was fairly high ($9.4 \cdot 10^{-2}$ mol/l) indicating that a precipitation of e.g. $SrCO_3$ is not unlikely. Another explanation could be sorption onto the walls of the injection hole.

Summary of INTRACOIN level 2

In summary several possible conceptual models have been applied in attempts to explain the experiments chosen for INTRACOIN level 2. It has been possible to tune most of the models to fit the experiments reasonably well. However, in this fitting process several free parameters have been used.

Although the experiments were selected on the basis that they were well defined and documented they still failed to form a good data set for model validations. In particular there is a lack of independent observations leaving to many degrees of freedom to the parameter fitting procedure. This pinpoints that there is a need for close cooperation between modellers and experimentalists to develop data sets suited for valdiating radionuclide transport models.

3.3 Sensitivity and uncertainty analysis

For INTRACOIN level 3 a scenario based on advection, dispersion and sorption on the fracture walls in a 100 m long fracture was defined as a central case. Twelve variations representing different combinations of dispersion, sorption, matrix diffusion and different source terms were defined and calculated (see Tables 1 and 2).

The results showed that the matrix diffusion was the by far most important retardation mechanism. Also the dispersion is very important when matrix diffusion is active since it causes a portion of the radionuclide to move significantly faster than the ground water.

3.4 State of the art in transport modelling

The results of the INTRACOIN study show that:

- there exists solution algorithms solve the radionuclide transport models currently applied. The choice of algorithm should be made based on the character of the problem at hand.

- the validation of radionuclide transport models requires input from several independent experiments. There is an advantage if the experiments could be designed in cooperation between the modellers and the experimentalists.

- the phenomena matrix diffusion and dispersion including different types of chaneling potentially have important impact on the results of the radionuclide transport modelling and should therefore be looked into carefully.

4. STATUS OF THE HYDROCOIN STUDY

The HYDROCOIN study has been running for two years and is anticipated to run for another year. As mentioned earlier in this paper a final draft report on the level 1 effort is being reviewed by the participants for publishing during the first half of 1987 /7/. Regarding levels 2 and 3 preliminary results have been presented to the group in workshops.

At level 1 seven test cases were defined according to the following brief descriptions.

1. Compares numerical solutions with an analytical solution to a problem involving transient flow from a borehole in a permeable medium containing a single fracture.

Bertil Grundfelt   Kjell Andersson   Alf Larsson

Table 1 Variations for INTRACOIN level 3

Variation number	Description[1)]
1	No dispersion, no sorption
2	No dispersion, no sorption, matrix diffusion
3	No dispersion
4	No dispersion, matrix diffusion
5	No sorption
6	No sorption, solubility limited source term
7	Solubility limited source term
8	Matrix diffusion
9	Matrix diffusion, solubility limited source term
10	Kinetically controlled sorption
11	Alternative exit boundary conditions
12	Transverse dispersion

1) The term sorption refers to sorption on the fracture walls. Matrix diffusion is diffusion through microfractures in the rock blocks and sorption on interior surfaces.

Table 2 Calculated maximum discharge rates (activity units/year)

Variation no.	KTH[1)]		UKAEA/AERE	VTT		EIR	Polydynamics
	Analytical	Numerical	NAMID	GETOUT	MMTID	RANCHN	TROUGH
Central			$1.97 \cdot 10^{-6}$	$1.53 \cdot 10^{-6}$	$1.62 \cdot 10^{-6}$	$1.97 \cdot 10^{-6}$	$1.96 \cdot 10^{-5}$
1	$1.50 \cdot 10^{-5}$	-	$1.49 \cdot 10^{-5}$	$1.50 \cdot 10^{-5}$	$1.50 \cdot 10^{-5}$	$1.49 \cdot 10^{-5}$	$1.49 \cdot 10^{-5}$
2	2)	-	$1.24 \cdot 10^{-29}$	-	-	$1.63 \cdot 10^{-29}$	$1.03 \cdot 10^{-29}$
3	$1.15 \cdot 10^{-5}$	-	$1.15 \cdot 10^{-5}$	$1.14 \cdot 10^{-5}$	$1.15 \cdot 10^{-5}$	$1.15 \cdot 10^{-5}$	$1.15 \cdot 10^{-5}$
4	2)	-	$9.57 \cdot 10^{-30}$	-	-	$1.26 \cdot 10^{-29}$	$1.28 \cdot 10^{-29}$
5	$1.15 \cdot 10^{-5}$	-	$1.49 \cdot 10^{-5}$	$1.50 \cdot 10^{-5}$	$1.50 \cdot 10^{-5}$	$1.49 \cdot 10^{-5}$	$1.49 \cdot 10^{-5}$
6	$1.70 \cdot 10^{-7}$	-	$1.69 \cdot 10^{-7}$	-	$1.72 \cdot 10^{-7}$	$1.69 \cdot 10^{-7}$	$1.70 \cdot 10^{-7}$
7	$1.32 \cdot 10^{-7}$	-	$1.38 \cdot 10^{-7}$	-	$1.32 \cdot 10^{-7}$	$1.38 \cdot 10^{-7}$	$1.45 \cdot 10^{-7}$
8	$1.76 \cdot 10^{-13}$	$7.72 \cdot 10^{-13}$	$2.97 \cdot 10^{-13}$	-	-	$2.89 \cdot 10^{-13}$	$2.69 \cdot 10^{-13}$
9	$8.21 \cdot 10^{-14}$	$3.23 \cdot 10^{-13}$	$1.37 \cdot 10^{-13}$	-	-	$1.33 \cdot 10^{-13}$	$9.87 \cdot 10^{-14}$
10.1	-	$3.49 \cdot 10^{-6}$ 3)	$1.95 \cdot 10^{-6}$ 3)	-	-	-	$6.37 \cdot 10^{-5}$ 3)
10.2	-	-	$2.16 \cdot 10^{-6}$ 3)	-	-	-	$9.82 \cdot 10^{-5}$ 3)
10.3	-	-	$1.43 \cdot 10^{-5}$ 3)	-	-	-	$9.82 \cdot 10^{-5}$ 3)
11.1	-	-	$1.50 \cdot 10^{-6}$	-	-	-	
11.2	-	-	$1.52 \cdot 10^{-6}$	-	-	-	

1) The discharge rates calculated by the KTH-team include only the convective part.

2) The team shows decay curves and break-through curves for a stable nuclide.

3) The results are not comparable because of different data and conceptual models for the kinetic sorption.

2. Simulates steady-state flow in a two-dimensional domain containing two permeable fracture zones interacting each other.

3. Simulates partially saturated flow through a sequence of alternating pervious and low permeability sedimentary rocks.

4. Compares analytical and numerical solutions of thermal convection driven flow where the heat is evolved from a spherical source with a decaying heat output.

5. Simulates water flow and salt transport in a two-dimensional domain with the fluid density dependent on the salt concentration.

6. Simulates steady-state flow in a three-dimensional domain representing a generic bedded salt geologic setting.

7. Simulates steady-state flow through a shallow land-burial site in argillaceous media.

The results /8/ show for six of those seven test cases a reasonable agreement. For the seventh case, Case 3, no team managed to get a converged solution with the data from the original test case specification. Some of the Project Teams tried to calculate the case with a data set that had been modified to decrease the non-linearity and the permeability contrasts close to the groundwater table. However, there is no concensus between these attempts about the way the data modifications should influence the solution.

In some of the test cases, in particular case 5, the agreement about the solution has been reached only after several reiterations including mesh refinement, reformulation of post processing algorithms etc. A special workshop was held in March 1986 to discuss the problems in conjunction with brine transport in general and especially Case 5.

It seems that the calculation of the primary field quantities, e.g. the groundwater pressure, is comparatively easier than the calculation of derived quantities such as fluxes. The latter generally require a higher discretisation density. It is obvious that the very non-linear test cases 3 and 5 have taxed the codes and seem to be frontline problems regarding flow modelling in a porous medium continuum. It should be pointed out that all efforts at level 1 of HYDROCOIN concern continuum approximations.i.e. there is no test case for fracture flow models included in level 1 of HYDROCOIN.

In summary, level 1 of HYDROCOIN has met it's objective to test the numerical accuracy of groundwater flow codes. In addition it has served as an efficient means for initiating research and development efforts. The response from the participants has been overwhelming resulting in slightly more than 1500 data files that have been compiled.

5. CONCLUDING REMARKS

The INTRACOIN and HYDROCOIN studies have provided an efficient means for model testing. The objective has been to test and evaluate models but not to rank them.

In both studies workshops have been held at regular intervals. Due to an informal atmosphere, the Poject Teams have been very frank in their presentations of results and to a degree included also failures. The workshops have therefore been extremely valuable in the prolifiration of "tricks of the trade" and in identifying problems associated with the different test cases. As a result many model developments and other research efforts have been initilised. This has been achieved through the labor of the Project Teams.

REFERENCES

/1/ INTRACOIN - Final report level 1, Code verification,
SKI 84:3, Swedish Nuclear Power Inspectorate, Stockholm,
September 1984

/2/ INTRACOIN - Final report levels 2 and 3,
Model validation and uncertainty analysis,
SKI 86:2, Swedish Nuclear Power Inspectorate, Stockholm, May
1986

/3/ PICKENS J F, JACKSON R E, INCH K J,
Measurement of distribution coefficients using a radial
injection dual-tracer test,
Water Resources Research 17 (1981), 529-544

/4/ GUSTAFSSON E, KLOCKARS K,
Studies on groundwater transport in fractured crystalline rock
under controlled conditions using nonradioactive tracers,
SKBF/KBS technical report 81-07, SKB, Stockholm (1981)

/5/ SKAGIUS K, SVEDBERG G, NERETNIEKS I,
A study of strontium and cesium sorption on granite, Nuclear
Technology 59 (1982), 302

/6/ SKAGIUS K, NERETNIEKS I,
Diffusion in crystalline rocks, Proc. Scientific Basis
for Nuclear Waste Management V,
Elsevier Science Publishing Co., 11 (1982) 509-518

/7/ ANDERSSON K, GRUNDFELT B, HODGKINSON D P, LINDBOM B,
JACKSON C P, (editors)
HYDROCOIN level 1 final report - verfication of
groundwater flow models, (to be published 1987).

/8/ HYDROCOIN - PROGRESS REPORT No. 4 January-August 1986, Swedish
Nuclear Power Inspectorate, Stockholm.

Bertil Grundfelt Kjell Andersson Alf Larsson

Appendix 1

List of parties participating in the INTRACOIN study, coordinating group members and project team leaders

Party	Coordinating group member	Project team leader
Atomic Energy of Canada Ltd (AECL)	Mr K Dormuth	Mr T W Melnyk
Commissariat à l'Energie Atomique/ Institut de Protection et de Sureté Nucléaire (CEA/IPSN)	Mr A Barbreau	Mr P Goblet
Nationale Genossenschaft für die Lagerung Radioaktiver Abfälle (NAGRA)	Mr C McCombie	Mr J Hadermann Mr R J Hopkirk
National Radiological Protection Board (NRPB)	Ms M Hill	Ms M Hill
Projekt Sicherheitsstudien Entsorgung (PSE)	Mr E Bütow	Mr E Bütow
Technical Research Centre of Finland (VTT)	Mr E Peltonen	Mr E Peltonen
Swedish Nuclear Fuel Supply Co (SKBF/KBS)	Mr I Neretnieks	Mr I Neretnieks
Swedish Nuclear Power Inspectorate (SKI)	Mr A Larsson	Mr B Grundfelt
United Kingdom Atomic Energy Authority/ Atomic Energy Research Establishment (UKAEA/AERE)	Mr D P Hodgkinson	Mr D P Hodgkinson
U.S. Department of Energy (U.S. DOE)	Mr G E Raines (ONWI)	Mr C R Cole Mr G Jansen Mr S Pahwa Mr T H Pigford
U.S. Nuclear Regulatory Commission	Mr N Eisenberg	Mr T J McCartin Mr B Ross Mr M Reeves Ms N N Finley

Managing participant:	SKI
Principal investigator:	KEMAKTA
Coordinating group:	
Chairman:	Mr A Larsson, SKI
Secretary:	Mr K Andersson, SKI
Project secretariate:	Mr K Andersson, SKI Mr B Grundfelt, KEMAKTA Mr A Bengtsson, KEMAKTA Mr J Hadermann, EIR Mr F Rösel, EIR

Appendix 2

LIST OF HYDROCOIN PARTICIPANTS

PARTY AND COORDINATING GROUP MEMBER	PROJECT TEAM(S) AND TEAM LEADERS
Atomic Energy of Canada Ltd (AECL) K.W. Dormuth	Atomic Energy of Canada Ltd T. Chan (AECL)
British Geological Survey (BGS) J.A. Barker	British Geological Survey D. Noy (BGS)
Commissariat à l'Energie Atomique/ Institut de Protection et de Sûreté Nucléaire (CEA/IPSN) J. Lewi	1. Commissariat à l'Energie Atomique (CEA) P. Raimbault 2. École Nationale Supérieure des Mines de Paris (EDM) P. Goblet
Gesellschaft für Strahlen- und Umweltforschung (GSF) E. Bütow	Technical Univ. of Berlin E. Bütow (TUB)
Japan Atomic Energy Research Institute (JAERI) H. Nakamura	1. Japan At. En. Research Inst. S. Muraoka (JAERI) 2. University of Kyoto (UOK) Y. Ohnishi 3. Hazamagumi Ltd (HAZA) 4. Okumuragumi Ltd (OKUM) 5. Central Research Institute of the Electric Power Industry (CRIEPI)
Nationale Genossenshaft für die Lagerung Radioaktiver Abfälle (NAGRA) P. Hufschmied	1. University of Neuchatel (UON) L. Kiraly 2. Motor Columbus (MCI) W. Huerlimann 3. ETH - Zürich (ETH) J. Troesch
Rijksinstituut voor Volksgezondheid en Milieuhygiene (RIVM) P. Glasbergen (Deputy: T. Leijnse)	Rijksinstituut voor Volksgezondheid en Milieuhygiene P. Glasbergen (RIVM) (Deputy: T. Leijnse)
Swedish Nuclear Fuel and Waste Management Co. (SKB) G. Bäckblom	The Royal Institute of Technology (KTH) R. Thunvik
Swedish Nuclear Power Inspectorate (SKI) A. Larsson	Managing Participant.
Technical Research Centre of Finland (VTT) S. Vuori	Tech. Research C. of Finland K. Meling (VTT)

PARTY AND COORDINATING GROUP MEMBER	PROJECT TEAM(S) AND TEAM LEADERS
United Kingdom Atomic Energy Authority/Atomic Energy Research Establishment Harwell (UKAEA/AERE) P. Jackson	1. Atomic Energy Research Est. P. Jackson (AERE) (Deputy: A. Herbert) 2. Atkins Research and Development (ARD) T. Broyd
U.S. Department of Energy (DOE) C. Cole	1. Basalt Waste Isolation Project, Rockwell, Hanford (BWIP) P.M. Clifton 2. Salt Repository Program, Office of Nuclear Waste Isolation (ONWI) S.K. Gupta 3. Office of Crystalline Repository Development, Battelle, Argonne (OCRD) A. Brandstetter 4. Tuff Repository Project, Nevada Nuclear Waste Storage Investigations (NNWSI) R. Prindle
U.S. Nuclear Regulatory Commission (NRC) T. Nicholson (Deputy: R. Codell)	1. U.S. Nucl. Reg. Commission T. McCartin (NRC) 2. Sandia National Laboratory P. Davis (SANDIA(NRC))
Organization for Economic Co-operation and Development/Nuclear Energy Agency (OECD/NEA) (Observer)	Member of Secretariat: Organization for Economic Co-operation and Development/Nuclear Energy Agency (OECD/NEA)

Managing Participant: SKI

Principal Investigator: Kemakta

Coordinating Group:

Chairman: A. Larsson, SKI
Vice chairman: T. Nicholson, NRC
Secretary: K. Andersson, SKI

Project Secretariat:
K. Andersson, SKI
B. Grundfelt, Kemakta
P. Jackson, AERE[1]
C. Thegerström, OECD/NEA[2]
U. Tveten, NKA/IFE

Modeling of Fluid Flow and Transport in Fracture Networks

by Jane C.S. Long

Earth Sciences Division
Lawrence Berkeley Laboratory
Berkeley, California 94720

ABSTRACT

Fracture hydrology is a relatively new science. Advances are slow because many classical techniques fail. To begin to solve these problems, we have put together an inter-disciplinary approach including the fields of hydrology, structural geology, statistics, geophysics, fluid mechanics, rock mechanics and geochemistry. Some efforts in this direction are described in this review paper. Our work can be conveniently divided into single fracture and fracture network studies. Within each, we have efforts to characterize the geometry and efforts to model the behavior. Eventually, what we learn about single fractures should be incorporated into the network models and what we learn about the networks should be incorporated into regional models. In the area of single fracture behavior, field and laboratory experience has shown that the assumption of parallel plate flow may not always be good. To study the affect of fracture geometry on flow behavior we have written a model to solve the Navier-Stokes equations in a single fracture whose voids have been described in detail. Photographs and profile data from fracture surfaces can be used to obtain this geometric data for the model. At the same time, we are modeling seismic rays passing through fractures and and studying the relationship of the fracture geometry to fracture stiffness and seismic wave attenuation. Such relationships will help in interpreting seismic survey data in terms of the hydrologic properties. In parametric studies of fracture networks, we have compared the behavior of flow in fracture networks to the behavior of an equivalent continuum. As the connectivity of fracture increases, the behavior is more like porous media. Percolation and fractal theory may help to explain scale effect observed in these networks. In another parameter study we examined how the variation in aperture decreases the permeability and causes the transport behavior to be less Fickian. If aperture is correlated to length, the opposite is true. These studies suggest techniques for deriving likely fracture models from borehole data. In efforts to model a real field site, data was incorporated in a 2D network model for the Fanay-Augeres mine. This model included the use of geostatistical simulation techniques to model spatial variability in the fracture pattern. An extension of this work to three dimensions is underway. In this model, fractures will be represented as discs in space and include a regionalized parent-daughter statistical model to generate fracture swarms. To enhance our ability to obtain data for these models, we have developed analytical solutions for well tests in composite systems which consist of a few fractures intersecting the well in the inner region and a network of fractures which behaves like an equivalent continuum in the outer region. These solutions allow an estimate of the aperture and length of the fractures. Seismic tomography has been identified as a potential mapping tool for fractures. In sum, this work represents a strong multidisciplinary approach to characterizing and modeling flow in fracture systems.

INTRODUCTION

The flow of fluids and contaminants through fractures in rock is controlled by the geometry of the fractures. On the scale of the individual fracture, it is the geometry of the void space that controls flow. On the regional scale, it is the geometry of the fracture network, ie the location, orientation, size of the fractures and in turn, the void space in each fracture, which control the flow. These facts have guided our study of flow and transport.

In fact, the geometry of void space controls groundwater flow in general. However, as opposed to fractured media, porous media voids are usually small compared to the scale of the problem and there are a great number of them in a field scale problem. Also, connection between the voids is virtually guaranteed in porous media. Problems of flow in such media are called problems at the "stochastic limit". As such they can often be treated as equivalent continuum problems by treating the parameters of the problem as average quantities.

At the other end of the scale are problems of flow through perfectly ordered systems, ie problems at the "crystal limit". (The terms "stochastic limit" and "crystal limit" were coined by Hasslacher, 1985.) An example of such a problem would be flow through sets of equally spaced, parallel, infinite fractures, as solved by Snow (1965), or flow through regularly packed spheres.

Relative to pores in porous media, there are few fractures in fractured rock, and they may be quite large compared to the scale of the problem. Connection between fractures may or may not exist. Further, any structural geologist who has looked at fractures can tell you that fractures are neither completely random nor completely regular. Thus the problem is between the stochastic and crystal limits and as such, between the two limits which we have known how to solve. Fracture geometry has a seemingly random component and a seemingly regular component. To characterize the geometry, both components must somehow be represented. For example, fractures may form as conjugate sets as a result of a compressional tectonic event. Thus the fractures will tend to be oriented in the conjugate directions, but certain heterogeneities in the boundary conditions or rock properties will cause the pattern to be imperfect. In this case the question is what is the theoretical pattern of fractures and how do the actual fractures vary from that pattern.

We can take at least four approaches to characterizing the geometry of fracture systems. The first is to observe fractures in outcrop, in underground openings, in core, in laboratory samples etc. From these observations we can propose models for the geometry and use these models to produce stochastic realizations which can in turn be used in a flow or transport model. Second, we can use hydraulic and tracer tests to measure properties of the fracture system insitu. We may be able to interpret these tests in terms of the specific geometry controlling the response, or in terms of average properties that can be related to geometric parameters. Third, we can find new ways to "see" fractures through geophysics such as radar or seismic tomography and link the tomographic results to fracture pattern. Finally, we can explore the genesis of fractures through the fields of rock mechanics and structural geology in order to identify fracture patterns as a function of stress history. The first of three of these are discussed in this paper. The last is a new area of research.

If characterizing the geometry were straight forward, modeling of flow and transport would be straight forward, at least from a theoretical point of view. The numerical models would simply solve the appropriate equations within the boundaries described by the geometry. However, a significant practical problem would remain in that huge amounts of data would be needed to describe that geometry. As a result of the difficulties involved in characterizing and incorporating the geometry, two types of modeling activities are useful. In the first we adopt simple models of fracture geometry and vary the parameters of the models to observe the effect on behavior. This type of modeling is usually done in two-dimensions as the computations are more facile. From this, we learn what features control flow and we may also learn something about bounding behavior. The second activity is to attempt to model specific cases with as much accuracy as possible. In this case the goal is to compare the behavior of the model with some observed behavior in the field or laboratory in order to confirm the model. In doing this, we hopefully learn something about predicting hydrologic behavior.

Fracture hydrology is a relatively new science. Advances are slow because many classical techniques fail. To solve these problems will require a strong inter-disciplinary approach including the fields of hydrology, structural geology, statistics, geophysics, fluid mechanics, rock mechanics and geochemistry. Some efforts in this direction are described in this review paper. Our work can be conveniently divided into single fracture and fracture network studies. Within each, we have efforts to characterize the geometry and efforts to model the behavior. Eventually, what we learn about single fractures should be incorporated into the network models and what we learn about the networks should be incorporated into regional models.

SINGLE FRACTURES

In studying single fractures, we are interested in three major characteristics: void geometry, flow behavior and mechanical behavior. The void geometry controls both the flow and the mechanical behavior and thus is a link between the two. If we can characterize the flow, then we can model it. If we can show the link between flow behavior and mechanical behavior, then we may have a key to interpreting the seismic response of a rock mass in terms of its hydrology.

Void Geometry

Efforts to characterize the void geometry of a fracture have used two experimental techniques. The first, profiling, has been used in many studies, Brown and Scholtz, 1985; Tsang, 1986; Gentier, 1986 for example. To collect profile data, one measures the elevation of the surface of the fracture along sample lines, preferably in two directions and along corresponding lines on both top and bottom surface. The second experimental technique is new (Myer et al., 1986) involving injection of a low melting point metal into the fracture under controlled stress and fluid pressure conditions. The result is a three-dimensional cast of the void space in the fracture.

Profile data is not void geometry data. To use this data to estimate the void geometry involves several steps. First one, must make some corrections to account for the fact that the profile lines do not line up with each other exactly. This results in moving the "location" of some lines relative to the others in a way which best achieves certain criteria. For example, one might find a rigid translation/rotation which minimizes the average aperture. This criteria might be used if the fracture sides were a tight fit to each other. Now we have two sets of profiles, one on each surface, but we have no aperture data because the profiles do not line up. To get aperture data, we must estimate the topography over both surfaces by using techniques such as Kriging. Finally, to obtain the void geometry at a specified state of stress we must calculate the deformation of these surfaces in contact. Techniques for calculating elastic deformation of the voids as they are compressed, are being developed by Hopkins (1986).

Metal injections can be performed on fractures under different normal loads. When the metal cools, the fractures are taken apart and photographed at several magnifications. Some metal sticks to both surfaces, so two approaches can be taken to reconstruct the void space from the photos. One can use stereoscopic techniques to obtain measures of the thickness of the metal. This is very usefull but such data may be difficult and time consuming to obtain. A second approach is to superimpose the photos. This can be done such that the void areas, ie. where the metal is, show up as white, and the contact areas show up as black. An example of such a photo prepared from a fracture in crystalline rock at 85MPa effective stress is shown in Figure 1 (from Myer et al., 1986). Such a photograph can be resolved to give the percentage of contact area and the distribution of the contact area. In combination with an analysis of profile data as described above, a complete description of the void volume can be estimated.

Flow Calculations

Given the void geometry, at some state of stress, we now wish to examine the hydraulic characteristics of the fracture. From the point of view of fluid mechanics, a fracture is an irregular three-dimensional channel with irregularly spaced and sized obstacles. In such channels we expect four possible flow regimes. If the fracture is sufficiently open the flow may behave like flow between parallel plates. As the fracture closes the distribution of the contact area will determine the characteristics of flow. If the contact area is not well dis-

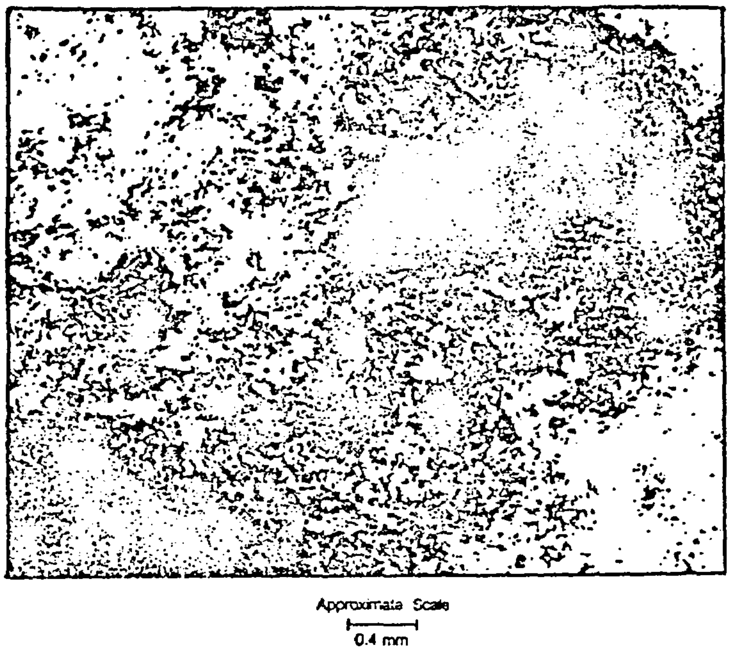

XBL 8610-12621

Figure 1. Composite photograph of sample E30 at 85 MPa effective stress; white is metal, black is contact area (after Myer et al., 1986).

tributed but occurs in sparse clumps, the flow may be non-linear, even at low Reynolds numbers. Thus flux will not be proportional to gradient. If the contact area is finely distributed, flow will behave like flow through porous media. Flux will be linearly related to gradient and potential theory can be used to describe head distributions. If the fracture is sufficiently closed, flow will only occur in tortuous channels. In this case, flow in the fracture plane becomes essentially one-dimensional.

The problem of fluid flow in an irregular geometry can be solved theoretically only if a numerical approach is adopted. Further, any such scheme must be able to handle boundary shapes which do not coincide with coordinate lines. We have developed a three-dimensional grid generation procedure which maps the interior of a complex region onto the interior of a rectangular parallelepiped (Muralidhar and Long, 1986ab). In the transformed region (computational space) the boundaries lie along lines which are parallel to one of the new coordinate axes. The flow computation is performed in this newly defined region, and an inverse transformation rule extracts values of flow velocities and pressure in the real geometry coordinates. The formulation has been developed in three dimensions, suitable for flow analysis in a single rock fracture.

Grid generation is accomplished through numerical solution of differential equations which insure that the transformed grid in the real space is smooth and has a certain degree of orthogonality. The more nearly orthogonal the grid is, the less truncation error results in the flow calculation. The grid lines in the physical plane are the contours on which the newly generated coordinates take on constant values. There is a one-to-one correspondence between nodal points in the physical space and nodal points in the computational space.

The grid generation procedure is actually done backwards. That is, it starts with the orthogonalized domain and calculates the location of each nodal point in the physical geometry, subject to the boundary shapes as constraint. Flow is computed in the regularized geometry, so it is only this inverse transformation law which is of interest.

Because we have transformed the spatial coordinates, we must also transform the governing equations for flow before they can be solved. In doing this, each term in the three-dimensional governing equations becomes 81 terms. Thus we have traded complexity in geometry for a large number of unknowns. The equations governing grid generation in three dimensions, including a method to improve orthogonality of the generated coordinates and the techniques for solving flow in the transformed region have been fully derived in Muralidhar and Long (1986a).

These techniques have been tested for a variety of problems and two examples are given here. Work on the full three- dimensional flow problem in a complex geometry is still in progress.

Figure 2 shows grid generation in a wavy channel. Figure 2a is the physical domain in which the flow process actually takes place. Figure 2b is the transformed domain in which the flow equations are solved. In the computational space, the wavy edges of the physical channel are represented by straight edges. In Figure 2a, orthogonality has been introduced in the calculation, both in the interior and at the boundary.

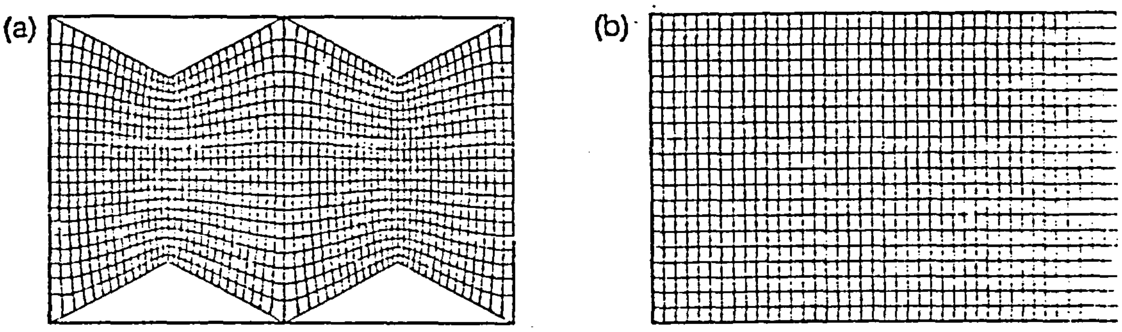

Figure 2. Grid generation in a channel with constriction, aperture = 2, length = 6. (a) Physical region. (b) Transformed region.

A real fracture is also expected to have a number of contact areas serving as obstacles to fluid flow. In this approach, the contact areas are mapped to rectangles, of about the same total area. An example of this procedure is shown in Figure 3. The actual contact area is circular (Figure 3a) and in the transformed plane. it is a square. (Figure 3b). The dimensionless duct is a size 6 × 6 × 2, dimensionless units and the obstacle is of size 1.2 × 1.2 ×2. The duct is closed at the top and the sides.The grid in the physical domain is gradually distorted to accommodate the boundary shape which is not coincident with a rectangular mesh pattern.

Once the grid generation has been performed, the flow field can be solved. Flow enters on the left side and leaves the right side. in response to a prescribed pressure drop. Results given below have been obtained for specified Reynolds numbers, Re, where Re is based on the pressure drop in the channel.

Figure 4 shows a velocity vector plot at the mid- plane of the duct, at Re = 25. A symmetric roll pattern is clearly visible on the rear side of the obstruction, and is a consequence of assuming the flow to be steady. As the Reynolds number is raised, the steady state computation retains the symmetric form of the recirculation region, except that it grows in size. It is known from experiments in flow past cylinders and spheres that the symmetric bubble is stable only for low Re. At higher flow rates, the flow becomes unsteady, with a trailing vortex street being produced behind the cylinder, which in turn destroys symmetry. The onset of unsteadiness in Figure 4 would have to be determined from a full transient calculation. More than one obstacle in the flow field provides a stabilizing influence to the flow. Many obstacles would provide Darcy flow.

Figure 5 shows plot of mean velocity as a function of Reynolds number for the three-dimensional duct considered above (curve 2) compared to a two dimensional parallel channel (curve 1). With increase in Re.

the flow in the duct encounters greater resistance and the non-linearities in flow bring out an overall non-linear behavior of the system.

The next step will be to obtain a data set from a real fracture as described above and use it to create an input file for the grid generation and flow calculation models. We can obtain the geometry for different states of stress and observe the changes in the flow regime.

At the same time that we are studying the hydrologic behavior, a parallel study examines the stiffness of the fracture. This is done theoretically using a numerical model which predicts deformation of both the voids (Hopkins, 1986). Stiffness is also studied in the laboratory using shear waves. The attenuation of the shear waves as they pass through the fracture has been shown to be a function of the stiffness, which in turn is a function of the fracture geometry (Myer et al., 1985). Such an understanding of the attenuation and stiffness of shear waves becomes critical to interpreting field measurements in seismic tomography as will be discussed later.

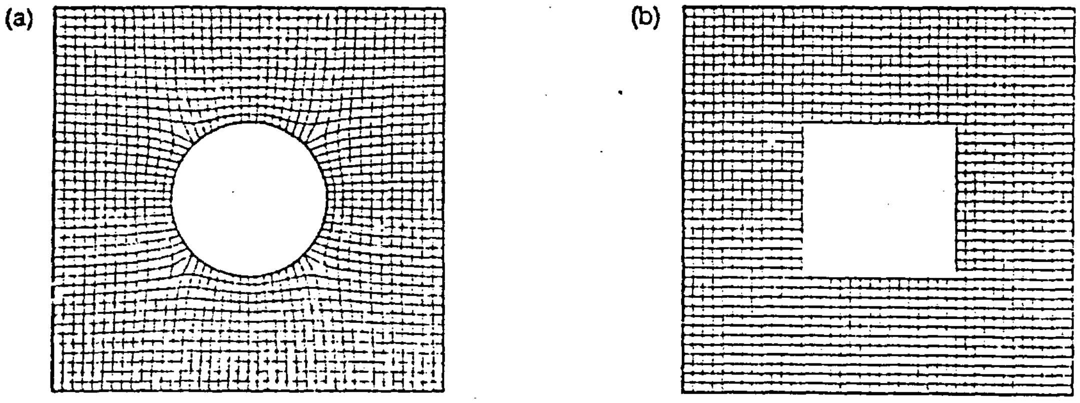

Figure 3. Grid generation in a square region with a circular obstacle (contact area). (a) Physical region; (b) Transformed region.

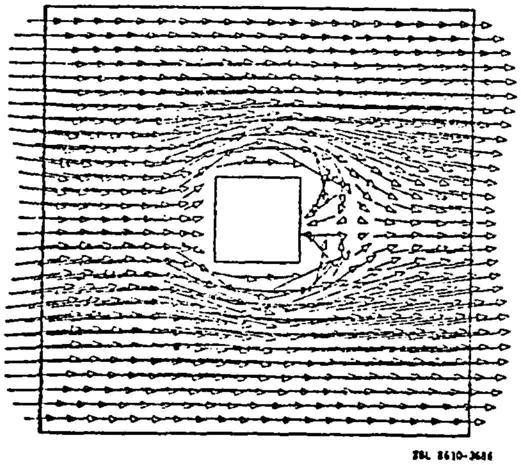

Figure 4. Velocity vector plot in a three-dimensional duct with an obstacle. Re = 25.

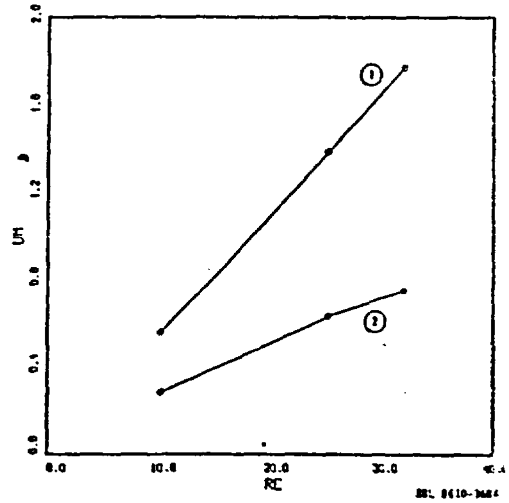

Figure 5. Plot of mean velocity in a three-dimensional channel as a function of pressure-based Reynolds number. (a) Flow in a parallel duct; (b) Flow in a duct with an obstacle.

FRACTURE NETWORK STUDIES

Our studies of fracture networks have been mainly concerned with parameter studies in two dimensions, modeling of field sites, well test solutions tailored for fracture systems, and most recently, the behavior of seismic rays in fracture networks. The parameter studies have been primarily focussed on learning how various geometric parameters affect flow. Under field site modeling, we have developed a two-dimensional simulation of the fracture system at the Fanay-Augeres mine in France (Long and Billaux, 1986). Extension of this model to three-dimensions is underway (Billaux et al, 1986). In the area of well testing, we have developed analytical solutions which are suited for determining the properties of the fractures intersecting the well. These are solutions for composite systems in which flow in the inner region is controlled by a few fractures intersecting the well and flow in the outer region is considered to behave on average like flow in a continuum. The newest area of research is in producing synthetic seismograms for the same fracture systems we study hydrologically. Such studies will hopefully lead to a hydrologic interpretation of seismic tomography. These studies are reviewed below.

Most of the parameter studies we have performed are, or will be available in the literature (Long and Witherspoon, 1985; Long and Shimo, 1986, and Long et al, 1982) so the review we give here will emphasize new results. These studies are all two-dimensional, but we feel that the results will apply qualitatively in three dimensions. In these studies, the fracture system is conceptualized as a Poisson model. That is the fractures are conductive line segments randomly located in the plane, where the orientation and lengths and conductivity of the line segments are randomly distributed. The construction of such networks has been discussed in Long et al (1982). We find all of the intersections between fractures. The intersections are called "nodes", and the portions of the fracture between the nodes are called "elements". Flow through a square region of such a network is calculated by assigning constant head values to the boundary nodes (i.e., the ends of the fractures which intersect the boundaries). The flow calculation is made by assuming that the steady flux in each element is proportional to the gradient in the element, i.e., the difference in the hydraulic heads at each of the associated nodes divided by the length of the fracture. Flux in each element can then be calculated essentially by solving Kirchhoff's laws.

By using boundary conditions which would produce a constant gradient in an anisoropic continuum, we can calculate the total flux through the system in the direction of the gradient. By orienting the rectangular sample in different directions, it is possible to measure the permeability in different directions. These directional permeability measurements can then be plotted as $1/\sqrt{K(\alpha)}$ where α is the direction of the gradient. If these measurements plot as an ellipse, the behavior of the system can be favorably compared to the behavior of a continuum. The more erratic the plot is, the less the behavior is like a continuum (Long et al, 1982; Long, 1983).

Connectivity

The first study was initially concerned with how much can be learned about a fracture system from a line sample such as that provided by a borehole. In this study we fixed the fracture frequency (average number of fractures intersected by a unit length of line sample, λ_l) and orientation distribution, as these data are often available. We assume all the fractures have the same conductivity. The aim of the study was to determine the effect of fracture length (l), and areal density (number of fractures per unit area, λ_A on the hydraulic behavior of the fracture network. Because the fracture frequency is fixed, appropriate values of λ_A and l are not independent. They are related by the probabilistic relationship:

$$\frac{\lambda_l}{\cos\theta} = \lambda_A \bar{l} \qquad (1)$$

where θ is the angle between the pole of a fracture and the borehole. Equation (1) means that the longer the fractures are and the more fracture there are the more fractures are likely to be intersected by a borehole.

We start with an arbitrary fracture network specified by values of fracture density, orientation distribution and constant fracture length. To create a series of fracture networks which all have the same fracture frequency, we can increase the fracture length and decrease the fracture density by the same factor, or vice versa. What we find is that as length increases at the expense of density, the connectivity of the fracture system increases. An example of a series of networks derived in this way is shown in Figure 6 along with the associated permeability plots.

If we could observe these systems on an infinite scale we would see the following: At high fracture densities (λ_A), but very small values of length, the fractures do not intersect and, given the impermeable matrix, the system has zero permeability. As the fracture length becomes larger at the expense of density, clusters of intersecting fractures begin to appear. Longer still, we reach a critical value of length and the clusters suddenly become infinite in size thus making the network permeable. Permeability increases as the fracture length increases and as the fracture length approaches infinity, the permeability approaches the assymtope equal to the value derived by Snow (1970).

However, we cannot observe the fracture systems on an infinite scale. On the finite scales possible for observation we tend overestimate the infinite permeability because otherwise unconnected fractures or fracture clusters are truncated by the boundaries of the finite flow region. We call this truncation error. In fact, if the length is below the critical value where permeability is theoretically zero, we can still measure a finite permeability if we choose a random sample located in a fracture cluster. On the other hand, if the length is above the critical value we could choose a random sample that is in a "hole" between clusters. In this case, even though the network is actually permeable on the infinite scale, some finite samples will not be permeable. Thus it may be difficult to know absolutely what the critical value of length is.

We can estimate the infinite permeability by performing a special kind of scale effect study. In this study, we create the fracture networks with parameters as described above. We then measure the permeability of the samples for different size nested sample squares (flow regions) by applying the boundary conditions successively to each square (Figure 7). At the same time that the the permeability of the flow regiom is calculated, the flow through the nested squares interior to the flow region (study regions) are calculated. The permeability of the study regions is then said to be equal to this flux divided by the field gradient imposed by

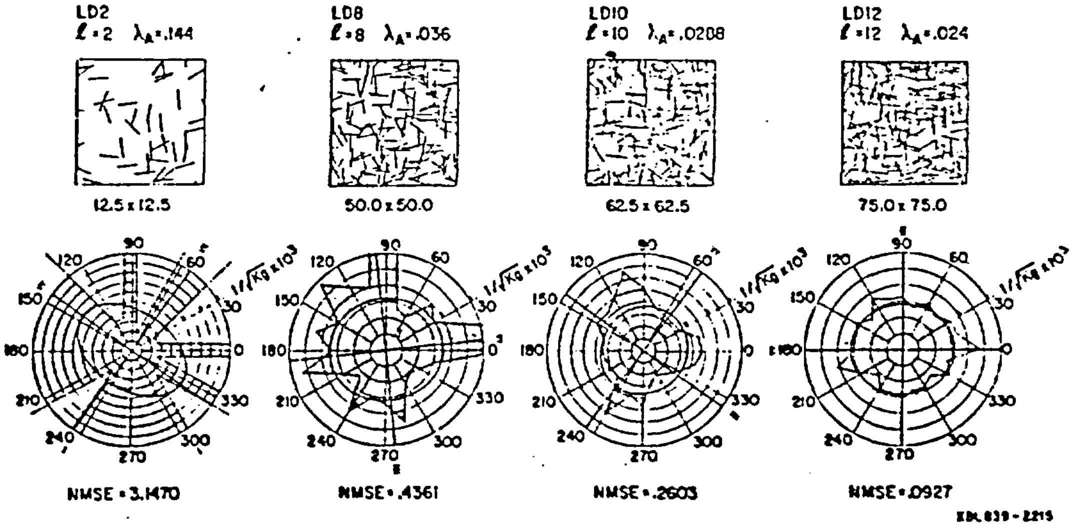

Figure 6. Permeability results for fracture lengths 2, 8, 10, and 12.

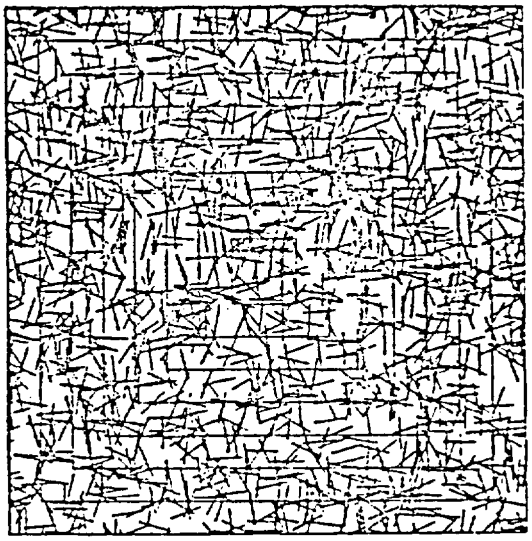

Figure 7. Fracture network for the case of l = 10 cm.

the boundary conditions. The permeability calculated in this way is the appropriate value to use in a regional flow model when the "study region" is an element in the model at a distance from the applied boundary conditions. Thus we have a study where we calculate permeability both as a function of scale and as a function of proximity to the applied boundary conditions.

For a given scale of measurement, when the permeability does not change as a function of distance to the boundary conditions, then we assume we have eliminated truncation error from the measurement. When the permeability does not change with increase in scale of measurement, then we have also estimated the assymtotic permeability. This assymptotic value of permeability is the same as the value of permeability one would find in a volume equal to or greater than the representative elementary volume (REV) of classical hydrology. An example of mean permeability results derived from the nested regions shown in Figure 7 is given in Figure 8. It is reasonably easy to confirm that we have eliminated truncation error. However, it may be difficult to determine the REV or the assymptotic value of permeability from the plots.

For systems where l is above the critical value, we expect that the permeability plots (like those shown in Figure 6) will be perfect ellipses if the scale of measurement is as large as the REV. However, we find that if the scale of measurement is smaller than the REV, the behavior may be erratic. Thus, systems which are connected and behave like equivalent continua on the infinite scale, may not behave like equivalent continua on a scale smaller than the REV. Thus if a system is above but near critical it may not behave like an equivalent continuum at practical field scales.

The results of these studies are plotted on Figure 9. The plot shows average directional permeability for systems with the same fracture frequency as a function of l. The relationship shown by the line on the plot is estimated based on the data from Figure 6 and other similar plots for different values of l. The "X"'s show data derived from plots like Figure 8. The assymptope for permeability is K_s where K_s, is taken to be the value which would be predicted using Snow's technique for infinite fractures. We estimate that the critical value of l to be about 9.

If this curve shown on Figure 9 can be fit to an analytical expression, then we have a relationship between permeability on the scale of the REV and fracture length for the fracture model we have adopted. It is worth repeating here that the fracture model we have adopted is a Poisson model, with constant length and aperture fractures and a specified orientation distribution. We would also like to know the theoretical

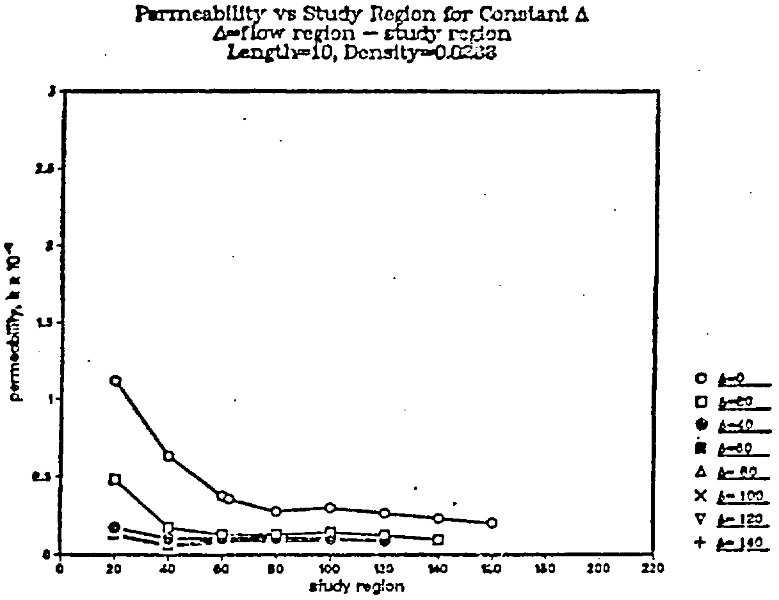

Figure 8. Permeability as a function of scale of measurement for various distances to the applied boundary conditions for the case of l = 10.

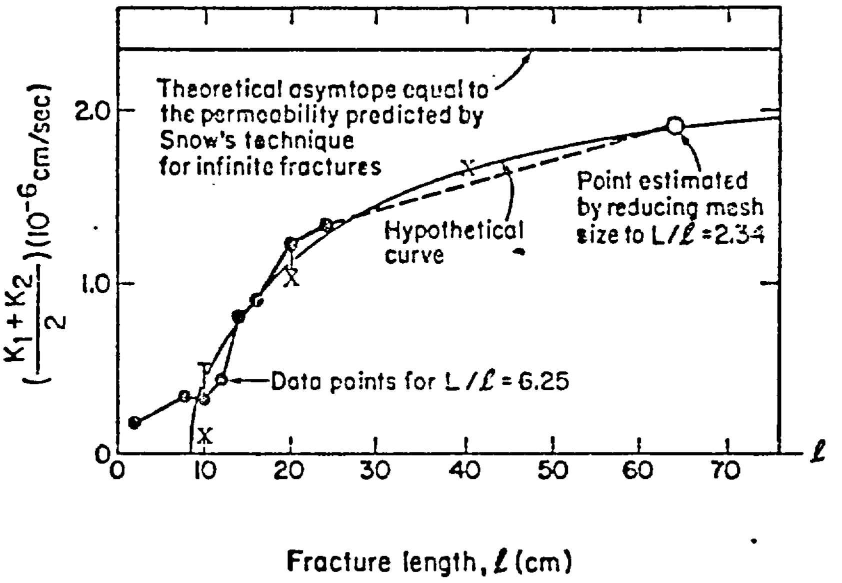

XBL 8410-9991

Figure 9. Previous data for average permeability as a function of degree of interconnection with X's showing new asymptotic data derived from the scale effect study.

relationship between the size of the REV and l. In other words, we would like to fit the curve shown in Figure 9 to an appropriate analytical expression. Further, we would like to know the expected value of permeability for scales of measurement smaller than the REV. In other words we would like to find an analytical expression to predict curves such those shown in Figure 8 for the case without truncation error. Answers to these questions may come from percolation theory.

Percolation theory has been extensively applied to lattice systems. Imagine, for instance a square lattice where the intersections of the lattice lines are called "sites" and the line segments between sites are called "bonds". Two types of problems are defined: site percolation and bond percolation. In bond percolation the bonds have some probability, p, of being present and conductive. When $p>p_c$, there is at least one infinite cluster of connected bonds where p_c is some critical value of p. Site percolation is similar. In this case we consider the probability of a site being occupied or not. Another type of site percolation looks at the squares formed by the lattice lines. In this case, p is the probability of a square being conductive, and $1-p$ is the probability of the square being non conductive.

Studies of conduction in such lattice systems use the conjectured relationship:

$$K \sim (p-p_c)^t \tag{2}$$

for $p \approx p_c$ and $p > p_c$; where K is the conductivity of the network on the infinite scale (Orbach, 1986; Englman et al., 1983: Balberg and Binenbaum, 1985, and others). At the other end of the scale, for $p = 1$, there is a maximum permeability which occurs when all the sites or bonds are occupied. Further, Orbach (1986) gives the relationship

$$\xi \approx a \mid p-p_c \mid^{-\nu} \tag{3}$$

Where a is the length of the sides of the squares in the lattice, ν is an exponent thought to be exactly equal to 4/3, and ξ is the correlation length or pair connectedness length for percolation. Orbach points out that between the limits of a and ξ, the percolating network exhibits self-similar geometry, that is, it is fractal. On length scales above ξ, the network appears to be homogeneous. In hydrologic terms, ξ is the REV.

We expect that similar relationships will hold for the random fracture systems we are studying. However we must find an expression for p in terms of the network geometry parameters if we are to use these equations. Robinson (1982) and Pike and Seager (1974) have suggested that the connectivity is a function of the average number of intersections per fracture. Hestir (1986) has shown that this number, which we call, ς is equal to

$$\varsigma = \lambda_A (\bar{l})^2 \int_0^{\pi} \int_0^{\pi} \sin \mid \theta_o - \theta \mid g(\theta) g(\theta_o)\, d\theta d\theta_o \tag{4}$$

where $g(\theta)$ is the orientation distribution of the fractures. This equation is of the form:

$$\varsigma = \lambda_A (\bar{l})^2 \Theta \tag{5}$$

where Θ is a function of the orientation distribution. This is consistent with the parameter study we describe above where we have fixed the product of λ_A and $\bar{l}$ so that our case, ς is proportional to l as we observed. With this in mind, our results are made dimensionless by plotting K/K_S versus ς. Because K_S is proportional to λ_l, these dimensionless results now apply to any value of λ_l.

This definition of ς differs from that used by Englman et al. (1983): $\varsigma_J = (\pi/4)\, \lambda_A \bar{l}^2$, which is based on making ς_J equal to the circular area swept out by rotating the fractures divided by the area of the sample. Besides not having the factor of $\pi/4$, our definition includes the factor Θ which accounts for the orientation distribution. Thus Θ, and therefore ς, will be zero if all the fractures are parallel which is not the case for ς_J.

Note also that in the above equation, ς is proportional to $\bar{l}^2$. Thus connectivity is a function only of the mean fracture length. However, Englman et al. show ς proportional to $\bar{l}^3$. Parameter studies using the same data as described above but allowing the fracture length to be distributed rather than constant have confirmed that permeability, which is controlled by connectivity, is only a function of $\bar{l}$. That is the moments of the distribution of fracture length, l have no effect. This is an important result, because it means that one only needs the mean value of fracture length, not the complete distribution to predict the permeability. So, we feel that ς is a better definition than ς_J for our purposes.

In order to apply Equations 2 and 3 it remains to define p as a function of ς. Jaeger et al. (1983) have suggested the use of the following:

$$p = 1 - e^{-\varsigma} \tag{6}$$

based on comparing p to the probability of N discs of diameter l overlapping, where $N = \lambda_A A$; A is the area of the sample. Hestir (1986) has shown that this definition of p is equal to the probability that a fracture of length $\bar{l}$ will intersect at least one other fracture. There may be a better way to define p, but for now if we accept this then we have from Equations 2 and 6:

$$K \sim C[(1-e^{-\varsigma}) - (1-e^{-\varsigma_c})]^t \tag{7}$$

or

$$K \sim C[(e^{-\varsigma_c} - e^{-\varsigma})]^t \tag{8}$$

which should apply for $\varsigma \approx \varsigma_c$. We know, as described above, that variation in the length distribution leaves this relationship unchanged. However, if the orientation distribution changes, Θ will change. It is not yet clear whether this change will leave t and ς_c invariant. We suspect that these parameters will not be invariant under changes in orientation distribution because lattices of different construction have different critical probabilities and exponents. However, this remains to be seen.

We now make the assumption that a in equation 3 is roughly equivalent to $\bar{l}$ and this gives:

$$REV = \xi \approx [(e^{-\varsigma_c}) - e^{-\varsigma})]^{-4/3} \tag{9}$$

or

$$REV = \xi \approx [(e^{-(\lambda_A(\bar{l})^2\Theta)_c}) - e^{-(\lambda_A(\bar{l})^2\Theta)})]^{-4/3} \tag{10}$$

If λ_l is substituted for $\lambda_A \cdot \bar{l}$, and $f(\theta)$ is measured, then the only unknown parameter needed to find the REV is $\bar{l}$. However, it is not clear that Equation 3, and therefore Equation 10 holds for variable fracture lengths. In fact, it is fairly certain that it does not. Clearly the REV will be larger if the fracture length is variable because it will take a larger sample to get a representative number of larger fractures. Perhaps we can find that a is a function of $\bar{l}$ and σ_l.

What is clear is that Equation 10 can be used to calculate only the minimum possible REV for a given fracture network. If length or aperture are variable, or if there are correlations between the various parameters, then the REV will be larger.

What now needs to be done is to find a rational expression for p as a function of ς and use our numerical data to determine the critical constants. Then we need to factor in the effect of the aperture distribution. Some promising work on this problem has recently been completed by Charlaix (1986). It also remains to show how correlations between length and aperture affect these relationships.

The Effect of Aperture Distribution on Transport Parameters

A second numerical study looked at transport in random fracture networks, Long and Shimo (1986). In this study the pattern of fractures in a two-dimensional network was fixed. It was assumed that the permeability is proportional to the aperture cubed, b^3 and the porosity is proportional to b. Then the apertures to the fractures were assigned in different ways but in all cases the mean value of b cubed, $E(b^3)$, is constant. Two factors were allowed to vary. These were the coefficient of variation of the hydraulic aperture ($\nu_b = \sigma_b/\mu_b$) and the correlation between fracture length and aperture, C. These cases are shown schematically in Figure 10. If the correlation between aperture and length is close to one, the long fractures get the larger apertures. The bulk average permeability of each network and the breakthrough curves under continuous injection were calculated .

The results in Figure 11 show that permeability and velocity decrease as the coefficient of variation of aperture increases. This is due to the fact that heterogeneity in conductivity in the network causes the larger conductors to have their flow restricted by smaller fractures which feed them. On the other hand, permeability and velocity increase as the correlation between length and aperture approaches 1. In the cases studied, dispersivity length increases slightly as the coefficient of variation of aperture increases or the coefficient of correlation decreases and it becomes increasingly difficult to find a unique fit based on the Fickian model. Correlation between length and aperture has the opposite effect from the behavior observed for coefficient of variation.

The Creation of Hypothetical Fracture Networks from Borehole Data

These results suggest a methodology for the hydrologic evaluation of homogeneously fractured rocks. One can develop a series of statistical parameter sets for the fracture networks which explain the measured permeability of the system conditioned by the observed fracture frequency, orientation distribution, and any other available data. Then from the breakthrough curve of a tracer test, velocity and dispersivity can be obtained. By comparing the transport behavior of the different fracture networks in numerical models (each defined by a different parameter set) to the field results we may be able to exclude many possibilities. This approach is attractive for sites where data is limited to surface and borehole investigations.

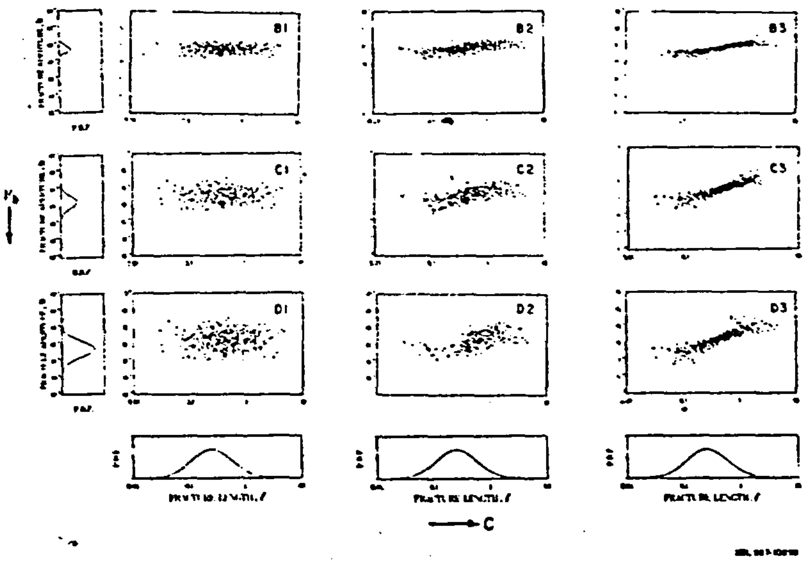

Figure 10. Cases of aperture variation versus correlation between length and aperture.

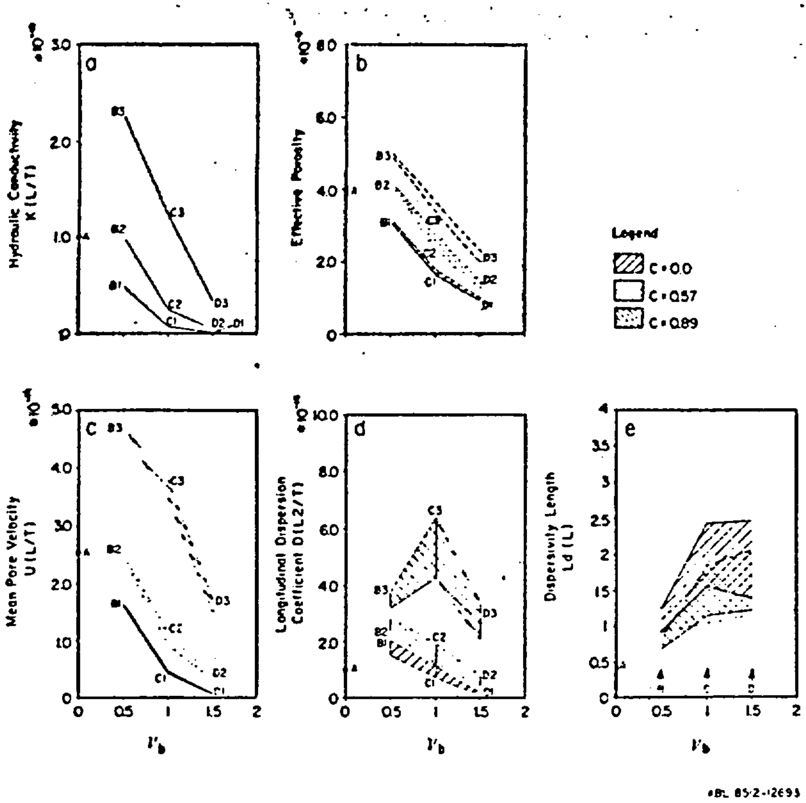

Figure 11. Results from the aperture variation parameter study.

In this approach, one first develops a conceptual model for the fracture network. In the present example, we used the same two-dimensional Poisson model as used in the previous study, where fractures are lines randomly located in space. This is rarely a good assumption and in general these techniques should be extended to three dimensions for accuracy and the Poisson model is not always appropriate. However, in a case where fracture are expected to be stratabound and sub-vertical, for example, a two-dimensional network may be appropriate.

Now, from the drilled, logged and well tested boreholes we have the following information: fracture frequency, λ_l; fracture orientation distribution, and values of permeability, K_m, estimated from pump tests. As explained above, we use the statistical relationship between λ_l, the mean fracture length, $\bar{l}$; the number of fractures per unit area, λ_A; and the orientation distribution of the fractures relative to the well. In the case that fractures are stratabound in sub-horizontal strata, the fractures are sub-vertical and the well is vertical the expression relating the length and density of traces in the horizontal plane of analysis to the frequency in the borehole is:

$$\frac{\lambda_l}{\cot\theta} = \lambda_A \bar{l} \qquad (11)$$

Given λ_l and the distribution of strike and dip, a variety of numerical models of fracture systems have been constructed by assuming the fracture length and calculating λ_A from Equation 11. An example plot of such models was shown in Figure 6. We can then calculate the permeability versus $\bar{l}$ for the value of λ_l observed in the borehole and different arbitrary values of b^3 as described above and in Long and Witherspoon

(1985) where b is the equivalent hydraulic fracture aperture. A schematic of such plots is shown in Figure 12a. Knowing K_m from the well test results then allows us to choose pairs of $\bar{l}$, λ_A, and b^3 which match the observed value of K_m, orientation distribution and fracture frequency.

The next step is to find networks with variable aperture which also can explain these observations. For each set of $\bar{l}$, λ_A, and $E(b^3)$, from Figure 12a, we can perform a parameter studies to prepare a plot like that shown in Figure 12b. This figure shows that a constant value of K_m, can be maintained by increasing $E(b^3)$ when ν_b, the coefficient of variation of aperture is increased.

At this point in our example we have identified four possible network parameter sets with constant equivalent hydraulic apertures which explain the data and for each of these four we have identified three more parameter sets with variable aperture which also explain the data. A total of 16 parameter sets have been found. This number can always be made larger by generating intermediate curves if necessary for matching data. However, our ultimate goal is to narrow the possibilities as much as possible. To that end we might look for independent information about the length and apertures of the fractures. This could come from well test analysis as suggested by Karasaki (1986) or geologic investigations. If we can determine that the fractures are more likely 10 m than 100 m or $E(b^3)$ is closer to 10^{-20} than 10^{-10} m for instance, then we might be able to ignore some of the points on Figure 12a and each of these would eliminate three more points on 12b from consideration.

So far we have ignored the distribution of fracture length. It seems that the connectivity of fracture systems depends much more strongly on the mean fracture length than it does on the standard deviation of

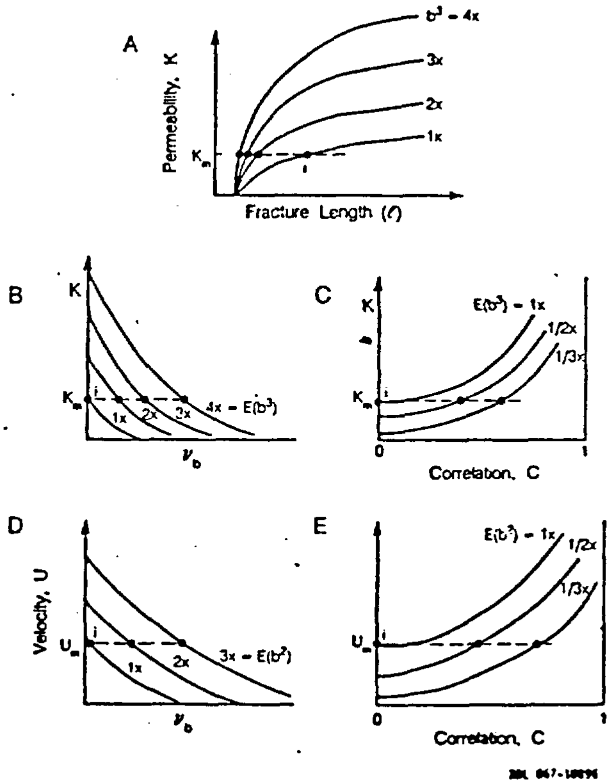

Figure 12. Schematic plots for deriving fracture network parameters.

fracture length (Long, 1986). So up to this point it is probably all right to ignore the standard deviation of length. However, if we wish to include a correlation between length and aperture we must allow length to be variable. We have not studied the effect of the standard deviation of length on transport parameters when the length is correlated to aperture. This may be important, but for now we will assume it is minor and pick an arbitrary, but realistic value for the coefficient of variation for length, ν_l, say 1.0. We continue in the same pattern and for each point on Figure 12b we construct the curves shown on Figure 12c. These curves tell us how to decrease $E(b^3)$ in order to maintain the same permeability when there is correlation between length and aperture. If we choose three curves on this plot we now have a total of 48 parameter sets to explain the data so far.

We now perform a tracer test in the boreholes. We obtain breakthrough curves and from these we obtain mean pore velocity, U, and dispersion length, L_l. We make the assumption that the hydraulic equivalent aperture, b is the same as the equivalent aperture for mixing b_m. This is not necessarily a good assumption. The actual relationship between b and b_m should be determined. Given the assumption, we model the tracer tests in fracture networks in order to produce of curves 12d and 12e for mean pore velocity instead of permeability. We look at mean pore velocity because it appears to be more sensitive to changes in network parameters than dispersion length. The curves generated in this manner will be similar to 12b and 12c, except that we plot of the curves for constant values of $E(b^2)$ because velocity is related to b^2 and permeability is related to b^3. Given $E(b^2)$ and ν_l we can calculate $E(b^3)$. Thus we should find a different set of values of ν_l, $E(b^3)$, and C which explain the mean pore velocity. Sets of ν_l, $E(b^3)$, and C which explain both the permeability and the pore velocity can now be identified. With luck, this will be a small but non zero subset of the original 48 sets.

Another attempt at refining our estimate of the fracture network parameters can be made by comparing the breakthrough curve from the field test with the breakthrough curves generated by the model results. High values of ν_l and low values of C result in flat breakthrough curves and large deviations from Fickian behavior. Small values of ν_l and large values of C result in steep breakthrough curves and small deviations from Fickian behavior. This information should give more confidence in some sets of parameters than others. Similar refinements to the estimate could be found by modeling other field tests such as resistivity measurements or cross hole tests or using other geologic information about the rock mass.

If we are able to reduce the probable fracture parameters to a small number, we can use these parameters to predict the behavior of the fractured rock mass under different conditions which is an important component of both reservoir engineering and waste storage problems.

Fracture Modeling of Fanay-Augeres

This section describes the approach to using field data to model three-dimensional fracture systems which we have developed over the past year in conjunction with BRGM of France. We recently completed a two-dimensional study of the fracture hydrology at the Fanay-Augeres mine in France (Long and Billaux, 1986). In this study we generated a network of fractures subregion by subregion where some of the properties of each subregion were predicted through geostatistics and some were randomly varied. Mean fracture length and fracture density in each subregion were the parameters obtained through geostatistical simulation. Fracture location within the subregion, actual fracture length, aperture and orientation were all chosen randomly. We have now designed an extension to this technique which generates three-dimensional disc-shaped fractures and allows regional fracture density variation through a simulation procedure which may be conditioned on data. Fractures are nucleated as "daughters" of a "parent" or seed which allows the simulation of swarms of fractures. The simulation allows for regional variation of density and orientation within each set of fractures.

The derivation of the model parameters from the field data has required refinement of the technique developed for two dimensional analysis. For three-dimensional analysis we must determine the disc diameter distribution from the trace length distribution. We also must develop parameters for the regionalized density and orientation distribution with a parent-daughter process rather than a simple Poisson distribution. These topics are briefly described below followed by an outline of the generation procedure. Application of this model to the site data will begin this year.

Determination of the Disc Diameter Distribution

In order to generate fractures in three dimensions from data which is essentially two-dimensional (drift wall mapping) or one-dimensional (well bore data) we need to make some assumptions about the shape and disposition of the fractures and derive the statistical relationships between the radii distribution, volumetric density, trace length distribution, frequency and areal density.

The two-dimensional analysis was designed to incorporate geostatistical simulation in fracture network analysis. Obtaining data for the two-dimensional analysis was relatively straightforward because the vertical plane of analysis was exposed in the drift. This made it possible to obtain the areal fracture density by counting the fracture traces in the plane and estimating the trace length distributions by direct measurement.

A three-dimensional analysis is necessary to achieve a realistic picture of the hydrology. However, can not see into the rock to count the number of fractures per unit volume and determine their shape. Perhaps geophysics will help us with this problem as described below, but for now we must use statistical geometry to estimate these parameters.

To make an estimate of fracture density we assume that the fractures are randomly located in space on the scale of the subregion (Poisson distribution). In order to estimate fracture size, it is necessary to make an assumption about the shape of the fractures and the type of distribution governing fracture sizes. We have assumed that fractures are discs. If the volume is cut by a plane, then the statistical relationship between λ_A, the areal density on that plane and λ_V, the volumetric density is:

$$\lambda_A = \lambda_V \, \bar{D} \, (\overline{\cos\theta}) \tag{12}$$

where $\bar{D}$ is the mean fracture diameter, $(\overline{\cos\theta})$ is a sampling orientation correction, and θ is the angle between the pole of each fracture and the plane of interest.

To determine λ_V we need to know $\bar{D}$, $\overline{\cos\theta}$, and λ_A. From the drift wall mapping we can obtain the θ, and λ_A and the distribution of trace length, l. Once we have the relationship between the distribution of l and $\bar{D}$, then we can calculate λ_V.

A functional relationship between the distribution of fracture trace lengths and the distribution of fracture diameters which has been developed by Warburton, (1980) is given below. In order to determine the parameters of the diameter distribution from this relationship one must assume the form of the distribution. Assuming that the fracture discs are orthogonal to the sampling plane. Warburton (1980) shows that:

$$\bar{g}(D) = \frac{1}{\bar{D}} D \, g(D)$$

$$f(l) = \frac{1}{\bar{D}} \int_{l}^{\infty} \frac{g(D)}{\sqrt{D^2 - l^2}} \, dD \tag{13}$$

Where

D = diameter of a given fracture
x = distance between the fracture center and the plane of intersection
l = h(x) = the trace length of the fracture in the plane

$g(D)$ = pdf (probability density function) of fracture diameters

$f(l)$ = pdf of fracture traces

$\tilde{g}(D)$ = pdf of disc diameters that intersect a given fixed plane

$\bar{D}$ = mean of $D \equiv \int_0^\infty D\, g(D)\, dD$

Given the above relationship one can assume the distribution of fracture diameters, $g(D)$ and evaluate the integral to obtain the distribution of trace lengths $f(l)$. One can then compare the computed distribution of trace lengths to that obtained from the field data. By trial and error, one can find a reasonable, but not necessarily unique distribution for fracture diameters.

To help frame the trial and error process we have extended Warburton's analysis to be able to calculate the relationship between the moments of $g(D)$ knowing the first two moments of $f(l)$ from the corrected distribution. This information in turn will guide initial choices of $g(D)$ in the trial and error process. The details of this derivation are given in Long and Billaux (1986). The results are given below.

If we call μ_l and σ_l the mean and standard deviation of trace length, then this analysis gives:

$$\mu_l = \frac{\pi}{4}\,\frac{E(D^2)}{E(D)} \tag{14}$$

and

$$\mu_l^2 + \sigma_l^2 = \frac{2}{3}\,\frac{E(D^3)}{E(D)}\ , \tag{15}$$

If we assume the diameter distribution is lognormal with mean μ_D and standard deviation σ_D, then

$$\mu_D = \mu_l \cdot \frac{128}{3\pi^3}\,\frac{1}{1+\frac{\sigma_l^2}{\mu_l^2}} \tag{16}$$

and

$$\sigma_D = \mu_l \cdot \frac{16}{\pi^2}\left\{\frac{2}{3[1+(\frac{\sigma_l}{\mu_l})^2]}\left[1-\frac{32}{3\pi^2[1+(\frac{\sigma_l}{\mu_l})^2]}\right]\right\}^{1/2} \tag{17}$$

Correction for Trace Length Truncation

A problem remains in that we do not have an infinite plane on which to observe l. Thus, we are not able to measure f(l) very well due to the truncation of visible traces. Baecher et al. (1977) and Warburton (1980) have both addressed this problem and a new approach was developed by Massoud and Chiles (1986) which does not require any a priori assumption on the shape of the distribution of length. This approach is described here.

Chiles and Massoud examined the trace length data from the Fanay- Augeres mine. They divided the data into three groups: fractures with no endpoint visible, fractures with one endpoint visible and fractures with both endpoints visible. For each of these groups, the relationship between the true distribution and the observed one were derived assuming all the fractures are parallel, at an angle θ with x axis.

The following notation is used in the development:

l	real length of a fracture trace
L	apparent length of fracture trace in the A by B box, $L \leq l$
$f(l)$	pdf of real length
$F(l)$	cdf of real length

$f_1(L)$	pdf of apparent length in group 1
$F_1(L)$	cdf of apparent length in group 1
u,x	axes of coordinates, see Figure 13
A	length of survey
B	height of survey
θ	angle between fractures and x axis
λ_A	density of trace centers

Figure 13 shows the survey plane.

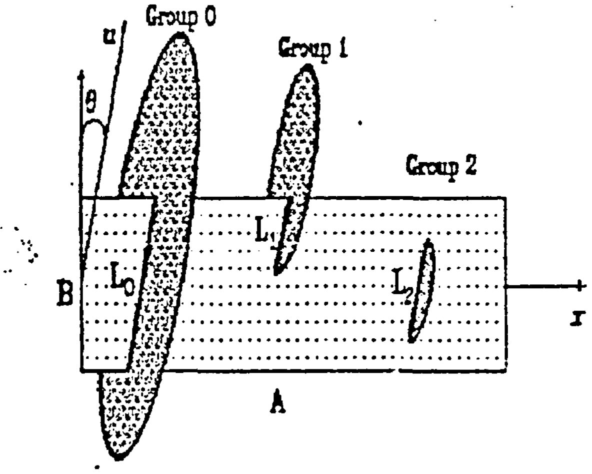

Figure 13. Survey Plane

For fracture traces with no visible end point (Group 0), the apparent length of all the fractures is only dependent on the angle θ because the fracture is truncated at both ends. Thus the trace length is $\frac{B}{\sin\theta}$. For a given fracture with center at (x,u), the probability of it to be in group 0 is equal to the probability for it to be long enough to transect the survey area. It can be shown that

$$E(N_0) = A\lambda_A \sin\theta \int_{\frac{B}{\sin\theta}}^{\infty} (l - \frac{B}{\sin\theta})\, f(l)dl \qquad (18)$$

This equation provides us with an estimate of the expected number of traces with no visible enpoints given the true distribution of trace lengths on an infinite plane.

If a fracture of length l has one visible end point, it is in Group 1. The value of l in this case can be either less than or greater than $\frac{B}{\sin\theta}$. By summing the integrals for these two cases we find that the expected number of traces with one truncated end is:

$$E[N_1(L_1,L_2)] = \int_{L_1}^{L_2} 2A\sin\theta[1-F(L)]dL \qquad (19)$$

If a fracture trace with both end points visible has a length l, then, it is in Group 2. The u coordinate of the center can have values which range over a distance $\frac{B}{\sin\theta} - l$. The x coordinate of the center can have values which range over a distance A. Thus the center must lie in an area of $(\frac{B}{\sin\theta} - l)A\sin\theta$. We can therefore show that:

$$E(N_2[l_1,l_2]) = \int_{l_1}^{l_2} (\frac{B}{\sin\theta} - l)\, A\sin\theta\lambda_A f(l)dl \tag{20}$$

Program LOI ("Law of lengths")

The program LOI, developed by Jean-Paul Chiles, uses the above equations as follows. Given $[A\lambda_A \sin\theta]$ and f(l), the integrals (equations 18, 19, 20) are computed over $]0,+\infty[$ for Group 0, and over specified intervals, $[x_i, x_{i+1}]$ for Groups 1 and 2. Doing this, we get the expected value of the number of fractures in Group 0, and each histogram interval in Group 1 and 2.

We then use trial and error to get λ_A and f(l). First, one makes a guess of the histogram of real length and of the number of trace centers in the survey area. The program, using the three derivations above, calculates:

- The number of traces with no endpoint, one endpoint and two endpoints
- The histogram of trace lengths with one endpoint
- The histogram of trace lengths with two endpoints

Both histograms are given in four classes from 0 to $\frac{B}{\sin\theta}$.

Now to find f(l) we first fit the 4 first classes using the "two endpoints" results and then fit the tail of the distribution, knowing that the 1 endpoint histogram is more sensitive to the middle of the distribution and the number of fractures with no endpoint is more sensitive to the tail. It is easy to fit the distributions, since we can fit the tail without changing the result for Group 2, and Group 2 depends only on the first four classes of real length.

Parent-Daughter Model

We often observe that fractures occur in swarms or zones. In order to model fractures in swarms we use a statistical description of this type of pattern called a "parent-daughter" model. In this model, the fracture swarms, or daughters are nucleated around seeds, or parents. The location of the parents may be purely random, ie a fixed rate Poisson process, or there may be a regional variation in the density of the parents. Once the parents have been determined, the daughters are found in some distance from the parents where this distance may, for example, have a normal distribution. The location of parents, location of daughters relative to their parents, and number of daughters are taken to be independent random quantities. Thus, implementation of the model requires that we know the distribution of the density of the parents, the distribution of the of the number of daughters per parent, and the distribution of the daughters around the parents.

There are two major difficulties in obtaining these distributions from the field data such as that available at Fanay-Augeres. The first problem is that it is not necessarily clear to which parent a fracture daughter belongs. This is further complicated by regional changes in the density of fractures. The second problem is that the parents and daughters are distributed in three-dimensional space but we can only observe traces. The centers of the traces are not the same as the centers of the fractures and the parent is a point that does not necessarily lie in the plane of observation. The first problem requires that we propose a parent daughter model and see how well it fits. Given a trial example of a three-dimensional parent daughter model with regional variation in density, Deverly (1986) worked out the statistics which would be observed on a plane. J. P. Chiles (1986) modified this derivation to account for the case that the daughters are disc shaped fractures rather than points. The result of Chiles work is that given assumed distributions for the parameters of the regionalized parent daughter model, we can calculate the theoretical variogram of fracture trace density on the plane. Then, we can compare the theoretical variogram with that derived from the drift wall mapping. Thus, we are now able to pick an appropriate regionalized parent daughter model by trial and error. This work is summarized below; details will be given in a later paper.

For the parent-daughter model, we have the following:

θ_G	density of parents (Poisson process)
M	number of daughters of a parent
θ_M	mean of M
σ_M^2	variance of M
F(x)	cdf of the location of a daughter relative to parent's location
f(x)	pdf associated with F
q	weight associated with a daughter
m_q	mean of q
σ_q^2	variance of q
x	point in R^n space of the process
B	domain of R^n corresponding to a sample
$I_B(x)$	indicator function, $I_B(x) = 0$ if $x \notin B$ $I_B(x) = 1$ $x \in B$
Q	a regionalized variable defined in B

Deverly's work was developed for application to the mining industry. He was attempting to understand ore deposits which were found as daughters around a parent (gold nuggets for example). Thus, the daughters were assigned a weight, q, that reflected the size of the ore body. In our problem, each daughter is a fracture with a weight of one. So, in this sense our problem is a subset of Deverly's problem. Deverly established that the regionalized variable Q(B) of the cumulative weights of the daughters included in B has the following moments (Deverly, 1986, p. 52 and Appendix A):

$$E[Q(B)] = \theta_G\, \theta_M\, m_q \int X(B,x)\, dx \tag{21}$$

$$\begin{aligned} \mathrm{Var}[Q(B)] &= \theta_G\, \theta_m (m_q^2 + \sigma_q^2) \int X(B,x)\, dx \\ &\quad + \theta_G\, E[M(M-1)]\, m_q^2 \int X(B,x)^2\, dx \end{aligned} \tag{22}$$

$$\begin{aligned} \mathrm{Cov}[Q(B),Q(B')] &= \theta_G\, \theta_M\, (m_q^2 + \sigma_q^2) \int X(B \cap B')\, dx \\ &\quad + \theta_G\, E[M(M-1)]\, m_q^2 \int X(B,x) X(B',x) dx \end{aligned} \tag{23}$$

where X(B,x) is the probability that a daughter of a parent located at x lies inside B. In this case for the vector U between the parent and a daughter:

$$X(B,x) = P\{x+U \in B\} = P\{U \in B_{-x}\} = F(B_{-x}) = \int I_B(y-x) f(y) dy$$

and

$$E[M(M-1)] = \theta_M^2 + \sigma_M^2 - \theta_M = \theta_M(\theta_M - 1) + \sigma_M^2 \tag{24}$$

So, given the parameters of a regionalized parent daughter model, Deverly has shown what the variograms observed on a plane, B will be.

Now we wish to extend Deverly's work to account for the fact that centers of traces are not necessarily center of fractures. Suppose one measures fracture density on a plane sample of the regionalized parent daughter process. Also, suppose the subregions over which density is measured are translations of the planar set B. The following assumptions are made and the results are relationships equivalent to those given above as derived by Deverly.

- Discs have a random diameter, D with expectation, $\overline{D}$
- The density of parents $\theta_G(x)$, $x \in R^3$, is a stationary random function with covariance C_θ that factors via

  $$C_\theta(x-x') = C_1(y-y')C_2(z-z')$$

  where $x = (y,z)$; $x' = (h',z')$; $x,x' \in R^3$; $y,y' \in R^2$; $z,z' \in R^1$.
- The pdf $f(u)$, $u \in R^3$ of daughter locations factors via

  $$f(u) = f_1(v)f_2(w)$$

  where $u \in R^3$; $v = (v,w)$; $v \in R^2$; $w \in R^1$.
- M has a Poisson distribution.
- $q=1$ with probability 1.

If B_h $h \in R^2$ is the translation of set B by h, then $Q(B_h)$ is the number of daughters in set B_h because $q = 1$. Chiles has shown that:

$$E(Q(B_h)) = \overline{\theta}_G\theta_M\overline{D}K(0)$$

where

$$E[Q(B)Q(B_h)] = \overline{\theta}_G[\theta_M\overline{D}K_1(h) + \theta_M^2\alpha\overline{D}g_1 * K_1(h)] + \theta_M^2\overline{D}^2\int C_1 * g_1(h+t)K(t)dt = C * K(h) \tag{25}$$

$$K_1(h) = \int I_B(x-h)I_B(x)dx,$$

and

$$g_1(h) = f_1 * f_1(h)$$

and

$$C(h) = \overline{\theta}_G[\theta_M\overline{D}K_1(h) + \theta_M\alpha\overline{D}g_1(h)] + \theta_M^2\overline{D}^2C_1 * g_1(h)$$

with α a constant, $0 \leq \alpha \leq 1$. Now, given the parameters of the regionalized parent-daughter process for discs in space we can calculate the variogram of fracture density as it would appear on a plane B.

Program SALVE

The preceding results have been incorporated in the program SALVE written by J.P. Chiles. To use this program we estimate the density of parents, mean number of daughters, distribution describing the dispersion of the daughters, distribution of the size of discs and the variogram of the density of parents. Given these and the size of the support sample (ie the subregion volume over which density is measured), the program calculates the variogram of the fracture density on a plane. This variogram can then be compared to the variogram derived from the field data. We can then change the estimates of the regionalized parent-daughter model until a good fit to the variogram is found. In this way we can derive a model which agrees with our data.

In implementing this trial and error process, the following guide lines may be used:

- The known number, N, of traces on the survey area is

  $$N = \theta_G \cdot \theta_M \bar{D} \cdot s \tag{26}$$

  where s is the known area of the survey, and $\bar{D}$ is the known mean fracture diameter. We then know the product $\theta_G \cdot \theta_M$. To separate θ_G and θ_M, one can use the variograms of the interdistances. These should contain two peaks, one at the typical daughter interdistance and one at the typical parent interdistance.
- When the variogram is computed from values averaged over an area, the range is longer than the range of the variogram of the same variable computed from point values. The difference is approximately equal to the length of the area over which the averaging took place.
- If σ_D is the standard deviation of daughters around parents, a_p is the range of the variogram of the density of parents, and a_d is the range of the variogram of the density of all points, then

  $$a_d \approx a_p + (c \cdot \sigma_D) \tag{27}$$

  where c is between 2 and 3.
- To increase the sill of the variogram of the fracture density calculated by SALVE, one can either increase the number of daughters per parent and decrease the density of parents, while keeping the produce constant, or increase the sill of the variogram of the density of parents.

When a good fit is found, we have obtained an estimate of the parameters for the parent daughter model which can be used to simulate the density of parents in each subregion. This simulation plus the other parent daughter parameters are used to generate realizations of the fracture system as described in the last section.

Orientation

Within a given set there may be a large dispersion in orientation. However locally, especially within a swarm, the orientation distribution may be quite narrow. Thus orientation has spatial structure. To account for this we can construct variograms for orientation. These variograms typically will have a nugget which represents the local random variation of orientation. If this nugget is subtracted from the variogram, the result can be used in a simulation to predict the spatial variation of mean orientation on a grid throughout the region. Now when a particular fracture is nucleated by the process described below the orientation can be found by interpolating the local mean orientation from the nearest neighbor grid points and adding to that a random component dictated by the nugget of the variogram. This results in fracture trace patterns as sketched in Figure 14.

Generation Scheme

The following steps are taken to create a realization of the fracture system once an acceptable parent daughter model has been obtained.

1. Using the parent-daughter model, a simulation of the spatial variations of the fracture model parameters (ie the density of the parents, distribution of the number of daughters per parent etc) is made in a three-dimensional region.
2. Define subregions on the same scale as the sample support.
3. For each subregion, read the strength of the parent Poisson process from the simulation.
4. From this Poisson process, pick the number of parents to be generated in the subregion.
5. To locate each parent, pick random values of x,y,z in the subregion.
6. Pick the number of fracture daughters from the distribution determined above.

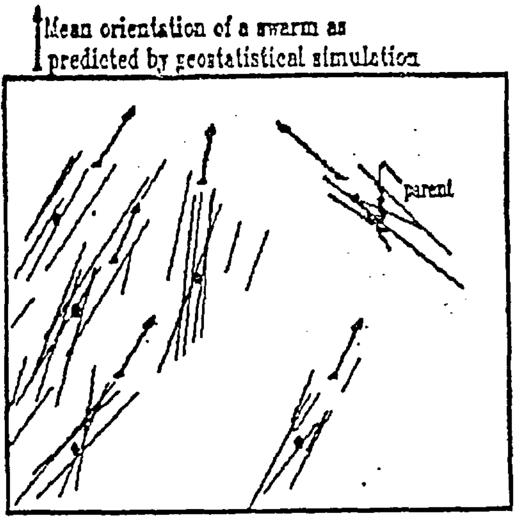
Mean orientation of a swarm as predicted by geostatistical simulation
parent

Figure 14. Fracture trace patterns for a regionalized parent-daughter model with regional orientation variation.

7. Pick the random locations of the fracture centers distributed around the parent. This may be an anisotropic distribution.
8. Pick the orientation in two steps. First, pick the continuous part from the simulation described above. Then add a random component as determined by the nugget of the orientation variogram.
9. Pick the fracture length and aperture from the global distributions.

Application of this statistical model to the Fanay-Augeres data is now underway.

Well Testing Results for Fractured Rock

From the above parameter studies, we have seen that fracture geometry, especially hydraulic aperture, controls hydrologic behavior. In our Fanay-Augeres studies, as well as many other field studies, the data on hydraulic aperture are the data in which there is the least confidence. The reasons for this are that the only way to obtain a good estimate of the hydraulic aperture is to perform a hydraulic test. Only an hydraulic test can integrate the effects of the void geometry in the fracture. The only available insitu hydraulic test is a well test of some kind. These tests should be designed and interpreted based on the likely behavior of a fracture network in an impermeable matrix.

Karasaki et al (1985) have developed a new well test solution particularly for fracture networks (Figure 15). This solution is based on a composite conceptual model of the flow system (Figure 16). In the inner region the flow is assumed to be linear through a finite number of fractures, n. These fractures have the same hydraulic equivalent aperture, b, permeability, k_1, and storage capacity $(\phi c_t)_1$. In the outer Region 2, the flow is radial and the permeability and storage capacity are k_2, and $(\phi c_t)_2$ respectively. The radius of the well is r_w and the radius between the inner and outer regions is r_f. The distance, r_f, is the distance from the wellbore where the radial flow regime takes over the system response under well test conditions. In practice, r_f is related to, but not necessarily equal to the fracture length. It is assumed that there is an infinitesimally thin ring of infinite permeability between the two regions so that otherwise incompatible boundaries can be matched.

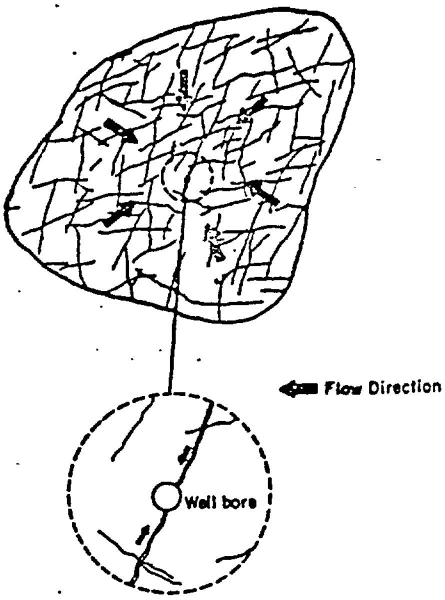
Flow Direction
Well bore

Figure 15. Flow to a well in a fracture-dominated system (after Karasaki, 1986).

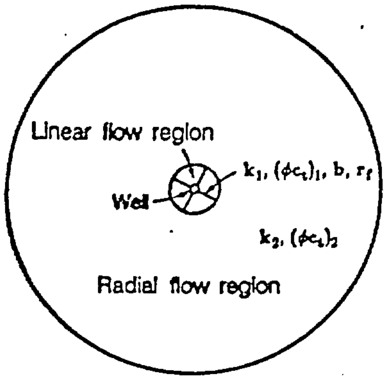
Linear flow region
$k_1, (\phi c_t)_1, b, r_f$
Well
$k_2, (\phi c_t)_2$
Radial flow region

XBL 8412-6193

Figure 16. Composite model of fracture dominated system with linear and radial flow regions (after Karasaki et al., 1985).

Karasaki et al. (1985) introduce the following dimensionless parameters:

$$p_D = \frac{2\pi k_2 h(p_i - p_w)}{q\mu}$$

$$t_{Dr_f} = \frac{k_2 t}{\mu(\phi c_t)_2 r_w^2} \cdot \frac{r_w^2}{r_f^2} = \frac{\alpha_2 t}{r_f^2}$$

$$r_D = \frac{r}{r_f} ,$$

$$r_c = \frac{r_w}{r_f} ,$$

$$\alpha_c = \frac{k_1}{\mu(\phi c_t)_1} \cdot \frac{\mu(\phi c_t)_2}{k_2} = \frac{\alpha_1}{\alpha_2} ,$$

$$\beta = \frac{nbk_1}{2\pi r_f k_2} .$$

In terms of these parameters, the solution for dimensionless pressure drop in Region 1 is:

$$p_{D_1} = \frac{4\alpha_c}{\pi^2} \int_0^\infty \frac{1 - e^{-\xi^2 \alpha_f}}{\xi^3} \cdot \frac{\cos\left(\dfrac{r_D - r_c}{\sqrt{\alpha_c}}\xi\right)}{\Psi^2 + \Lambda^2} \, d\xi$$

$$(r_c \le r_D \le 1) \qquad (28)$$

and in Region 2, the solution is:

$$p_{D_2} = -\frac{2\sqrt{\alpha_c}}{\pi} \int_0^{\infty} \frac{1 - e^{-\xi^2 t_{D_r}}}{\xi^2} \times$$

$$\times \frac{\Lambda \cdot J_o(\xi r_D) + \Psi \cdot Y_o(\xi r_D)}{\Psi^2 + \Lambda^2} \, d\xi$$

$$(1 \le r_D < \infty) \tag{29}$$

where:

$$\Psi = -\sqrt{\alpha_c}\, J_1(\xi) \cdot \cos\left(\frac{1-r_c}{\sqrt{\alpha_c}}\,\xi\right) + \beta J_o(\xi) \cdot \sin\left(\frac{1-r_c}{\sqrt{\alpha_c}}\,\xi\right)$$

$$\Lambda = \sqrt{\alpha_c}\, Y_1(\xi) \cdot \cos\left(\frac{1-r_c}{\sqrt{\alpha_c}}\,\xi\right) - \beta Y_o(\xi) \cdot \sin\left(\frac{1-r_c}{\sqrt{\alpha_c}}\,\xi\right)$$

Details of the development of these equations as well asymptotic solutions for small and large values of time are presented in Karasaki (1986).

Equations 28 and 29 have been evaluated and the results plotted in the form of type curves for use in evaluating the results of field data (Karasaki et al., 1985; Karasaki, 1986). Figure 17 presents an example of these type curves for Region 1 ($r_c < 0.05$) to illustrate the effect on transient pressures of β, which is the ratio of permeability in inner Region 1 to that of outer Region 2. It may be seen that at early time, the curves exhibit the expected half slope for linear flow in Region 1. At later times, the effects of radial flow in Region 2 become dominant.

Figure 18 presents the results obtained by taking the partial derivative of Equation 28 with respect to $\ln(t_{D_r})$ for the same conditions as used in obtaining the results shown on Figure 17. It is apparent that as the β term increases from 0.1 to 100, the time for the start of infinite acting homogeneous behavior increases more or less proportional to β.

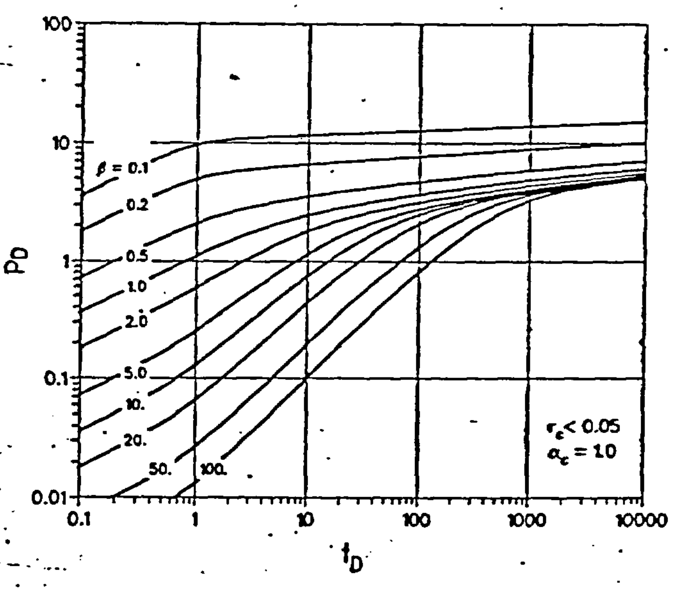

Figure 17. Dimensionless pressure versus dimensionless time for fracture dominated system (after Karasaki et al., 1985).

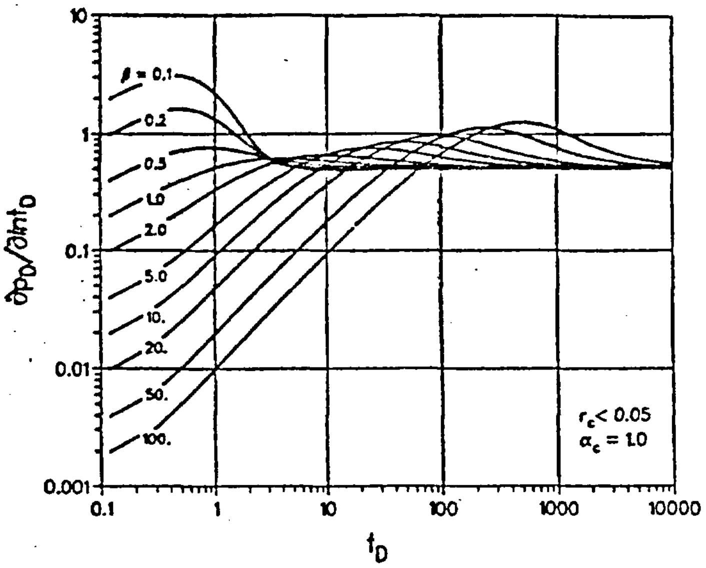

Figure 18. Derivative of dimensionless results for fracture dominated system (courtesy K. Karasaki).

These and similar results developed by Karasaki (1986) can be used in interpreting well tests in fractured rock. If successfully matched they will provide an estimate of the hydraulic aperture b, of the fractures intersecting the test zone, and estimate of the length scale of the fractures, and a better estimate of the average formation properties.

Seismic Tomography Studies for Fracture Detection and Characterization

Geophysical methods provide one of the best potential tools for obtaining the geometric data we would like to have to analyze fracture network behavior. In particular, LBL is investigating the use of three component vertical seismic profiling (VSP) for fracture detection and characterization. Fracture detection using P and S waves in VSP studies is not a new idea, (Stewart et al., 1981). It is becoming increasingly apparent, however, that to utilize the full potential of VSP, 3-component data should be acquired. It is important to record the three components of signal because of the phenomenon of shear wave splitting. When a shear wave passes through a fracture, the shear component splits into two parts, one faster than the other, (Crampin 1978, 1984a,b, 1985). The fast wave is unaffected by the fracture as it is associated with the component of particle motion parallel to the fracture. The slow part is associated with the component of particle motion perpendicular to the fracture. It is attenuated and slower slower because the stiffness across the fracture is less than that along the fracture.

Recent laboratory (Myer et al., 1985) and theoretical work Schoenberg (1980, 1983) explains shear wave anisotropy in terms of fracture stiffness. The fracture stiffness theory differs from Crampin's theory in that at a fracture, or a non-welded interface, the displacement across the surface is not required to be continuous as a seismic wave passes, only the stress must remain continuous. This displacement discontinuity is taken to be linearly related to the stress through the stiffness of the discontinuity.

The implication of the fracture stiffness theory is that for very thin discontinuities, for example fractures, there can be significant effect upon the propagation of a wave. In fact, the thickness of the fracture can be much much less than the seismic wavelength. This stiffness theory is also attractive from several other points of view. Schoenberg (1980, 1983) shows that the ratio of the velocity of a seismic wave perpendicular and parallel to a set of stiffness discontinuities is a function of the spacing of the discontinuities as well as the stiffness. Thus, given the stiffness and the velocity anisoptropy, one could determine the average fracture spacing of density. Or, alternatively, given independent information on fracture density, one could determine the fracture stiffness and hopefully relate this stiffness to actual fracture properties such as discriminating between filled and open fractures or hopefully hydraulic conductivity. In any case, there is sufficient reason to expect fracture content and properties to be reflected in the velocity, amplitude, and polarization of the shear waves.

In addition to describing structure and fracture content we are also hoping to relate the seismic response of the rock mass to the hydrologic response. The idea is to tomographically map the variation in the P-, SV-, and SH-wave properties and relate the resulting anomalies to the actual fracture density, orientation, and spacing. In order to learn how to do this, we have begun a numerical study. In this study we take the same two-dimensional fracture networks used for hydrologic parameter studies and model the progress of a seismic wave through the network. In this way we can compare the seismic response to the hydrologic response. In the programs that we have developed we have incorporated the effect of fracture stiffness (Myer et al. 1985) in addition to the effect of the bulk rock properties. In fact, as described at the begining of this paper, we are studying the relationship between fracture void geometry and both hydraulic behavior and stiffness. Such a study will allow us to create a fracture network with values of fracture stiffness and permeability which both conform to the same geometry.

An example of this approach is shown in Figure 19. Shown are ray paths through a model of fractured rock. The area modeled in Figure 19 is 1 km by 1 km. The fracture pattern is non-uniform and two distinct densely fractured regions are near the center of the section. The upper fractured region is more densely fractured than the lower. Only one set of cross-hole ray paths are shown on the plot, but many were calculate from the assumed boreholes on the left and right sides of the plot. Figure 20 shows an initial crude tomographic reconstruction based only on the P-waves velocities. The darker areas are slower velocity indicative of higher fracture density. Because this was cross hole tomography, there is poor horizontal resolution. However, we do see darker patches at two levels which correspond to the two highly fractured zones. We also have the capability to model SV- and SH-waves as well which should greatly improve the interpretation. As explained above, the aim is to use the times, amplitudes and polarizations of the P-, SV-, and SH-waves to map fracture properties.

A significant question that remains to be answered is the scale effect of stiffness. If we use stiffnesses of fractures that have been measured in the laboratory in our kilometer size model, we see no effect on the seismic waves. To see an effect we must assume that stiffness scales as the square of the length of the fracture. Because we have in fact observed effects of fractures in field cases at kilometer size scales, (Majer et al 1986), we assume that there must be a scale effect.

In conclusion, we are carrying out field and modeling studies to determine the effect of fracture on the propagation of seismic waves. The goal is to be able to map the orientation, density, and spacing of fracture sets in the field and to be able to provide useful hydrologic information. To date we have seen that fractures do have a significant effect on seismic waves. Hopefully, through modeling and controlled field experiments we will be able to quantify this effect.

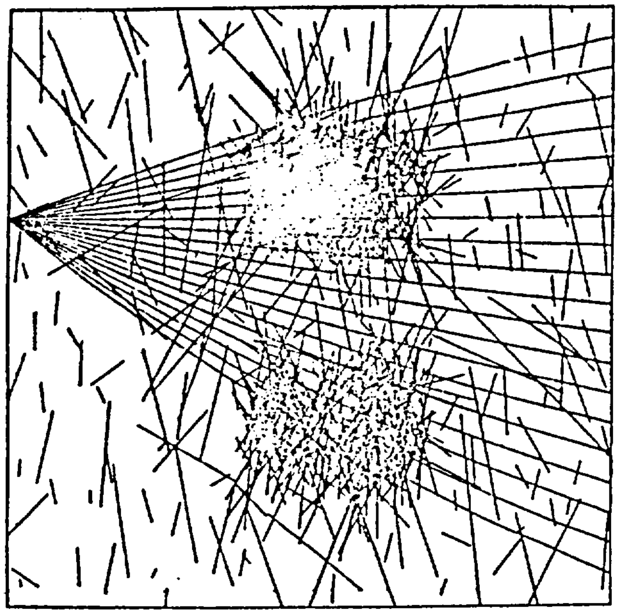

Figure 19. Model of a two-dimensional heterogeneous fracture network shown in ray paths (courtesy of J. Peterson).

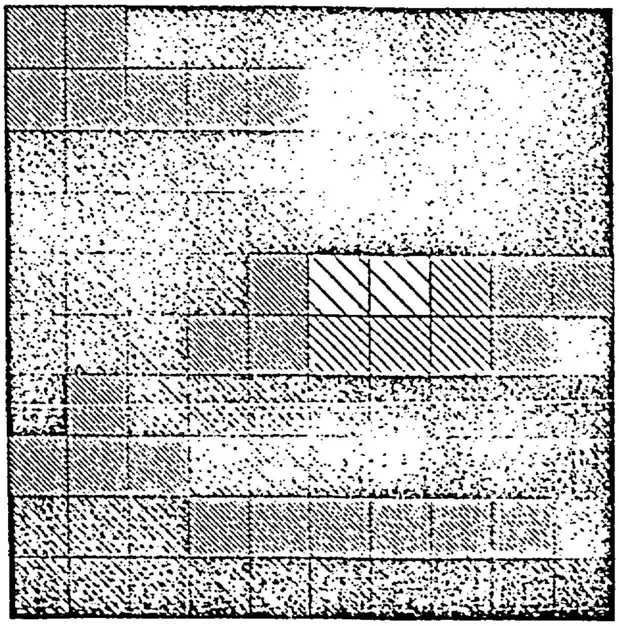

Figure 20. Tomographic inversion of the synthetic seismograms derived from Figure 18 based on P-wave velocities (courtesy of J. Paterson).

CONCLUSIONS

This paper is a review of recent work which represents various aspects of our approach to modeling flow and transport in fractures. There is very little in this paper describing actual modeling techniques, vis-a-vis finite element or boundary element methods etc. The application of such models to fractures can be complex, but for the most part, the numerical problems are well posed and solvable, if not always efficient. It is rather, the definition of the problem to be solved by numerical techniques that is difficult. As such the approach we are pursuing is largely concerned with the definition of the geometry of fractures. Further studies then are aimed at determining how the geometry controls the behavior.

Because defining the geometry is difficult, we are trying to use every tool available. We bring geology and statistics to bear on data we can observe and we use improved well testing and geophysics to expand our ability to observe. Parameter studies of the behavior of fractures helps to point out what is important to observe. In general, when we can not understand the behavior on a given scale, we try to characterize the geometry on a finer scale and determine how this geometry controls the behavior. Thus we study single fracture behavior so that we can correctly model flow in a network. Finally, attempts to analyze field data and match insitu behavior serve to identify areas where the development of new techniques are needed.

ACKNOWLEDGMENTS

I would like to acknowledge the scientists whose work is represented in this paper: Daniel Billaux, Jean-Paul Chiles, Neville Cook, Kevin Hestir, Satoshi Immamura, Deborah Hopkins, Kenzi Karasaki, Ernest Majer, K. Muralidhar, Larry Myer, John Peterson, Laura Pyrak-Nolte, Michito Shimo and Paul Witherspoon. This work was supported by the U.S. Department of Energy under contract No. DE-AC03-76SF00098.

REFERENCES

Baecher, G. B., N. A. Lanney, and H. H. Einstein, (1977). Statistical descriptions of rock properties and sampling, *Proceedings 18th U. S. Symposium Rock Mechanics*, pp. 5C1-1-5C1-8.

Balberg, I. and N. Binenbaum, (1983). Computer study of the percolation threshold in a two-dimensional anisotropic system of conducting sticks, *Physical Review B*, Vol. 28 (7) p. 3799.

Billaux, D., J. Long, J.-P. Chiles, K. Hestir, (1986). Modifications to the three-dimensional disc model, Earth Science Division, Lawrence Berkeley Laboratory, Progress Report for CRP, in preparation.

Charlaix, E., E. Guyon, S. Roux, (1986). Permeability of a random array of fractures of widely varying apertures, paper in preparation.

Crampin, S., (1978). Seismic-wave propagation through a cracked solid: polarization as a possible dilatancy diagnostic, *Geophys. J. Roy. Astron. Soc.*, Vol. 53, pp. 467-496.

Crampin, S., (1981). A review of wave motion in anisotropic and cracked elastic-media: *Wave Motion*, Vol. 3, pp. 343-391.

Crampin, S.,(1984a). Effective anisotropic propagation through a cracked solid, Proceedings of the First International Workshop on Seismic Anisotropy, S. Crampin, R. G. Hipkin, and E. M. Chesnokov, eds. *Geophys. J. Roy. Astron. Soc.*, Vol. 76, pp. 135-145.

Crampin, S., (1984b). Anisotropy in exploration seismics, *First Break*, Vol. 2, pp. 19-21.

Crampin, S., (1985). Evaluation of anisotropy by shear wave splitting, *Geophysics*, Vol. 50 (1), pp. 142-152.

Deverly, F. (1984). Echantillonnage et Geostatistique, These l'Ecole National Superierure des Mines de Paris.

Englman, R., Y. Gur, Z. Jaeger, (1983). Fluid Flow Through a Crack Network in Rocks, *Journal of Applied Mechanics*, Vol. 50 p. 707.

Hasslacher, B., (1985). Tiling, Complexity and Statistical Scaling in Chaotic Systems, Los Alamos Preprint, LA-UR-85-2435, Los Alamos National Laboratory, Los Alamos, New Mexico 87545, submitted to *Physica D.*

Hestir, K., (1986). Lawrence Berkeley Laboratory, personal communication.

Hopkins, D. L., N. G. W. Cook, L. R. Myer, (1986). Estimation of Joint Stiffness, Abstract in 33rd Pacific N.W. Regional Meeting of AGU, University of Washington, Seattle, September 4-5.

Karasaki, K., (1985). Well Test Analysis in Fractured Media, Ph.D. Dissertation, University of California, Berkeley, 239 pp.

Long, J. C. S., J. S. Remer, C. R. Wilson, P. A. Witherspoon, (1982). Porous media equivalents for networks of discontinuous fractures, *Water Resources Research* Vol. 18, (3) pp. 645-658.

Long, J. C. S., (1983). Investigation of Equivalent Porous Medium Permeability in Networks of Discontinuous Fractures, Ph.D. Dissertation, University of California, Berkeley.

Long, J. C. S. and P. A. Witherspoon, (1985). The relationship of the degree of interconnection to permeability in fracture networks, *Journal of Geophysical Research,* Vol. 90 (B4) pp. 3087-3098.

Long, J. C. S. and D. Billaux, (1986). From field data to fracture network modeling - An example incorporating spatial structure, submitted to *Water Resources Research.*

Long, J. C. S., (1986). Permeability of homogeneous fracture systems, in preparation.

Long, J. C. S. and M. Shimo, (1986). The control of fracture aperture on transport properties of fracture networks, submitted to *Water Resources Research.*

Massoud, H., and J. P. Chiles, (1986). La modelisation de la petite fracturcation par les techniques de la geostatistique, BRGM report in preparation

Majer, E. L., T. V..McEvilly, F. S. Eastwood, and L. R. Myer, (1986). Fracture detection using P- and S-wave VSP's at The Geyers Geothermal Field, *Geophysics*, (in press).

Muralidhar, K. and J. C. S. Long, (1986a). A scheme for calculating flow in fracture channels using numerical grid generation in three-dimensional domains of complex shapes, report in preparation.

Muralidhar, K. and J. C. S. Long, (1986b). A new approach to characterizing flow in single fractures, Abstract submitted to the 1986 AGU Fall Meeting, San Francisco.

Myer, L. R., L. J. Pyrak-Nolte, N. G. W. Cook, (1986). Experimental determination of fracture void geometry, LBL Progress Report for CRP, Lawrence Berkeley Laboratory, University of California, Berkeley in preparation.

Myer, L. R., D. L. Hopkins, and N. G. W. Cook, (1985). Effects of an interface in partial contact on attenuation of acoustic waves, *Geophysics*, (in press).

Orbach, R. (1986). Dynamics of Fractal Networks, *Science*, Vol. 231, p. 814.

Pike, G. E. and C. H. Seager, (1974). Percolation and conductivity: A computer study I and II, *Phys. Rev. B*, Vol. 10, p. 1421.

Robinson, P. C., (1982). Connectivity of fracture systems - A percolation theory approach, report, Theoretical Physics Division, AERE Harwell, Oxfordshire.

Schoenberg, M., (1980). Elastic wave behavior across linear slip interfaces, *Journal Acoust. Soc. Am.*, Vol. 68, (5), pp. 1516-1521.

Schoenberg, M., (1983). Reflection of elastic waves from periodically stratified media with interfacial slip, *Geophysical Prospects*, Vol. 31, pp. 265-292.

Snow, D. T., (1965). A Parallel Plate Model of Fractured Permeable Media, Ph.D. Dissertation, University of California, Berkeley, 331 pp.

Stewart, R. R., R. M. Turpening, and M. N. Toksoz, (1981). Study of a subsurface fracture zone by vertical seismic profiling, *Geophysical Research Letters*, Vol. 8, pp. 1132-1135.

Warburton, P. M., (1980). A stereological interpretation of joint trace data, *International Journal Rock Mechanics Mining Science and Geomechanical Abstracts*, Vol. 17, pp. 181-190, Pergamon Press Ltd.

RADIONUCLIDE MIGRATION BY WATER FLOW AND DIFFUSION THROUGH SMECTITE BARRIERS

ROLAND PUSCH

Swedish Geological Co, and Lund University of Technology and Natural Sciences, Lund, Sweden

Interlayer or "internal" water forming a large part of the total water content at high bulk densities is strongly attached to the smectite lattices. Water flow as well as anion diffusion through dense clays of this sort therefore only take place in a relatively small number of interconnected, wider pores. This number increases very rapidly when the density drops, which explains why the hydraulic conductivity of dense smectite clays is extremely low, while it is orders of magnitude higher when the density is increased by as little as 30 %. This phenomenon is particularly obvious in Na montmorillonite, which is discussed in the article.

The heterogeneous microstructure causes a large variation in flow rate over an arbitrary cross section, such that reasonably correct flow models should be based on probabilistic reasonings.

1 Introduction

For accurate mathematical modelling of coupled processes like thermally affected water migration, ion diffusion, and creep, the physics involved in the respective process must be known in detail. This is a complex matter even in the apparently simple case of soils consisting of rock-forming minerals as illustrated by the wellknown difficulty of predicting, accurately, water/vapor movement in partly saturated tilled ground exposed to cyclic thermal gradients [1]. The complexity is much greater for strongly hydrophilic minerals like smectites since they affect the mobility of the porewater, and their microstructure, which is strongly dependent on the porewater chemistry, density, and temperature, is a determinant of the hydraulic conductivity and ion diffusivity. Since these two properties are of major importance for the isolating function of engineered smectite-based barriers, they deserve special attention. This article deals with the relation between the microstructure and the permeability and ion diffusivity of such barriers on a microscopic scale, with special respect to the possibility of relevant mathematical modelling. The discussion is confined to the smectite family member montmorillonite in sodium form.

2 Hydration of Na montmorillonite

The exact nature of the uptake of water by expandable clay minerals is still not completely understood since this process is very much dependent on the crystal lattice constitution of montmorillonite, of which there are two possible versions (Fig 1). The hydration of the Edelman & Favejee structure has been explained as the formation of an ice-like water lattice that grows from the protruding hydroxyls of the basal planes when the interlamellar cations are monovalent and small (Li and Na). A number of metastable and stable states of the H-bonded lattice appear, implying a successive establishment of 1, 2 and 3 interlayer hydrates as manifested by diagnostic basal layer spacings in X-ray diffractograms.

On wetting of the Hofmann, Endell & Wilm structure the orientation and mutual interaction of th water molecules as well as their association with interlayer cations and crystal lattices ar altered in the successive build-up of interlayer hydrates, the expected degree of ordering bein low, particularly of the second and third hydrates.

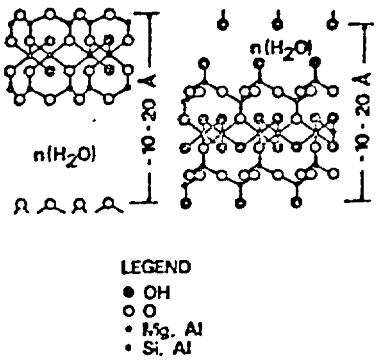

Fig 1 The montmorillonite crystal lattice. Left: The Hofmann/Endell/Wilm structure. Right: The Edelman/Favejee version

Spontaneous expansion beyond 3 hydrates of montmorillonite stacks in unconfined gels, yielding complete dispersion of the lamellae would be expected at low electrolyte concentration according to classical colloid chemistry and it has also been observed in Li montmorillonite. Recent research indicates that the hydration of Na montmorillonite leads to a stable condition of fully expanded stacks separated by rather large volumes of "external" water. Thus, the expansion of the stacks or domains does not seem to proceed beyond 3 hydrate layers and do not yield dispersion [2, 3]. The lattice-associated hydrates in interlayer positions are termed "internal" water.

3 Microstructure of engineered smectitic barriers

3.1 Soft Na montmorillonite gels

It follows from the preceding text that Na montmorillonite, if free to expand, forms an open microstructural pattern which is honeycomb-like as verified by electron microscopy (Fig 2). The regularity is very obvious for expanded soft gels of this type, a practical example being the front part of Na bentonite injected in rock fractures for sealing purposes. A microstructure of this sort is expected to be very uniformly percolated by flowing water and penetrated by diffusing ions, which means that the macroscopically determined average hydraulic conductivity as derived from permeameter tests is valid, in principle, also on a microscopic scale. This would be the case also for diffusion.

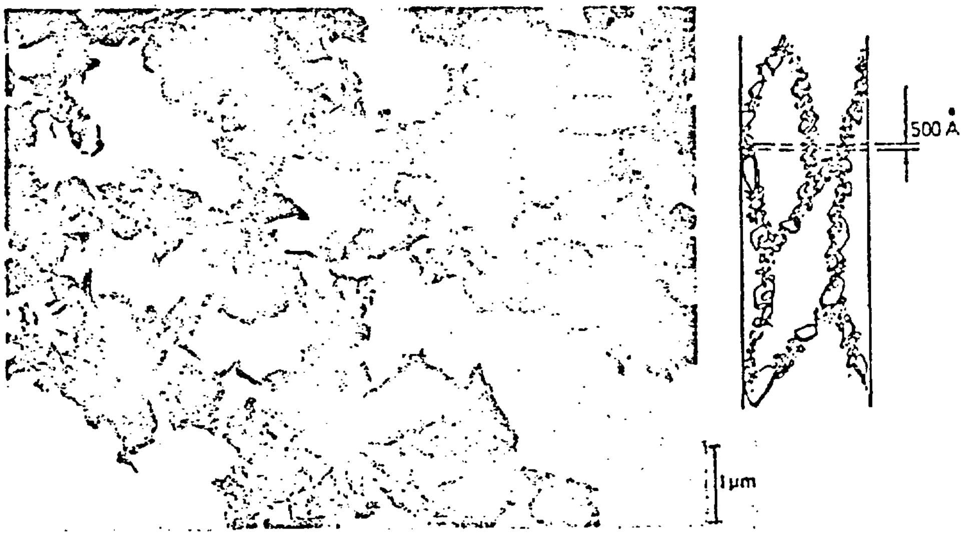

Fig 2 Transmission electron micrograph of ultrathin section of commercial sodium bentonite (GEKO/QI) expanded to a density of about 1.3 t/m³ in water saturated state. The section is illustrated in the tactoid-type structure suggested for water-rich clays [4].

3.2 Dense Na montmorillonite clays

The compaction of air-dry Na-montmorillonite granules, i.e. the technique used in Sweden to produce blocks that can be applied in boreholes, shafts and tunnels as well as in deposition holes as HLW canister envelopes, results in densely grouped aggregates as illustrated in Fig 3. We identify three types of pores: interlayer space, small isolated voids and larger continuous voids. On wetting, water first enters the system of wide continuous pores by "capillary suction", which then serves as a source for the successive build-up of the strongly adsorbed interlayer water. With a specific surface area of 600-800 m² of montmorillonite we find that 1 hydrate layer is fully developed in completely water saturated clay with a bulk density of 2.1-2.4 t/m³ (dry density 1.75-2.22 t/m³) leaving about 20 % of the total water content as external, pore water. Allowing such a clay element to expand by letting it take up water, 2 hydrate layers in interlayer positions are fully established at a bulk density of 1.9-2.1 t/m³ (dry density 1.43-1.75 t/m³) leaving about 30 % of the total water content as external pore water. Further expansion to a bulk density of less than 1.7-1.9 t/m³ (dry density 1.11-1.43 t/m³) yields 3 hydrate layers in interlayer positions, leaving about 30-40 % of the total water content as external water. Summarizing these data we find the relation between interlayer, i.e. internal, and external water to be as shown in Fig 4.

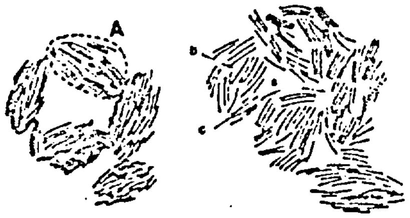

Fig 3 Schematic particle arrangement in highly compacted Na bentonite granulates. Left picture: powder grains in air-dry state. Right picture: "homogeneous" state after saturation and particle redistribution

A=particle aggregate, a=large interparticle void, b=small interparticle void, c=interlayer space

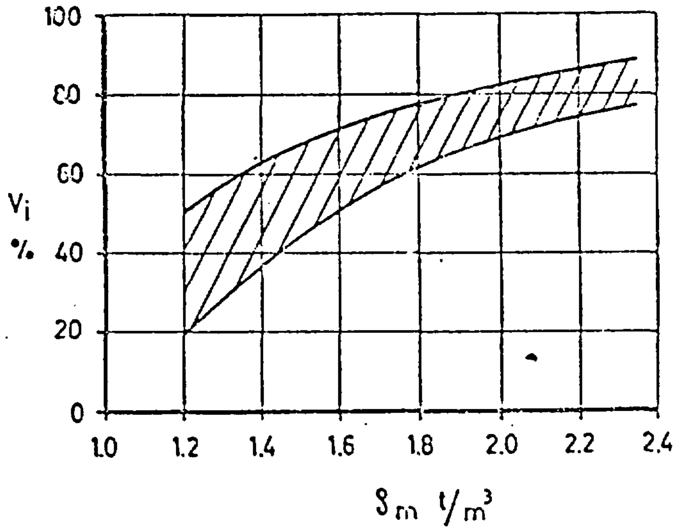

Fig 4. General relationship between bulk density and content of internal water in percent of the total pore water volume of smectite clays

From the diagram we can draw some important conclusions concerning the water flow and ion diffusion patterns. Thus, since only external water readily flows under the action of a hydraulic gradient we have a plausible explanation of the wellknown dramatic drop in the mean, macroscopically recorded hydraulic conductivity at increasing density (Table 1).

Table 1 Mean hydraulic conductivity as determined in permeameter tests. MX-80 Na bentonite cla (distilled water)

Bulk density ρ_m t/m^3	Hydraulic conductivity, m/s 25°C	70°C
2.1	$1.5 \cdot 10^{-14}$	$1.5 \cdot 10^{-13}$
2.0	$2.0 \cdot 10^{-14}$	$2.0 \cdot 10^{-13}$
1.9	$3.0 \cdot 10^{-14}$	$5.0 \cdot 10^{-13}$
1.8	$5.0 \cdot 10^{-14}$	$8.0 \cdot 10^{-13}$
1.7	$8.0 \cdot 10^{-14}$	$\leq 10^{-12}$

This table also demonstrates that the conductivity at 70°C is 10-15 times higher than at room temperature, which is explained mainly by heat-induced contraction of the montmorillonite stacks and the associated widening and increase in interconnectivity of the voids.

As to diffusivity it has been demonstrated that diffusion coefficients derived from analyses of tracer distribution in laboratory-scaled experiments may be similar for cations and anions (Table 2). However, the diffusive transport is much lower for anions than for cations due to Donnan exclusion of the anions; i.e. anion diffusion can only take place in the external water, while cations can diffuse in external and internal water and - depending on size and character - even through the crystal lattices [5]. Logically, therefore, the diffusive transport of cations and anions would tend to become similar at lower bulk densities, which has also been verified experimentally [6]. As to the detailed diffusion migration mechanisms, the diffusion rate of cations seems to be related to their size and hydration properties.

Table 2 Characteristic diffusion coefficients (D) as determined in laboratory diffusion cells [5] Bulk density 2.1 t/m³; MX-80 Na bentonite clay

Specie	D, m^2/s
Sr^{2+}	$23 \cdot 10^{-12}$
Cs^{+}	$8 \cdot 10^{-12}$
Cl^{-}	$6 \cdot 10^{-12}$
I^{-}	$4 \cdot 10^{-12}$

We conclude from these considerations that neither water flow nor ion diffusion occur uniformly through dense sodium montmorillonite clay on a microscopic scale. Thus, water percolation and anion diffusion take place only through continuous larger voids, while cation diffusion occurs more uniformly (cf Fig 3). The rather extreme property of dense sodium montmorillonite to self-heal, i.e. to redistribute water and minerals forming a largely homogeneous structure, tends to reduce the pore size to much less than in soft gels but arching effects prevent the particles to move into perfectly regular arrangements. The voids thus formed will not be distributed in a regular fashion and will not be equally shaped. Still, the spectrum of void size - expressed in terms of the equivalent diameter - and lengths of flow and anion diffusion paths will have a moderate width. Naturally, these spectra are functions not only of the bulk density but also of the purity, i.e. the content and distribution of other minerals and of the pore water chemistry.

3.3 Clay/ballast composites

For certain purposes clay-poor buffer materials offer better properties than pure smectites, one example being beds of low compressibility and permeability for heavy waste-containing structures such as the silo for LLW and MLW which is presently constructed at depth in granitic rock in Sweden. Natural soils with smectite as one component are frequently found and can be used as raw materials for such beds but artificial mixtures of properly graded ballast and smectite clay may represent more homogeneous composites. They can be prepared by mixing a properly composed ballast with finely ground Na bentonite, the aim being to obtain a continuous skeleton of ballast grains (silt, sand, gravel) with a minimum porosity and with the pores filled with the clay component. If clay and ballast materials are mixed in an air-dry condition, the microstructure will be as shown in Fig 5.

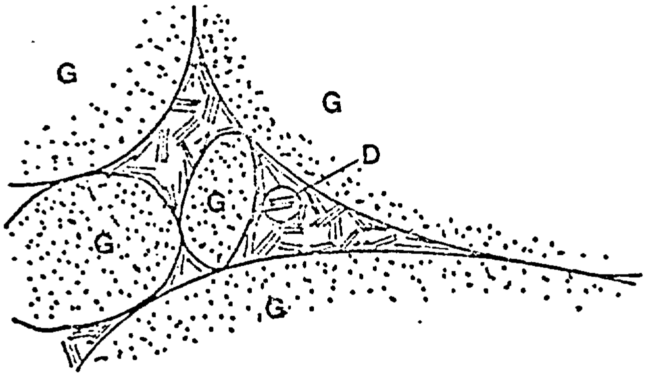

Fig 5 Schematic particle arrangement in a graded ballast with clay filling in the fine pores

Depending on the shape of the voids, the degree of filling and density of the clay gel may vary very much and it is immediately realized that these factors are major determinants of the spectra of the size of permeable voids and of the length of paths of flow and diffusion. They are, in turn, functions of the following variables:

- Homogeneity of mixture
- Shape of ballast grains
- Gradation of ballast grains
- Shape of mixed-in clay aggregates
- Density of mixed-in clay aggregates

4 Physical modelling and mathematical analogies

4.1 Microstructural analyses

The system of continuous, wider pores that is responsible for the permeability and anion diffusi can be described as a three-dimensional pipe network with a variation in diameter of the individu open passages that is illustrated by the spectra in Fig 6.

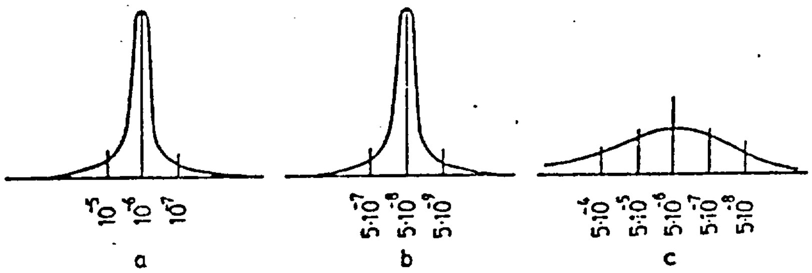

Fig 6 Schematic distribution curves of the diameter of intersected pores of a) soft Na montmorillonite gel, b) dense Na montmorillonite clay, c) dense, clay-poor mixture of Na montmorillonite and graded ballast (in meters)

The associated strong variation in flow is amply demonstrated by comparing microstructural parameters with the macroscopically determined hydraulic conductivity. Such parameters can be derive from electron micrographs using simple statistical methods [7] provided that the ultrathin sections have a standard thickness (300-500 Å). The total sectioned pore area (P) in percent of the tota area (T) of the micrograph, and the pore size (a_p) are characteristic measures of microstructural features. The pore size is defined as the longest intercept (Fig 7).

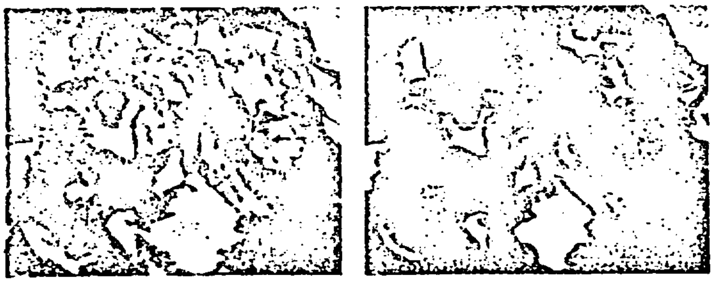

Fig 7 Example of micrograph normalized for microstructural analysis

The measurements of pore size (individual measurements) and pore area (continuous line integration) are based on drawn images of the micrographs in which no discrete particles are depicted. Hence, the drawings show black areas for the clay particle matrix with no sectioned pore space. Depending on particle size and arrangement, this matrix has a varying density which is not illustrated by the even black areas. This means that the true porosity cannot be judged from the drawings. Although the sections are extremely thin they naturally contain very small pores which are embedded in the clay sections and are thus not revealed. The observed frequency of such pores, which host internal water, therefore needs to be corrected. Characteristic data of some representative montmorillonite soils are shown in Table 3.

Table 3 Microstructural and flow data of Na-montmorillonite soils

Clay	Bulk density t/m³	Poro-city (<μm) %	Clay content %	Main clay minerals*	Microstr.param. Median pore size μm	P/T %	Hydraulic conductivity** m/s
Ordovician bentonite (natural)	1.98	43	38	S>H>Chl>K	0.12	1.5	10^{-13}
Matured Na bentonite granulate	1.60	65	90	S	0.25	23	10^{-10}
Matured Na bentonite granulate	1.25	85	90	S	0.5	31	$\leq 10^{-8}$

* S=Na smectite and mixed layers, H=hydrous mica, Chl=chlorite, K=kaolinite

** Slightly brackish, synthetic groundwater

We see from this table that the dramatic increase in hydraulic conductivity on reducing the bulk density is associated with only moderate changes in microstructural and macrostructural porosities and median pore size. The explanation of this apparent discrepancy is that the probability of the development of wider, continuous passages traversing the percolated sample increases very much when the density is reduced. This has the following two major implications on the processes of percolation and anion diffusion:

1 At the experimentally observed insignificant average percolation rate of dense smectite clay, water still flows at a high rate through a relatively small number of continuous passages of low tortuosity, which are thus determinants of the bulk conductivity. Such high flow rates are expected to cause internal material transport and plugging, which is a major reason for the often observed time-dependent reduction in average flow rate in permeameter tests (Fig 8).

In mixtures of clay/ballast materials, such permeable passages are numerous because of the incomplete filling of the pores. Also, several very dominant flow-determining paths are expected to appear per m³ volume of fillings compacted on site since the preparation, application and compaction using ordinary techniques are bound to yield variations in composition and density. This phenomenon is expected to be scale-dependent.

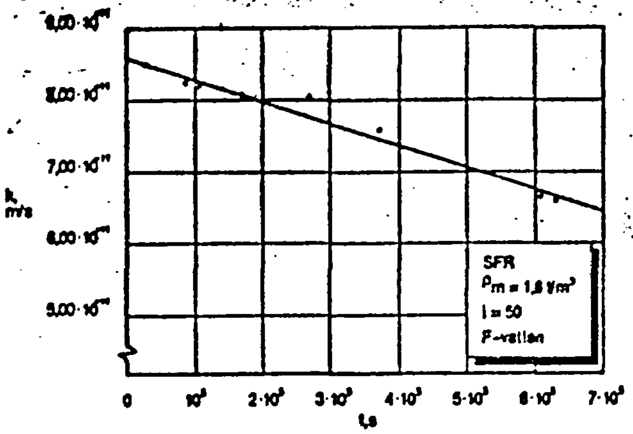

Fig 8 Average hydraulic conductivity of commercial Na bentonite with a bulk density of 1.6 t/m^3. Hydraulic gradient = 50. (Brackish groundwater)

2 Anion diffusion takes place relatively unhindered in wide passages, which yields fast migration through a fraction of the pore system and delayed diffusion in the more tortuous passages in the rest of the sample. This seems to be one reason for the skewed concentration profiles in diffusion experiments* (Fig 9).

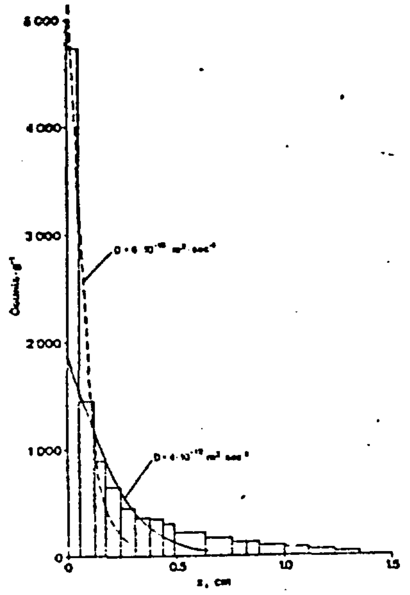

Fig 9 Example of concentration profile of ^{131}I in diffusion test of dense Na bentonite [8]

---

* Personal communication Prof Trygve Eriksen, Dep Nuclear Chemistry, Royal Technical Institute, Stockholm, Sweden

4.2 Flow modelling

Since the detailed features of the flow-determinant passages are not known, stochastic methods would offer a suitable basis for mathematical modelling. A simple analysis serves to demonstrate the potential use of such techniques, the applied method allowing for three-dimensional flow. It has been developed for the study of consolidation rates in soil mechanics and illustrates the variation in flow path length assuming standard normal distribution functions [9]. According to this method, porewater flow is treated as a "random walk" process using the similarity between the configurations of flow paths and polymer chains for determining the probability density function of the total length of flow lines. Fig 10 shows an element of the soil with a flow path that corresponds to coupled links of a chain. Assuming m links the total flow path length is a random variable:

$$r = \sum_{i=1}^{m} r_i \tag{1}$$

where r_i = length of i:th link

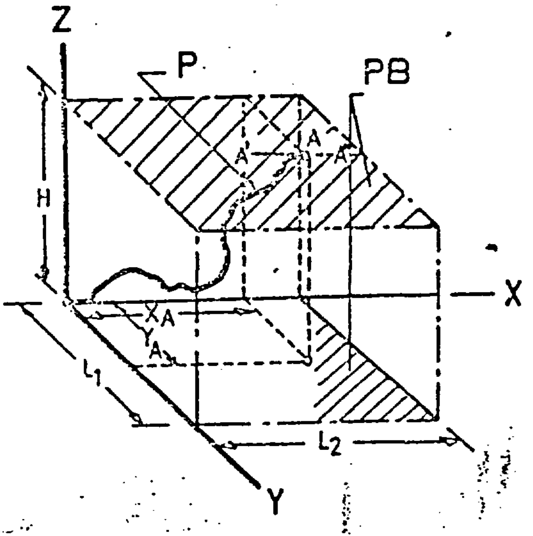

Fig 10 Flow path P through soil element. PB are pervious boundaries

Analytically, the length r is taken as the sum of the thickness H and the absolute value of the random length x for $-\infty<x<\infty$, which leads to the following probability (f_r) density and cumulative (F_r) distribution functions of r:

$$f_r(r) = 2f_x(r-H), \quad r \geq H \tag{2}$$

$$F_r(r) = 2F_x(r-H), \quad r \geq H \tag{3}$$

where f_x is taken as a normal density distribution function, and F_x as a cumulative distribution function (Fig 11).

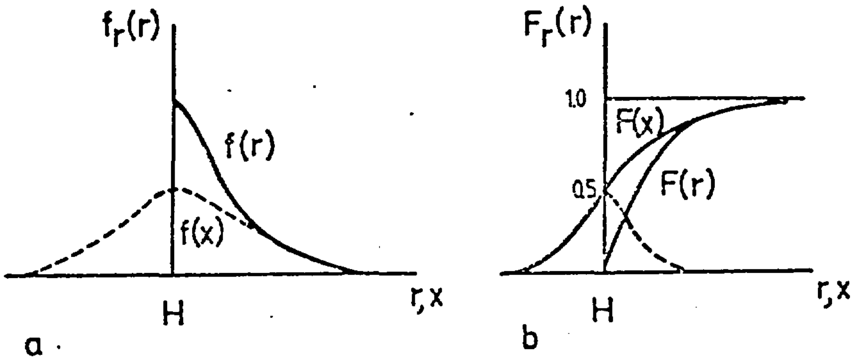

Fig 11 Left: probability density function. Right: cumulative distribution of the length r [9].

The mean value of r and the variance V(r) can be expressed as:

$$\bar{r} = \int_H^{\infty} f_r(r)r \, dr \tag{4}$$

$$V(r) = \int_H^{\infty} f_r(r)(r-\bar{r})^2 dr \tag{5}$$

Taking as an example Na montmorillonite clays with bulk densities ranging between 2.0 t/m³ and 1.2 t/m³, the corresponding mean values of the total number of links per meter length are estimated at $m=10^4$ to $m=10^8$. The value $m=10^5$ would correspond to a bulk density of about 1.5 t/m³, keeping in mind that the montmorillonite stacks behave as grains belonging to the fine silt fraction.

Following [9] we introduce a random variable u, being the ratio of x/H, which is taken to have a standard normal distribution, i.e:

$$f_u(u) = \frac{1}{\sqrt{2\pi}} \exp\left(-\frac{u^2}{2}\right), \; -\infty<u<\infty \qquad (6)$$

Then the length of the flow path r is given by the basic Eq. (1):

$$f_r(r/H) = 2\, f_u(r/H), \; 1 \leq r/H \leq \infty \qquad (7)$$

The probability density function of r/H has the form:

$$f_{r/H}(r/H) = k\, f_r(r/H) \qquad (8)$$

where k is derived from $k\int_1^\infty f_{r/H}(r/H)d(r/H)=1$

Introducing k back in Eq. (8) we obtain the mean value of r/H and the standard deviation of this same quantity:

$$\bar{r}/H = \frac{2k}{\sqrt{2\pi}} \int_1^\infty e^{-(r/H)^2/2}(r/H)d(r/H) \qquad (9)$$

and

$$\sigma^2_{r/H} = \frac{2k}{\sqrt{2\pi}} \int_1^\infty e^{-(r/H)^2/2}(r/H - \bar{r}/H)d(r/H) \qquad (10)$$

It can be shown that k has a finite value of 3.15, which yields the mean value 3.05 and the standard deviation value 1.57 of r/H.

We conclude from this that when normal distribution functions are applied, the probable existence of long tortuous paths results in a mean flow path equal to about three times the theoretical minimum distance.

The dispersion of flowing water and diffusing anions is thus considerable. In particular, this example serves to show that accurate prediction of the transport of anions by diffusion cannot be based on the simple diffusion equation.

Much more advanced analyses of flow and diffusion can be made by applying advanced techniques like the use of fractal concepts [10]. Such work requires access to microstructural data and is presently focussed on in the ongoing buffer material study of SKB .

5 Comments

Naturally, many of the processes that need to be considered in safety analyses of long term repository function, may well be described by rather simple mathematical analogues. This is also the case for waste canister envelopes of clay, which are determinants of the operational lifetime of the containers since the clay creates their chemical environment. The choice of relevant mathematical models, however simple and practical, needs to be based on a deep insight in the involved physics, particularly as concerns flow and diffusion as demonstrated in this article.

6 Acknowledgements

The author is greatly indebted to the Swedish Nuclear Fuel and Waste Management Co (SKB) for financing part of the study.

7 References

1 Pusch, R., Börgesson, L. & Ramqvist, G. Final Report of the Buffer Mass Test - Vol. II: Test results. Stripa Project 85-12, 1985

2 Tessier, D. Etude experimentale de l'organisation des materiaux argilleux, INIRA, (361 p)

3 Pusch, R. Identification of Na smectite hydration by use of "humid cell" high voltage microscopy (In press)

4 Pusch, R., & Karlsscn, R. Shear strength parameters and microstructure characteristics of a quick clay of extremely high water content. Proc. Geot. Conf. Oslo, 1967

5 Pusch, R. & Carlsson, T. The physical state of porewater of Na smectite used as barrier component. Engineering Geology, Vol. 21, 1985 (pp. 257-265)

6 Low, Ph. Viscosity of interlayer water in montmorillonite. Soil Sci. Soc. Am. J. Vol. 40, 1976 (pp 500-505)

7 Pusch, R. A technique for investigation of clay microstructure. J. Microscopie, Vol. 6, 1967

8 Eriksen, T., Jacobsson, A., & Pusch, R. Ion diffusion through highly compacted bentonite. SKBF/KBS Technical Report 81-06, 1981

9 Athanasiou-Grivas, D. & Harr, M.E. The path of flow and its effect on consolidation rates. Third International Conf on Numerical Methods in Geomechanics. Aachen, 2-6 April 1979

10 Williams, J.K. and Dawe, R.A. Fractals. An overview of potential applications to transport in porous media. Transport in Porous media. Vol. 1, 1986, Reidel Publ. Co., (pp. 201-209)

Radionuclide Release and Transport Modelling;
Specific Applications and Requirements for Further Developments

Charles McCombie

National Cooperative for the Storage of Radioactive Waste (NAGRA)
Baden/Switzerland

SUMMARY

Release and transport of radionuclides from geologic repositories is most likely to be caused by moving groundwater. The modelling of these processes within a system performance asssessment is discussed. Emphasis is laid upon identifying the important processes determining final release rates and on reviewing the status of their modelling. Recent assessments in various projects tend to reveal a common set of key safety issues and these are summarized in this paper.

1 INTRODUCTION

The general aim of this paper is to discuss the modelling of radionuclide release and transport from a nuclear waste repository. For most geologic repository concepts, the most likely release mechanism for radionuclides is by transport in groundwater and modelling efforts have accordingly concentrated upon studying this scenario. Hydrogeologic modelling on a large scale, as discussed in other papers, gives the natural water-flows through the host-rock formation and more detailed analyses can allow for the perturbations induced by the presence of the repository system. We thus typically arrive at a predicted groundwater flow field around a backfilled underground excavation containing waste packages. The subsequent modelling steps involve prediction of the radionuclide release rate out of the immediate surroundings of the waste (the "near field") into the relatively undisturbed geologic medium (the "far field") and thereafter the transport rate through the geosphere and biosphere.

Fig. 1 gives one representation of a typical modelling chain. I shall confine discussion here to the near-field and far-field areas represented at the centre of the figure, i.e. I shall leave discussion of hydrogeology and of biosphere transport to other speakers. Furthermore, a detailed treatment of near-field transport in clay buffers will be given by R. Pusch and the general mathematical background to transport modelling will be covered by G. de Marsily. Following some general observations on mathematical modelling and a review of important near-field and far-field issues, some selected important conclusions on the current state of release and transport modelling are summarized.

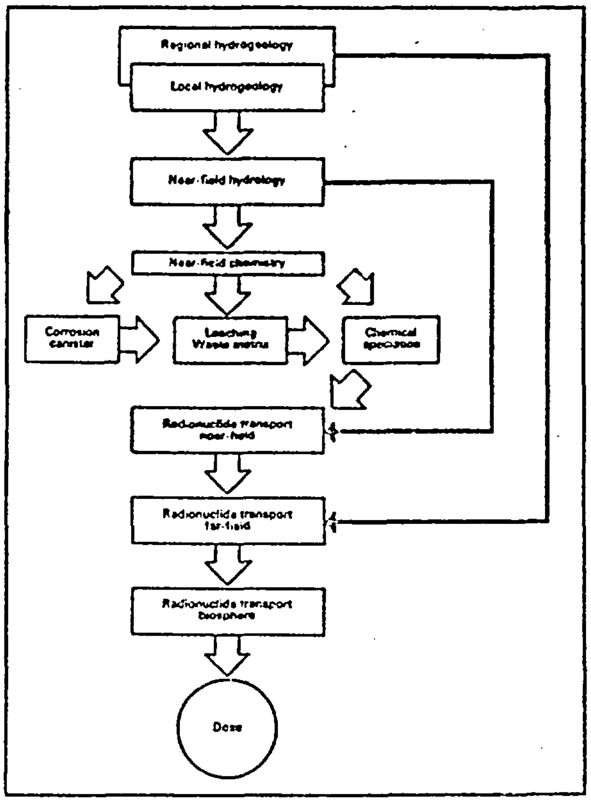
Regional hydrogeology
Local hydrogeology
Near-field hydrology
Near-field chemistry
Corrosion canister
Leaching Waste matrix
Chemical speciation
Radionuclide transport near-field
Radionuclide transport far-field
Radionuclide transport biosphere
Dose

Fig. 1: Model chain for safety analysis

2 BASIC MODELLING ISSUES

2.1 Performance assessment models

It is not possible to prove in a rigorous mathematical sense that radiation doses from a repository will at no time exceed a certain limit and direct experimental checking of calculated results is not possible because of the long time periods involved. All meaningful safety studies of final disposal must therefore be based on predictive models of physical, chemical and geological processes.

The most important step is the formulation of a conceptual model which is capable of adequately describing the processes to be considered, with appropriate approximations if justifiable. The validation of this model, i.e. checking how well the approximation corresponds to physical reality, is very important. A calculation model is usually derived from the conceptual model and this simplifies routine use in conjunction with other models. A calculation model is understood to be a mathematical representation of a real system which allows quantitative results to be obtained. Verification of such models is defined as the process of proving that the mathematical solution correctly reproduces the properties of the conceptual model. These steps are shown schematically in Fig. 2.

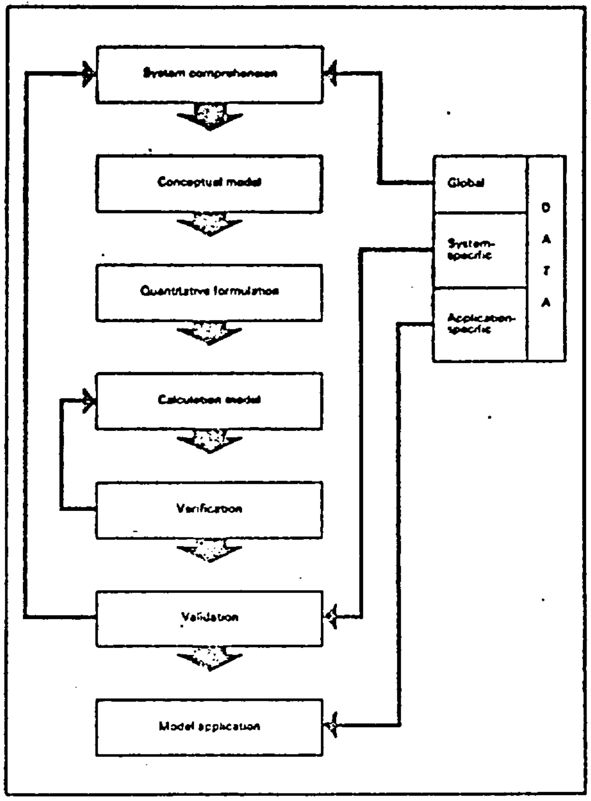
System comprehension
Conceptual model
Quantitative formulation
Calculation model
Verification
Validation
Model application
Global
System-specific
Application-specific
DATA

Fig. 2: Modelling steps

It is often practical to make separate models of sub-systems. Chemical and physical processes which can be quantitatively characterized through measurements and experiments and observations of geological and hydrological processes can be described and extrapolated in time in models of individual sub-systems. Finally, an integrated assessment of the whole repository system is necessary in order that the interactions of the individual systems and their effect on overall safety can be taken into account. Also, it is possible to estimate the relative importance of the individual barriers only in an integral model study. An important task in the area of repository safety analysis is checking the validity of the models. This involves detecting and clearly describing their range of application and identifying possible inaccuracies which can be caused on the one hand by approximations in the conceptual and calculational models and, on the other hand, by uncertainties in the input data used.

2.2 Selection of methods and data

Quantitative predictions require certain simplifications and approximations and it is therefore important to be able to assess the resulting uncertainties. A possible method would be a study carried out according to stochastic principles with defined probability distributions for the input data values. Such methods have already been developed for repository analyses; they are currently being put to use, but cannot yet completely replace deterministic analyses because the procedures selected contain extensive simplifications of the system and it is often impossible to achieve the necessary degree of detail in the data acquisition.

A different safety analysis method has been followed in analyses in which it has to be ensured that the simplifications and selection of data are always conservative. This is justified when the main goal is a bounding analysis, i.e. a demonstration that a certain degree of safety can be achieved under all circumstances. However, if the safety analysis is used for planning of a specific project, for defining research programmes or for realistically assessing the potential consequences of waste repository, the use of "best guess" data or estimates is more appropriate. This approach minimises the danger of obtaining too distorted a picture of the whole system since a significant deviation from reality must be expected when linking individual over-conservative steps. Procedures which are based on deterministic methods and conservative data are being increasingly complemented by probabilistic methods. It is acknowledged that these probabilistic/statistical approaches still have limitations in their methodology and, even more so, in their databases. However, future assessments of overall repository safety will certainly include comparison of probabilistic predictions with risk acceptance criteria - even if these continue to be accompanied by deterministic dose predictions based on bounding-value cases.

3 RELEASE AND TRANSPORT IN THE NEAR FIELD

The near field of the repository system is generally taken to mean the waste matrix itself, its overpack, the backfilling of the excavation and those parts of the surrounding host rock substantially affected by the presence of the repository. In 1980 an NEA Symposium devoted to near-field effects gave a good overview of the modelling situation /Ref 1/, and this was partly updated by an IAEA Working Group which met in 1984 to produce a further document /Ref 2/.

The processes modelled in the near field and far field include heat transport, water movement, engineered barrier corrosion, waste form leaching, dissolution and precipitation processes in the groundwater, gas generation, convective or diffusive mass transport and chemical sorption effects. Many of these processes are interrelated and the final predicted repository safety will depend on all of them.

Fig 3 gives a schematic example (from Swiss work - /Ref 3/) of a near-field system, for the particular case of vitrified waste in a steel overpack within a repository tunnel backfilled with bentonite clay.

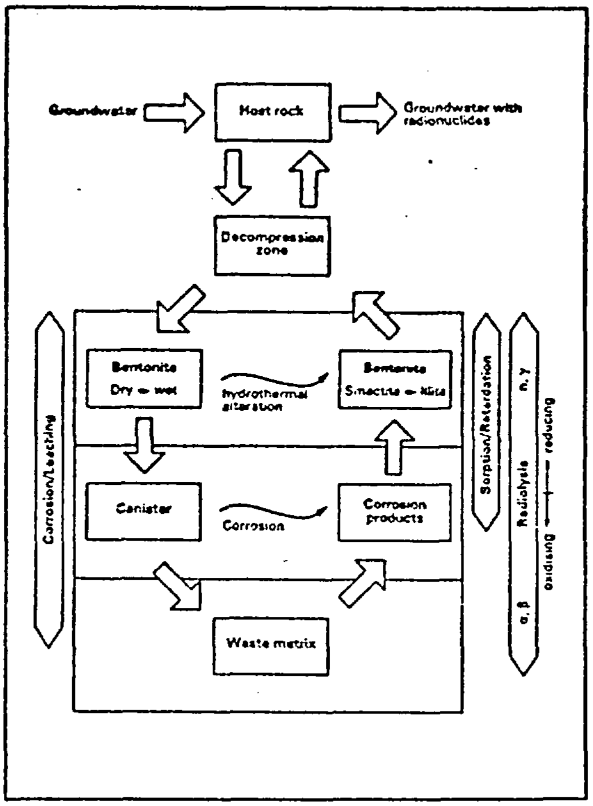
Groundwater
Host rock
Groundwater with radionuclides
Decompression zone
Bentonite
Dry ⇒ wet
hydrothermal alteration
Bentonite
Smectite ⇒ Illite
Canister
Corrosion
Corrosion products
Waste matrix
Corrosion/Leaching
Sorption/Retardation
Radiolysis
n, γ
α, β
oxidising
reducing

Fig. 3: Radionuclide release from the near field

3.1 Chemical thermodynamic modelling

The chemical environment and its evolution with time are of extremely high importance in determining the repository performance. The corrosion rates of waste and overpack, the solubilities of radionuclides, and their sorption on other system components are all strongly dependent on the chemistry (in particular on Eh and pH which determine the speciation). Therefore the application of chemical thermodynamical models is important.

Most models today are based on equilibrium thermodynamics in aqueous solutions. Models currently used to check the consistency of measured hydrochemistry data or to predict the future chemical environment and the concentrations of radionuclides include MINEQL, EQ3/EQ6, PHREEQ, etc. Important developments being worked upon are the improvement and extension of the basic thermodynamic data, the inclusion of kinetic effects, and the coupling of the chemical modelling to a solution of the transport equations. This last item is difficult because the scale of the computational problem which must be solved for a direct approach is so large that simplifications based on a good scientific understanding of system behaviour must be sought.

Various applications of chemical modelling to date have emphasized the importance of potential future changes in Eh, pH, etc. within the near field. Oxidising conditions might develop due to radiolysis of groundwater after overpack failure has allowed intimate contact of water with spent-fuel pellets; chemical buffering by specific additives or by reducing corrosion products can influence this; changes in pH will occur in bentonite buffers or due to cement structures within the repository. It is important to quantify such effects if we wish to take full credit in our performance assessment for the substantial safety barrier effect due to the normally low solubilities of important actindes in the disposal system.

3.2 Corrosion and waste-form release modelling

Corrosion rates of metallic overpacks are important in varius disposal concepts. An overpack can certainly provide complete containment during an initial time period which is longer than the duration of a waste-induced heat pulse within the repository; it may also provide very much longer containment if properly chosen materials are used in a suitable environment (c.f. Swedish work with Cu-container lifetimes of over 10^5 y). Mostly the corrosion processes are not directly modelled; container lifetimes are derived either by assuming reactions occur with all oxidants transported by groundwater to the container or by using empirical corrosion rates derived from experiment and observation. There are, however, codes which simultaneously calculate the development of mechanical stresses and corrosion processes in the overpack; the most obvious application of these is in an attempt to quantify the expected spread in container failure times.

For the waste-form itself, there have been many modelling studies of the rate of radionuclide release. At a macroscopic scale, release is often taken to be due to a nuclide-independent matrix corrosion rate together with a nuclide-dependent diffusion out of the waste matrix. Innumerable leaching experiments have been performed to provide data for such models. Complications which arise include the practical problems of achieving realistic conditions (e.g. water/waste volume ratios low enough to represent those expected in the repository) and the difficulty in predicting the physical and chemical behaviour of surface films which can have an important influence on effective corrosion rates.

One example of a current programme aimed at studying release rates from vitrified waste, using varied experimental techniques together with appropriate modelling, is the JSS Programme. Some experiments use high ratios of waste surface area to water volume and involve explicit examination of corrosion films; other experiments have a deliberatly chosen high glass surface area in order to achieve chemical equilibrium in the leachate in reasonable times; all practical work is accompanied by release modelling which also takes into account the changing chemical composition of the leachant solution.

In practical, integrated performance assessments of complete disposal systems little or no use has been made to date of detailed microscopic corrosion models which treat the build up and dissolution of specific solid phases. Most studies assume simple congruent release from the corroding waste matrix, although refinements to account for restricted elemental solubilities, including the sharing of solubilities amongst different isotopes, have been implemented.

3.3 Near-field transport modelling

Nuclides released from the waste matrix must be transported through the backfill or buffer material. Details of this process for the common case of clay barriers are discussed in the contribution of R. Pusch. Here we shall mention only some important conclusions which can be drawn from recent modelling studies.

For normal buffer dimensions and for the low water flows expected in most repository host rocks, the diffusion rate through the buffer is not a factor which limits ultimate releases of long-lived nuclides to the geosphere. However, slow diffusion can delay the break-through of radionuclides for times which are long enough to allow decay of even relatively long-lived radionuclides. Moreover, the diffusion resistance of the buffer provides a mechanism which can restrict release rates to values determined only by the concentration gradients - even if greatly increased groundwater flow rates should occur at some future time.

The modest, direct contribution to long-term safety predicted for the buffer is to some extent a consequence of the modelling of the interface between buffer and host rock and of the flow of radionuclides across this interface. If no transfer resistance is assumed, i.e. if nuclides can freely move into the host rock at all places, the results indicated above are valid. More realistic modelling, however, should account for the fact that, in hard rocks with discrete water bearing features, diffusion will occur only to these features - and they are normally relatively sparsely distributed through the host rock. The major problem in calculating this effect reliably is not the computational model, but rather the difficulty in gathering adequate data on the future systems in the host rock.

3.4 Comments on near-field release and transport modelling

The notes above indicate that proper near-field analyses must involve modelling of spatially heterogeneous and chemically complex systems over long time periods. Methods are available for adequately treating those processes known to be important; improvements of methods and data are however possible. Some few effects which could in some circumstances be important (e.g. colloid formation, microbial effects, etc.) have not been modelled in any depth. Efforts are underway to investigate possible symbiotic effects when different processes are coupled together. Results of analyses show that the near field of a waste repository can provide a highly efficient nuclide containment which is not strongly dependent upon the more remote geologic setting.

4 TRANSPORT IN THE FAR FIELD

4.1 Transport models

Most processes already mentioned as occurring in the near field, take place also during transport through the geosphere. An important difference is that the environment in the geosphere is not expected to be significantly affected by the presence of radionuclides being transported in the groundwater. The main processes involved are advection, diffusion, dispersion, sorption, dilution and radioactive decay - and these are normally all included in the coupled transport equations solved by standard computational models.

Many computer models exist for geosphere nuclide transport, some including also other processes like hydrology, heat transport, etc. Extensive work has been done on verification of these models by cross comparisons and on validation by comparison with experimental results. Some of this work is described in the contribution by B. Grundfelt on the Intracoin and Hydrocoin projects. In the following section, therefore, emphasis will again be laid upon describing the conclusions which can be drawn from recent applications of geosphere transport codes in performance assessments.

4.2 Conclusions from applications

From the time of the earliest analyses it has been clear that the geosphere can be an *extremely effective safety barrier. Even with highly conservative assumptions on nuclide* sorption, many radionuclides are extremely immobile in the geosphere. This qualitative conclusion is easily verified by experiments and field observations. For some important nuclides, however, (e.g I-129) solubility and mobility can be high, so that concentrations at the geosphere outlet are dependent mainly upon dispersivities and upon dilution.

The results of geosphere calculations are particularly sensitive to the conceptual modelling of *some parts of the system. For example,* if we use conventional, large-scale hydrogeologic models to predict bulk volumetric groundwater flow rates, we must thereafter model the details of the flow systems through which the water moves - and the predicted transport properties of host rocks can vary greatly according to our conceptual model of these flow systems. Results exist for cases where it has been assumed that flow is uniform (porous medium), in discrete fractures, or in discrete one-dimensional networks (channels within fractures, veins in altered rock, etc.).

The precise description of the rock around the water bearing feature is also important. Minerals lining fracture surfaces can determine the effective sorption; the diffusivity of rock adjacent to the flow path will determine how easily and how far nuclides can diffuse into the rock matrix. *One example of this point is illustrated in Fig 4*; this illustrates the variation with time of Np-237 concentrations at the geosphere outlet for a 500 m linear flow path for different cases with varying volumes of rock around the flowing water availabe for matrix diffusion. Many orders of magnitude in concentration can result from small factors in diffusion depth. It is then clear that flow path characterization and the development of corresponding conceptual models is of utmost importance in radionuclide transport modelling. This means that careful characterization of the host rock is essential, and that the problems of sparse data will always be present because of the fine scale description needed for large rock volumes.

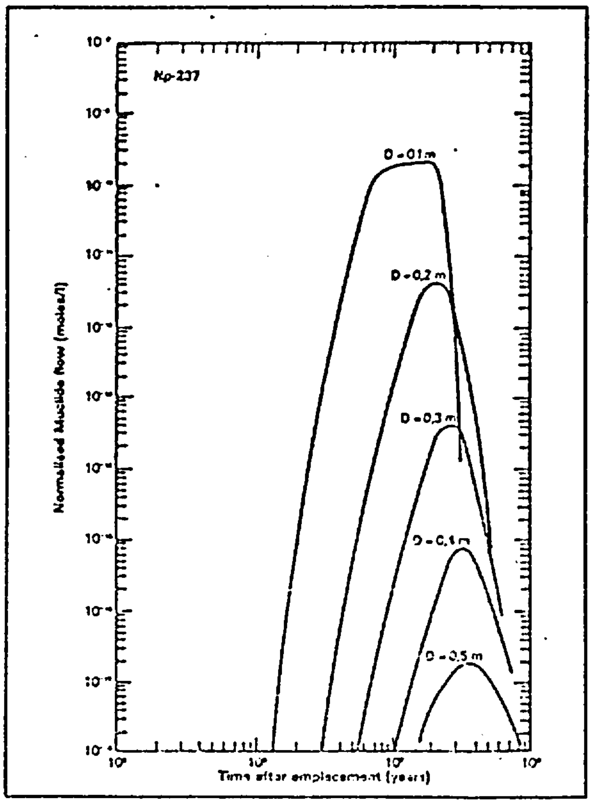

Fig. 4: Normalised nuclide flow (Np-237) leaving the 500 m long transport path in the middle crystalline as a function of time and the maximum depth of penetration into the kakirite (D)

5 CONCLUSIONS

From the remarks made in the preceeding sections of this paper and from a broad look at the project work in different countries, we can draw together some general conclusions on the current state of radionuclide release and transport modelling.

Basic modelling issues:
In mathematical modelling of any system the most important single issue is the choice of an appropriate conceptual model; this depends upon our having an adequate quantitative understanding of how the processes involved affect total system behaviour. In relatively few areas is the calculational model the restrictive issue, although there are examples (e.g. probabilistic modelling with many parameters, fully coupling of transport processes, etc.) where increasing demands for computing power can arise. For very many model applications the database needs improvement. This is true on a small distance scale (microprocesses in waste matrices, in the fine structure of the rock, etc.) and on a large scale (adequate characterization of the geologic and hydrologic environment of a repository) - and in both cases for unusually long timescales.

Radionuclide Release and Transport Modelling; Specific Applications and Requirements for Further Developments

Current status of models:

Models are available now which allow quantitative analysis and prediction of radionuclide release and transport processes. Improvements are, however, necessary. On one side, conservative, relatively unrealistic assumptions have sometimes been made in order to be sure that models overpredict release and transport (e.g. linear sorption, fast kinetics in all chemical reactions); with increasing understanding of processes involved, this approach should become less common. On the other side, we must improve modelling of certain processes which could affect disposal system safety in a negative or in an as yet unknown way (e.g. colloid formation and transport, strong channeling in flow paths, gas production and transport). In virtually all of the important modelling areas associated with waste disposal safety analyses, validation of the concepts is and will continue to be a key issue. A full validation will in many cases never be possible in a rigorous sense; we can speak only of increased confidence in the modelling tools. Verification and quality assurance of computer models are also very important - these tasks should not, however, be confused with the fundamental validation process.

Application of models:

The number of applications within the framework of complete safety assessments of repository systems continues to increase and the results show some common trends. The importance of understanding the chemical and geochemical environments, including their evolution with time, is very high. Radionuclide release or transport rates can vary by many orders of magnitude under different chemical conditions. Total system analyses quantifying the efficiency as a safety barrier of both near field and far field of a repository show that both can be highly effective. Even in a geologic setting of relatively modest quality, the near field can provide effective containment of radionuclides for very long times (c.f. recent Swedish or Swiss work); in a well-chosen geologic environment (favourable hydraulic regime, good chemical conditions, assured dilution, etc.). almost no demands need be placed on the waste package nuclide release rates. The accepted principle of including both near-field and far-field safety barriers in a multi-barrier system is confirmed to be appropriate. All applications of modelling of repositories suffer from inadequate databases, particularly at a site-specific level; the numerous characterization programmes which are in progress should improve this situation. Databases will, however, never be complete. Accordingly an issue of major - and still growing - importance is the quantification of the uncertainties in model predictions which are caused by our imperfect knowledge of the input data needed to quantitatively describe the repository system at the present and at future times.

6 ACKNOWLEDGEMENT

The ideas in this paper have been developed together with colleagues involvement in performance assessment within Nagra and at the Swiss Federal Institute for Reactor Research.

7 REFERENCES

/1/ NEA, "Near-field phenomena in geologic repositories for radioactive waste"; Proceedings of the NEA Workshop, Paris, 1981

/2/ IAEA, "Deep underground disposal of radioactive waste - Near-field effects"; 1984 (Draft)

/3/ Nagra, "Nuclear waste management in Switzerland: Feasibility studies and safety analyses; Nagra Project Gewähr Report NGB/85-09, Baden/Switzerland, 1985

Pathways to Man for Radionuclides Released to the Biosphere from Land-based Waste Disposal Facilities

Graham H Smith

National Radiological Protection Board
United Kingdom

This paper discusses the potential for release of radionuclides into the biosphere following disposal of radioactive waste in land-based facilities, the modelling of subsequent transport of radionuclides in the environment, and estimation of the associated doses to man. Some example results are presented based on the application of a particular model, called BIOS, and these are used to illustrate some of the major difficulties, and areas where further development is appropriate.

1. INTRODUCTION

In a comprehensive radiological assessment of any waste disposal method it is necessary to consider all the events and processes which could lead to the transport of radionuclides back to man, or could influence transport rates. Some of these events and processes are natural, others are caused by the effects of the waste on the repository, yet others are human induced. The modelling of these processes can be divided conveniently into three areas: the near and far fields from the waste repository, which essentially include all of the geosphere, and the biosphere.* The purpose of this paper is to examine the different kinds of release from the geosphere, the modelling of the subsequent transport and accumulation of radionuclides, and the associated doses to man. Because a full assessment must include estimates of doses and risks to the most exposed individuals and to populations as a whole[1] the models used should cover the area local to the point where radionuclides are initially released into man's environment, the region around it, and the remainder of the biosphere. In other words, it is necessary to attempt to model the whole environment.

2. RELEASE OF RADIONUCLIDES FROM THE GEOSPHERE

The most likely mechanism to result in transfer of activity from a land-based waste disposal facility through the geosphere and into the biosphere is carriage by groundwater. Contaminated groundwater may then be discharged into the freshwater environment (rivers or lakes), into sub-soil, or into the coastal marine environment. Given the nature of the geosphere transport processes it follows that release into the biosphere is likely to continue over very long periods of time, and that only relatively long-lived radionuclides will be released, particularly from deep geological facilities.

---

*For the purpose of this paper the term geosphere is taken to mean that part of the globe which is below the ground surface and beyond the normal range of man's access. Biosphere is taken to include all those areas to which man normally has access, including soils, the atmosphere, fresh water and marine environments, but not below ground as in mining activities.

In addition to the natural discharge into the biosphere of contaminated groundwater, releases may arise as a result of abstraction of groundwater from contaminated aquifers. This water may be used directly for human consumption, or for irrigation or other purposes.

Finally, intrusion into the repository or the region of contaminated geosphere, for example as a result of exploratory borehole drilling, could result in direct transfer of activity into the biosphere.

All these features of potential release have to be considered when considering the structure of the biospheric transport model.

3. STRUCTURE OF BIOSPHERIC TRANSPORT MODELS

3.1 General

The type of model which is most frequently used to predict rates and patterns of radionuclide transfer through the environment following releases from geologic repositories is the donor controlled linear compartment model. In these it is assumed that as soon as a radionuclide enters a compartment, instantaneous mixing occurs so that there is a uniform concentration of the radionuclide over the whole compartment. Each compartment must therefore be chosen to represent a region of the environment for which this assumption is reasonable. Depending on the situation being considered, compartments can be as large as the global oceans or as small as a dew pond. In general, the tendency should be to reduce the number of compartments to the minimum consistent with the validity of the instantaneous mixing assumption. Transfer between compartments is described by "transfer coefficients" which represent the fraction of activity in one compartment transferred to another in unit time. These transfer coefficients can be functions of time, so that, for example, changes in compartment sizes can be taken into account.

The advantages of compartment models are that they are mathematically straightforward, can be fairly easily interfaced with models for radionuclide release from the geosphere and, in the case of short term predictions, are not too difficult to validate. In addition, these models can readily deal with actinide decay chains, which are a major concern in assessments of disposal of long-lived and highly active wastes. To illustrate how a compartment model for use in geologic disposal assessments is structured, I will use as an example the BIOS model[2] developed at the National Radiological Protection Board (NRPB), with partial funding from the Commission of the European Communities (CEC). Similar models are in use in other countries (see, for example, SKBF/KBS[3]; Matthies et al[4]; Kuhne et al[5]) and other UK organisations (Mann and Thorne[6]).

3.2 Structure of the BIOS Model

The highest doses to individuals from disposal on land will arise where radionuclide concentrations are highest, which is likely to be in the vicinity of the release to the biosphere. Hence, in developing a model such as BIOS greatest attention is paid to the locality of the release. The local part of the model must permit calculation of radionuclide concentrations in all the local environmental compartments which could lead to irradiation of man, and must take into account radionuclide transport into the region beyond the release. Also, because releases may occur over very long periods (thousands of years or more), allowance must be made for feedback into the local area of radionuclides which have been more widely dispersed, and possible changes which may occur in the environment during and after the release must be incorporated into the calculations.

Depending on the type of release and the characteristics of the local environment, major contributions to collective dose may come from the local area where concentrations of activity are comparatively high. On the other hand, significant population exposure may also arise in the long term from more widely dispersed activity. It is neither feasible, nor necessary, to provide the same degree of detail in the part of the model dealing with this wider dispersal as is given to the local i.e. Two broad areas are sufficient, regional and global, provided that the major transport mechanisms and environmental compartments are included, so that contributions to collective dose from all exposure in all places at all times can be calculated.

Compartments representing the major global reservoirs for activity, and the transport between them, can be represented in a global model. This part of the biosphere model is used to calculate the contributions to collective dose arising from relatively low concentrations of activity leading to low doses to large numbers of people. The model for the region between the local and global compartments (the regional model) is necessary to provide an accurate representation of transport between the local and global compartments, and to allow calculation of collective doses arising at intermediate levels of individual dose. It is also possible that in some circumstances maximum individual doses could arise in this area.

The requirements outlined above led to the broad structure of the BIOS model, which is illustrated in Figure 1. The transport processes included in each part of the model are outlined below. Fuller description is provided in reference [2].

3.2.1 Freshwater environment

Radionuclides transported from an inland repository via groundwater can enter freshwater bodies such as lakes and rivers directly, or via soil compartments. During subsequent transport downstream to the sea, the radionuclides will interact with freshwater sediments, and may also be transported to adjacent land areas as a result of flooding, irrigation practices or sediment movement. If the water is used in domestic or industrial supply, radionuclides will re-enter river systems via drains. All these transport processes are included in BIOS. Furthermore, any number of freshwater compartments may be specified, and connected in any order, so that discharges into and transport through river-lake systems can be modelled.

3.2.2 Terrestrial environment

Radionuclides may enter the terrestrial environment directly from the geosphere, or via freshwater, or the sea. The transport processes modelled include interception by plant surfaces (during irrigation with contaminated freshwater), root uptake, transfer into grazing animals, and radionuclide migration down through soils and back into freshwater bodies. Following release into deep soil from the geosphere it is necessary to consider the transfer from deep soil to surface soil as a result of processes such as animal activity and the intermittent rising of the water table during periods of heavy rain. In addition, river and lake bed sediments can be dispersed over farmland as a result of periodic flooding, or dredging to avoid flooding, or, in the longer term, as a result of sediment accumulation drying out lakesides or altering river courses. Because of the various feedback mechanisms BIOS includes consideration of all these processes whatever the initial source of activity to the terrestrial environment. In BIOS this is modelled through the use of a transfer coefficient from the sediment compartments to soil compartments, the coefficient being determined from the rate of accumulation of bottom sediments in rivers and lakes, the depth of the relevant water compartments, and assumptions about dredging activities.

Activity may also be brought to the surface inadvertently through borehole drilling. Samples from drilling activities could be closely examined before it is discovered that they are contaminated. Most of the material might then be dumped close to the drilling site, where the liquid fraction could enter freshwater and the solids become mixed with soil. If the borehole has been sunk in order to provide a water supply, then the subsequent transfer of activity can be assumed to be similar to that for abstracted river water.

3.2.3 Marine environment

In the case of a repository sited on the coast, radionuclides could enter coastal waters directly. In other cases transfer will be by rivers (through estuaries), and both transport to the sea in water (either dissolved species or suspended particulates) and in sediments needs to be included. Once radionuclides are in the ocean, the processes to be considered are advection, diffusion, interactions with suspended and bed sediments, and uptake by marine organisms which are consumed by man. In BIOS this is again achieved using a compartment system, in which a larger number of compartments are used to represent coastal waters close to the release, and others to represent the rest of the world's oceans. The coastal compartments have been chosen in BIOS so as to represent dispersion of activity throughout the continental shelf of the North East Atlantic and the Mediterranean.

3.2.4 Atmospheric and global circulation

Environmental transport of radionuclides through the atmosphere is not a major transport mechanism for all the most likely releases from land disposal sites. However, sea to land transport of all radionuclides (via sea spray) does need to be included in the local marine environment, and, in addition, for the long-lived, mobile radionuclides (primarily ^{14}C and ^{129}I) it is necessary to consider transport from ocean surfaces to the global terrestrial environment via the atmosphere. In BIOS, global dispersion is not considered explicitly because there are particular models for global circulation of ^{14}C and ^{129}I which allow a simpler approach to be used (Bush et al[illegible], [illegible] and White[illegible]). The approach is to define a single global atmosphere compartment, in which the concentrations of ^{14}C and ^{129}I are determined according to their transport across the ocean surface, and to use parameters chosen to be consistent with the special models referred to above. It is then assumed that all terrestrial carbon and iodine is in equilibrium with the atmosphere. This assumption is reasonable in the long term for long releases.

3.3 Exposure Pathways in BIOS

The transport model outlined above provides an estimate of the concentration of radionuclides in each of the major environmental compartments. In combination with relatively simple functions which relate environmental concentrations to concentrations in foodstuffs or external dose rates, these results can be used to estimate doses.

The exposure pathways included in BIOS are listed in Table 1. Typical data requirements are presented in Section 6, where example calculations are presented. For a particular application not all of these pathways may be relevant. It should also be noted that care is required in summing doses over pathways, so as not to implicitly consider situations which are impossible (eg simultaneous use of the same piece of land for two types of farming).

Thus, in summary, the output of BIOS consists of:

i) concentrations of each radionuclide in each environmental compartment, as a function of time;
ii) time-integrated concentrations of each radionuclide in each compartment;
iii) annual individual doses in each compartment for each pathway and each radionuclide, as a function of time;
iv) collective dose rates in each compartment for each pathway and each radionuclide, as a function of time;
v) as (iv) but summed over compartments;
vi) as (iv) but summed over radionuclides and compartments;
vii) collective dose rates summed over compartments, radionuclides and pathways
viii) as (iv) - (vii) but with collective doses integrated over various time periods, including infinity.

4. MODEL VALIDATION

Model validation is a separate activity from model verification. The latter consists of [illegible] only [illegible] hand, [illegible] complete agreement [illegible] should [illegible] compared [illegible] predictions of the model [illegible] Furthermore, [illegible] full validation is not possible. The most that can be achieved is a partial validation. [illegible] can be done in two complementary ways.

The first way is to ensure that all the relevant processes are included in the model, if only in a simplified fashion. This is done by allowing experts in particular areas (eg terrestrial ecology, marine science, hydrology) to examine the model and its data base. Preferably, it should be done on an international basis. An example of an international study, [illegible], for the validation of [illegible] has been launched by the Swedish National Institute for Radiation Protection. In the context of waste disposal assessments this study proceeds on the basis of each participant providing model results and estimates of uncertainties for environmental concentrations for a range of different radionuclide release scenarios. The scenarios are only loosely defined in order to permit the widest possible discussion of processes which may be relevant to them.

The second way is to directly validate the separate parts of the model, using field observations. For example, [illegible] in terrestrial foodchains can be validated using fallout data and [illegible] (see, for example, [illegible]), while both fallout data and [illegible] distribution of natural radionuclides can be used to validate models of the [illegible] of [illegible] with deep ocean sediments ([illegible]).

5. UNCERTAINTIES

The uncertainties involved in modelling radionuclide transfer through the biosphere and in predicting doses to man from waste disposal can be divided into three categories:

i) those related to predictions of future biosphere conditions (for example, climatic changes);

ii) those related to changes in human characteristics, habits and locations;

iii) those associated with the approximations introduced by reducing the complex processes occurring in the transfer of radionuclides through the environment to a few mathematical equations.

These categories of uncertainties differ in both the extent to which they can be reduced by further research and in the way in which they are treated in assessments of the radiological impact of waste disposal options.

Uncertainties in the third category indicated above can be reduced by further research and the remaining irreducible uncertainties can be quantified by use of laboratory and field data. This situation does not exist for uncertainties in either the first or second categories. In the case of uncertainties related to predictions of future biosphere conditions, there is some scope for reduction through research (generally not related to radioactive waste disposal) and considerable prospects for scientific agreement on the range of future conditions to be considered. Thus it should be possible to include enough biosphere scenarios within an assessment to span the range of likely future conditions, even if information is lacking on their probabilities of occurrence. It may be noted that in many studies of deep geological repositories, discharge of activity in to the biosphere is predicted to continue for such long periods that a wide range of biosphere conditions is probable during the period of significant geosphere release.

Uncertainties about human characteristics, habits and locations are more difficult to deal with. When estimating maximum risks to individuals the approach used is to assume that an individual is present at the location where risks would be highest, and that this individual has habits and characteristics (metabolism etc) similar to those of people today (NRPB[12], NEA[13]). The rationale for this approach is that it ensures that no individual in a future generation is subject to a risk which would be regarded as unacceptable now. The approach works well for scenarios in which the highest doses will be received through consumption of water or food, and depend primarily on predicted radionuclide concentrations in environmental materials. However, it is more difficult to apply to scenarios involving inadvertent intrusion because assumptions must be made about actions taken prior to and after the discovery of the waste.

For populations the situation is more complex because the results of collective dose and risk calculations are to be used in comparisons between disposal options. For such comparisons to be valid the estimates must be as realistic as possible and uncertainties must be quantified. It is clearly not possible to predict changes in the location and habits of populations over the time periods of concern in assessments of geologic disposal, nor changes in human characteristics. (For example, 10^5 years ago marked the start of the development of human speech, so how can we tell what society will be like 10^5 years from now?) The best that can probably be achieved is to indicate the range of uncertainty in calculated collective doses and risks, and to take account of these uncertainties when comparing disposal options.

6. IMPORTANT RADIONUCLIDES, PATHWAYS AND PROCESSES

In early work on land disposal of long-lived and highly active radioactive wastes, the models used to predict rates of radionuclide transfer through the biosphere were rather simple ones which did not include all the possible pathways. The tendency was to focus on those pathways which were most direct, in particular on drinking water for inland repositories and on seafood consumption in the case of coastal repositories. These assessments indicated that the radionuclides which are likely to give rise to the highest doses are those which are either very long-lived or which grow in from long-lived parent radionuclides, and which were assumed to migrate relatively rapidly through the geopshere. For example, several studies showed that ^{129}I, ^{99}Tc, ^{226}Ra and ^{237}Np were likely to give rise to the highest doses to individuals from disposal of spent fuel or vitrified high level waste.

Since the early studies both models and their data bases have been improved, but the general pattern of results in terms of the dominant radionuclides has not changed a great deal. For example, in the KBS study[3] of disposal of spent nuclear fuel in crystalline rock formations in Sweden ^{129}I (half-life 16 million years) is predicted to be the most important contributor to both individual and collective doses from spent fuel disposal. The dominant exposure pathways for individuals are consumption of drinking water and consumption of freshwater fish obtained from a lake close to the repository. In the case of collective doses there is a substantial contribution from these, local, pathways but in the very long term it is circulation of ^{129}I throughout the global environment which dominates the cumulative collective dose. It is important to recognise that this global circulation dose is made up of extremely small doses to a large number of people, and is independent of the characteristics of the disposal site.

To investigate the environmental transfer processes and parameters which have most effect on predicted doses, NRPB has carried out a number of example calculations using the BIOS model[1]. The two radionuclides considered are ^{239}Pu (half-life 24,000 years) and ^{99}Tc (half life 213,000 years). Plutonium tends to become fixed to soils and sediments, while technetium is relatively mobile in the environment. Figure 2 shows schematically the characteristics of the local biosphere which were assumed for these example calculations. Table 2 gives the data assumptions for the local biosphere, Table 3 element dependent data (including those for the radioactive daughters of ^{239}Pu), and Table 4 assumptions for human behaviour. All these data were presented in reference [1] and are reproduced here to indicate the amount of information required even for quite a simple set of calculations.

Table 5 shows some of the results obtained for a release of 1 MBq y^{-1} of each radionuclide for 10^3 years into three different parts of the biosphere. For these two radionuclides, both individual and collective doses are dominated by exposure arising close to the release point. With the assumptions made here, terrestrial exposure pathways are more important than direct consumption of contaminated drinking water when the release occurs directly into a river. However, this would not be the case if the river had a lower flow rate. For ^{99}Tc the importance of farming pathways arises from the high factor assumed for uptake from soil into pasture and crops, while for ^{239}Pu it is long term retention and hence accumulation in soils which leads to high doses via terrestrial pathways. Despite the relatively high concentration factors of both radionuclides in certain types of marine foodstuffs, doses from a release into the marine environment are calculated to be much lower than those for a release into freshwater or soils. Work carried out in other contexts shows that interactions with marine sediments will be important in determining doses from ^{239}Pu, but much less so for ^{99}Tc [GESAMP, 1983].

The results given in Table 5 assume constant biosphere conditions. Further calculations are presented in reference [2] which take account of the consequences of the lake (see Figure 2) substantially drying out over a period of 3 10^3 y, and of lake bed sediments being used for farmland. In the case of geosphere release to the river predicted doses for ^{99}Tc were not substantially higher than given in Tabel 5. For ^{239}Pu, which unlike ^{99}Tc, would tend to accumulate in lake bed sediments before the lake dries, both maximum individual doses and collective doses are predicted to be an order of magnitude or so greater. If the drying out of the lake were to occur abruptly, for example if it were drained by man, then predicted doses would be substantially higher still.

Overall, the results discussed above show that it is necessary to include all the relevant pathways and processes, because any one or more could have the greatest effect on predicted doses from a given radionuclide. Our experience from carrying out these calculations and other studies has indicated a number of problem areas for environmental transport modelling. More information and a better understanding is required for the mechanisms for retention and accumulation of radionuclides in soils and their long term availebility for uptake into crops. At present little seems to be known about the potential for transfer of radionuclides from deep soil into the rooting zone, which may be particularly important in the context of releases from shallow land burial facilities. For long-lived alpha emitters resuspension of activity from soils and inhalation (eg during ploughing) has been identified as an important exposure pathway but this is on the basis of relatively little information about the resuspension process.

7. CONCLUSIONS

The difficulties involved in modelling the transfer of radionuclides through the environment and calculating doses to man from land disposal of radioactive wastes are related to lack of data, rather than to lack of modelling techniques. It is possible to construct models to predict doses to individuals and populations from releases of radionuclides from repositories and to verify these models. Validation of these models is more difficult, but can be partially achieved through traditional methods and expert review. When considering priorities for further research in this area it is necessary to bear in mind that the major uncertainties in predicting doses and risk to populations are inherently irreducible, and that maximum risks to individuals may well arise from scenarios involving inadvertent intrusion into repositories. Thus, while the long term behaviour of radionuclides in the environment is of considerable interest, the problem of the assessment of the intrusion hazards should not be ignored.

REFERENCES

[1] International Commission on Radiological Protection. Radiation Protection Principles for the Disposal of Solid Radioactive Waste. ICRP Publication 46. Ann ICRP, 15, No. 4 (1985).

[2] Lawson, G. and Smith, G. M. BIOS: a model to predict radionuclide transfer and doses to man following releases from geological repositories for radioactive waste, NRPB-R169, London, HMSO (1985).

[3] SKBF/KBS. Final storage of spent nuclear fuel - KBS-3, Stockholm, Swedish Nuclear Fuel Supply Co/Division KBS (1983).

[4] Matthies, M. et al. Evaluation of radiation exposure due to radioactive release into the biosphere from a salt dome repository IN Radioactive Waste Management, Proc. Int. Conf., Seattle 16-20 May 1983, Vol 5 p 227-240, Vienna, IAEA (1984).

[5] Kane, P. and Thorne, M. C. User's guide to the biosphere code ECOS. DoE SYVAC TN-ANS-9, London, Department of Environment (1984).

[6] Wushke, D. M. et al. Environmental and safety assessment studies for nuclear fuel waste management, Vol 3: Post-closure assessment. AECL TR-127-3, Whiteshell Nuclear Research Establishment, Pinawa, Manitoba (1981).

[7] Bush, R. P., White, I. F. and Smith, G. M. Carbon-14 waste management, AERE-R10543, Harwell, United Kingdom Atomic Energy Authority (1983).

[8] Smith, G. M. and White, I. F. A revised global circulation model for iodine-129, NRPB-M81, Chilton, National Radiological Protection Board (1983).

[9] National Institute for Radiation Protection. BIOMOVS Progress Report No. 1 Stockholm January (1986).

[10] Haywood, S. M. et al. The development of models for the transfer of ^{137}Cs and ^{90}Sr in the pasture-cow-milk pathway using fallout data, NRPB-R110, London, HMSO (1980).

[11] Group of Experts on the Scientific Aspects of Marine Pollution (GESAMP), An oceanographic model for the dispersion of wastes disposed of in the deep sea, GESAMP Reports and Studies No 19, Vienna, IAEA (1983).

[12] National Radiological Protection Board (NRPB). Radiological protection objectives for the disposal of solid wastes, NRPB-GS1, London, HMSO (1983).

[13] Nuclear Energy Agency (NEA). Long-term radiation protection objectives in radioactive waste disposal (Expert Group report), Paris, NEA (OECD) (1984).

Table 1

Exposure Pathways included in the BIOS Model

Inhalation	- resuspension of soils, river and lake sediments, beach sediments
	- air contaminated through global circulation
	- sea spray
Ingestion	- drinking water
	- freshwater fish
	- terrestrial foodstuffs (milk, meat, crops)
	- marine foodstuffs (fish, crustacea, molluscs, seaweed, plankton)
	- desalinated water
External irradiation	- soils
	- sediments
	- fishing gear

Table 2 Local Biospheric-Transport Parameters

Parameter	Adopted for example calculation
(a) Terrestrial compartments	
Volumetric flow rate ($m^3\ y^{-1}$) This is a combination of the following three model parameters:	$3.2\ 10^{7}$ (1st river) $6.3\ 10^{7}$ (lake) $9.5\ 10^{8}$ (2nd river)
Water velocity ($m\ y^{-1}$)	$6.3\ 10^{7}$ (1st river) $1.3\ 10^{4}$ (lake) $3.2\ 10^{7}$ (2nd river)
Length (m)	$5\ 10^{3}$ (1st river) $1\ 10^{3}$ (lake) $5\ 10^{4}$ (2nd river)
Volume (m^3)	$2.5\ 10^{3}$ (1st river) $5\ 10^{6}$ (lake) $1.5\ 10^{6}$ (2nd river)
Bed-sediment velocity ($m\ y^{-1}$)	$6.3\ 10^{3}$ (1st river) 0 (lake) $3.2\ 10^{3}$ (2nd river)
Suspended sediment load ($t\ m^{-3}$)	$2\ 10^{-5}$ (1st river) $4\ 10^{-5}$ (lake) $6\ 10^{-5}$ (2nd river)
Sedimentation rate ($t\ m^{-3}\ y^{-1}$)	* (1st river) $2\ 10^{-4}$ (lake) * (2nd river)
Water depth (m)	* (1st river) 5 (lake) * (2nd river)
Annual depth of irrigation ($m\ y^{-1}$)	$5\ 10^{-2}$ (each compartment)
Fraction of volumetric flow used for irrigation	10^{-2} (each compartment) (25% pasture, 75% arable)
Coefficient for transfer of river and lake sediment to land (y^{-1})	10^{-3} (1st river) $3\ 10^{-4}$ (lake) $2\ 10^{-3}$ (2nd river)
Transfer coefficient from surface to deep soil (y^{-1})	$6.9\ 10^{-3}$ (each compartment)
Transfer coefficient from deep to surface soil (y^{-1})	$5\ 10^{-2}$ (each compartment)
Residence time for mobile water in deep soil (y)	1.8 (each compartment)
(b) Local marine compartment	
Depth (m)	20
Sedimentation rate ($t\ m^{-3}\ y^{-1}$)	$5\ 10^{-6}$
Suspended sediment load ($t\ m^{-3}$)	10^{-5}
Volume (m^3)	$2\ 10^{9}$
Volume exchange with adjacent regional compartment, English Channel West ($m^3\ y^{-1}$)	$4\ 10^{10}$
Fraction of local marine water transferred to coastal strip (y^{-1})	10^{-5}
Length of coastline (m)	$2\ 10^{4}$

*Parameter not used in the model for river compartments.

Table 3 Element Dependent Data

Parameter	Tc	Pu	U	Pa	Ac
Distribution coefficients ($m^3\ t^{-1}$)					
Fresh water - sediment	2 10^{2}	3 10^{4}	1 10^{4}	1 10^{5}	1 10^{3}
Soil - ground-water	0	1 10^{3}	3 10^{2}	6 10^{3}	3 10^{3}
Sea-water - sediment: coastal	1 10^{3}	1 10^{5}	1 10^{3}	1 10^{5}	1 10^{4}
deep ocean	1 10^{3}	1 10^{5}	5 10^{2}	1 10^{5}	1 10^{4}
Concentration factors (t dry soil/ t fresh crop)					
Soil - root vegetables	10	1 10^{-3}	3 10^{-3}	3 10^{-3}	3 10^{-3}
Soil - grain	10	1 10^{-6}	3 10^{-3}	3 10^{-3}	3 10^{-3}
Soil - green vegetables	10	1 10^{-4}	3 10^{-3}	3 10^{-3}	3 10^{-3}
Soil - pasture	10	1 10^{-4}	3 10^{-3}	3 10^{-3}	3 10^{-3}
Fresh water - fish (m^3 filtered water/t fresh edible part)	15	10	10	11	25
Sea-water - fish "	3 10^{1}	5 10^{1}	0.1	5 10^{1}	5 10^{1}
Sea-water - crustacea "	1 10^{3}	2 10^{2}	1 10^{1}	1 10^{1}	1 10^{3}
Sea-water - molluscs "	1 10^{3}	2 10^{3}	1 10^{1}	1 10^{1}	1 10^{3}
Sea-water - seaweed "	1 10^{3}	2 10^{3}	1 10^{1}	1 10^{2}	1 10^{3}
Sea-water - sea spray ($m^3\ m^{-3}$)	1	10	10	10	10
Fraction transferred to animal products (day kg^{-1})					
Beef	1 10^{-2}	1 10^{-5}	2 10^{-4}	0.0	4 10^{-4}
Cow liver	1 10^{-2}	1 10^{-5}	2 10^{-4}	1 10^{-1}	1 10^{-1}
Milk	1 10^{-2}	1 10^{-7}	6 10^{-4}	5 10^{-6}	2·10^{-5}
Mutton	1.3 10^{-1}	1.3 10^{-4}	2.6 10^{-3}	0.0	5.1 10^{-3}
Sheep liver	7.5 10^{-2}	7.5 10^{-5}	1.5 10^{-3}	0.75	0.75

Table 4

Assumptions of human behaviour used in example calculations

Maximum individual doses

For each pathway which may potentially lead to exposure of man it is assumed that an individual is present to receive the dose. The characteristics of the individual are chosen so as to maximise the potential dose. Thus individual consumption rates for each foodstuff are at the top of the ranges persisting. It is possible that the same individual may be exposed via more than one pathway. However, in this event it is unreasonable to assume maximum values for all the pathways.

Individual consumption rates

drinking water	0.6 $m^3\ y^{-1}$	green vegetables	80 kg y^{-1}
freshwater fish	20 kg y^{-1}	grain	130 kg y^{-1}
beef	60 kg y^{-1}	root vegetables	120 kg y^{-1}
cow liver	20 kg y^{-1}	marine fish	219 kg y^{-1}
milk	300 kg y^{-1}	crustacea	36.5 kg y^{-1}
mutton	30 kg y^{-1}	molluscs	36.5 kg y^{-1}
sheep liver	20 kg y^{-1}	seaweed	36.5 kg y^{-1}

Occupancy (hours y^{-1})	External irradiation	Inhalation
beach	10^3	8760 (sediment) 10^3 (sea spray)
fishing gear	876	-
farmer ploughing	300	300
other	8760	8760

Inhalation rate 1 m^3 hour^{-1}

Collective doses

Fraction of each freshwater-compartment volumetric flow

consumed as drinking water 2×10^{-3}

(equivalent to about 20% of flow abstracted for domestic supply)

used for spray irrigation purposes 10^{-2}

(25% to pasture, 75% to arable land)

Terrestrial food yields (kg km^{-2})

beef	1.6 10^4	green vegetables	1.0 10^6
cow liver	6.4 10^2	grain	4.0 10^5
milk	6.3 10^5	root vegetables	2.5 10^6
mutton	1.3 10^3	pasture (dry weight)	1.0 10^5
sheep liver	6.9 10^1		

Marine harvests maintained at current regional and global levels; all fish, crustacea and molluscs assumed to be for human consumption; 10% of seaweed harvest assumed to be for human consumption. Local seafood harvests, fish 20 t, crustacea 60 t, molluscs 70 t, and seaweed 1 t. Percentage of landing weight assumed to be edible

fish	50%	molluscs	15%
crustacea	35%	seaweed	10%

Table 5

Results of Example Calculations for ^{99}Tc and ^{239}Pu using the BIOS Model

Compartment into which release occurs	Maximum annual individual dose (Sv) and dominant pathway	Collective dose[(c)] commitment (man Sv) and dominant pathway
^{99}Tc		
river(a)	2.10^{-11}, milk	9.10^{-3}, farming
deep soil(b)	2.10^{-10}, milk	2.10^{-2}, farming
local marine	3.10^{-13}, seafood	3.10^{-5}, seafood
^{239}Pu		
river(a)	6.10^{-9}, inhalation of resuspended soil	5.10^{-1}, drinking water, farming
deep soil(b)	6.10^{-7}, inhalation of resuspended soil	1.10, farming
local marine	1.10^{-10}, seafood	2.10^{-3}, seafood

Notes

(a) River water is assumed to be used for irrigation of farmland.

(b) Contamination of farmland arises through upward migration from the deep soil. No irrigation is assumed.

(c) Results for collective dose commitment are those assuming that farmland is used to produce those products which give rise to the largest dose.

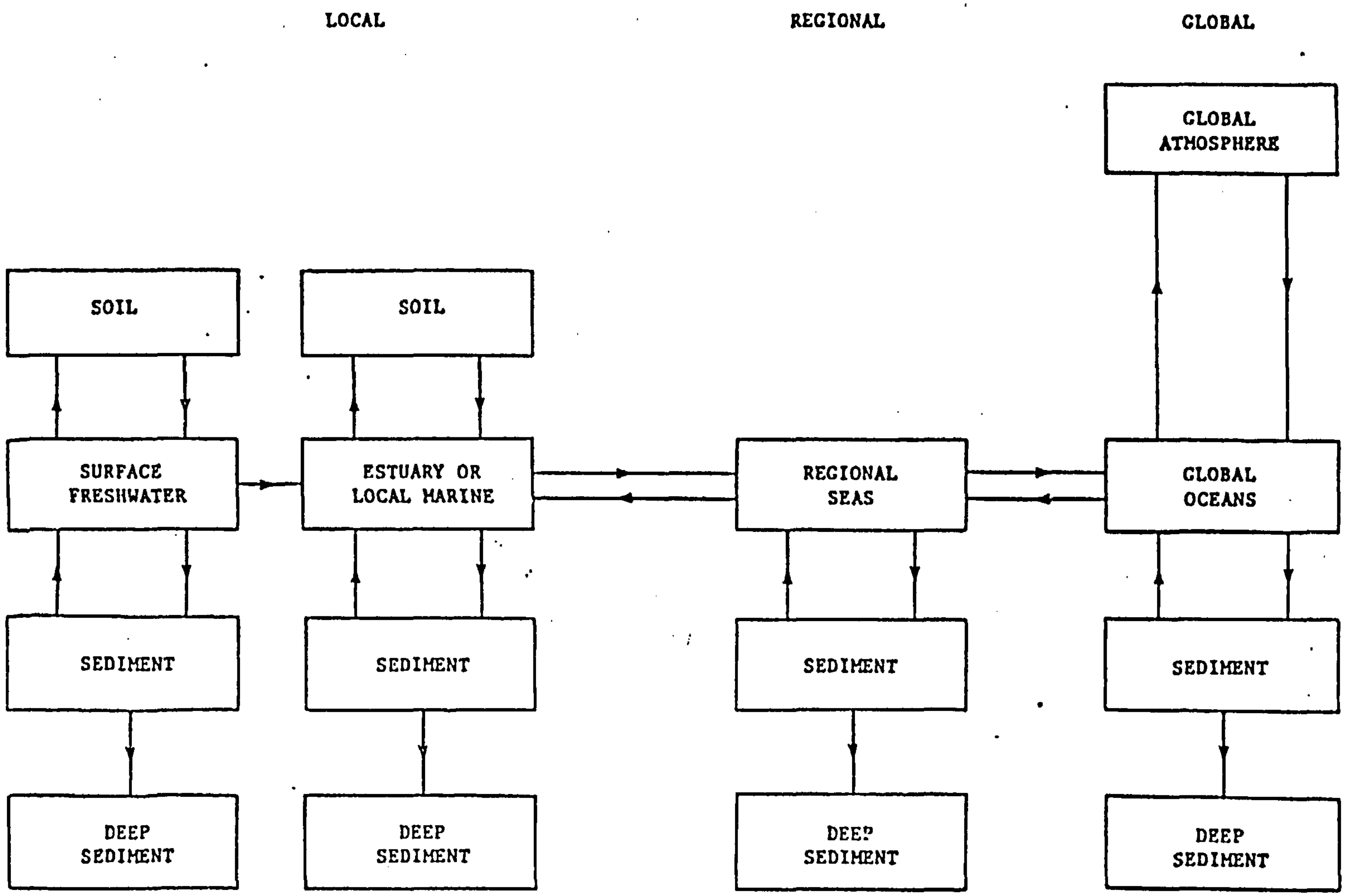
LOCAL
REGIONAL
GLOBAL
GLOBAL ATMOSPHERE
SOIL
SOIL
SURFACE FRESHWATER
ESTUARY OR LOCAL MARINE
REGIONAL SEAS
GLOBAL OCEANS
SEDIMENT
SEDIMENT
SEDIMENT
SEDIMENT
DEEP SEDIMENT
DEEP SEDIMENT
DEEP SEDIMENT
DEEP SEDIMENT

Figure 1 Schematic of biospheric-transport model

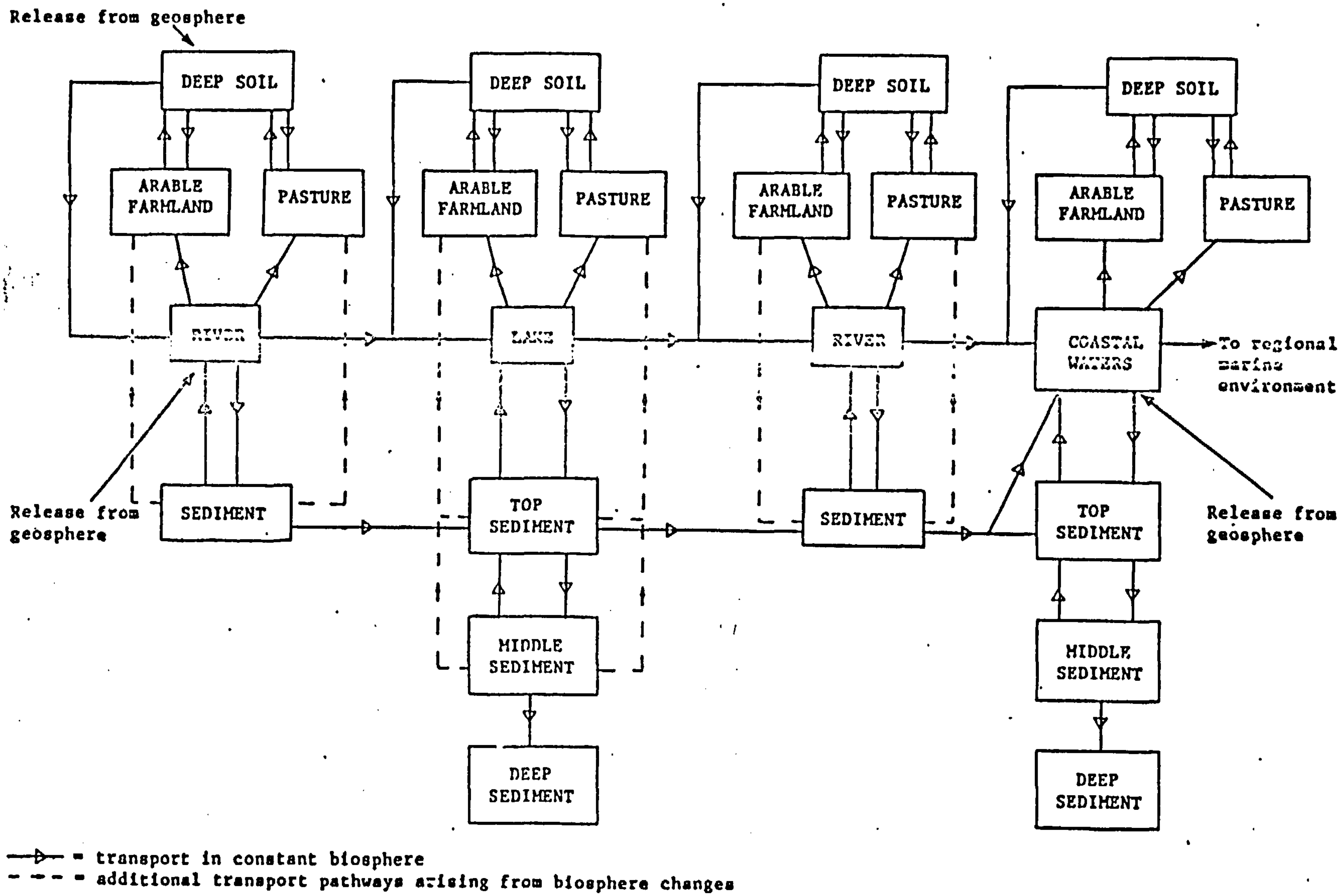
Release from geosphere
DEEP SOIL
ARABLE FARMLAND
PASTURE
RIVER
SEDIMENT
Release from geosphere
DEEP SOIL
ARABLE FARMLAND
PASTURE
LAKE
TOP SEDIMENT
MIDDLE SEDIMENT
DEEP SEDIMENT
DEEP SOIL
ARABLE FARMLAND
PASTURE
RIVER
SEDIMENT
DEEP SOIL
ARABLE FARMLAND
PASTURE
COASTAL WATERS
To regional marine environment
Release from geosphere
TOP SEDIMENT
MIDDLE SEDIMENT
DEEP SEDIMENT
= transport in constant biosphere
= additional transport pathways arising from biosphere changes

Figure 2 Schematic of the assumed local biospheric transport for the example calculations

MODELLING OF SPENT NUCLEAR FUEL LEACHING

Jordi Bruno.
Dept. of Inorganic Chemistry. The Royal Institute of Technology.
S-100 44 Stockholm. (Sweden).

SUMMARY

The current trends on thermodynamic and kinetic modelling of the dissolution of spent nuclear fuel in groundwater are discussed. Special emphasis is put in the processes connected to $UO_2(s)$ dissolution. Some examples of the validation of the thermodynamic data base for uranium are given.

INTRODUCTION

A combination of engineered barriers and deep geological burial is a current concept in all repository designs. The overall performance of a repository cannot be tested prior to its construction. All kind of security analysis and the optimization of the design depends on the understanding and the consequent modelling of the behaviour of the different barriers.

The innermost of the barriers consists on the limited solubility in groundwater of UO_2(s), the major component of the spent fuel. A number of experiments have been performed in order to study the dissolution rates of [illegible] fuels of various burnups. From these, so called, leaching studies [illegible] information has been obtained on the empirical behaviour (dissolution rates and solubility limits) of spent fuel in contact with groundwater. In the other hand, the solubility behaviour of $UO_2(s)$ have been widely studied both from the thermodynamic[1] and the kinetic point of view[2-7].

The aim of this communication is to review the current trends in the thermodynamical and kinetic modelling of spent nuclear fuel dissolution, particularly in connection with the behaviour of $UO_2(s)$. At the same time, some practical examples of the validation of the thermodynamic data base for [illegible] will be given.

Uranium release from $UO_2(s)$ spent fuel leaching. An experimental evidence. Experimental studies of $UO_2(s)$ spent fuel leaching have shown that a fraction of the fission product as Cs and I are rapidly released. This is followed by preferential grain boundary dissolution and dissolution of the $UO_2(s)$ grains. This last process depends very much on the redox state of the surface as well on the composition of the groundwater in contact with. The existing data are far from sufficient in order to completely understand the mechanisms of uranium release under these circumstances. However, based on the results so far obtained some conclusions can be drawn. Independent studies of spent fuel dissolution in simulated groundwaters containing total bicarbonate concentrations in the range 10^{-3} mols/l and in contact with the air, indicate that the uranium release reaches a constant concentration in the range $[U(VI)]_{tot} \simeq 10^{-6}$ mols/l [8,9]. The time for the attainment of constant uranium concentrations is approximately 14 days. This is shown in Figure 1, where the measured uranium concentrations are plotted as a function of the contact time in the leaching experiments performed at pH=8.1 and $[HCO_3^-]_{tot}=2\ 10^{-3}$ mols/l. In Figure 2 the dissolved uranium concentrations in contact with solutions at different pH values are plotted. These two plotts indicate that the uranium release from spent nuclear fuel is solubility limited[8].

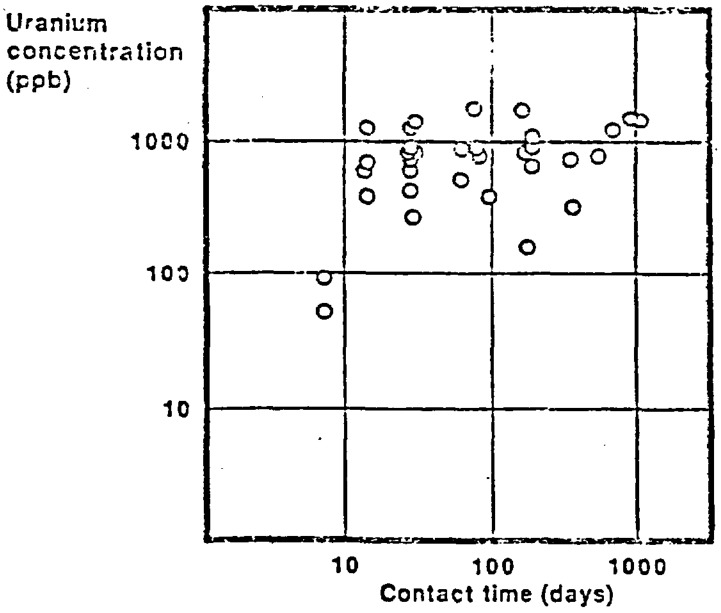

Figure 1. Measured concentrations of uranium in leach solution centrifugates as a function of time.

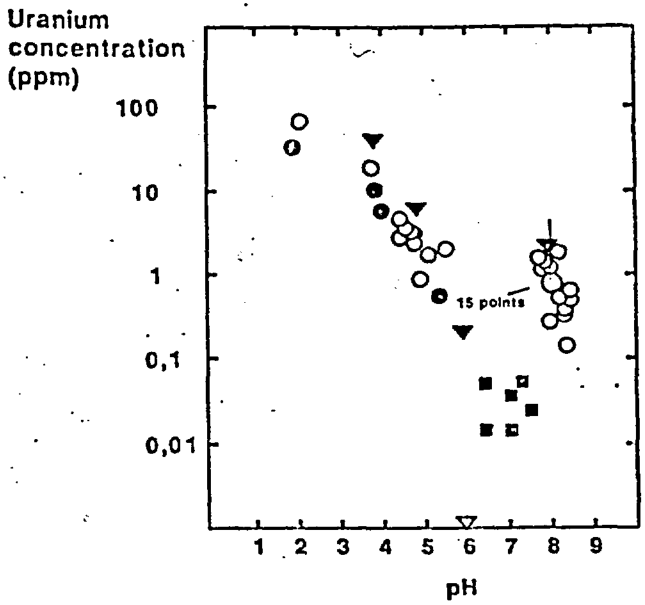

Figure 2. Measured concentrations of uranium at different pH. ○ In acidic range, 91 days exposure. ◉ At pH=3.2, 14 days to 3 years exposure. ⊠ Exposed in DI water. ▼ Calculated solubilities for synthetic groundwater. ▽ Calculated solubility in DI water.

The thermodynamics of $UO_2(s)$ dissolution.

In order to model the processes connected with $UO_2(s)$ spent fuel dissolution an independent knowledge of the thermodynamical data of relevance is critical. Since, uranium release is clearly thermodynamically constrained, as we have previously indicated. Furthermore, even in the cases where equilibrium is not reached, the progress towards the equilibrium will conditionate the dynamics of the system.

The thermodynamic datum which directly defines the solubility of a solid phase is the solubility constant. In the case of $UO_2(s)$ the solubility equilibrium is defined :

$$UO_2(s) + 4\,H^+ = U^{4+} + 2\,H_2O \qquad (1)$$

where the equilibrium constant for the reaction is given by:

$$K_{s0} = [U^{4+}]/[H^+]^4 \qquad (2)$$

The determination of this solubility constant has been matter of controversy. The direct investigation of this equilibrium reaction is difficulted by two factors:

1) The characteristics of the solid phase. $UO_2(s)$ can be easily oxidized to higher $UO_{2+x}(s)$ oxides, and the measured solubilities will consequently be erroneous if strict control is not taken on the redox conditions. On the other hand, different $UO_2(s)$ solids of various degrees of crystallinity have been measured, this being a factor that affects the magnitude of the solubility constant (2).

2) In traditional solubility measurements the total uranium concentrations are analytically determined in solutions of different pH, in contact with $UO_2(s)$. The U^{4+} cation is a very strong acid and even at very low pH values it is strongly hydrolyzed. This means that uranium is no longer present as U^{4+} but it participates in reactions of the type :

$$U^{4+} + n\,H_2O = U(OH)_n^{4-n} + n\,H^+ \qquad (3)$$

As a consequence, the measured total uranium concentration [U(IV)] is not equal to $[U^{4+}]$, but also the concentration of the hydrolysis species $U(OH)_n^{4-n}$ have to be taken into consideration. The main problem arises from the fact that no direct reliable determination of the different hydrolysis complexes of U(IV) is available, and most of the solubility data treatment has been done based in estimates[10]. We have devoted some of our experimental efforts to solve part of these problems. We have measured the solubility of different well characterized $UO_2(s)$ solid phases, under controlled redox conditions. We have directly determined the variation of $[U^{4+}]$ with pH in solutions saturated with $UO_2(s)$, by measuring the variation of the redox potential of the couple UO_2^{2+}/U^{4+}, previously determined[11]. As a result of, we have established the value for the solubility constant K_{s0} of reaction (1), for different types of crystalline solids, among them an unirradiated $UO_2(s)$ fuel pellet[1] ($[U(IV)]_{total} \approx 10^{-7}$ mols/l, pH: 7-9, under reducing conditions, $[HCO_3^-] = 2\ 10^{-3}$ mols/l)

Although the bulk of $UO_2(s)$ spent fuel can be thought to be crystalline, the formation of amorphous superficial $UO_2(s)$ phases cannot be excluded. This will be particularly the case, in the event of a solubilization of the spent fuel under oxidizing conditions (caused perhaps by α-radiolysis), and a later re-precipitation of $UO_2(am)$ when the reducing conditions are restored. Hence, under these circumstances uranium release may be controlled by an amorphous phase of higher solubility than the crystalline one. We have determined the solubility of a freshly precipitated, but reproducible $UO_2(am)$ phase, we obtain uranium solubilities which are 200 times higher than the expected uranium concentrations from crystalline $UO_2(s)$, ($[U(IV)]_{tot} = 2\ 10^{-5}$ mols/l, in the pH range 7-9, under reducing conditions and $[HCO_3^-] = 2\ 10^{-3}$ mols/l). At the same time, by studying the dependence of log [U(IV)] vs pH (see Figure 3), we have been able to establish the predominant $U(OH)_n^{4-n}$ hydrolysis species in the pH range 3 to 11, as $U(OH)_3^+$ and $U(OH)_4$[10]. In this way, some of the ambiguities concerning the solubility of $UO_2(s)$ have been solved (see Fig 3). Nevertheless, some uncertainities are still present for the U(IV) speciation in groundwaters. Experimental and modelling work is on progress in our laboratory concerning the actinide(IV) speciation in carbonate waters[12,13].

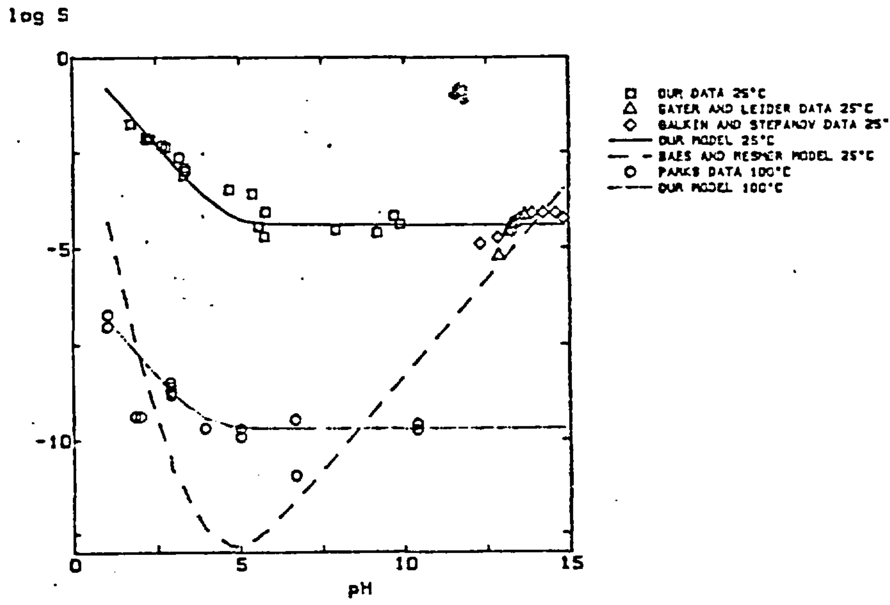

Figure 3. Experimental $UO_2(s)$ solubility as a function of pH for different types of solid phases at T:25-100°C. Comparison with calculated model solubilities.

Some test cases for the validation of the thermodynamic data base of uranium. The validity of a certain thermodynamic data base and the methodology involved in its use should be tested by comparing the predicted values with parameters experimentally collected in the conditions of application. In the case of uranium, the ultimate goal of the thermodynamic data base and the consequent thermodynamic modelling is to predict long-term uranium concentrations under repository conditions. The data summarized in Figure 2 provides us with a good test case. The leaching data have been obtained under drastically different conditions of pH and complexating agents[8], the fact that the calculated uranium solubilities as a function of pH, reproduce the behaviour experimentally observed, indicates that the critical parameters in the thermodynamic data base for uranium are correct enough to modellate the experimental behaviour of uranium. At the same time, this also gives support to the hypothesis of solubility limits for uranium release from spent fuel.

The measured uranium concentrations in different groundwaters, under various pH, total carbonate, and pE conditions, provide us with another test case. In the course of the site characterization program, uranium analysis have been performed in different boreholes[14]. The development of the field equipment made possible the measurement in situ of pH and pE, the parameters of relevance for uranium solubility. In Figure 4, we include a predominance diagram for the different uranium species as a function of E_h and pH. This diagram has been calculated with the thermodynamic data base compiled in our laboratory[8]. The result of the uranium analysis have been also plotted as a function of the measured E_h and pH. The good agreement between theoretical and experimental values indicates that the measured parameters in the field can be reproduced by the thermodynamic data base. As an additional conclussion it appears that the uranium solubilities in groundwater agree with the hypothesis of $UO_2(am)$-$UO_2(c)$ as the solubility limiting phases. This gives support to the idea that much information can be extracted from natural analogues for the understanding of the spent fuel solubility processes, particularly in the long term behaviour.

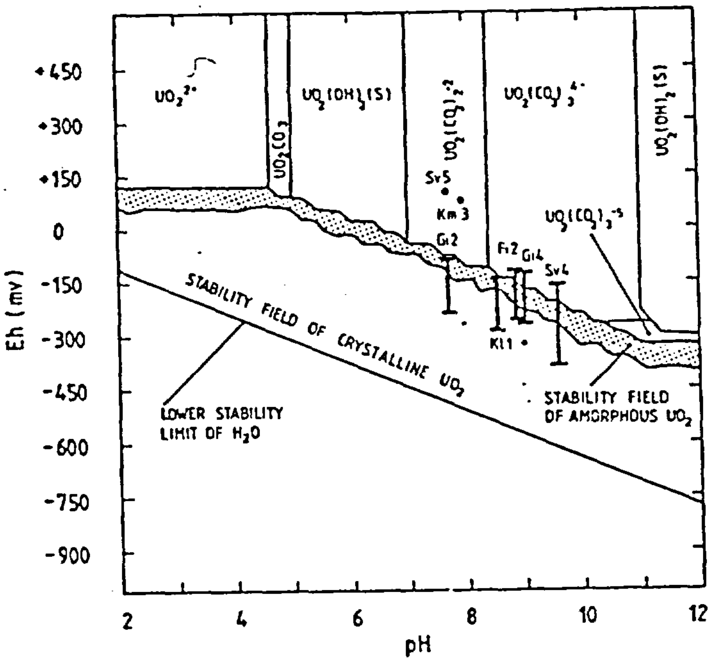

Figure 4. *In situ* measured pH, E_h and uranium concetrations for different boreholes in Sweden. The experimental measurements are superposed to the theoretical predominance diagram for uranium in groundwater conditions.

The kinetics of UO_2(s) dissolution

The information here included is part of a major Technical Report on the kinetics of UO_2(s) dissolution[15]. Experimental work has been done in order to study the rates of dissolution of UO_2(s) in various conditions[2-7]. These investigations have been in general directed to establish the dependence of dissolution rates on different critical parameters. In this way empirical reaction rates are obtained. In order to model the dissolution behaviour of UO_2(s) and to attempt long-term predictions it is not sufficient with a knowledge about the overall reaction rates. In opposition to thermodynamic functions, the kinetics of a system is very dependent on the way the overall reaction proceeds. On the other hand, the rate parameters of elementary reactions (processes occuring at the microscopic level, including reaction intermediates), can be applied in any other process in which the specific elementary reaction occurs. This means that a detailed knowledge on the kinetics of the elementary reactions (e.g. elementary reaction rates and elementary mechanisms) is needed.

The mechanistic information so far obtained can be summarized in the following way :

a) no experimental information is available on the rates and mechanisms of dissolution of $UO_2(s)$ under reducing conditions. The kinetic study of the dissolution of uraninite by D.E. Grandstaff[5] was performed under different partial pressures of $O_2(g)$, but the author used natural samples of uraninite with a large content of $UO_3(s)$. A.R. Amell and D. Langmuir[6] studied the kinetics of $UO_2(s)$ dissolution under anoxic conditions but they specifically investigated the effect of oxidizing agents, e.g. Fe^{3+}.

b) Much more experimental work has been done under oxidizing conditions. It is reasonable to assume that the initial step on the dissolution mechanism of $UO_2(s)$ under oxidizing conditions will be the surface oxidation of $UO_2(s)$, according to the general reaction :

$$UO_2(s) + x/2\ O_2(g) \dashrightarrow UO_{2+x}(s) \qquad (3)$$

The extent of this reaction, and consequently the magnitude of x is dependent on the presence and amount of oxidizing species (p_{O_2}, H_2O_2, Fe(III)). R.L. Pearson and M.E. Wadsworth found in their pioneer work[2] a direct dependence between p_{O_2} and the rate of dissolution of $UO_2(s)$. F. Habashi and G.A. Thurston[3] were the first to propose an anodic reaction for the oxidative dissolution of $UO_2(s)$, being the reduction of $O_2(aq)$ the corresponding cathodic reaction. M.J. Nicol and C.R.S. Needes[4] found that their steady state potentiostatic and cyclic voltammetric measurements were consistent with the anodic dissolution involving a two-electron transfer and the formation of U(VI)-oxide films on the surface. The same behaviour has been found by Shoesmith et al[16] in their extensive studies of UO_2-spent fuel dissolution by electrodynamic measurements. D.E. Grandstaff[5] carried out an investigation of the dissolution of uraninite and he found a direct dependence of the rate of dissolution on p_{O_2}. A.R. Amell and D. Langmuir[6] made an interesting study of the $UO_2(s)$ dissolution in the presence of acid waters containing Fe(III) and SO_4^{2-} species. They proposed several Fe(III) species as direct oxidants on the uranium dioxide surface, since the reaction rates were found to be dependent on the concentration of Fe(III) but not on the E_h of the solution.

The identification of the oxidized phase has been subject of much experimental effort. In the initial studies $UO_3(s)$ was proposed. It is now clear that the oxidation of the surface does not easilily proceed further than to $U_3O_8(s)$. In their studies Taylor et al[16] found by an X-ray diffraction, a conversion of the upper 3µm layer of UO_2 to U_3O_7 under oxidizing conditions at 250-275 °C. These results were later on corroborated by an XPS investigation of air-oxidized pellets at 200-250 °C by G.C. Allen[17]. However, it is not clear in which way the results obtained by these investigators can be applied to the situation in which spent nuclear fuel is put in contact with groundwater at 25-70 °C. In fact, A. Stenborg[18] found by ESCA measurements that the surface oxidation of $UO_2(s)$ by oxygen containing water did not proceed further than to the formation of $UO_{2.25}$. The disagreement between different investigators is partly explained by the interpretation of the ESCA results, but also by the different oxidazing situations they studied.

The second step on the dissolution mechanism of $UO_2(s)$ should be the surface reaction between the oxidized UO_{2+x} solid phase and the major complex formating ions present in the groundwaters, e.g. $HCO_3^-/CO_2(aq)$ in the case of granitic groundwaters, to form the corresponding uranyl carbonate complexes. Different alternatives have been proposed. The investigations conducted in carbonate media have been mostly directed to the optimation of in situ leaching of uranium ores by highly concentrated carbonate solutions. In granitic groundwaters, the total bicarbonate concentrations are of the order of magnitude of 10^{-3} mols/l. At the average pH values found in groundwaters (6.5 - 9), HCO_3^- and $CO_2(aq)$ are the predominant carbonate species. Different dependences with bicarbonate and carbonate concentrations have been found. The reaction orders oscillate between 0.5 and 1 for carbonate. J.B. Hiskey[7] proposed that HCO_3^- takes directly part on the anodic dissolution according to the general mechanism:

$$UO_2(s) + HCO_3^- = UO_2HCO_3(s) + e^- \qquad (4)$$

$$UO_2HCO_3(s) + CH^- = UO_2CO_3(s) + H_2O + e^- \qquad (5)$$

$$UO_2CO_3(s) + 2\,CO_3^{2-} = UO_2(CO_3)_3^{4-} \qquad (6)$$

R.L. Pearson and M.E. Wadsworth[2] proposed $CO_2(aq)$ as the surface active species and they observed a competition between $CO_2(aq)$ and $O_2(aq)$. It is well known that in processes such the carboxilation of metal hydroxides in aqueous solution $CO_2(aq)$ is the active species in the reaction up to $pH \simeq 9$[19]. It is thus reasonable to expect that $CO_2(aq)$ will participate actively in the process, particularly in groundwaters with partial overpressure of carbon dioxide. Hence, an hypothetical second step in the oxidative dissolution of $UO_2(s)$ would be :

$$UO_{2+x}(s) + CO_2(aq) \dashrightarrow UO_2(CO_3)_3^{4-} \qquad (7)$$

In this second step the formation of secondary phases play an important role. The dissolution of $UO_2(s)$ proceeds until saturation of a U(VI) solid phase is attained. Under oxidizing groundwater conditions the saturation of $UO_2(OH)_2$ can be easily reached[8]. Other secondary phases have been proposed, $UO_4(s)$ in the presence of H_2O_2[6], $UO_2CO_3(s)$ at high carbonate concentrations[7]. The formation of these secondary phases may pasivate the $UO_2(s)$ surface.

Finally, it is interesting to compare the results so far obtained for the spent fuel dissolution, with the ones obtained with other kind of $UO_2(s)$ materials. The $UO_2(s)$ dissolution rates for uranium, oscillate between 10^{-6}-10^{-8} g cm^{-2}day, depending if oxidizing or reducing conditions have been studied. The same order of magnitude for uranium release is found for other types of $UO_2(s)$. The magnitude of the energy of activation, E_a ranges between 30-60 kJ mol^{-1}, the variation depending on the mechanism proposed and not on the kind of $UO_2(s)$. The value of E_a indicates that the overall process is chemically and not diffusion controlled. Nevertheless, the first oxidation step (3), may be diffusion controlled, if $O_2(aq)$ is the oxidazing agent.

CONCLUSSIONS

From the information here reviewed we may draw the following conclussions.

The knowledge about the thermodynamic behaviour of $UO_2(s)$ is fairly good. The experimentally determined thermodynamic data for the solubility of uranium dioxide shows a correlation with the degree of crystallinity, but not with the type of $UO_2(s)$ material used, microcrystalline oxide shows the same solubility as unirradiated $UO_2(s)$ pellets. The theoretically calculated uranium solubilities agree well with the uranium concentrations found in "real" cases. Still, some uncertainities are present regarding the speciation model for the $U(IV)-H_2O-CO_2(g)$ system, we believe that the work at the present going on at our lab will solve some of these questions.

The knowledge about the mechanisms of $UO_2(s)$ dissolution and their implications on the dissolution of $UO_2(s)$-spent fuel is far more uncomplete. Experimental and theoretical work has to be done in addition to the ongoing spent fuel leaching studies in order to understand the elementary processes involved. Particular stress should be put in the study of the phenomena occurring in the $UO_2(s)$-solution interfase under both oxidizing and reducing conditions.

REFERENCES

1- J.Bruno, D.Ferri, I.Grenthe and F.Salvatore. *Acta Chem. Scand.* (1986) A 40, 428.

2- R.L.Pearson and M.E.Wadsworth. *Trans. Metall. Soc. AIME.* (1958), 212, 294.

3- F.Habashi and G.A.Thurston: *Energ. Nucl.* (1967), 14, 238.

4- M.J.Nicol and C.R.S. Needes. *Electrochem. Acta.* (1975), 20, 585.

5- D.E.Grandstaff *Econom. Geolog.* (1976), 71, 1493.

6- A.R. Amell and D.Langmuir. Bureau of Mines OFR-84-79. Washington D.C. 1978

7- J.E.Hiskey. *Trans. Inst. Min. Metall.*,(1979), C 88, 145.

8- R.S.Forsyth, L.O.Werme and J.Bruno. *J. Nucl. Mater.* (1986), 138, 1.

9- L.H.Johnson. Report AECL Whiteshell Nucl. Res. Est. Pinawa, Manitoba, Canada (1982).

10.- J.Bruno, I.Casas, B Lagerman and M.Munoz. To be presented in the X Scientific Basis for Nuclear Waste Management Meeting. Boston. December 1986.

11.- J.Bruno, I.Grenthe and B.Lagerman. *Mater. Res. Soc. Symp. Series.* (1986), 40, 299.

12.- J.Bruno, I.Casas, I.Grenthe and B.Lagerman. To be published.

13.- J.Bruno, I.Casas, I.Grenthe and B.Lagerman. To be published.

14.- J.Smellie, N.A.Larsson, P.Wikberg and L.Carlsson. SKB Technical Report [illegible]. Stockholm 1985.

15.- J.Bruno, I.Casas and I.Puigdomenech. To be published.

16.- S.Sunder, D.W.Shoesmith, M.G.Bailey F.W.Stanchel and N.S. McIntyre. J.

Electroanal. Chem. (1981), 170, 165. P.Taylor, E.A.Burgess and D.G.Owen. *J. Nucl. Mater.* (1980), 88, 153.

17.- G.C.Allen. *Philos. Magazine* (1985) B51, 465.

18.- A.Stenberg. UPTEC 84 122 E. Teknikum, Inst. Of Technology. Uppsala University. Uppsala 1984 (Sweden).

19.- E.Chaffee, T.P.Dasgupta and G.M.Harris. *J. Am. Chem. Soc.* (1973), 95, 4169. T.P. Dasgupta and G.M. Harris. *J. Am. Chem. Soc.* (1977), 99, 2490. [illegible] [illegible], D.A. Palmer and G.M. Harris. *Inorg. Chem.* (1974), 13, [illegible].

ACKNOWLEDGMENTS. This investigation has been economically supported by SKB (Swedish Fuel Supply Co.).

DATA UNCERTAINTY IN LONG-TERM PREDICTION. PRESENT TRENDS IN RISK ANALYSIS WITH MONTE CARLO TECHNIQUES.

A. SALTELLI, G. BERTOZZI

Joint Research Centre of the European Communities, Ispra (I)

ABSTRACT

As the analysis of the risk linked to the existence of radioactive waste repositories into geological formations must extend over geological time periods, the parameters and models utilised are unavoidably affected by uncertainties. A methodology recently applied to Waste Disposal Performance Assessments involves the use of probability distributions for the uncertain parameters. Such distributions, which account for intrinsic parameter variability as well as for their degree of uncertainty, are then fed into a computer code able to produce a distribution of the model results. In this note some of the statistical techniques usually applied in the various steps of the Monte Carlo Analysis shall be shortly illustrated.

1. INTRODUCTION

Radioactive waste is an unavoidable consequence of the use of nuclear energy at an industrial level. Its disposal into properly selected geological formations is considered at present as a solution which can be technically implemented, with no major problems. In fact, in the different European countries, it is possible to identify formations which are likely to remain unaltered for geological periods of time, thus assuring that the enclosed waste will be kept adequately segregated [1].

The experts' judgement cannot, however, be considered as a demonstration that the disposal of radioactive waste into a given site in consistent with future public health: it is necessary to validate this statement by showing, on scientific bases, that present-day technology allows to create geological repositories of nuclear waste in a manner that meets the preestablished safety requirements for sufficiently long time periods.

Predictive modelling of repository evolution and radionuclide behaviour in the specific environment can offer the required answer to the demand for such a demonstration: the release and transport processes of radionuclides through the various barriers and food chains are described in quantitative terms, having regard of the site-specificity of the analysis.

This predictive modelling, however, is of necessity hampered by relevant uncertainties which affect both models and data, and whose importance increases with the length of the time span considered. A reliable analysis can only be effected through appropriate quantification of the uncertainty linked to the analysis results, and through identification of the areas and parameters which contribute more substantially to the overall uncertainty.

Substantial efforts are being made in Western Europe by individual countries and the CEC in order to create the methodological bases for such kind of analysis. To this aim, the CEC coordinates a concerted action in order to establish a common background for this type of performance assessment [2].

The methodological approach which has been so far developed, and the related mathematical and statistical issues are briefly described in the following sections.

2. METHODOLOGY

The assessment methodology consists of an analysis of probabilistic character, in which a number of probability terms are involved; their use is necessary in order to deal with the non-deterministic behaviour of different components of the system, like geological and climatic events, and human habits and actions.

It consists of the following steps:

1) identification and description of the different scenarios involving radionuclide release from the repository;
2) assessment of the probabilities of occurrence of the various events capable of triggering or perturbing the release scenarios;
3) modelling of the radionuclide release and transport through the various system components, following the scenario considered; modelling of the radionuclide dispersion in the environment, assessment of their concentrations in food chains and related intakes to man;
4) assessment of the radiological consequences to individuals, in terms of radiation exposure;
5) conversion of doses to risk;
6) investigation of the relative importance of the various input parameters in governing the output.

Points 1 and 2 require the identification of all the events and processes which could cause the release of radionuclides from the waste and govern their transport through the geosphere and the biosphere. For any given type of geologic formation, there will be some processes which are certain to occur: they constitute the 'Normal Evolution Scenario'. The assumptions used in analysing this scenario are based on extrapolations into the future of present geological and climatic trends. Probabilistic events and processes, having the capability to perturb the normal situation lead to the definition of the 'Altered Evolution Scenarios', characterized by sets of parameter values which are outside the normal range. The probabilities that the phenomena will occur are taken into account in the analysis.

A third type of scenario is that in which the radionuclide release is triggered by probabilistic events and occurs in a completely different way, being thus described by a different model. Again, the probabilities of the triggering events have to be considered, when assessing the risk for such scenarios. Events having the potential to cause direct releases of radionuclides into the biosphere are grouped into a fourth class, 'Disruptive Scenarios'. They are very unlikely and - in general - can be ruled out on the mere basis of their probabilities.

Probability evaluation in a geological context is an especially debated point, as most of the events considered are rare, and their probabilities of occurrence can hardly be inferred from a body of statistically significant data. A codified procedure for the assessment of probabilities of goelogical events and processes does not exist. In the past, we have described a few applications of the Fault Tree Analysis for this aim, with satisfactory results; however, we feel that the binary logic of this tool imposes a too strict working scheme, which is not especially suited for such a multiform context. Thus, for many geological processes the evaluation of the corresponding probabilities is often derived from expert's subjective judgements, on the basis of the current state of knowledge.

As the analysis must extend over very long time periods, the numerical values attributed to the various parameters in the mathematical equations used to describe the system are very often affected by uncertainties, which, in some cases, may be very important. Uncertainties associated with the models can be overcome by systematically adopting conservative choices, and uncertainties due to scarce knowledge of physical quantities can be reduced through adequate laboratory and in-field research. There are uncertainties, however, which are linked to an intrinsic variability of parameters in space and time as well as to unforeseeble future hydrogeological conditions and mankind habits. They may be handled with a specific treatment, previously developed for Reactor Safety Analysis [3]: probability density functions are assigned to each uncertain variable, to cover its entire range of variability; such distributions are then fed into a computer code, which generates the corresponding distribution of the model results, following a Monte Carlo technique.

The assessment is then completed by performing different kinds of statistical analysis of the results: estimate of the expectation values, convergence analysis, computation of confidence bounds etc. It is also important to investigate how the variability of any individual parameter governs the variability of the overall system (sensitivity analysis)[4].

The way of expressing the results is still the subject of some debate. The present trend is towards a comprehensive approach, in which risks are calculated as the product of the probability of occurrence of the scenario, the dose and the dose-to-risk conversion factor [5,6,7]. Such an approach is in line with recent recommandations of the ICRP [7].

The following relationship is used:

$$R = H.r.P \tag{1}$$

where: R = risk to an individual (1/a)

H = committed annual dose equivalent (Sv/a)

r = dose to risk conversion factor ($0.01\ \mathrm{Sv}^{-1}$, [8])

P = probability that the annual dose, H, will be received by an individual.

The output is a distribution of the risk. It is built, first, by generating a large number of dose rate curves as a function of time (Fig. 1), each curve being associated with a particular set of input data; then, the doses are gathered into a histogram. This latter is finally transformed into a histogram of the risk, by multiplying each column by the risk factor.

For probabilistic scenarios the doses are also multiplied by the probability of the scenario itself, which is assumed to identify with the probability P (Eq. 1) that individuals will receive exposures. Thus, a distribution of the risk linked to the given accidental scenario is generated.

In the following sections, the problems related to different sampling methodologies, and to sensitivity and uncertainty analysis will be discussed more in details.

3. SOME STATISTICAL TOOLS IN MONTE CARLO SIMULATIONS

The implementation of a probabilistic risk assessment (PRA) involves the use of a considerable number of mathematical and statistical tools. In this section only those techniques shall be discussed which strictly pertain the Monte Carlo simulation of repository system evolution. Techniques for selecting and screening release scenarios and mathematical modelling of the individual barriers are not addressed here. It is assumed that a complete description of the repository system has been made and that each barrier - e.g. canister, buffer, backfilling and so on - has been modelled. This may involve, for instance, a set of differential equations. It is also assumed that each uncertain parameter has been given a proper value distribution through some kind of previously formalized procedure.

Two major tasks are then takled in the Monte Carlo approach.

The first one is to estimate the distribution of one or more output variables given the distributions of the input variables and is commonly indicated as Uncertainty Analysis (UA). The second task is to investigate how the output is influenced by each one of the input variables and constitutes the object of Sensitivity Analysis (SA).

To fix ideas let the input variables be presented as a vector

$$X = (X_1, X_2, \ldots, X_K) \tag{2}$$

where K is the number of variables and let $Y = Y(X)$ be the output under consideration.

As far as UA is concerned an empirical distribution function for Y, F(Y), can be obtained by repeatedly sampling the input vector X and running the code; under certain conditions it is also possible to evaluate confidence bounds for the empirically estimated F(Y). For SA purposes, the influence of the variables X_j on the output Y can be investigated by generating statistics on the coupled $(Y, X_j)_i$ values, where $i = 1, 2, \ldots, N$ and N is the sample size, i.e. the number of times the computer code has been run.

In the following sections the various steps of the analysis shall be discussed. Sampling algorithms shall be illustrated first focusing on the Latin Hypercube Sampling. Techniques for uncertainty Analysis and Sensitivity Analysis shall then be presented.

3.1 Sampling Algorithms

The purpose of the sampling is to generate an input data matrix of the form:

$$\underline{\underline{X}} = \begin{pmatrix} x_{11} & x_{12} & \cdots & x_{1K} \\ x_{21} & x_{22} & \cdots & x_{2K} \\ \cdot & & & \\ \cdot & & & \\ \cdot & & & \\ x_{N1} & x_{N2} & \cdots & x_{NK} \end{pmatrix} \tag{3}$$

containing the values assigned to the K variables in the N runs.

For each variable X_j, the N values X_{ji}, $i = 1, 2, \ldots, N$ must represent a sample from the distribution of the variable X_j, or - in other words - once plotted in a histogram, the X_{ji}'s must resemble the input distribution of the variable X_j. The simplest method to obtain such a sample is to generate random a number r between zero and one, and the solve for x the integral equations:

$$r = \int_{-\infty}^{x} f(u)\,du \tag{4}$$

where f(u) is the distribution of the variable under consideration.

Repeating the above procedure N times for each variable results in a "purely random" sample of the input vector.

Whenever the barriers submodels are relatively simple and the computer code is not particularly time consuming, Random Sampling is probably the best technique to use.

Very often - instead - the computer program involves time consuming steps, such as numerical solutions of differential equations, series approximations of analytical formulae and so on. In this case a rationalization of the sampling procedure is seeked in order to reduce the number of runs to be performed. In fact other sampling strategies are available which are more efficient than the purely random sampling, in the sense that the convergence of the output distribution is more rapid.

One of the most widely used techniques is the Latin Hypercube Sampling (LHS) [9,10].

According to LHS the range of variability of each variable is divided into a number N of non overlapping intervals of equal probability where N equals the number of model runs to be performed.

Once this partition is done for all the K variables the sample space is divided in N^K cells. When using LHS, N such cells are selected in the sample space in such a way that each interval is sampled exactly once so that the entire range of each variable X_j is explored.

LHS can be considered as a method for selecting, out of the possible N^K cells, a subset of N cells in such a way that the scanning of the sample space is optimized.

Because of the random pairing of the input values, spurious correlations among the input variables may be introduced. Correlations are particularly undesirable when the sample has also to be used for sensitivity analysis purposes. A technique has been developed by Iman and Conover [11,12] to eliminate the spurious correlations. This technique, in fact, allows any kind of prespecified correlation to be imposed on the input variables, so that the sample matrix $\underline{\underline{X}}$ (Eq. 3) can be elaborated either to eliminate all the undesired correlations or to impose correlations among two or more variables when this is desired.

The Iman technique has been implemented in the LISA code [13] and is also available as a separate package from the Sandia Laboratories [12]. A discussion of the relative performances of purely random sampling and LHS is given in [9].

One shortcoming of the LHS method is that it gives a biased(*) estimate of the output variance [9,14].

On the other side the bias can be proved to be negligible when the input-output relationship is monotonic for all the variables [15].

Other sampling algorithms are also available, such as stratified sampling [9] and importance sampling [16]. The latter in particular can be used to explore the tails of the output distribution

---

(*) An estimator is said "unbiased" if its average performance tends to equal the quantity being estimated. Example: $y = \sum y_i/N$, where the y_i's are obtained through LHS of the input variables, is an unbiased estimator of the output mean, in the sense that the average values of y over different runs tends to equal the actual mean.

(the upper tail, generally), as the risk for a given scenario and simulation is very often determined by the few high dose outcomes. In this case the sampling of the input variable can be forced in a subinterval of the input distribution to produce higher doses, so that the upper tail of the output distribution is better explored. This can only be made for those variables whose monotonical relationship with the output has been ascertained.

3.2 Uncertainty Analysis

Uncertainties in PRA may arise from scenarios, models and input data. The Monte Carlo method is specially suited to deal with uncertainties due to input parameters.

A simple method to present the results from a Monte Carlo simulation consists of giving the probability distribution of the calculated annual doses at some reference times.

In Fig. 2 one such histogram is shown. This histogram is an estimate of an empirical distribution function, and the problem here is to characterize the true underlying distribution, producing, for instance, confidence bounds on the distribution itself or estimating the error associated with its mean.

Confidence bounds are needed to quantify the uncertainty in the dose distribution f(H) or - better - that part of the overall uncertainty which is due to the finite number of runs employed to estimate f(H).

The Kolmogorov confidence bounds can be computed for the empirical cumulative distribution function (cdf) of the dose as shown in Fig. 3. In this figure F(H) represents the empirical cdf, while U(H) and L(H) are the upper an lower confidence bound respectively. U(H) is computed by adding to F(H) the appropriate quantile W(y) of Kolmogorov test statistic, where y is the desired confidence level (e.g. $y = 0.9$ for a 90% confidence bound). Of course the value of W(y) depends on the sample size, i.e. the smaller the sample the larger the uncertainty on F(H). Analogously L(H) is computed by substracting W(y) from F(H) [17]. It can be noted that, as any cdf is bounded to the interval (0,1), U(H) was not extended beyond unity, neither was L(H) prolonged below zero.

The results of probabilistic calculations can be used to evaluate the risk due to the considered scenario. The risk is defined as

$$R = \int_{H_{min}}^{H_{max}} H\, p(H)\, r(H)\, dH \qquad (5)$$

where:

R = risk

H = annual dose rate

p(H) = probability of the annual dose

r(H) = risk conversion factor

If $H_{max} < 1$ Sv/y then $r(H) = 0.01$ 1/Sv

and $$R = r \int_{H_{min}}^{H_{max}} H\, p(H)\, dH \qquad (6)$$

$$R = r\,E(H) \tag{7}$$

where E(H) is the expectation value or mean.

It can be seen that the risk is related to the expectation value or the arithmetic mean of the calculated doses.

A problem which arises here is the difficulty to estimate a stable value of the arithmetic mean of a parameter whose distribution is spread over several orders of magnitude. In this case the mean is completely determined by a few very high values. The shape of the curve of the relative incremental contributions to the mean of the different ranges of calculated annual doses (Fig. 4) can give an indication of the convergence of the estimated value for the mean. For the example given one outlier is contributing for about 40% to the expectation value of the annual dose; this gives a strong indication that convergence of the mean is not reached for the considered simulation (Fig. 2).

Importance sampling [16] may give a faster convergence of the mean for a smaller number of runs than LHS does, because more realisations will be generated in the high dose tail of the output distribution.

Another possibility presently under study involves the determination of the true output distribution. This is obtained by solving, in the Laplace space, all mass transfer equations constituting the model. Such solutions are then integrated over the various parameter distributions to get the expectation value of the consequence (i.e. the risk) in the Laplace space. Actual risks as a function of time are then computed by numerically inverting the Laplace risk [18].

Although attractive this approach is not yet at a mature stage of development. Only single nuclide chains can be considered in conjunction with very simple source term and biosphere submodels. Yet this method can be used to check results from Monte Carlo simulations.

For the purpose of the risk calculations, confidence bounds on the risk can be computed once a confidence bound on E(H) is available.

If the H values were normally distributed it would be possible to use standard parametric statistical techniques, such as the t test, to compute confidence bounds on E(H) depending on the sample size. Actually the hypothesis of sample normality is likely to be unrealistic as far as dose distribution functions are concerned. Experience from previous assessments [6,19] indicates instead that the dose distribution can be roughly log-normal.

When the distribution function of a variable is unknown (or simply non normal) a non-parametric method based on the Tchebycheff's Theorem can be used to estimate confidence bounds on the mean [20]. Given a stochastic variable x whose distribution function is unknown the Tchebycheff's Theorem states [21]:

$$P(|x-\mu| \leqslant \alpha\sigma) > 1 - \frac{1}{\alpha^2} \tag{8}$$

for any value of α, where μ and σ the distribution mean and standard deviation respectively. Substituing in (8) $\overline{x}$ for x and $\sigma_{\overline{x}}$ for σ, as $\sigma^2_{\overline{x}} = \frac{\sigma^2}{N}$, the following inequality is obtained.

$$P(|\overline{x}-\mu| \leqslant \frac{\alpha\sigma}{\sqrt{N}}) > 1 - \frac{1}{\alpha^2} \tag{9}$$

For $P = 0.95$, $\alpha = 4.472$.

Hence the 95% confidence bound for is given by

$$\mu = x \pm \frac{\alpha\sigma}{\sqrt{N}} = x \pm 4.472 \frac{\sigma}{\sqrt{N}} \tag{10}$$

Eq. (10) is very similar to the equivalent parametric formula for the confidence interval on the mean base on the Student's t test

$$\bar{\mu} = \bar{x} \pm t_{0.95} \frac{\sigma}{\sqrt{N}} \tag{11}$$

For large sample size $t_{0.95} = 1.96$.

The t test is commonly defined as parametric because the distribution function of the sample is assumed to be normal. When the assumption of normality is droppd (Tchebycheff's theorem) the confidence interval is more than doubled.

Summarizing, it can be said that whenever the output under consideration is a certain kind of "consequence", such as an individual dose rate to the most exposed individual of a critical group, uncertainty analysis can produce histograms and quantify the uncertainty on a given predicted distribution by attaching confidence bounds on the estimated cumulative distribution. Analogously if the risk is being evaluated the Tchebycheff's theorem can be used to quantify the uncertainty on the predicted risk.

3.3 Sensitivity Analysis

The objective of Sensitivity Analysis (SA) is to ascertain the degree of influence of any input variable X_j on the output under consideration.

This is done by applying proper statistics to the sample matrix $\underline{\underline{X}}$ and to output vector $Y = (y_1, y_2, \ldots, y_N)$. Some statistics, such as the Spearman test, simply elaborate on the bivariate sample (y_i, x_{ji}), $i = 1,2, \ldots, N$, disregarding any information on the remaining variables X_m, $m \neq j$.

In other techniques the entire matrix $\underline{\underline{X}}$ is considered, in order to estimate the relationship between Y and any of the X_j's. The Partial Correlation Coefficient - for instance - looks at the true degree of correlation between Y and X_j, removing the effect due to the correlation of both Y and X_j with any other variable X_m, $m \neq j$. This technique, in fact, works on a multi (K+1) variate sample, $(x_{i1}, x_{i2}, \ldots, x_{iK}, y_i)$ $i = 1, 2, \ldots, N$.

There are also statistics where the matrix $\underline{\underline{X}}$ is partitioned, according to the values calculated for the dependent variable Y; one possible partition, for instance, is to take in one matrix all the row vectors (samples) $(x_{i1}, x_{i2}, \ldots, x_{iK})$ for which y_i is below the 50th percentile of its distribution F(Y), and all the vectors corresponding to y_i values above the 50th percentile in an other matrix (50/50 partition).

These latter statistics work on two monovariate samples of (generally) different sizes N_1 and N_2: (x_{ij}), $i = 1, 2, \ldots, N_1$ and (x_{nj}), $n = 1, 2, \ldots, N_2$, without any consideration for other variables X_m, $m \neq j$, and they try to estimate whether or not there is a difference between the two samples. If such a difference can be detected, then the parameter under consideration is an influental one.

For the risk analysis exercises the partition (50/50) is not the most convenient. Because extremal Y values are generally the most important as far as risk is concerned, a (90/10) partition is preferred, where the 10% subsample consists of the runs yielding the highest Y values.

The Smirnov test is an example of this type of statistics.

In this section a few tests shall be illustrated, such as the Pearson and Spearman correlations, the Partial Correlation Coefficient and the Standardized Regression Coefficient, the Smirnov Test and the Cramer - von Mises statistics.

Other sensitivity analysis techniques can be found in [4,15,22], where the relative performances of the various methods are also discussed.

Pearson and Spearman correlation coefficients

The Pearson product moment correlation coefficient (PEAR) is the most widely used measure of correlation and is proportional to the covariance of Y and X_j.

For non-linear models the Spearman coefficient (SPEA) is preferred as a measure of correlation, which is simply the same as PEAR, but the ranks R of both Y and X_j are used in place of the raw values [17].

$$\mathrm{SPEA}(Y,X_j) = \mathrm{PEAR}\ (R(Y),\ R(X_j))$$

The numerical value of SPEA, commonly known as the Spearman "rho", can also be used for hypothesis testing, to quantify the confidence in the correlation itself. The following base hypothesis is first made:

"no correlation exists between Y and X_j"

SPEA(T, X_j) is then computed from - say - a 500 runs simulation and its value is compared with the quantiles of the Spearman test distribution. The comparison is made at a certain preestablished level of significance α, and the hypothesis of no correlation is rejected if SPEA is either lower than $W_{(\alpha/2)}$ or higher than $W_{(1-\alpha/2)}$, where the W's are the quantiles of the test distribution. The level of significance is the probability of erroneously rejecting the hypothesis, i.e. - in this context - the probability that the test indicates a correlation when Y and X_j are actually uncorrelated.

The quantiles can be computed by the asymptotic formula (for high N values) [17]:

$$W = \frac{W'_\alpha}{\sqrt{N-1}} \qquad (12)$$

where N is the sample size and W' is the quantile for the normal distribution. W' can be obtained by solving the integral equation

$$\alpha = \frac{1}{\sqrt{\pi}} \int_{-\infty}^{W'} \exp(-v^2)dv \qquad (13)$$

To apply the test at a 0.05 significance level $W'_{0.025}$ and $W'_{0.975}$ must be computed

$$W'_{0.025} = -1.96$$
$$W'_{0.975} = +1.96$$

Taking for instance N = 500 the Spearman quantiles are (Eq. 12)

$$W_{0.025} = -0.088$$
$$W_{0.975} = +0.088$$

The hypothesis of no correlation is rejected if SPEAR, as computed from a 500 runs simulation, falls outside the range (- 0.088, 0.088), and the probability of an erroneous rejection, when Y and X_j are actually uncorrelated, is 0.05.

Partial correlation and standardized regression coefficients

Partial Correlation Coefficients (PCC) and Standardized Regression Coefficients (SRC) are two very powerful correlation estimators, which can be used also on the ranks of the (Y,X_j) values (Partial Rank Correlation Coefficients PRCC and Standardized Rank Regression Coefficient SRRC). A description of how PCC and SRC are obtained is given in [23]. PRCC and SRRC are straightforwardly obtained by transforming Y and X_j into their ranks and then applying the same procedure.

The SRC (Y,X_j) are the coefficients of the regression model for Y; they may provide an approximation to Y in the form

$$Y^* = \sum_{j=1}^{K} \mathrm{SRC}\,(Y,\, X_j)\, X_j^* \tag{14}$$

where X^*_j are the normalized variables

$$x^*_{ji} = \frac{x_{ij} - \bar{x}_j}{\sigma(X_j)} \tag{15}$$

and $\bar{x}_j$ and $\sigma(X_j)$ are respectively the sample mean and standard deviation.

When computing the SRC's the model coefficient of determination R^2 is also calculated, which gives a measure of how well the linear regression model based on the SRC's can reproduce the actual sample y_i. In particular:

$$R_Y^2 = \sum_{j=1}^{N} \frac{(y^*_i - \bar{y})^2}{(y_i - \bar{y})^2} \tag{16}$$

where y is the sample mean, so that R_Y^2 represents the fraction of the variance of the sample explained by the regression. The closer R^2 is to unit, the better is the model performance.

The coefficients SRC $(Y,\, X_j)$ can themselves provide a very effective measure of the relative importance of the input variables. Of course the validity of the SRC's as a measure of sensitivity is conditional to the degree to which the regression models fits the data, i.e. to R^2.

The PCC can be considered as an extension of the usual correlation coefficients, and represent that part of the correlation between two variables which is not due to correlation between these two variables and the remaining ones. When PCC are used they can provide a ranking of the various variables by indicating the strength of the linear relationship between Y and X_j. If PRCC are used the linear relationship between the ranks of Y and X_j is measured. This gives an effective estimation of sensitivity. Unlike the SPEA statistic, PRCC and SRRC are not used directly for hypothesis testing.

Smirnov and Cramer - von Mises Statistics

The Smirnov Statistics SMIR (Y, X_j) and the Cramer von Mises CRAM (Y, X_j) belong to the same class of nonparametric tests. They are based on the empirical cumulative distribution $F(X_j)$ of a given input variable X_j for two different subsamples.

In order to apply the statistics, the Y values arising from a given simulation (sample) are first divided into two subsets, for instance by taking the values exceeding the F(Y) 90th percentile in one sample and the remaining values in the other sample (10/90 partition).

At this point, for each variable X_j, the empirical cumulative distributions $F(X_j)$ are computed on the two samples and the two distributions are compared with each other. Intuitively, if a given parameter X_j has no influence on the output, then the two samples will give a similar distribution, or, better, they will be two different estimates of the same true underlying distribution (i.e. the input distribution for that parameter X_j in this case). If the two distributions are different, it can be said that the parameter influences the output, and that high outputs are preferentially associated with high, or low, parameter values.

More quantitatively, a test statistics is available to decide - at a given significance level - whether or not the two samples come from the same population. The Smirnov statistics is defined as the maximum vertical distance between the cumulative distributions of the two samples, and the test hypothesis to be accepted or rejected is that the two distributions are not significantly different.

The decision rule in this case, for accepting or rejecting the hypothesis "the two samples have the same distribution" at the level of significance   is to compare SMIR with the (1-) test quantile W_{1-} of the Smirnov distribution, as given by tables [17] or computed by asymptotic formulae. For   = 0.05

$$W_{(1-\alpha)} = W_{0.95} \simeq 1.36 \left(\frac{N_1+N_2}{N_1 N_2}\right)^{1/2} \tag{17}$$

where N_1, N_2 are the two subsample sizes. If $\text{SMIR} > W_{1-\alpha}$ the hypothesis is rejected. The probability of having made an error in rejecting the hypothesis is equal to the level of significance (0.05 in this case). Comparing SMIR values for different variables allows the variable importance to be ranked, exactly as with the preceeding sensitivity estimators.

The Cramer - von Mises statistics resembles very much the Smirnov one [17].

Because in this statistics the total area of the two distributions is scanned, it may be more appropriate for sensitivity analysis when the $Y(X_j)$ is a non monotonic function.

Also for this statistics a significance test is available [6].

4. CONCLUSIONS

A short and necessarily incomplete presentation has been given of some current issues in Risk Assessment for Nuclear Waste Disposal. Of course, both the proposed methodology and the choice of the computational tools reflect the Authors' viewpoint and preferences. Yet it is the Authors' opinion that the real problem with this kind of assessments is not linked to the sampling strategy, nor to the algorithm chosen for detecting sensitivities but rather to the correct definition of realistic input distributions, and to the correct assessment of the probabilities of occurrence for various types of rare events. The statistical tools required to analyze satisfactorily the probabilistic behaviour of any geological system do exist, provided that the starting information is correctly utilized.

On the other hand experience from the Reactor Safety Studies has shown that uncertainties in Risk Assessment can be much higher than risk assessors claim. The limitations of this kind of treatment should always be kept in mind, to avoid, for instance, that a confidence bound on a risk figure (computed on purely statistical basis) be taken or presented as the real uncertainty on such a risk. A Risk Assessment study, performed at the best of our present knowledge of the system, should always be performed to ensure that all what can be done will be done to ensure the safety of chosen option. Yet these studies should always be performed in a comparative fashion as any energy production system is linked to the production of related risks. The huge amount of studies recently devoted to the safety of nuclear systems should ensure a carefully considered technology, but, at least within the scientific communities, it must be aknowledged that the ability of predicting accidents is severely limited for those systems where very few accidents have occurred (reactor systems) or where accidents did not occur at all because no such system has yet been created (the waste disposal system).

REFERENCES

[1] "Geological confinement of radioactive wastes within the European Community", CEC Tech. Rep. EUR 6891 EN.

[2] N. Cadelli, F. Girardi, S. Orlowski, "PAGIS, common European methodology for repository performance analysis", 2nd Europ. Community Conference, Luxembourg, April 22-26, 1985.

[3] M. Astolfi, J. Elbaz, Report EUR 5804 EN (1977).

[4] A. Saltelli and J. Marivoet, Performance of nonparametric statistics in sensitivity analysis and parameter ranking, Submitted for publication on Nuclear Technology.

[5] Long term radiation protection objectives for radioactive waste disposal, NEA, OECD publication (1984).

[6] G. Bertozzi, M. D'Alessandro and A. Saltelli, Commission of the European Communities, Report EUR 9641 EN (1984).

[7] ICRP publicaton 46, Radiation protection principles for the disposal of radioactive waste , Annals of the ICRP, 15(4), Pergamon Press (1985).

[8] ICRP publication 26, Recommendations of the ICRP, Annals of the ICRP, 1(3), Pergamon Press (1977).

[9] M.D. Mc Kay et al., Technometrics, 21(2), pp. 239-245 (1979).

[10] R.L. Iman, W.J. Conover, Comm. Statist. - Theor. Meth., A9(17), pp.1749-1842 (1980).

[11] R.L. Iman, W.J. Conover, Comm. Statist. - B11(3), pp. 311-334 (1982).

[12] R.L. Iman, M.J. Shortencarrier, Sandia Natl. Laboratories report NUREG/CR-3624, SAND83-2365 (1984).

[13] A. Saltelli, G. Bertozzi and D. Stanners, Report EUR 9306 EN, (1984).

[14] A. Saltelli and G. Bertozzi, Risk assessment for geological disposal or radioactive waste: uncertainty propagation and sampling techniques. Joint Research Centre (Ispra). Technical Note No. 1.07.03.82.49 (1982).

[15] R.L. Iman, J.C. Helton, Sandia Natl. Laboratories, Report NUREG/CR-3904, SAND 84-1461 (1985).

[16] R. Middleton, Statistical techniques for the development and application of SYVAC; CAP Scientific, London; Report TR-STH-1 (1983), DOE, London, Report DOE/RW/83.125.

[17] W.J. Conover, Practical Nonparametric Statistics, John Wiley & Sons, New York (1980).

[18] P.C. Robinson and D.P. Hodgkinson, AERE, Report AERE-R-12125 Harwell (1986).

[19] D.M. Wuschke et al., Atomic Energy of Canada, Ltd., Report AECL TR-127-3 (1981).

[20] A. Saltelli, J. Marivoet, "Safety Assessment for Nuclear Waste Disposal. Some observations about actual risk calculation", Submitted for publication in Radioactive Waste Management and the Fuel Cycle.

[21] A. Hold, Statistical Theory with Engineering Applications. John Wiley & Sons, New York (1952).
[22] R.L. Iman, J.C. Helton and J.E. Campbell, Journal of Quality Technology, 13, 3, 4 (1981).
[23] R.L. Iman, M.J. Shortencarrier, J.D. Johnson, Sandia Natl. Laboratories, Report NUREG/CR 4122, SAND85-0044 (1985).

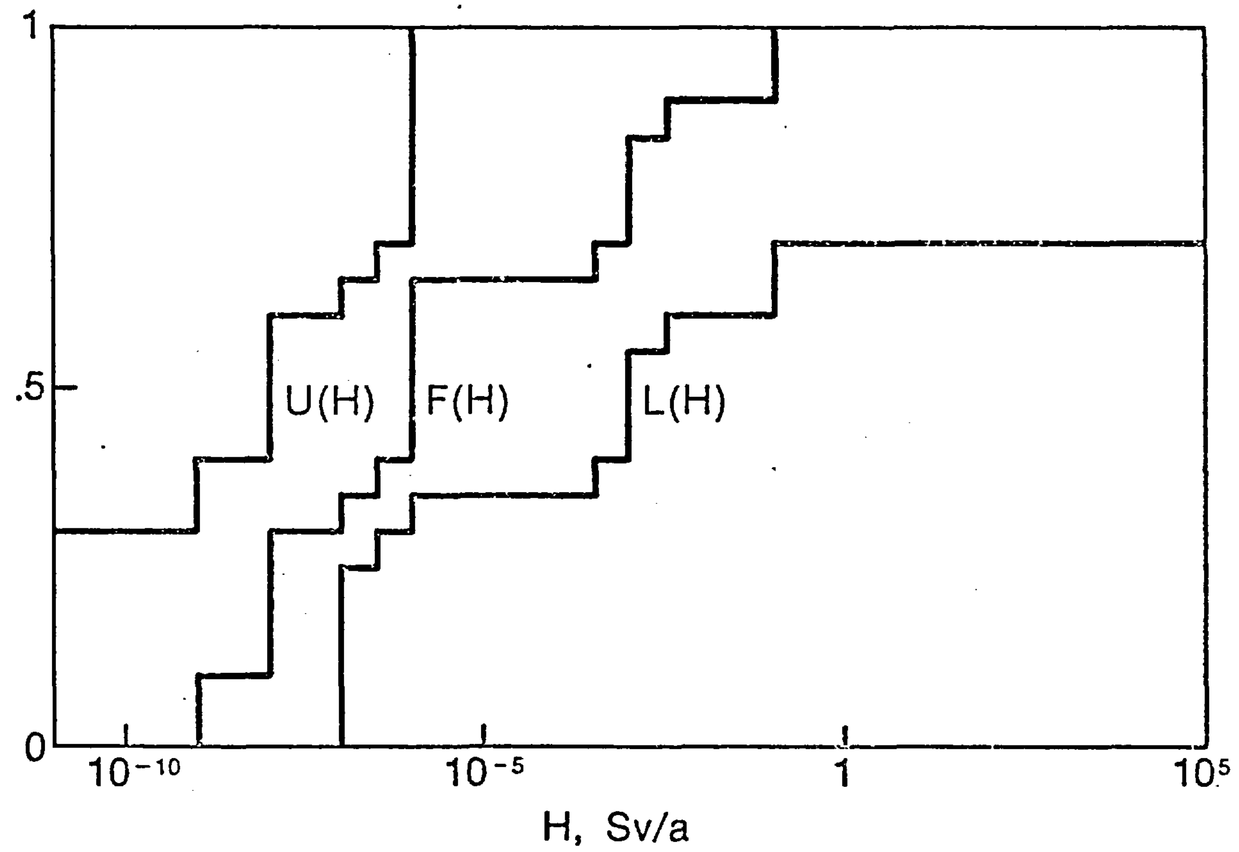

FIG. 3. EXAMPLE OF AN EMPIRICAL DOSE CUMULATIVE DISTRIBUTION WITH CONFIDENCE BOUNDS

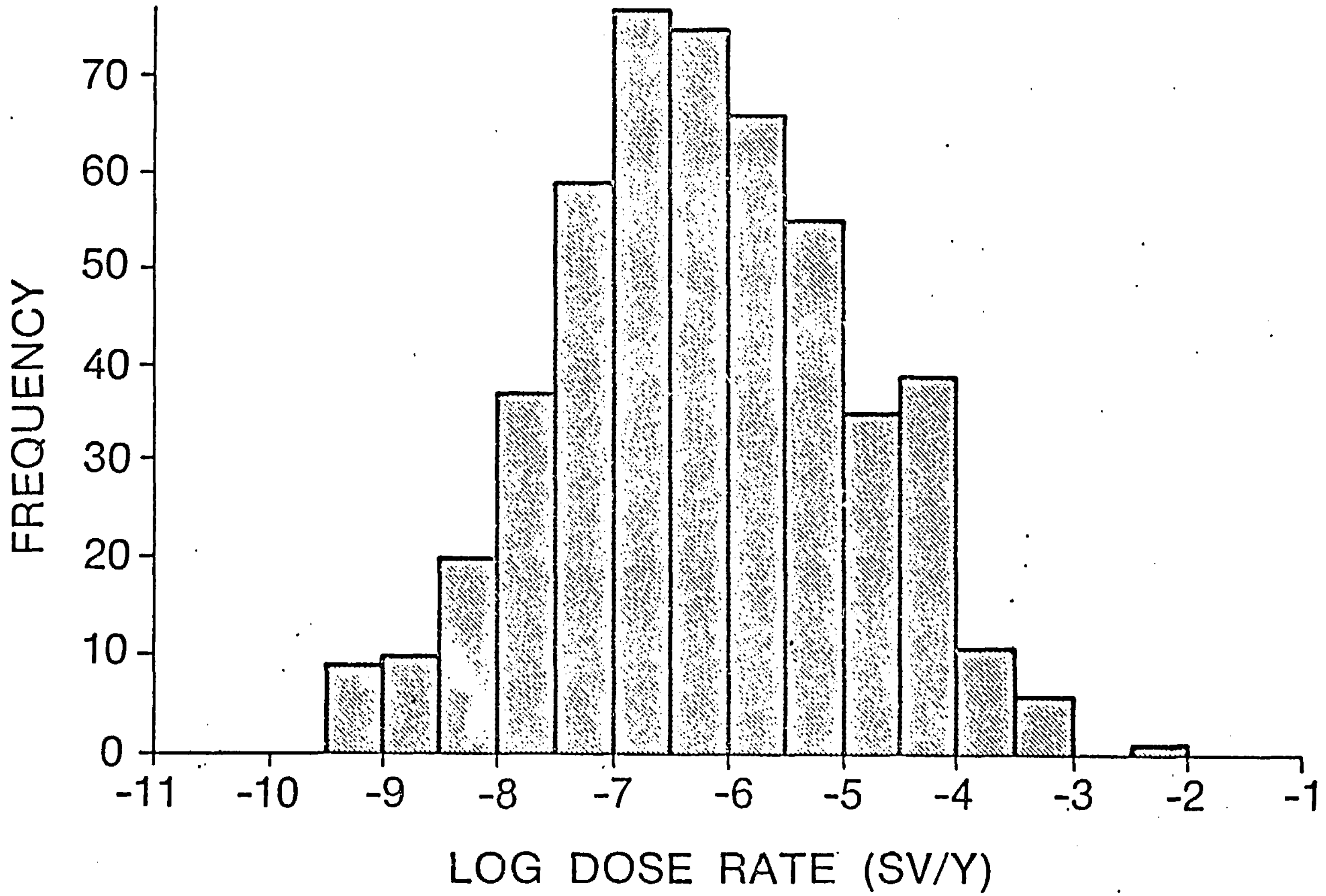

FIG. 2. DOSE RATE HISTOGRAM FROM A MONTECARLO SIMULATION

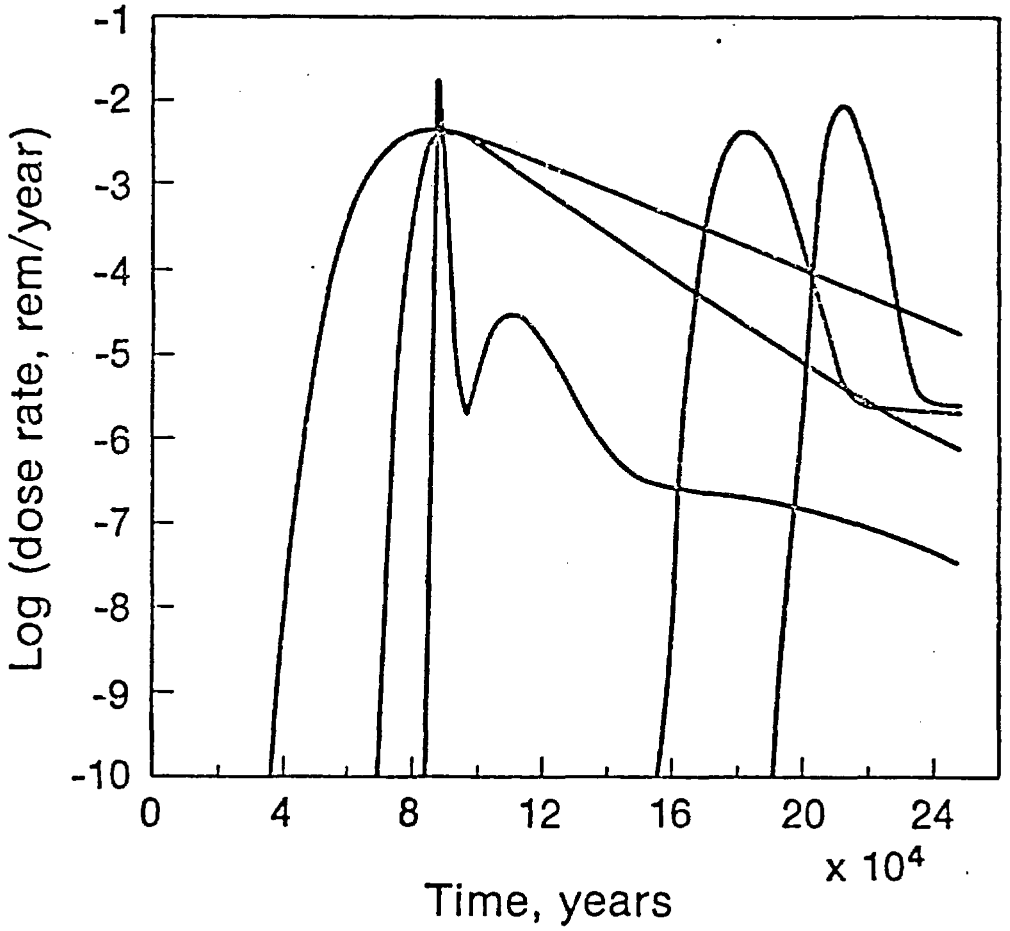

FIG. 1. DOSE RATE VERSUS TIME CURVES FOR THE RUNS OF A MONTECARLO SIMULATION GIVING THE 5 HIGHEST PEAK DOSES

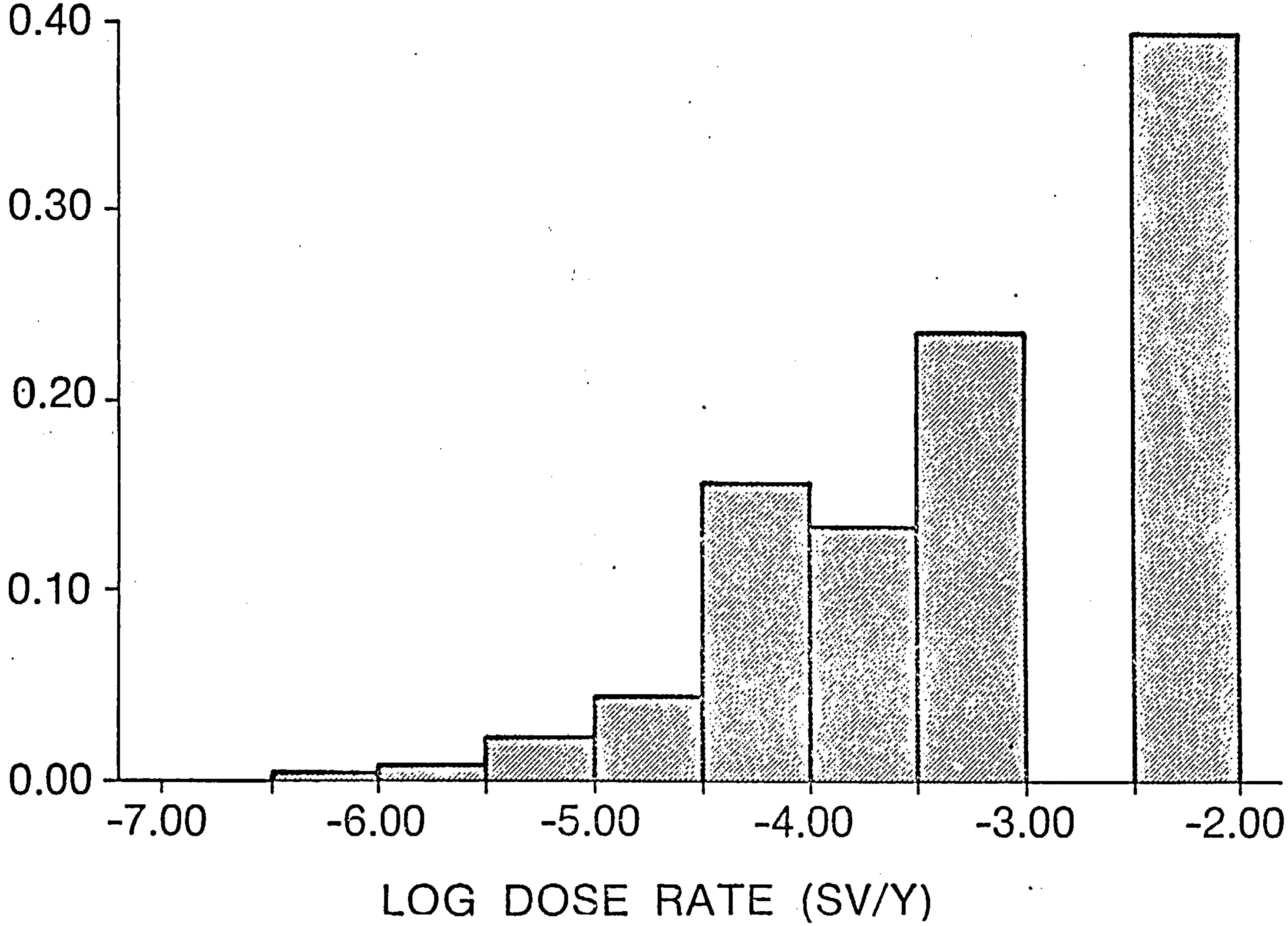

FIG. 4. RELATIVE INCREMENTAL CONTRIBUTION TO THE EXPECTED VALUE OF DOSE RATE E(H) FOR DIFFERENT RANGES OF THE CALCULATED DOSE (FIG. 3)

ENRESA SEMINAR ON NUMERICAL MODELLING IN WASTE DISPOSAL
MADRID, 10th-12th DECEMBER 1986

INTEGRATED APPROACH TO PERFORMANCE ASSESSMENT OF NUCLEAR WASTE DISPOSAL SYSTEMS INCLUDING RADIATION PROTECTION CONSIDERATIONS

Claes Thegerström, Stefan Carlyle
Radiation Protection and Waste Management Division
OECD Nuclear Energy Agency
Paris, France

ABSTRACT

The paper discusses the role of performance assessment in the evaluation of the potential radiological impact of a nuclear waste disposal system. International co-operation in this field is highlighted and the related NEA activities are presented. The main elements of performance assessment - scenarios, data, models - and their integration are discussed against the background of long-term objectives for radiation protection in waste disposal.

1. INTRODUCTION

Performance assessment is a global term for all the steps involved in predicting the potential radiological impact of a nuclear waste disposal system. The correct modelling of repository subsystems is a necessary element in the performance assessment. Equally important, however, is the coherent integration of the various components of a comprehensive safety assessment. It encompasses all the steps starting with a systematic procedure for scenario identification and selection through modelling of subsystems and the total system, to the clear presentation of results and conclusions.

In the present program of the NEA Radioactive Waste Management Committee (RWMC) performance assessment-related activities play a major role. It is an area under rapid development where there is a strong need for international co-operation and co-ordination.

The results of a safety assessment have to be evaluated against existing regulations and long-term objectives for waste disposal. Here the NEA, through its Radioactive Waste Management Committee and its Committee on Radiation Protection and Public Health (CRPPH), plays an active role in the formulation of internationally accepted guidelines and long-term objectives.

Recent and ongoing activities initiated by the RWMC and the CRPPH in these areas are presented in this paper and discussed in the context of the integrated performance assessment of nuclear waste disposal. First the role of performance assessment is briefly presented based partly on discussions and presentations at a recent NEA workshop [1]. The question of scenario identification and selection is then discussed before reviewing the ongoing activities on modelling and related data bases. Finally the integrated evaluation and presentation of results is discussed especially in relation to radiation protection considerations and long term objectives for radioactive waste disposal.

2. THE ROLE OF PERFORMANCE ASSESSMENT

2.1 General

The fundamental function of a disposal system is to contain and isolate the radioactive materials so they cause no undue harm to man or his environment, either now or in the future. This means that one is confronted with the problem of predicting the behaviour of the system over long time periods. It will not be necessary to predict the future behaviour in minute detail. What is needed is to understand enough to be assured that no harmful releases will occur. To gain this level of understanding and to describe it to responsible authorities and the public is one of the major tasks in any nuclear waste disposal programme.

The basis for an analysis of the safety is a good scientific understanding of all parts or the system. This encompasses for instance:

- the physical/chemical and radioactive properties of the waste materials and canisters (the source)

- the chemical interactions and transport phenomena within or close to the repository (the near-field)

- the chemical interactions and transport phenomena in the geological formation surrounding the repository (the far-field)

- the effects of dispersion and/or reconcentration of possible releases to the biosphere.

In all these areas research is performed through experiments and observations in laboratories or in the field. Mathematical models are developed to describe important processes that might occur. The large amount of data obtained from experiments and field tests are collected in a systematic way and stored in data bases.

In a safety assessment the available information is used as appropriate as possible to assess the future effects of the repository on the environment. The quality of such a total system performance assessment and the relevance of its results will depend on:

- that all important events or processes that may influence the releases from the repository have been identified (scenarios)

- that the mathematical models give a correct description of these processes (i.e. are validated), at the level of detail needed for this particular purpose

- that the input data used is representative of the actual site conditions and repository design, and finally

- that the calculations and the interpretation of results are made in an appropriate way.

For the geological disposal of high-level waste no country has yet reached the stage of making a formal safety assessment for the licensing of a repository at a specific site. However, extensive formal assessments of the feasability of implementing safe disposal have been carried out in some countries e.g. Sweden and Switzerland, and are planned soon in other countries e.g. Canada.

2.2 International co-operation within NEA

The last years a great deal of effort in countries with a waste disposal programme has been devoted to the further development and application of performance assessment methodologies. In this context the exchange of information and the co-operation at an international level is extensively used to avoid duplication of work and to benefit from the open exchange of ideas and know-how between specialists in different countries. In addition, it has particularly been recognized that there is a need to discuss at an international level how to rationalise all the various elements that combine together in carrying out performance assessments. Figure 1 gives a schematic representation of the main elements and linkages in system performance assessments. These were discussed at an NEA workshop in October 1985 [1] and based on the outcome of the discussions a program of NEA activities on performance assessment related matters was outlined. A Performance Assessment Advisory Group (PAAG) has been set up by NEA to give general guidance and advice within this area. The group consist of member countries representatives with key positions in the national performance assessment programs, covering both program responsible organisations and regulatory bodies.

LINKAGES IN SYSTEM PERFORMANCE ASSESSMENTS

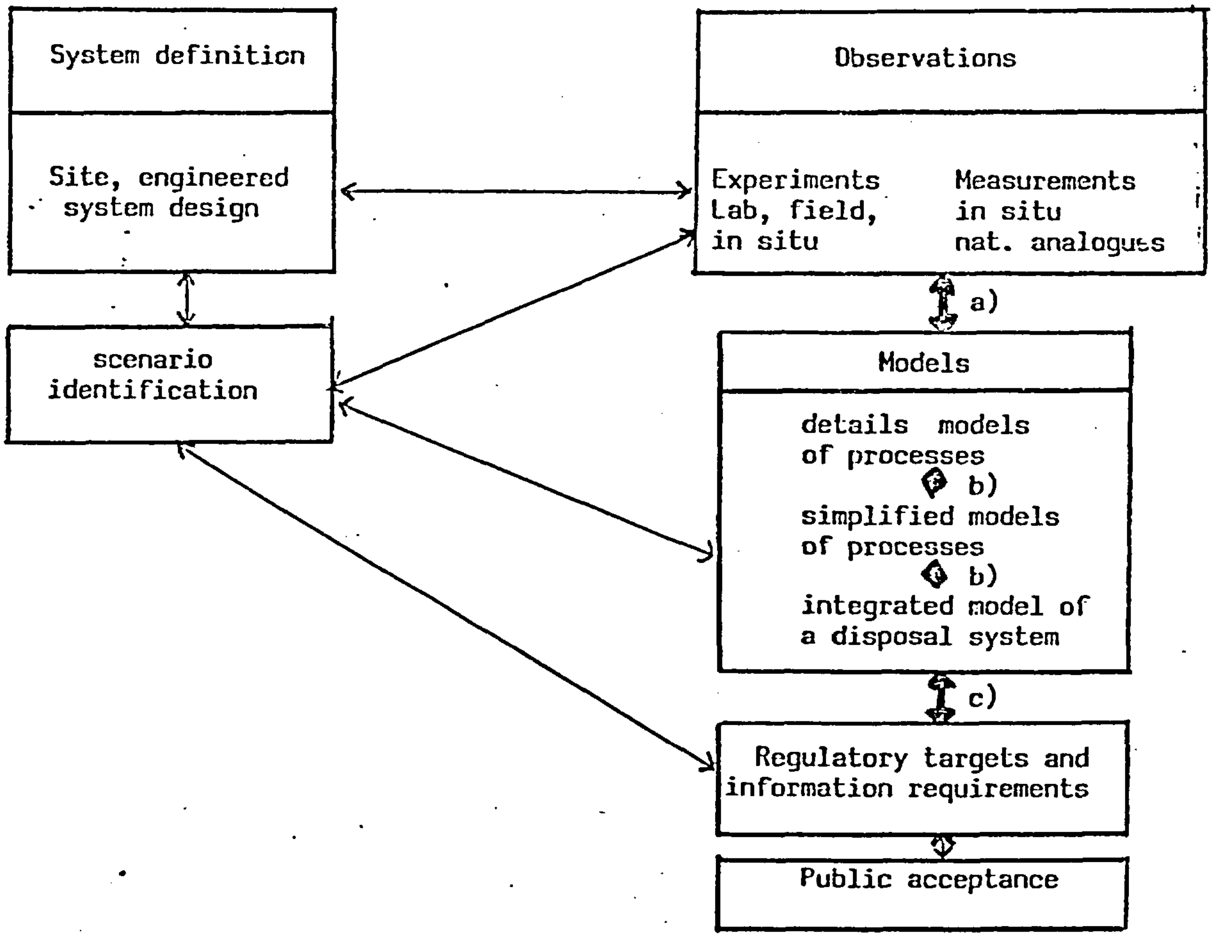
System definition
Site, engineered system design
Observations
Experiments Lab, field, in situ
Measurements in situ nat. analogues
scenario identification
a)
Models
details models of processes
b)
simplified models of processes
b)
integrated model of a disposal system
c)
Regulatory targets and information requirements
Public acceptance

a) Link between the development of models andobservations (validation)

b) Link between detailed models and simple models and
Link between separate models and an integrated system model

c) Link between the output of performance assessments and regulatory equipments.

The scope of the PAAG embraces all radioactive waste types with the emphasis on post-closure performance assessments, particularly in the long-term: the objective is to build confidence within the technical community.

In meeting this objective, the group would:

i) exchange information and experience to further the development of performance assessment methodologies, and avoid duplication of effort;

ii) identify initiatives for co-operation on the development and use of performance assessment methodologies, in particular in the area of model development, data acquisition and regulatory requirements;

iii) advise the RWMC on scientific and technical aspects of performance assessments by periodic reports to the Committee on the current state-of-the-art, and

iv) assist the RWMC in the co-ordination of existing and new activities of NEA in the area of performance assessments, including peer reviews on request.

In particular, the following technical areas will be covered by the group, i.e.

- Model development - including verification, validation and code development and exchange.

- Data acquisition including data base development, assessment of uncertainty in data and data frome site investigation, and co-ordination with in situ research and laboratory studies.

- Regulatory needs - including the development of performance objectives and criteria.

It is believed that for the coming years the PAAG will provide an efficient guidance not only for the NEA activities on long-term performance assessment of radioactive waste disposal, but alo for participating countries which can confront their own views and benefit from discussion among the specialists.

It has initiated and will continue to initiate specific activities in selected areas, some of which are briefly described in below. It may also have an important role to play in focussing, at an international level, all the elements of performance assessment to provide the type of integrated understanding upon which the long-term radiological acceptability of nuclear waste repositories need to be evaluated.

3. ELEMENTS OF PERFORMANCE ASSESSMENT AND THEIR SIGNIFICANCE FOR THE LONG-TERM SAFETY

Referring to figure 1 three main elements of a full system performance assessment can be distinguished:

- The identification, selection and specification of possible release scenarios

- The collection/compilation of data relating to the selected site,engineered systems and observations in the field and in the laboratory

- The modelling of possible releases from the repository through man-made and natural barriers to the environment and man.

These elements are highly interrelated. For instance much of the data collection and experiments are planned with certain release scenarios and model needs in mind. Raw data from the field are generally evaluated by the help of and in the context of certain models describing the phenomena under study.

For a complete system performance assessment all the above mentioned elements (scenarios, data, models) are equally important. Further, for the usefulness of any system performance assessment a clear presentation of all its aspects is indispensable. Only then will it be possible for regulatory bodies and independent reviewers to evaluate the results obtained.

3.1 Scenario identification and selection

Any assessment of the safety of a nuclear waste repository must begin by selecting the proper scenarios to analyse. The correct identification, selection and specification of scenarios is thus fundamental.

The identification and specification of scenarios is based on accumulated knowledge from R & D, field studies and site investigations. Further it has to relate to actual design and siting of the repository. It will set the scene for the model calculations to be performed and it will give the basis for assigning input parameter values and boundary conditions for such calculations.

In the evaluation of a scenario its consequences as well as its probability of occurence have to be considered. A simple but illustrative way of categorising scenarios is given in table 1 below.

Table 1: Combination of probability/consequences for scenarios

I High probability High consequences	III Low probability High consequences
II High probability Low consequences	IV Low probability Low consequences

I: High probability, high consequences. In this category we find those scenarios that have to be avoided by chosing an appropriate design and site for the repository. They are normally not displayed in the safety assessments simply because they have already, implicitly or explicitly, been considered when defining requirements for the disposal system. Examples of measures of this category are limiting the thermal load to avoid excessively high temperatures or siting the repository so that there is a very low probability that people in the future drill into it for drinking water.

II: High probability, low consequences. In this category we normally find the base-case scenarios. By analysing them in detail confidence is gained that their consequences will be low which will make it possible to accept the disposal system proposed.

III: Low probability, high consequences. Scenarios in this category are sometimes problematic to identify and to evaluate. A strict calculation of their probability of occurence is not always feasible. Subjective judgement based on available expert knowledge and experience might be used as one tool in evaluating their importance. An example of a scenario in this category is the existence of fast preferential pathways initially undetected or later created by natural phenomena. Examples of another type are extreme events like intrusion in case of war, large scale sabotage, natural catastrophes like meteorite impact or magmatic explosion. In many of these cases it can be argued that the possible consequences due to release from the repository are small compared to the effects of the initiating events.

IV: Low probability, low consequences. In this category we find scenarios which can be rejected at an initial qualitative screening due to that their probability of occurence is low and their consequences would be low in any case.

The identification of a set of scenarios that need to be considered is normally rather straight forward. Most often a base-case scenario is analysed in detail and in addition a few altered (disturbed, disruptive..) scenarios are also considered. The difficulty, however, is to be assured that all important scenarios have been identified and that no important processes or phenomena have been overlooked in specifying the scenarios. This is directly related to the level of understanding we can gain of the disposal system and to the quality of a systematic analysis of its safety. An example of a systematic listing of potentially relevant phenomena is given in table 2 below [2].

Table 2

TABLE 1
IAEA List of Phenomena Potentially Relevant to Scenarios for Waste Repositories

Natural processes and events

- Climatic change
- Hydrology change
- Sea-level change
- Denudation
- Stream erosion
- Glacial erosion
- Flooding
- Sedimentation
- Diagenesis
- Diapirism
- Faulting/seismicity
- Geochemical changes
- Fluid interactions
  - Ground water flow
  - Dissolution
  - Brine pockets
- Uplift/subsidence
  - Orogenic
  - Epeirogenic
  - Isostatic
- Undetected features
  - Faults, shear zones
  - Breccia pipes
  - Lava tubes
  - Intrusive dikes
  - Gas or brine pockets
- Magmatic activity
  - Intrusive
  - Extrusive
- Meteorite impact

Human activities

- Faulty design
  - Shaft seal failure
  - Exploration borehole seal failure
- Faulty operation
  - Faulty waste emplacement
- Transport agent introduction
  - Irrigation
  - Reservoirs
  - Intentional artificial ground water recharge or withdrawal
  - Chemical liquid waste disposal
- Large-scale alteration of hydrology
- Undetected past intrusion
  - Undiscovered boreholes
  - Mine shafts
- Inadvertent future intrusion
  - Exploratory drilling
  - Archaeological exhumation
  - Resource mining (mineral, water, hydrocarbon, geothermal, salt, etc.)
- Intentional intrusion
  - War
  - Sabotage
  - Waste recovery
- Climate control

Waste and repository effects

- Thermal effects
  - Differential elastic response
  - Nonelastic response
  - Fluid pressure, density, viscosity changes
  - Fluid migration
- Mechanical effects
  - Canister movement
  - Local fracturing
- Chemical effects
  - Corrosion
  - Waste package—rock interactions
  - Gas generation
  - Geochemical alterations
- Radiological effects
  - Material property changes
  - Radiolysis
  - Decay-product gas generation
  - Nuclear criticality

The PAAG has proposed that NEA consider a set of questions related to scenario identification and selection. They are for instance:

- the need for a common terminology;
- general approaches to the selection of scenarios;
- time-dependent processes like long-term changes in the biosphere and geosphere;
- the role of probabilities and ways to assign probabilities to scenarios and to parameters used in scenario analysis; and
- the use of methods like scientific judgement, fault tree analysis, influence diagram analysis in the scenario specification process.

These and related questions are being discussed within an NEA consultants group and a workshop on scenarios will probably be held during 1987.

3.2 Data

Another main element of performance assessment is the collection and compilation of data on the disposal system, the site and relevant release phenomena. Laboratory experiments, field observations and site-investigation activities provide these data. These activities constitute a substantial part of the present nuclear waste disposal programs. Here, however, we will only mention the setting-up, within NEA and the NEA Data Bank in Saclay, of two data base systems in support of performance assessment activities.

International Sorption Information Retrieval System (ISIRS)

The ISIRS is a data base system for the storage and handling of information related to experiments on the sorption of radioelements onto different kinds of materials and minerals. The data base currently contains data from ten countries with about 2500 distribution coefficients (K_d's) for

18 elements on eight general classes of geological material in a variety of physico-chemical conditions. The opinion on the usefulness of ISIRS is divided. Some scientists consider it of little value, referring, for instance, to that K_d values are purely empirical and do not provide a good ground for description of the basic processes in sorption and retardation phenomena. Others, however, while recognising this fact, point out that presently K_d values are being used in practice when modelling nuclide transport. NEA is now exploring means to improve further the usefulness of ISIRS. Most important would be to get a fully representative data base of K_d values at least in some selected areas like sorption on near-field materials (concrete, clay, ...) and/or for elements of special interest, like Neptunium.

The NEA Thermochemical Data Base (TDB)

The development of an international chemical thermodynamic data base is a recent activity of the NEA Data Bank carried out jointly with the Division of Radiation Protection and Waste Management of NEA. It was initiated to account for the increasing need of such data for modelling purposes in safety analyses for nuclear waste repositories.

Most modelling groups supporting the performance assessment of radioactive waste disposal, have developed their own data base from the scientific literature. These individual data bases often differ considerably from each other, especially in the data of the actinides. It is thus not surprising that radionuclide speciation and maximum solubilities calculated by different groups, with different geochemical computer codes and data, but for similar conditions, often turn out to differ by orders of magnitude. It has been recognized that the reason for these discrepancies are not the different codes but the different data bases. The needs for a comprehensive, internally consistent and internationally recognized chemical thermodynamic data base meeting the requirements of the modellers have thus been acknowledged by a number of technical groups within the NEA Member countries. It is in response to this need that the NEA has undertaken its thermochemical data base development.

The development of this data base involves not only a compilation of all relevant published thermodynamic data, but also a detailed critical review and, finally, the selection of a "best data set" which will be recommended. Each review is being performed by a group of four to five internationally acknowledged experts in chemical thermodynamics. The first 10 elements to be reviewed are: Uranium, neptunium, plutonium, americium, technetium, cesium, strontium, radium, iodine and lead. The thermodynamic data being compiled and reviewed for each species include:

the standard Gibbs free energy of formation
the standard enthalpy of formation
the standard entropy of formation
the standard heat capacity (at constant pressure)

together with uncertainties and, if available, the temperature functions.

In addition, an interface program is being developed which makes it possible to extract specific data from the thermodynamic data base and to convert them into a form in which they are readable by geochemical modelling codes, such as PHREEQE, MINEQL and EQ3/6, all of which are widely used geochemical reaction path computer codes. The data could also be made available in a form compatible with other computer codes if there is any demand from users.

A schematic presentation of NEA's chemical thermodynamic data base development system is given in figure 2 [4].

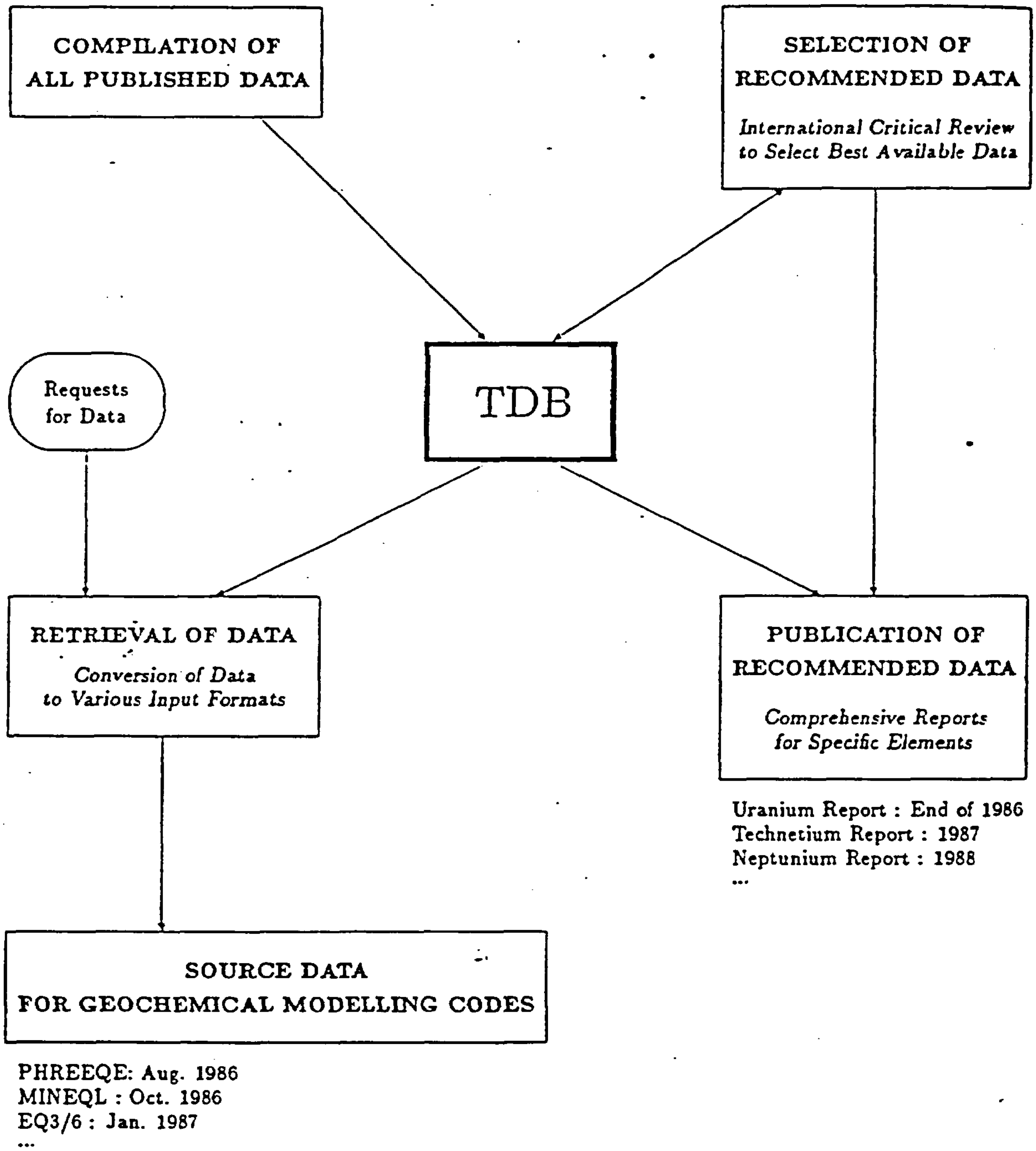
COMPILATION OF ALL PUBLISHED DATA
SELECTION OF RECOMMENDED DATA
International Critical Review to Select Best Available Data
Requests for Data
TDB
RETRIEVAL OF DATA
Conversion of Data to Various Input Formats
PUBLICATION OF RECOMMENDED DATA
Comprehensive Reports for Specific Elements
SOURCE DATA FOR GEOCHEMICAL MODELLING CODES

Uranium Report : End of 1986
Technetium Report : 1987
Neptunium Report : 1988
...

PHREEQE: Aug. 1986
MINEQL : Oct. 1986
EQ3/6 : Jan. 1987
...

Figure 2 Structure of the NEA Thermochemical Data Base System

3.3 Models

A central part of any performance assessment is of course the modelling of the total system as well as single subsystems or even individual processes of special importance.

The whole area of development of models and computer codes for these various purposes is under rapid development. New more complex models and approaches are developed and taken into practice as the tools for computer calculations are developing and as the needed supporting data are being collected.

At an international level the questions of verification and validation of the concepts, models and codes being used are given special attention. Examples are the INTRACOIN and HYDROCOIN projects where the verification and validation of nuclide migration codes and hydrological codes respectively have been studied in international co-operation.

The results within these two projects are summarised in another paper at this seminar.

The high degree of sophistication reached in systems performance assessments, compared for example to performance assessment for the disposal of equivalent chemical wastes, has led to new challenges for those developing currently preferred methodologies. Recently, there has been a move away from exclusive reliance on deterministic calculations to the balanced use of deterministic and probabilistic models. This is in response to the need to take into account the many uncertainties in carrying out performance assessments covering the long term, due mainly to the intrinsic variability of natural processes.

In view of this the NEA Probabilistic Systems Assessment Codes user Group (PSAC) was established in early 1985 to aid the development in OECD Member countries of PSA Codes for assessments of the performance of radioactive waste disposal systems. A major part of the activities of PSAC is devoted to the intercomparison of codes in order to provide confidence in their ability to adequately represent the system being modelled and therefore their capability to provide reliable information for safety assessments.

The NEA Data Bank provides support in the form of computer services for PSAC and has fully tested, documented and packaged SYVAC 1 and 2 from Canada, SYVAC A/C from the United Kingdom and the LISA Code from JRC/CEC. Work is also in hand on the development of a library of certain computer modules such as random number generators or sampling routines for the purposes of exchange between members.

At the meeting of the PSAC users group topical workshops are also organised. Most recently the subject of reduction of research models to sub-models in probabilistic system assessment codes was treated.

In this context it should also be mentioned that NEA is organising a workshop on uncertainty analysis for system performance assessments in February 1987. The role of uncertainty analysis in performance assessment will be described and the steps necessary to carry out such analyses in large complex systems will be covered in detail. The focus will be on practical and proven methods in meeting the objective of the workshop which will be to develop a better understanding of the available methods, and to formulate general recommendations for their use based on the lessons learned to date. It may also help clarify the role of uncertainty analysis in the broader context of performance assessment as seen by regulators and decision-makers.

4. LONG TERM OBJECTIVES AND RADIATION PROTECTION CONSIDERATIONS FOR NUCLEAR WASTE DISPOSAL

Compared to other activities involving the use and handling of radioactive materials the final disposal of nuclear waste is different in three specific ways:

1) the long time perspectives involved

2) the total isolation of the active materials from the environment for very long-time periods, in many cases probably "for ever"

3) the ultimate absence of active control and possibility to prompt corrective measures if needed.

It is generally agreed that performance objectives can be formulated in a number of different ways and yet still ensure that radioactive wastes are disposed of safely. General objectives relating to radiation dose, health risk (to individuals or populations) or to environmental contamination have been proposed and are under discussion; There appears to be a trend towards individual risk limitation in several European countries and in Canada, which are similar to the recommendations of an NEA Expert Group on Long-term Radiological Protection Objectives for Radioactive Waste Disposal [5] and more recently to principles published by the ICRP [6]. Other European countries may prefer a system of individual dose limitation for reasonable scenarios of radiation exposure. In United States the regulatory bodies have developed limits on radionuclide releases to the environment and also criteria for hydrogeological conditions and the performance of the waste package. The comparison with natural fluxes of radioactivity in the environment is also being discussed as a suitable reference in judging radiological safety in the very long term.

The report published by NEA in 1984 on long term objectives for waste disposal [5] was discussed at a workshop in Paris in 1985 on the interface between radiation protection, waste management and nuclear safety [7]. The individual risk concept adopted in this report to take account of both the level of radiation exposure of individuals and the probability of that exposure in time, is now widely endorsed. The maximum risk objective of 10^{-5} per year advocated in the report, which is in line with ICRP guidance, seems to be generally acceptable. Its practical application, however, raises some concern among the waste management community particularly because of the difficulty to assess probabilities and the need to apply it in the spirit of the relevant recommendations of the ICRP (i.e. with an ALARA approach). It must be emphasised that, as with all guidance documents, their recommendations require interpretation in the context that they are made. The complexity of this issue is well recognised but it should not become an issue of major concern for the following reasons:

- first, provided a long term radiological objective for waste disposal purposes is chosen within a range of values considered reasonable by present radiation protection standards and experience, suitable disposal solutions are most likely to be found;

- second, radiation protection is not, in most situations, a critical parameter in waste management decisions. In the NEA Long-Term Objectives Report, a multi-criteria approach for decision making is advocated, illustrating the need to consider other factors in an organised priority system;

- third, given the uncertainties inherently associated with long term performance assessments, we cannot expect very accurate estimates but rather orders of magnitude. In this respect, any long term risk objective should be looked more as a boundary condition for designers and licensing authorities than as a strict regulatory limit, since in most cases the existence of uncertainties makes it necessary to remain orders of magnitude below.

Another topic which is also often controversial is the need for collective dose calculations. Here again the NEA report on long term objectives makes a plea for common sense. Obviously such calculations can be useful as long as their results can be trusted and indicate marked differences in the potential impacts between various options. The NEA report says that in an optimisation approach such calculations are potentially useful for the comparison between options, but that they should not really be used as an absolute measure of the potential impact of a given disposal practice.

5. CONCLUDING REMARKS

In discussing the details of radiation protection criteria we have perhaps a tendency to forget that our main objective in radioactive waste disposal is isolation of the radioactive materials from the biosphere for as long as we feel it desirable, which in practical terms means something of the order of 100 000 years or more for long-lived waste. By anyone's standards, what we try to achieve by geological disposal is isolation practically forever and what we do with our performance assessments is essentially to check the degree of reliability of this isolation. This points to the importance of using system performance techniques that are broad, systematic and integrated so that they really give a correct picture of the overall safety characteristics of our disposal systems. This also points to the importance of a very clear presentation and documentation of the approaches and results of performance assessments. Only then can they be subject to an efficient review by scientists and regulatory bodies, which would gradually establish a firm confidence in the acceptability of the proposed methods of nuclear waste disposal. It is in this context that international co-operation will have an important role to play in the area of performance assessment during the coming years. Exchange of ideas, experiences and different viewpoints at an international level will promote development in this area and it will be one of many means to ensure a high quality of the analysis upon which the acceptability of nuclear waste disposal is to be judged.

REFERENCES

[1] Proceedings of the NEA Workshop on SYSTEM PERFORMANCE ASSESSMENTS FOR RADIOACTIVE WASTE DISPOSAL, Paris, 22-24 oct. 1985, OECD/NEA, Paris 1986

[2] IAEA Safety series No. 68
Performance Assessment for Underground Radioactive Waste Disposal Systems, IAEA, Vienna, 1985

[3] MULLER A.B. (1985), International Chemical Thermodynamic Data Base for Nuclear Applications, Radio. Waste Manage. Nucl. Fuel Cycle 6(2), 131-141

[4] Wanner H. (1986), THE NEA THERMOCHEMICAL DATA BASE, OECD Nuclear Energy Agency, NEA Data Bank, Saclay

[5] Long-term Radiation Protection Objectives for Radioactive Waste Disposal, OECD/NEA, Paris 1984

[6] Radiation Protection Principles for the Disposal of Solid Radioactive Waste, ICRP Publication 46

[7] Interface Questions in Nuclear Health and Safety, Proceedings of a NEA Seminar, OECD/NEA, Paris 1985

oooOooo

LINKAGES IN SYSTEM PERFORMANCE ASSESSMENTS

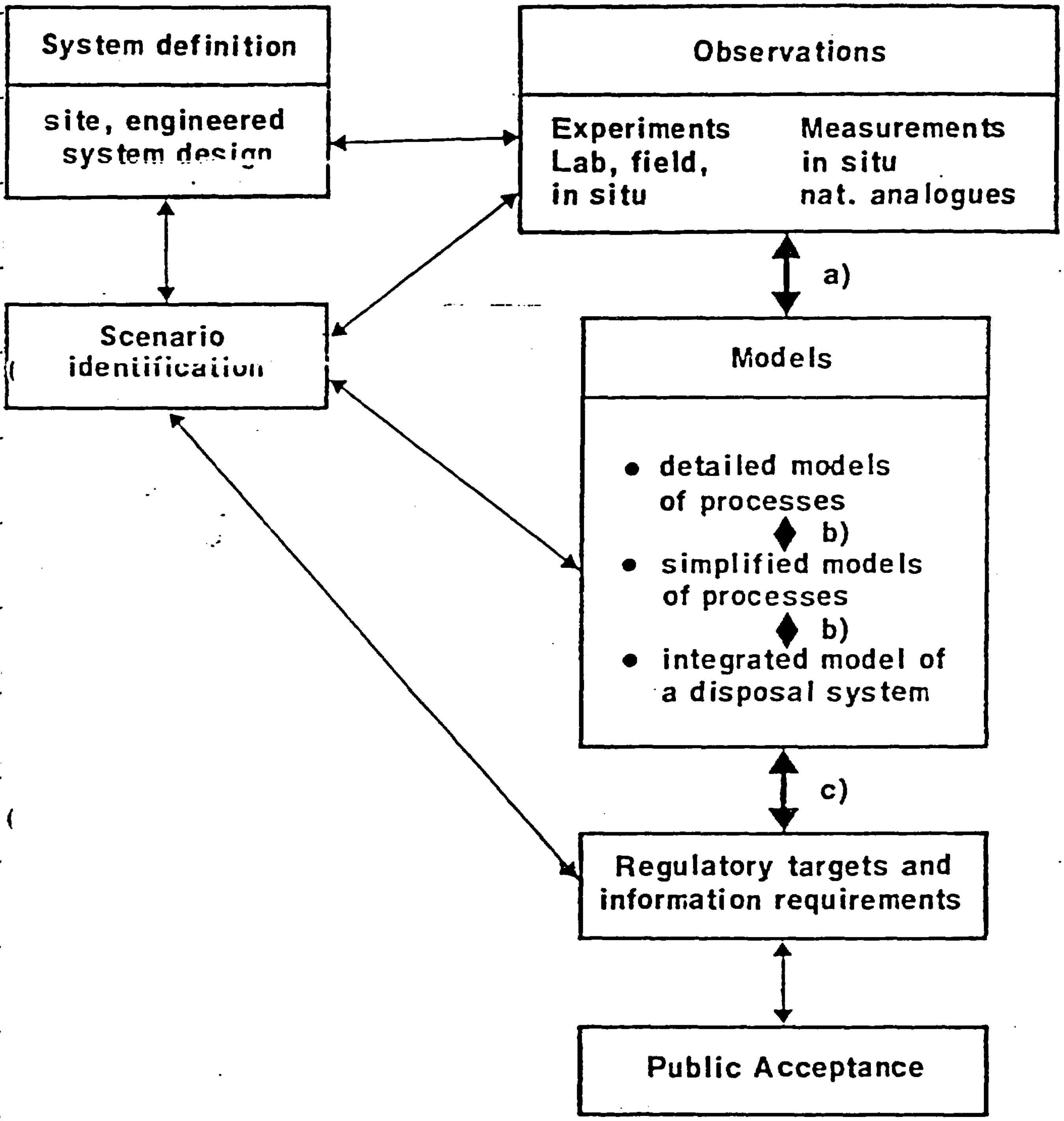
System definition
site, engineered system design
Observations
Experiments Lab, field, in situ
Measurements in situ nat. analogues
a)
Scenario identification
Models
• detailed models of processes
b)
• simplified models of processes
b)
• integrated model of a disposal system
c)
Regulatory targets and information requirements
Public Acceptance

a) Link between the development of models and observations (validation)

b) Link between detailed models and simple models and Link between separate models and an integrated system model

c) Link between the output of performance assessments and regulatory requirements.

MELODIE : A GLOBAL RISK ASSESSMENT MODEL FOR RADIOACTIVE WASTE REPOSITORIES

- J. LEWI, M. ASSOULINE, J. BAREAU, P. RAIMBAULT -

Commissariat à l'Energie Atomique/Institut de Protection et de Sûreté Nucléaire
BP n°6
92265 Fontenay-aux-Roses Cedex France

The Institute of Protection and Nuclear Safety (IPSN), which is part of the French Atomic Energy Commission (C.E.A.) develops since 1984 in collaboration with different groups inside and outside the C.E.A. a computer model for risk assessment of nuclear waste repositories in deep geological formations. The main characteristics of the submodels, the data processing structure and some examples of applications are presented.

INTRODUCTION

The modelling activity at the IPSN is based on the development of the global risk assessment code MELODIE 1 .
MELODIE is a deterministic code which can perform best estimate calculations by using detailed models; a selected set of representative scenarios is then studied. Sensitivity analysis and uncertainty calculations can also be performed, using simplified models.
The present version of MELODIE is based on the coupling of a groundwater flow model, a source term model, a radionuclide transport model and a biosphere model.
We will present hereafter the main characteristics of the sub-models, the data processing structure and some examples of applications.

I) MODEL DEVELOPMENT

1) Source term model

The source term modelling development is performed at the CEA/DRDD (Département de Recherche et Développement sur les Déchets). The first version of the code CONDIMENT, fitted for high-level wastes in a glass matrix, has been made available : it is a 1D code where the near field is represented in axisymetric geometry; it includes the glass matrix, the engineered barrier (for instance bentonite) and a layer of the host rock formation.
The code solves the advection-dispersion equation in the various media for a Nusselt number smaller than unity. The chemical interactions between radionuclides are represented by linear isotherms (retardation factor formalism).

In its present version, CONDIMENT considers the transport of radionuclides in the different source compartments and describes the degradation of the glass matrix related to the dissolution and transport of silica.
The flux out of the glass matrix of the radionuclides more soluble than silica (like caesium) is determined by the displacement velocity of the interface between the sound glass and the altered glass (gel layer). The radionuclides less soluble than silica (like the actinides) precipitate into the gel layer : their concentration at the limit of the gel layer is equal to their saturation value.

The corrosion of the container cannot presently be described by a realistic model; it is modelled as a failure time (experience shows that this failure time may be neglected when compared to radionuclide's travel time through geosphere), where the glass comes directly in contact with the bentonite. A statistical distribution of container failure times will eventually be introduced.

The future developments of CONDIMENT will allow to take into account chemical interactions such as precipitation reactions related to the chemical properties of the leaching water. Non-linear isotherms will be considered as well.

The CONDIMENT model can be used to describe the evolution of temperature in the near field and thus the heat flux to the geosphere. Parameters will be allowed to vary with local temperature.

2) Groundwater flow and radionuclide transport models

The submodels for groundwater flow and radionuclide transport in MELODIE are derived from the METIS code developed at the Ecole Nationale Supérieure des Mines de Paris. METIS is a 2D finite element code which solves the diffusivity equation and the advection-dispersion equation for an equivalent porous medium. First order adsorption kinetics as well as matrix diffusion and nuclear decay chains are included.
A recent development of the code was to implement explicit fracture representation for groundwater flow and radionuclide transport. Fractures are considered as linear elements with specific transmittivity : this simplifies mesh generation and saves computer time.

The possibility to solve the groundwater flow problem using water pressure instead of hydraulic head has been implemented, as well as a submodel for 2D heat transfer. This allows to take into account the variable density and viscosity of water with temperature for modelling buoyancy effects.

Specific models for flow in aquifers surrounding a salt formation are being developed as well. A simplified salt dissolution model has been implemented in the code and is used in connection with METIS in order to calculate the concentration of brines in aquifers. The coupling between groundwater flow and brine transport is then introduced by the variation brine density with salt concentration.

The question of time step management is of critical importance for advection-dispersion code since very large permeability contrasts may exist in the geosphere and the optimum time ste depends on the region which is considered. An automatic time step evaluation has bee implemented in the code which allows to use less stringent criteria and thus reduce compute time.

3) Biosphere model

The biosphere model, called ABRICOT, which has been developed at the IPSN/DPT (Département de Protection Technique), is based on a water and food consumption description. Individual, regional or collective doses may be calculated from the ingestion of radionuclides corresponding to menus which components originate from different agricultural systems in the pathways of radionuclides. Doses commitments from inhalation and direct exposure are taken into account as well.

A specific biosphere model valid for a coastal site is being developed. This code participates in the BIOMOVS international validation exercice.

4) Other model developments

- **Thermomechanics**

Several options will be investigated in order to determine to what extent thermomechanics should be introduced in a risk assessment code. These options range from taking these effects into account by modifying the statistical distribution of the parameters which are altered, performing a sudden change in the value of series of parameters, using specific laws of variation between parameters or coupling of thermomechanical model to the risk assessment code.

The choice will be made after specific studies performed with generic codes and associated sensitivity studies.

- **Geochemistry**

A general investigation has been conducted at the Ecole Nationale Supérieure des Mines de Paris in order to determine the state of the art in geochemical models and coupling methods between geochemistry and transport.

Tests will be conducted on the coupling of a simplified sorption model to a transport code.

- **Geoprospective**

The evolution of the geosphere for long periods of time will be taken into account by impact models corresponding to different climatic and neotectonic scenarios. Geoprospective studies are being performed in order to precise relevant scenarios on a specific site.

II) THE DATA PROCESSING STRUCTURE

An important effort have been made on the data processing structure of the MELODIE model. We present hereafter the reasons of this effort and the solutions adopted.

1) Presentation of the objectives

We may distinguish three main objectives :

- the first one is to give to the MELODIE code users the ability of adapting the tool according to their specific calculation needs : the evaluation of the consequences of nuclear wastes repositories induces different types of studies, in strong dependance with the nature of the mediums concerned (for instance : transient flow after refilling, hydrogeological conditions and the time scales considered at steady state, implementation of thermal effects...).

- the second objective is to insure the easiness of any further development or maintenance : the nuclear wastes management being a field where techniques and knowledge are in constant progress, it is clear that improving the existing models or developping new ones becomes a necessity.

- the last one is to make the system user friendly by optimizing the execution times for the different tasks, and creating utility fonctions for data processing or for development.

We may summarize these objectives in :

- flexibility
- easy maintenance and development
- user friendliness

2) The problems encountered

Performance assessment of a nuclear wastes repository requires the knowledge of the various physical phenomena to be described, the optimization of numerical techniques used to solve the systems of equations, the adequation of computer techniques and languages to set up the environment, and to carry out the calculations.

Scheme 1 describes the level of knowledge which is necessary in order to access to any level of activity related to the system.
It is first necessary to disconnect entirely the process of running the code from the programming tasks. Because, on one hand, little computer knowledge should be required to use the programs, and on another hand, because system maintenance, updating and development should never perturbate its utilisation.

A second source of problems is related to development constraints : it is necessary to obtain a modular structure allowing an evolutive organization of the code (updating of the different modules, implementation of new parameters and new physical processes), an evident solution being the realization of a specific binary modules library, easily transportable and maintenable.

A third difficulty will consist in making the use of the system as comfortable as possible : its heaviness must be ignored by the user and assistance will be required during :

- pre-processing tasks (data set building and management),
- post-processing operations (exploitation of results, curve drawings),

3) Practical solutions adopted

The realization of the MELODIE software has been accomplished in four phases :

- Phase 1 : Definition of the system's elementary functions
  A librarian utilities organization has been set up providing for functional separation and modularity of the tasks. The library organization is represented by scheme 2.

- Phase 2 : Definition of the hardware resources.
  The efficiency of the organization represented by scheme 2 will be governed by the choice of best adapted computers and systems. Among the possible configurations available we have developped the following one, described by scheme 3, characterized by the use of a CRAY-XMP as a central computer :

. calculations are executed by CRAY-XMP via the batch utility. Programs are all written in CRAY extended FORTRAN.

. pre and post processing are performed on IBM 4341 under VM/CMS exploitation system. Procedures are written in CMS/EXEC2 language and standard FORTRAN.

- Phase 3 : Implementation of the general structure.
  The conversational VM/CMS system allows the repartition of hardware resources into user's independant virtual machines, between which links may be pre-defined via the system's disk management utilities.

In our configuration, one virtual machine is continuously devoted to program development and another one to pre and post processing procedures : this provides for the physical separation required between the two types of activities.
These two virtual machines are accessible by all the users. Program sources and procedures are installed on read only accessed disks in order to avoid any false manoeuvre from the users. The permanent binary modules library is installed on the CRAY-XMP central computer, modules being created or updated through an UPDATE procedure, exclusively accessible from the development machine itself. Tasks are assembled on the frontal computer,

then sent to the CRAY-XMP batch utility and results files are sent back to the users own virtual machines for post-processing.

- Phase 4 : Development of the pre and post processing utilities and development of the code.

  Procedures are using many development languages :
  - FORTRAN 77,
  - CMS/DIOF conversational screen management,
  - Graphic IBM library,
  - EXEC2 procedure language,

The organization of the procedures functions is modular as described by shemes 4 and 5 and tasks are defined under a conversational environment.

Program development modularity occurs at two levels :
- for the physical processes description : the scheme 6 presents an example of a simulation structure organization,
- for the program development and especially for the parameters management : usually COMMON blocks or dummy arguments are used to modify or implement new parameters, and this induces modifications of the main program and of the subroutines. Another method is allowed by the CRAY-XMP FORTRAN compiler : the use of pointers.

Let's summarize this technique :
- each parameter is associated to an address in computer's central memory,
- a common memory zone is reserved for all of them,
- each subroutine may access this zone in order to retrieve its input arguments and store its output arguments.

The advantage is that the modules become perfectly interchangeable, and that the main program is never affected by the introduction of new developments. This technique requires however a rather sophisticated computer knowledge and practice : a solution resides in creating environment utilities to simplify the pointers use such as parameters list glossaries, modules creation and update assistance.

As a conclusion we may summarize the main characteristics of the MELODIE software :

- modular structures intervening at each functional level such as physical processes description, task definition, program development,
- a clear separation between development and user functions,
- maintenance and development utilities,
- comfortable use provided by acceptable response times and conversational environment,
- high level of flexibility to treat different problems provided by a dynamic modules assembling.

III) EXAMPLES OF APPLICATIONS

The characteristics of the MELODIE submodels which are today available for the description of the different physical sub-systems involved in the risk assessment of nuclear wastes repositories and the specific software organization developed at the IPSN allow to perform several kinds of applications.

In this part we will review different aspects of model validation and performance assessment exercises. Pictures illustrating different results of the proposed exercises, are giving an idea of the pre and post processing utility functions of the code.

1) Participation to the international project Hydrocoin

The validation of the groundwater flow module of the METIS code is performed by participation to the HYDROCOIN international project [2]. The level 1 of the project was dealing with the verification of the numerical accuracy of the codes. METIS was used to perform calculations on 5 cases dealing with :

a) Transient flow from a borehole in a fractured permeable medium.
b) Steady state flow in a rock mass intersected by fracture zones.
c) Thermal convection in a saturated permeable medium.
d) Steady state flow from a hypothetical bedded salt repository.
e) Saturated 2D flow through a shallow land disposal facility in argillaceous media.

Excellent agreement with analytical solutions and other codes was found for hydraulic heads and water velocities. More spreed was obtained in particle trajectories (see fig 1, 2, 3).

Levels 2 and 3 of HYDROCOIN deal with comparisons of calculated results and experimental data and sensitivity analysis. A 3D version of the METIS is being developed to solve the proposed cases.

2) Performance assessment exercise on a bedded salt site

A vertical cut of an hypothetical bedded salt site is currently used for a performance assessment exercise.

The cut is 60 km wide and 3000 m deep (figure 4).
Two 100 to 300 m thick salt layers are surrounded by shale.
The permeability of salt is 10^{-15} m/s and the permeability of shale is 10^{-10} m/s.

A complete grid generation of the site was performed with GIBI (grid generator developed by CEA/DEMT (Département d'Etudes Mécaniques et Thermiques) to 1343 elements (figure 5).

A description of the groundwater flow system around the salt formation have been computed with MELODIE. Figure 6 shows the Darcy velocity chart.

Pathlines were computed and will allow to use a simplified representation for calculating the radionuclide migration in relation with non normal scenarios such as sealing deficiencies around the shafts or fracture openings.

3) Participation to the PAGIS (Performance Assessment of Geological Isolation Systems) project [3]

For this European project dealing with high level vitrified wastes repositories, started since 1982, four formations have been selected : clay, salt, granite and sub-seabed. The French team is responsible for the granite option calculations.

Two types of calculations are essentially performed at CEA/IPSN with MELODIE :
- "Best-Estimate",
- Sensitivity analysis according to the parameters variability.

"Best Estimates" calculations require a high level of sophistication for the source, geosphere and biosphere descriptions. The logical sequence of the different steps performed for the global assessment of the granite reference site (Auriat) in the case of a normal evolution scenario are presented through picture 7 to 15 :

- Step 1 : 2 dimensional mesh generation and data processing (figure 7).

- Step 2 : hydrogeological calculations leading to :
  - hydraulic head field representation (figure 8),
  - pore-water velocities under steady state conditions (figure 9),
  - particle trajectories and identification of the main discharges (figure 10).

- Step 3 : Implementation of the repository in the mesh (figure 11) and simulation of the joint evolution of the radionuclides transfer in the source term and the geosphere (CONDIMENT/METIS) providing for :
  - radionuclide activity profiles in 2D cut versus time (figure 12),
  - activity releases to the discharges as a function of time.

- Step 4 : Implementation of the biosphere (ABRICOT) model to the previous structure and evaluation of dose rates to individuals, versus time (figure 13).

Sensitivity analysis to parameters are also to be carried out to achieve the reference case study.

A specialized structure has been set up for the calculations as described in figure 14.
The 2D "Best Estimates" provide for a 1D flow tube representative of the geosphere (figure 15).
Statistical distribution curves are associated to the concerned parameters (in the example 11 parameters) and sets of values are sampled for each run being performed (60 runs in this case).

The results are then stored, and, at last, statistically analyzed according to the RSM multilinear regression technique.

CONCLUSIONS

The modelling activity performed at the CEA/IPSN has permitted to develop a first version of the code MELODIE, which associates a source term model, a geosphere model and a biosphere model. Each of these submodels is developped and tested in specialized teams (ENSMP, CEA-DRDD, CEA-IPSN-DPT). The confrontation to experimental results (obtained in laboratory) and the participation to existing international projects (HYDROCOIN, BIOMOV, PAGIS) reinforces the confidence we may have in the code quality.

REFERENCES

[1] Development of the code MELODIE for long term risk assessment of nuclear waste repositories - P. Raimbault, P. Goblet, P. Guetat, J. Levi, J. P. Mangin, G. de Marsily - 9th symposium on the scientific basis for nuclear waste management MRS-Stockholm (september 1985).

[2] HYDROCOIN - Progress report n° 3 - July-December 1985 - SKI-Stockholm.

[3] PAGIS - Summary report of phase 1 - EUR 9220 EN - 1984

		KNOWLEDGE OF PHYSICS		KNOWLEDGE OF NUMERICAL AND COMPUTER TECHNIQUES			
		DATA	PHYSICAL PROCESS	NUMERICAL ANALYSIS	FORTRAN 77	FORTRAN 77 CRAY	OTHER COMPUTER LANGUAGES
USER	LEVEL 1	X	X				
	LEVEL 2	X	X		X		
DEVELOPMENT	OF PROGRAMS		X	X	X	X	
	OF COMPUTER ENVIRONMENT				X	X	X

SCHEME 1

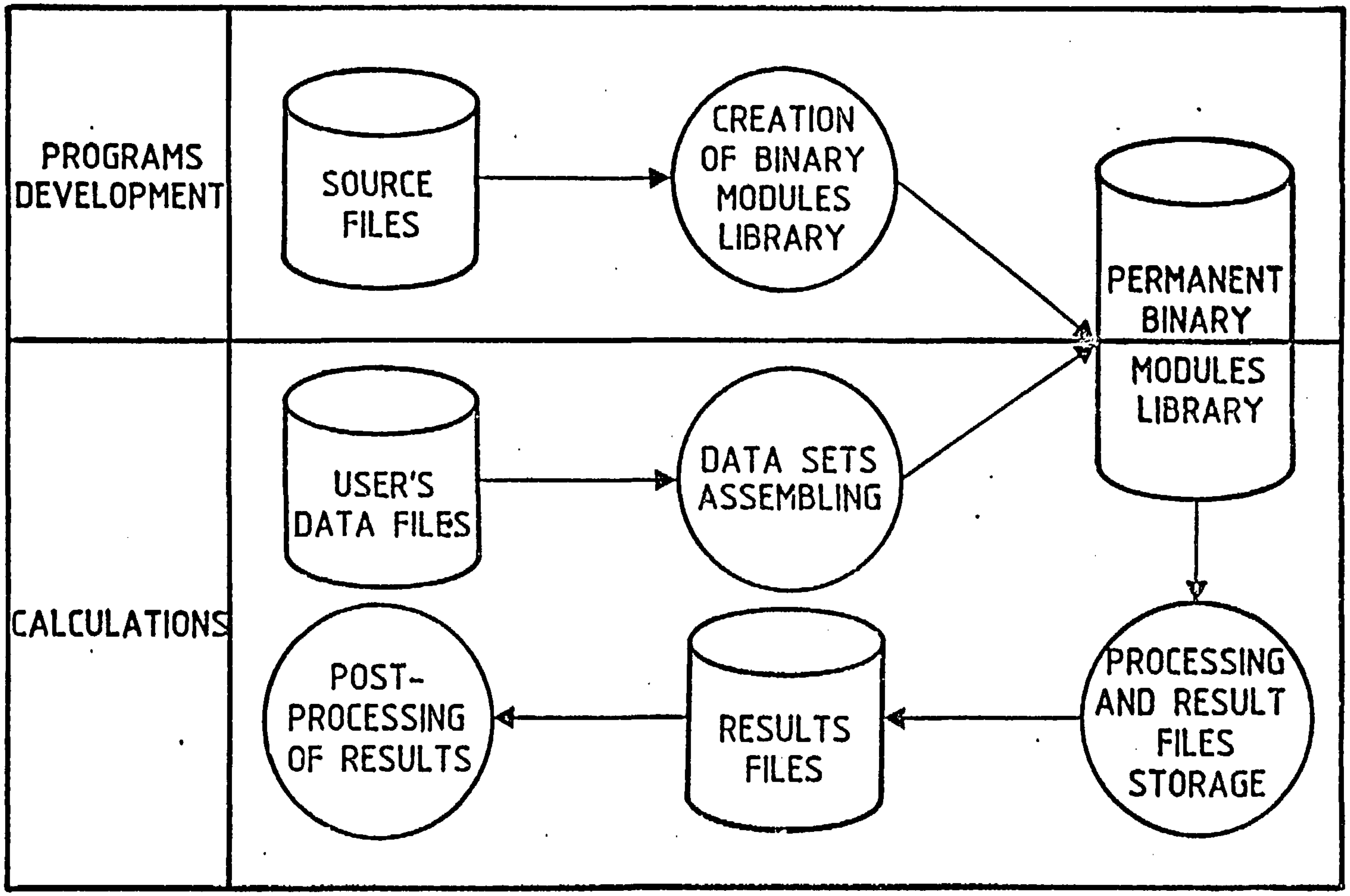
PROGRAMS DEVELOPMENT
CALCULATIONS
SOURCE FILES
CREATION OF BINARY MODULES LIBRARY
PERMANENT BINARY MODULES LIBRARY
USER'S DATA FILES
DATA SETS ASSEMBLING
PROCESSING AND RESULT FILES STORAGE
RESULTS FILES
POST-PROCESSING OF RESULTS

SCHEME 2

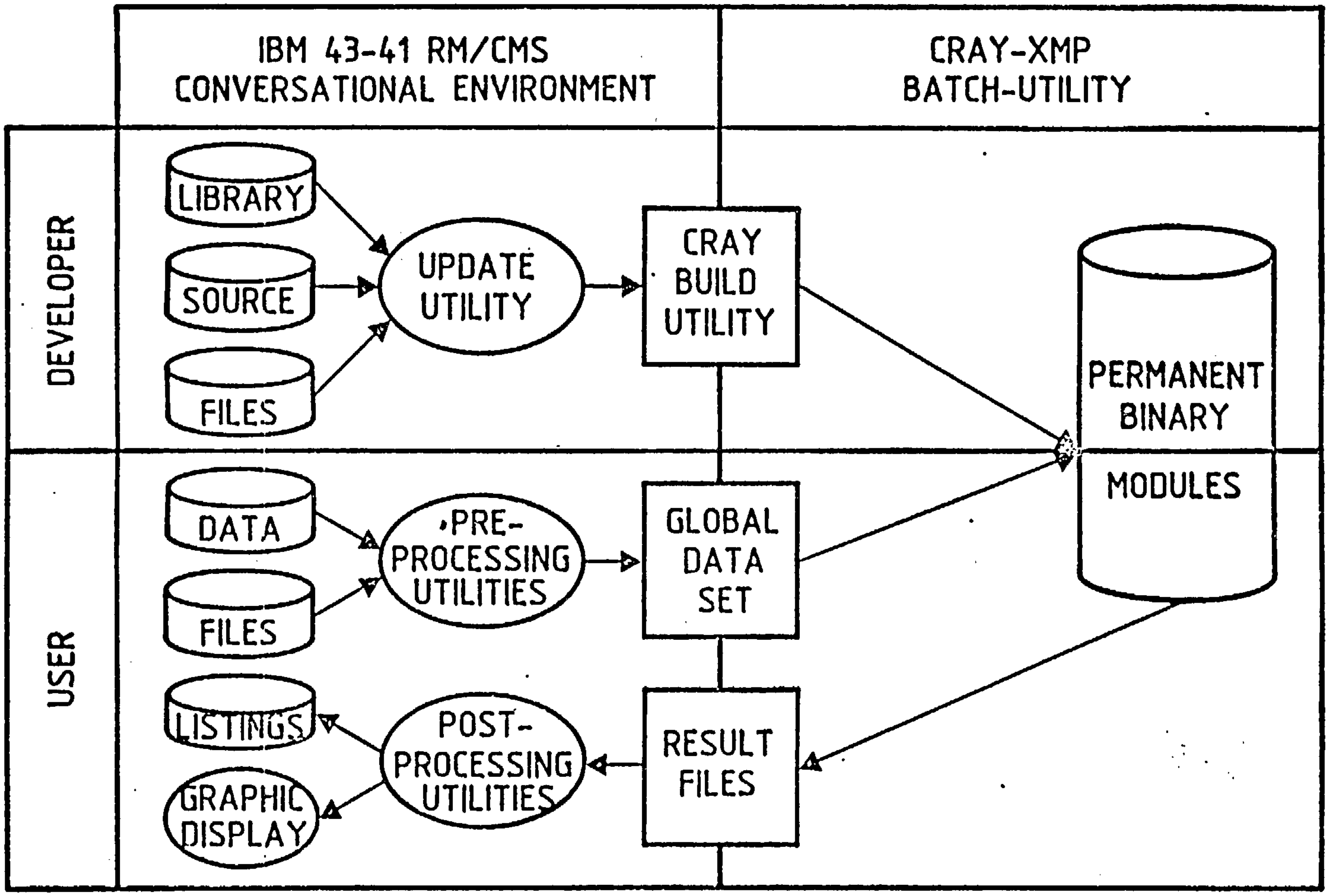
IBM 43-41 RM/CMS
CONVERSATIONAL ENVIRONMENT
CRAY-XMP
BATCH-UTILITY
DEVELOPER
USER
LIBRARY
SOURCE
FILES
UPDATE UTILITY
CRAY BUILD UTILITY
PERMANENT BINARY MODULES
DATA
FILES
PRE-PROCESSING UTILITIES
GLOBAL DATA SET
LISTINGS
GRAPHIC DISPLAY
POST-PROCESSING UTILITIES
RESULT FILES

SCHEME 3

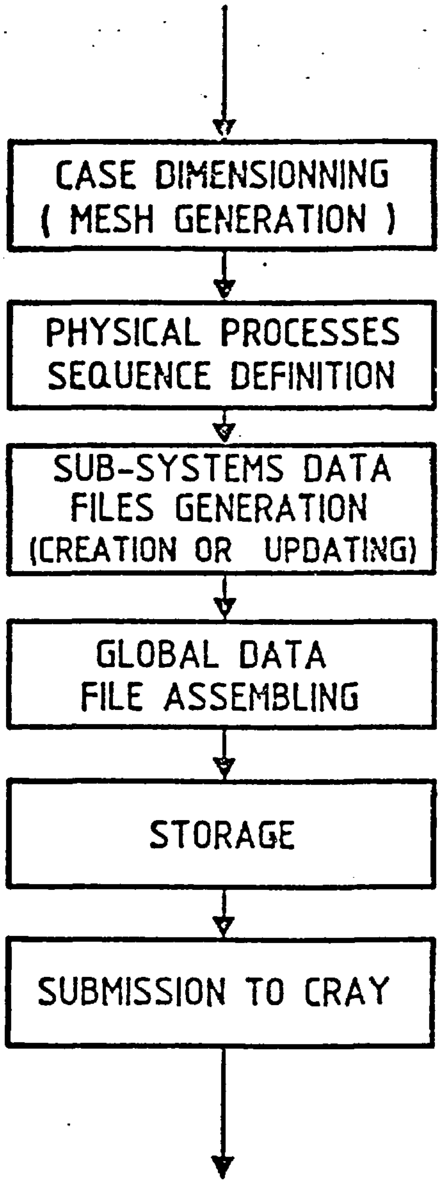
CASE DIMENSIONNING
(MESH GENERATION)
PHYSICAL PROCESSES
SEQUENCE DEFINITION
SUB-SYSTEMS DATA
FILES GENERATION
(CREATION OR UPDATING)
GLOBAL DATA
FILE ASSEMBLING
STORAGE
SUBMISSION TO CRAY

PRE-PROCESSING
GENERAL TASKS

SCHEME 4

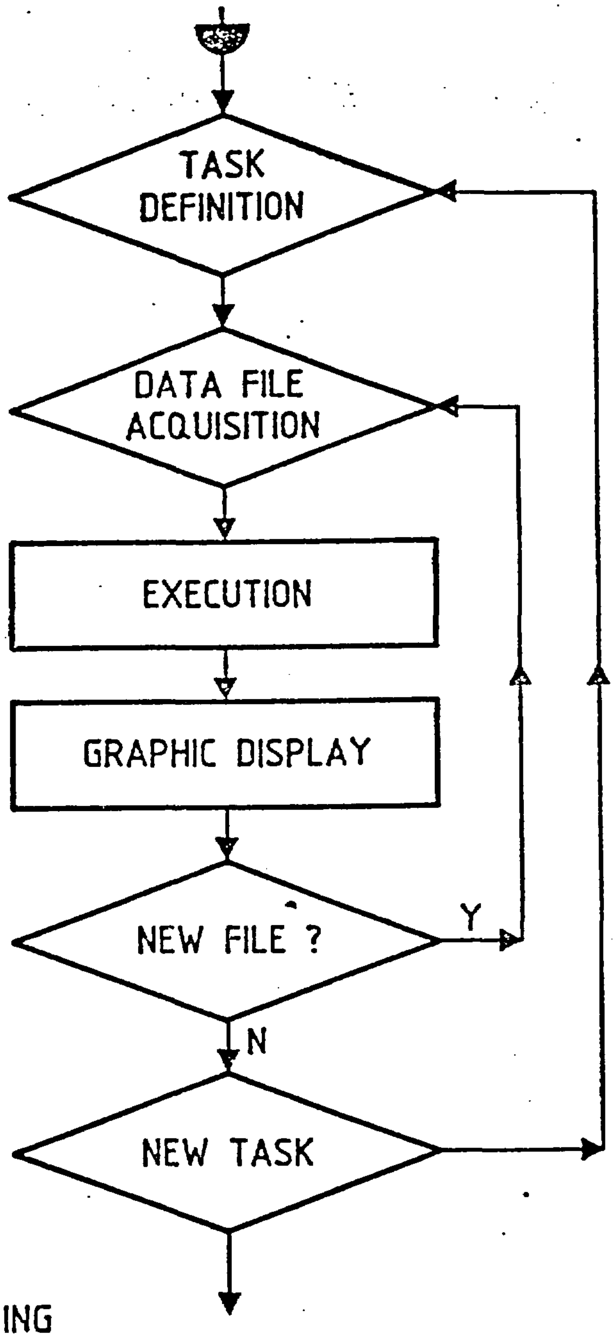
TASK DEFINITION
DATA FILE ACQUISITION
EXECUTION
GRAPHIC DISPLAY
NEW FILE ?
Y
N
NEW TASK

POST-PROCESSING
GENERAL TASKS

SCHEME 5

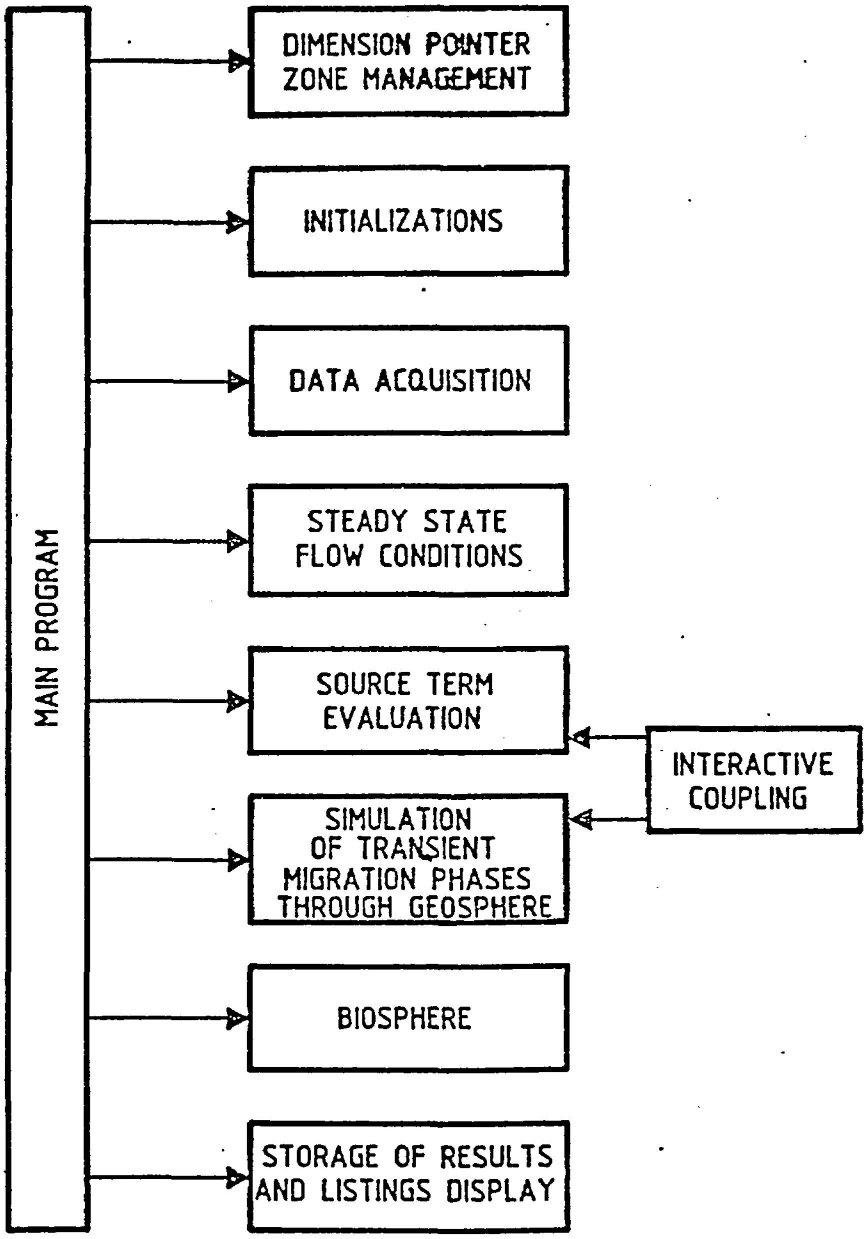
MAIN PROGRAM
DIMENSION POINTER ZONE MANAGEMENT
INITIALIZATIONS
DATA ACQUISITION
STEADY STATE FLOW CONDITIONS
SOURCE TERM EVALUATION
SIMULATION OF TRANSIENT MIGRATION PHASES THROUGH GEOSPHERE
BIOSPHERE
STORAGE OF RESULTS AND LISTINGS DISPLAY
INTERACTIVE COUPLING

DATA MODULING TASK ORGANIZATION

SCHEME 6

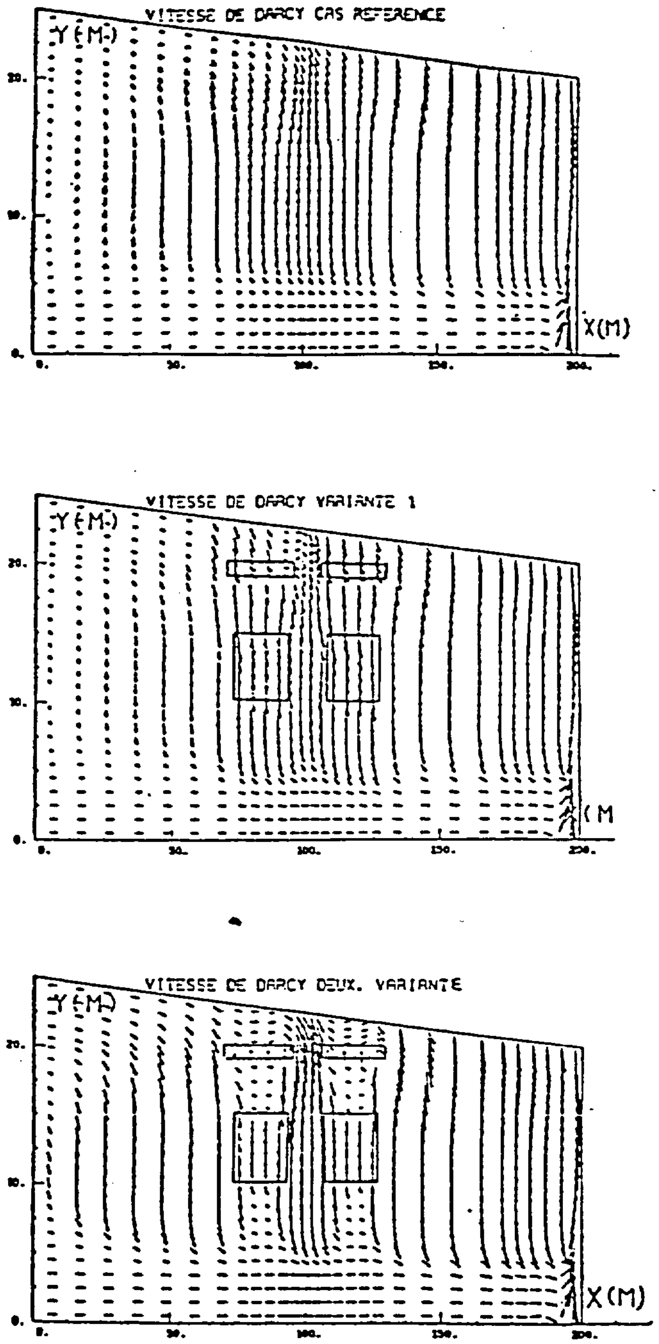

Darcy velocity chart

Figure 1 : HYDROCOIN : argillaceous medium : case 7

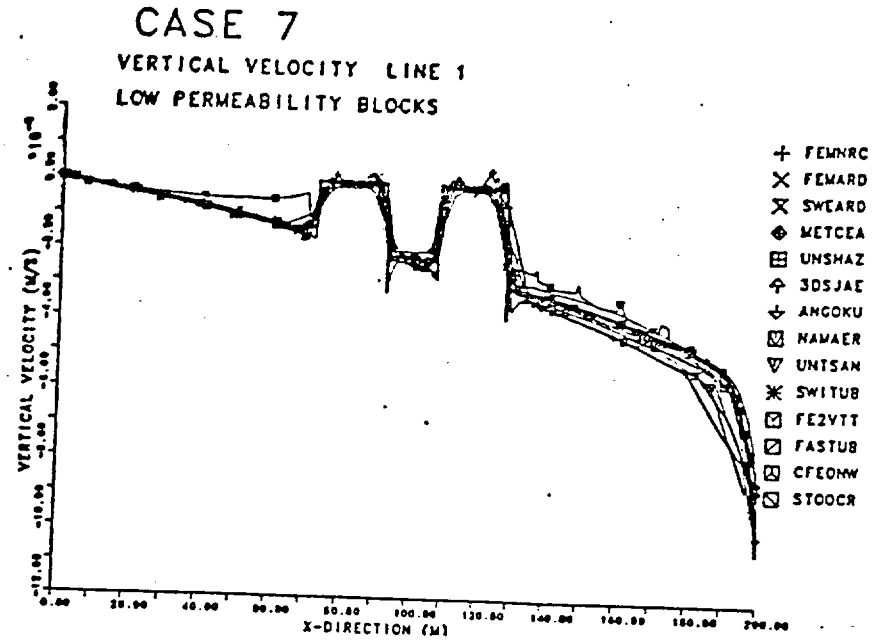

Figure 2 : Code intercomparison : velocity profiles

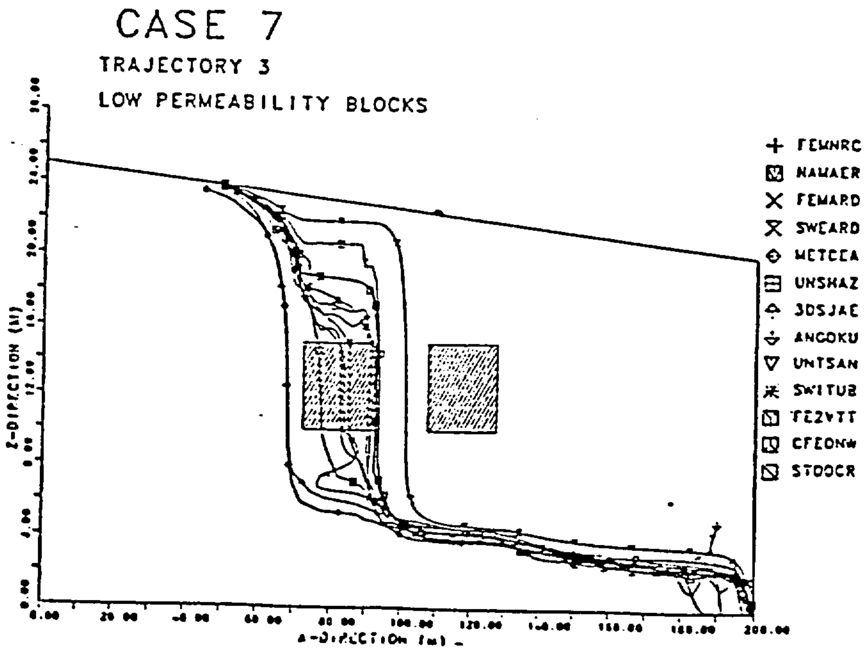

Figure 3 : Code intercomparison : particle trajectories

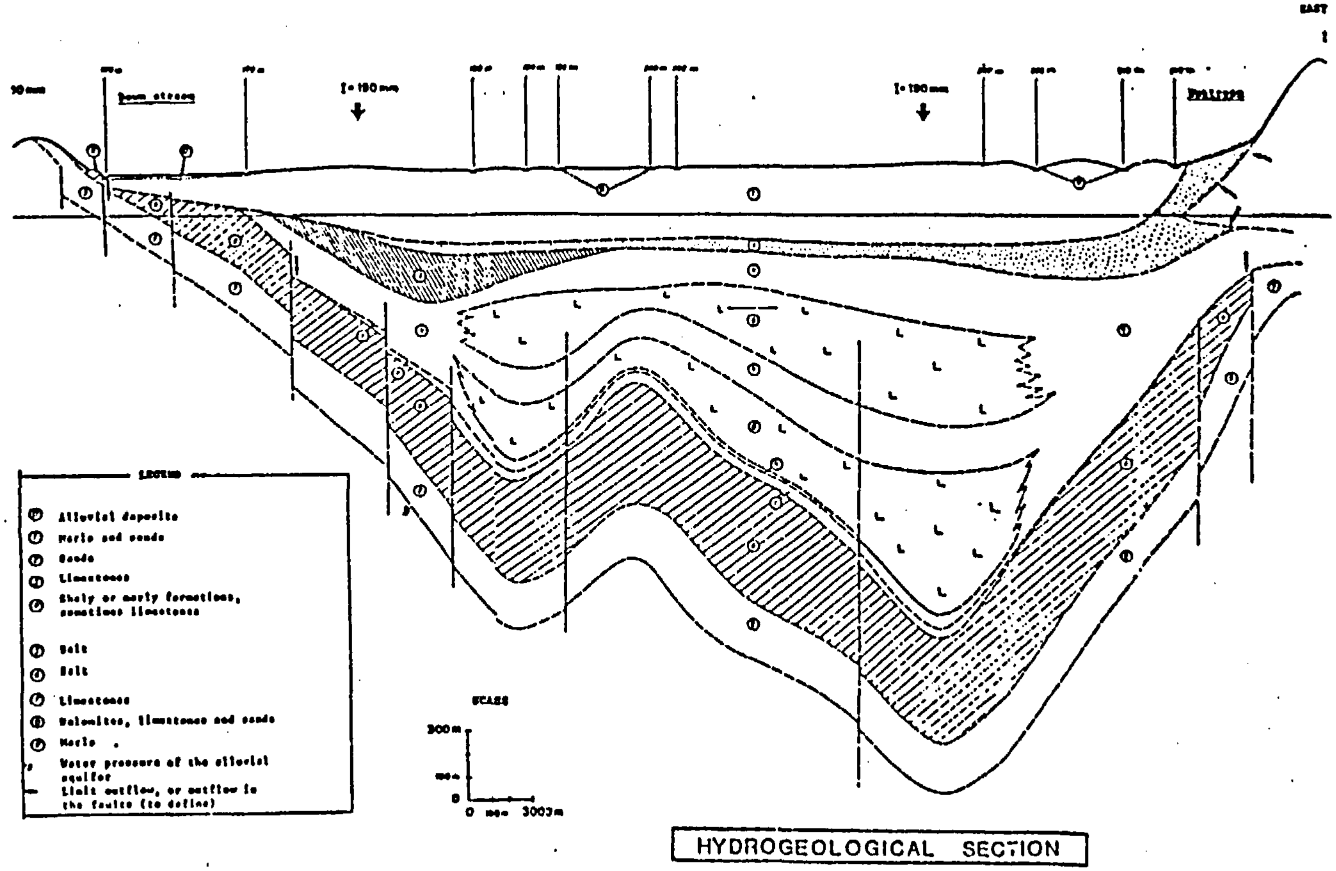
EAST
10 mm
Down stream
I=190 mm
I=190 mm
Upstream
LEGEND
Alluvial deposits
Marls and sands
Sands
Limestones
Shaly or marly formations, sometimes limestones
Salt
Salt
Limestones
Dolomites, limestones and sands
Marls
Water pressure of the alluvial aquifer
Limit outflow, or outflow in the faults (to define)
SCALE
300 m
0
0 mm 3000m
HYDROGEOLOGICAL SECTION

Figure 4 : Hypothetical site for the bedded salt

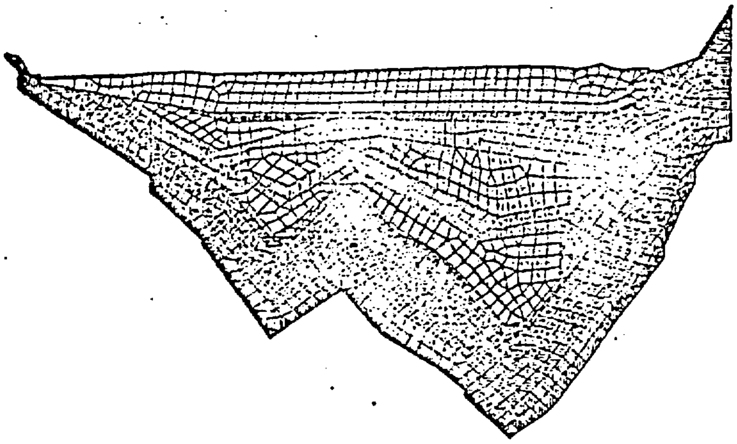

Figure 5 : Finite elements discretization

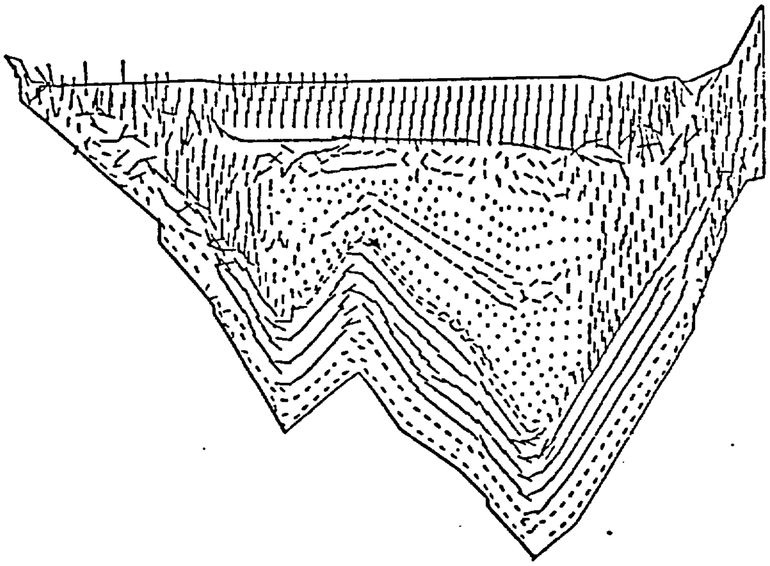

Figure 6 : Darcy velocity chart

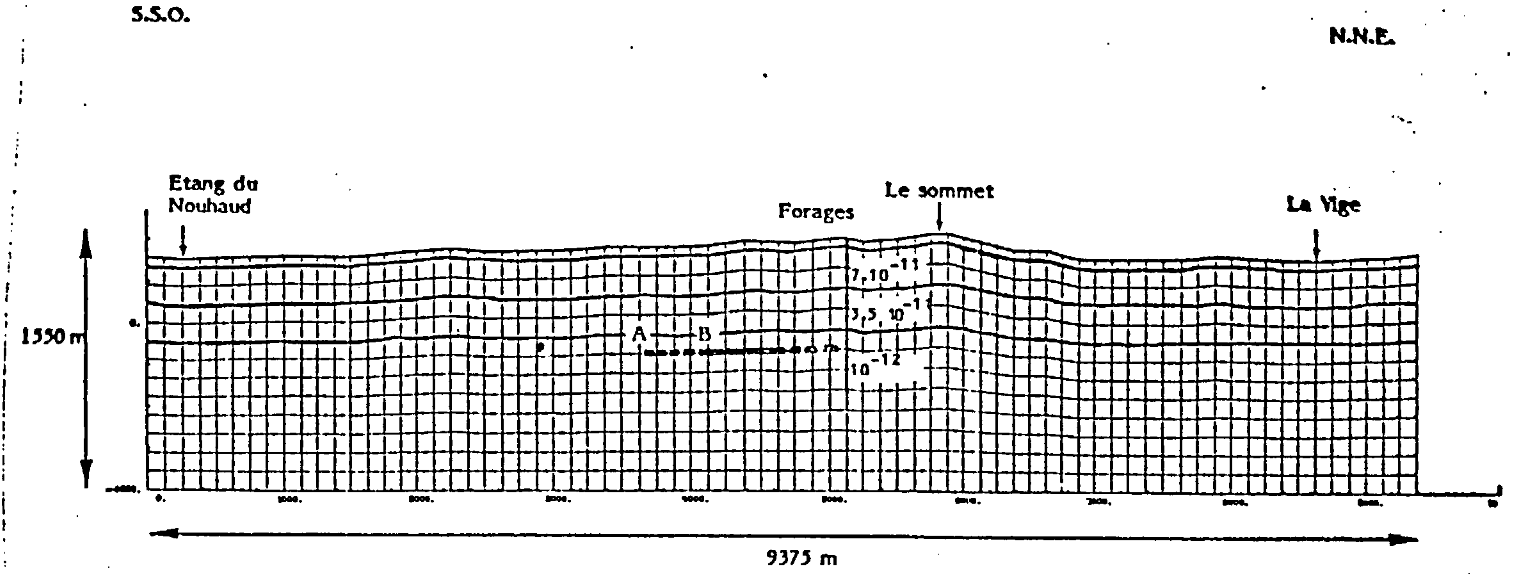

S.S.O.
N.N.E.
Etang du Nouhaud
Forages
Le sommet
La Vige
7,10^-11
3,5, 10^-11
10^-12
A
B
1550 m
9375 m

Figure 7 : 2D mesh for Aurlat site representation

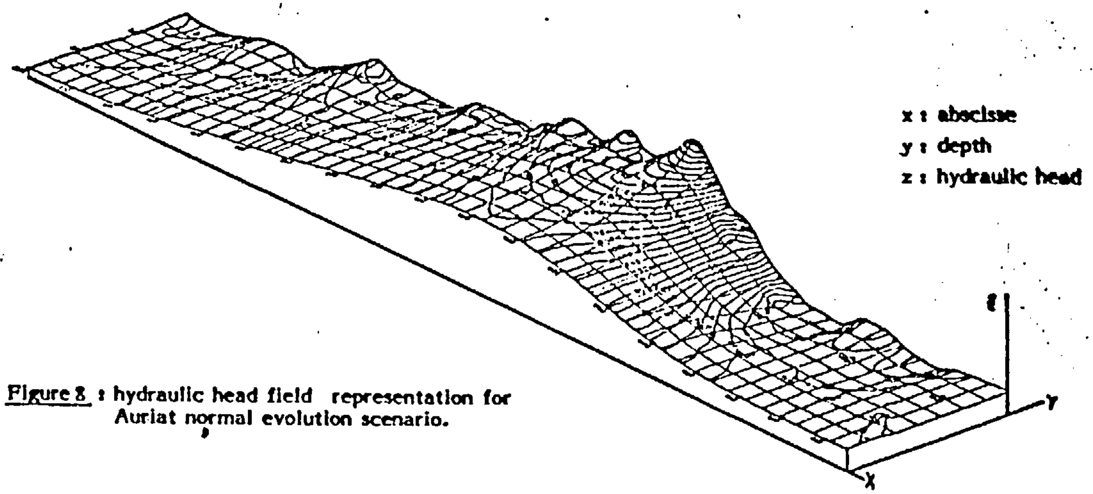

Figure 8 : hydraulic head field representation for Auriat normal evolution scenario.

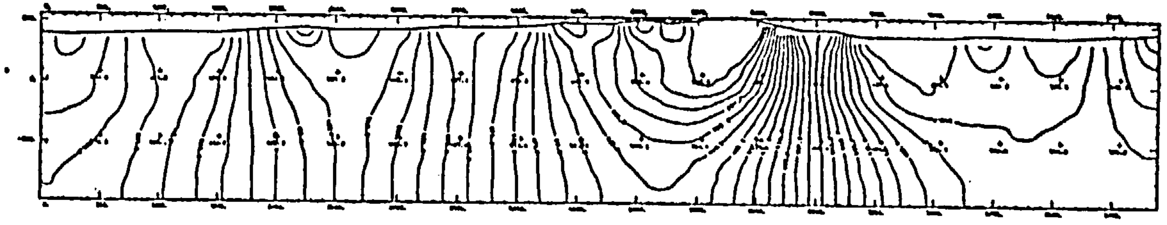

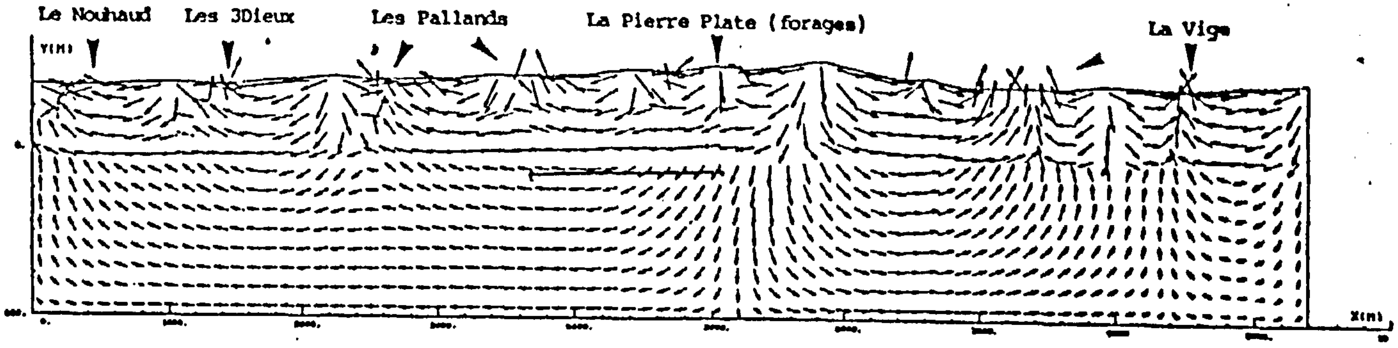

Figure 9 : pore-water velocities under steady state conditions
Auriat - normal evolution scenario

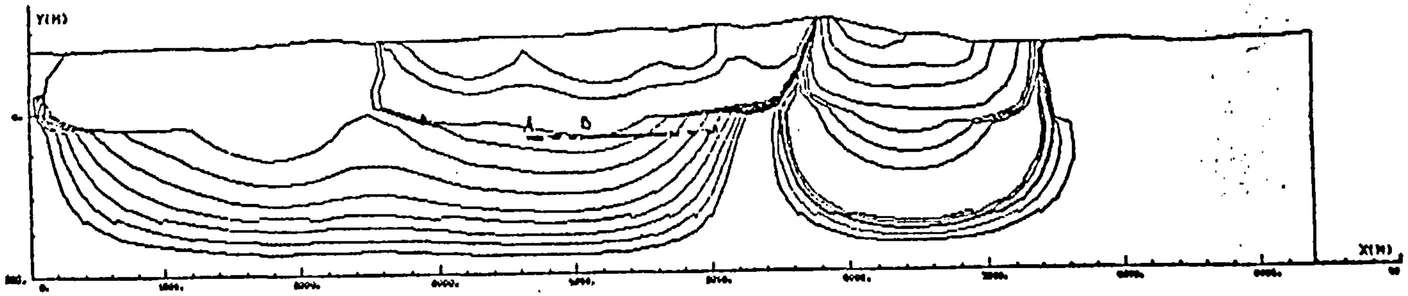

Figure 10 : particle trajectories in Auriat 2D representation

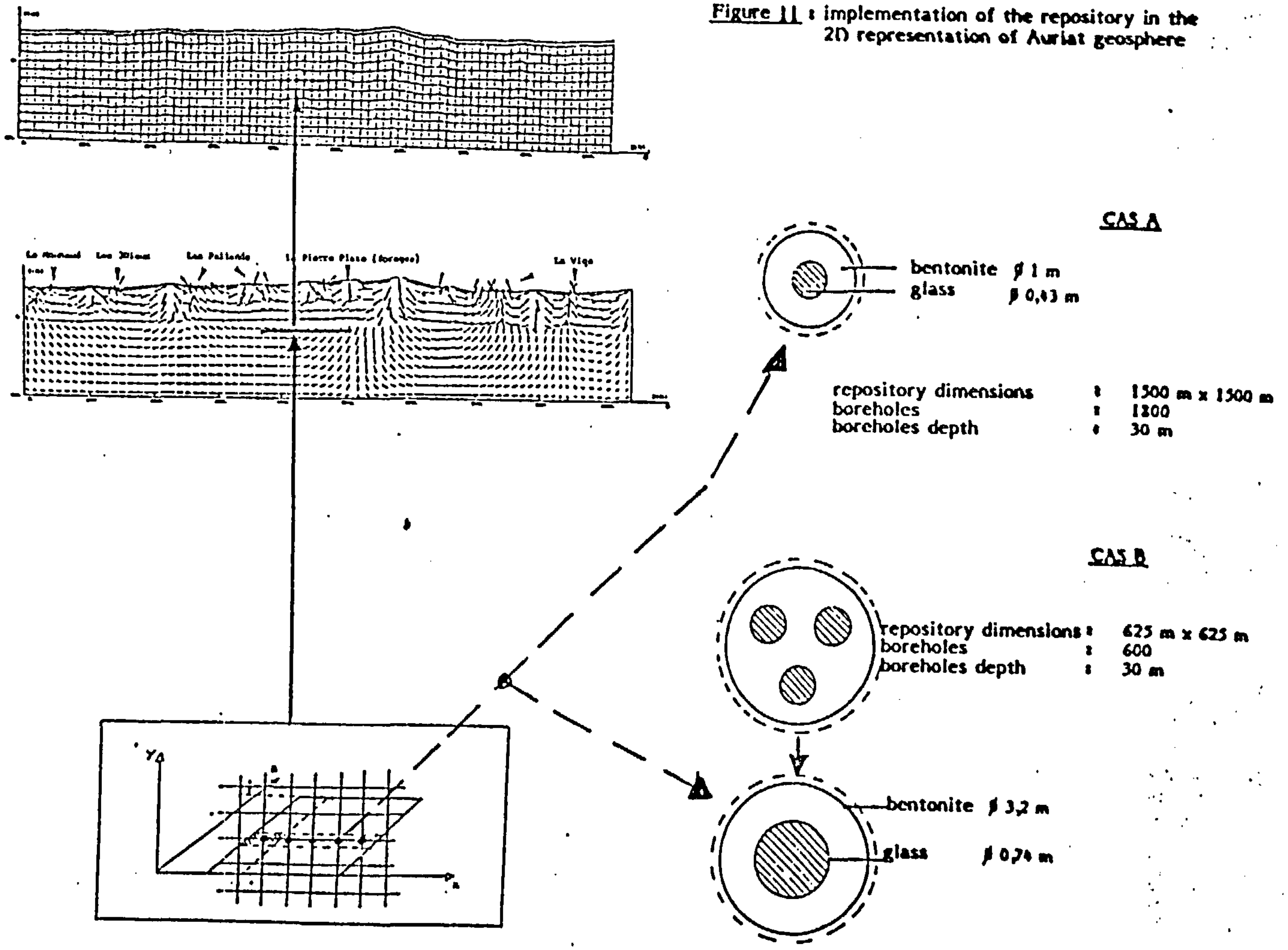
La Pierre Plate (forages)
La Vige
CAS A
bentonite ∅ 1 m
glass ∅ 0,43 m
A
CAS B
bentonite ∅ 3,2 m
glass ∅ 0,74 m
A
B
Y
x

Figure 11 : implementation of the repository in the 2D representation of Auriat geosphere

CAS A

repository dimensions : 1500 m x 1500 m
boreholes : 1200
boreholes depth : 30 m

CAS B

repository dimensions : 625 m x 625 m
boreholes : 600
boreholes depth : 30 m

Figure 12 : radionuclide activity profiles versus time - Auriat - case B - normal evolution scenario (cesium 135)

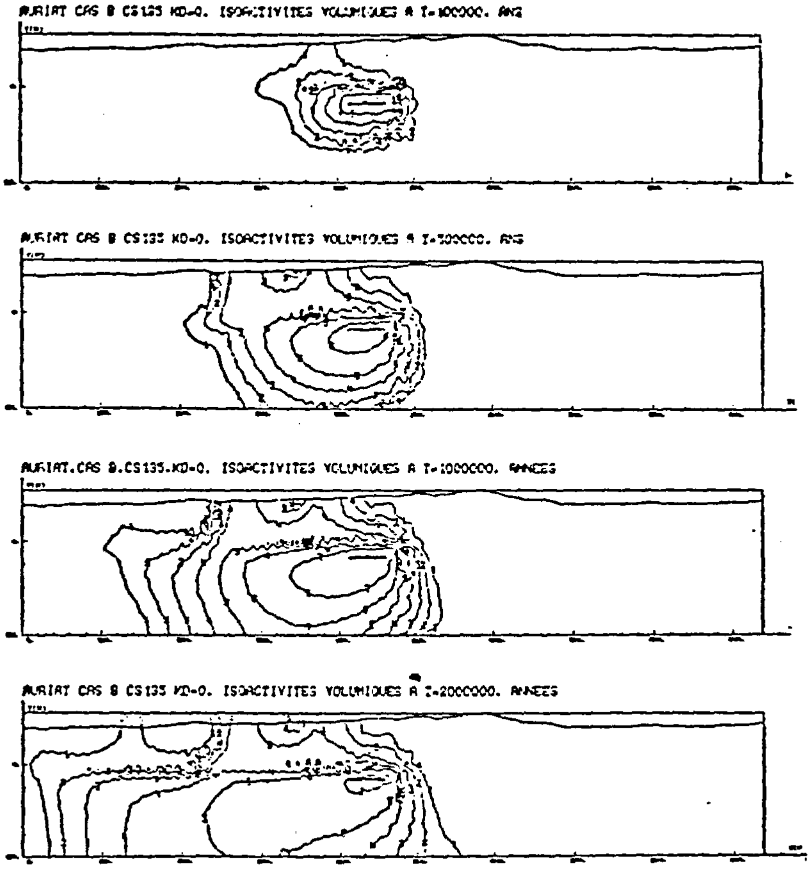

AURIAT CAS B CS135 KD=0. ISOACTIVITES VOLUMIQUES A T=100000. ANS

AURIAT CAS B CS135 KD=0. ISOACTIVITES VOLUMIQUES A T=500000. ANS

AURIAT.CAS B.CS135.KD=0. ISOACTIVITES VOLUMIQUES A T=1000000. ANNEES

AURIAT CAS B CS135 KD=0. ISOACTIVITES VOLUMIQUES A T=2000000. ANNEES

Figure 13 : individual annual dose rates for fission products - Auriat - case A - normal evolution scenario

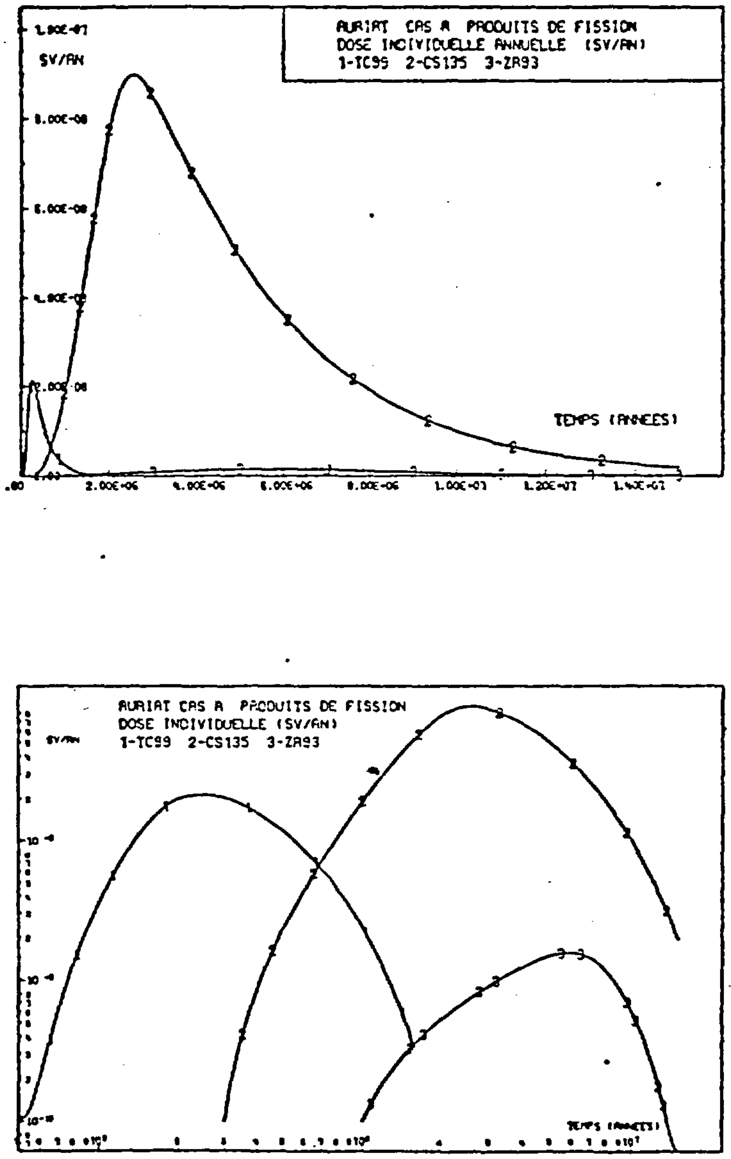

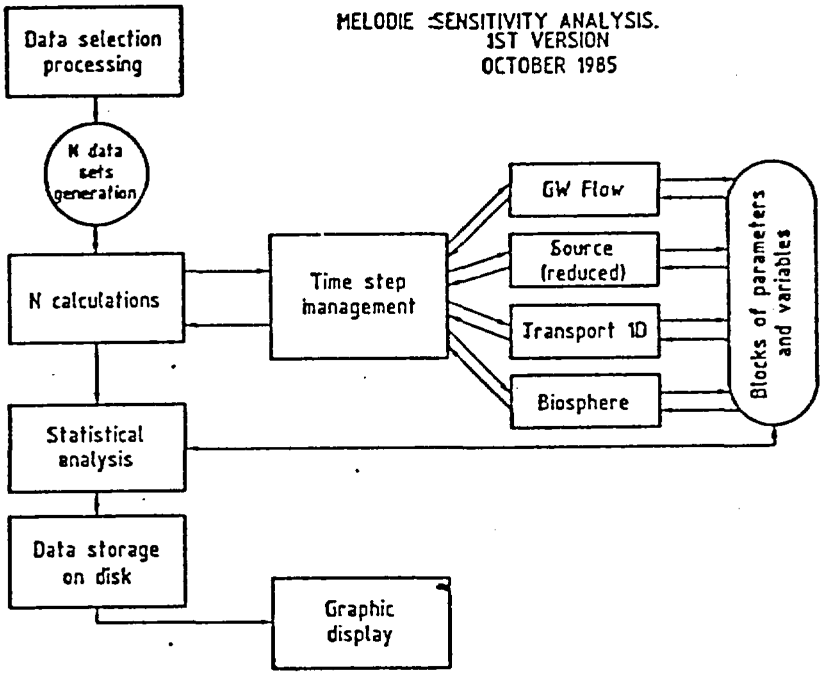

Figure 14

MELODIE SENSITIVITY ANALYSIS.
1ST VERSION
OCTOBER 1985
Data selection processing
N data sets generation
N calculations
Time step management
GW Flow
Source (reduced)
Transport 1D
Biosphere
Blocks of parameters and variables
Statistical analysis
Data storage on disk
Graphic display

Figure 15 : one dimensionnal reduction of Auriat site for sensitivity analysis

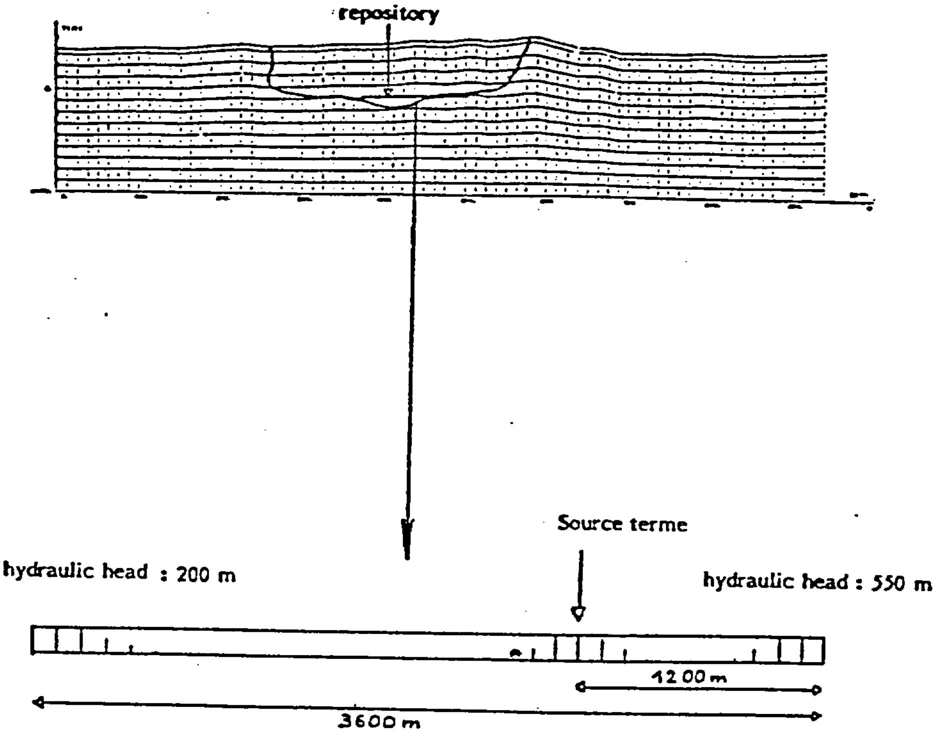
repository
Source terme
hydraulic head : 200 m
hydraulic head : 550 m
1200 m
3600 m

mean permeability : 1.10^{-4} m/an

TITULO DEL ARTICULO O NOMBRE DEL AUTOR

[illegible] mecanografiado
en todas las páginas
excepto la pág 1)
debe comenzar aquí →

Project COSA - A Benchmark of Computer Codes for the Thermo-Mechanical Behaviour of Rock Salt.

N C Knowles, Atkins Research and Development, Epsom, Surrey, UK

ABSTRACT

A review of a benchmark exercise involving 10 organisations using some twelve computer codes is presented. Interest centres around the reliability of predictions of the thermo-mechanical creep behaviour of rock salt in the context of geological disposal of high level radioactive waste.

1. INTRODUCTION

Research studies dealing with the geomechanical behaviour of repositories for radioactive waste in rock salt, have now been pursued for nearly two decades. Such studies rely increasingly on fairly sophisticated computer calculations to predict the long term stress and deformation history within the host strata and a number of computer programs have now been developed (1). Project COSA (comparison of computer codes for salt) was organised to compare the capabilities of these codes.

It was set up by the Commission of the European Communities as part of its research programme into 'Management and Storage of Radioactive Waste' following a meeting of CEC research contractors in December 1983 (2). The first phase was completed in July 1986, the second phase commenced in November 1986 and will run for a further 2 years.
Ten organisations have participated to date, with the British engineering consultants Atkins R&D of Epsom acting as the non participating (and hopefully impartial) coordinator and scientific secretary. The participants are :

In Belgium : The company FORAKY, in association with the Centre d'Etude de l'Energie Nucleaire (CEN/SCK) and the Laboratoire de Genie Civil of the University of Louvain-la-Neuve (LGC).

In Germany : The Rheinisch-Westfalische Technische Hochschule (RWTH), Aachen; The Gesellschaft fur Strahlen-und Umweltforschung (GSF), Braunschweig; The Kernforschungszentrum Karlsruhe (KFK), Karlsruhe.

In Denmark : The Engineering Department of the RISO Laboratory (RISO), Roskilde.

No escriba por debajo de esta linea

In France : The Laboratoire de Mecanique des Solides of the Ecole Polytechnique (LMS), Palaiseau; The Centre de Mecanique des Roches of the Ecole des Mines (EMP), Fontainebleau; The Laboratoire d'Analyse Mecanique des Structures, Departement des Etudes Mecaniques et Thermiques, of the CEA-Saclay (CEA-DEMT).

In Italy : The Istituto Sperimentale Modelli e Strutture (ISMES), Bergamo.

In the Netherlands : The Energieonderzoek Centrum Nederlands (ECN), Petten.

In all some 12 'mechanical' computer codes have been used together with complimentary or associated codes for thermal calculations. All but one, (CYSIPHE) are based on the finite element method. They ranged from relatively small special purpose programs specifically developed for this generic problem (e.g. GOLIA, CREEP) to large scale general purpose codes which are commercially available (e.g. ADINA, ANSYS). It should be noted that all participants have considerable experience of geomechanical finite element analysis and can be categorised as 'expert users' of their particular codes. The participants and the codes used are listed in Table 1.

Participant	Country	Thermal Code(s)	Mechanical Code(s)
ECN	Holland	ANSYS	GOLIA MARC ANSYS
RISO	Denmark		ADINA
RWTH	W Germany	FAST-RZ	MAUS
KfK	W Germany	ADINAT	ADINA
FORAKY & CEN/SCK + LGC	Belgium	HEAT	CREEP
LMS	France	ASTHER	ASTREA
CEA	France	DELFINE	INCA
EMP	France	CHEF	VIPLEF CYSIPHE
ISMES	Italy	GAMBLE*	GAMBLE*
GSF	W Germany	ANTEMP	ANSALT

* N.B. GAMBLE is a pseudonym for a general purpose commercial code.

Table 1. Participants and Codes

2. ORGANISATION OF THE EXERCISE

'Benchmarking' is an increasingly popular means of increasing confidence in the reliability of complex computer predictions of situations where an accepted solution is not available (e.g. from experimental or direct measurement). The term has a range of connotations; the key element being that a common problem is 'solved' by several computer codes and the results are compared. Depending on how the problem is defined, the exercise may range from a direct assessment of the capabilities of the codes against a theoretical solution (this is sometimes referred to as 'verification') to situations where the analyst's judgement, skill and experience in modelling real physical situations is also involved. Project COSA was intended to progress from a verification exercise in its first stage to more complex exercises in later stages where codes are asked to predict real-life behaviour. Accordingly 3 benchmark problems have been planned, of which two have been completed.

Benchmark 1 was deliberately chosen to be a simple hypothetical creep problem, complex enough to demonstrate the strengths and weaknesses of the particular codes, yet sufficiently well-posed for there to be semi-analytical solutions available for comparison. It was intended principally to assess numerical and mathematical performance, with particular emphasis on the temporal integration capabilities of the codes. It was also anticipated that a solution could be obtained in two days, during which the coordinators were present as observers.

Benchmark 2 was based on a laboratory experiment, the intention being that the codes would attempt to replicate the observed behaviour. Interest nevertheless still centred on code performance and capability. For this reason the modelling of the problem was fully discussed a priori by the participants and a mutually agreeable 'common' specification of the problem to be solved was drawn up by the coordinators. This specification defined the geometry, boundary conditions, loading history and material law. It was left to the individual participants to decide on the most appropriate spatial and temporal discretisation (i.e. number, type and arrangement of elements, time step and solution method) and other aspects peculiar to their codes. In short all participants were to solve the same mathematical model in a manner most appropriate to the codes available to them.

A common mathematical model, of course, implies that the codes were restricted to use only those capabilities that were available in all. The 'quality' of the solutions is thus limited by the approximations necessary to allow it to be modelled by the 'weakest' code. For this reason attention focussed more on comparing the individual computer predictions with each other rather than with the experimental behaviour.

In addition to purely technical aspects it was initially felt desirable to attempt to compare the 'user friendliness' and computational efficiency of the codes. Accordingly each team was asked to run the same small program on their computer to provide a basis for normalising the cost of their calculation runs. This 'computational cost parameter' program (ccp) was intended to approximate the demands that a 'typical' finite element program makes on a computer system. User friendliness was assessed qualitatively by the coordinators during the course of the visit to each participant. In fact both user friendliness and computational efficiency assumed a relatively minor importance during the project for a variety of reasons.

3. BENCHMARK 1

3.1 The Problem

The problem posed was a thick spherical shell subjected to internal pressure (Figure 1). It was spherically symmetric in all respects. The creep behaviour was described by a Norton type temperature and stress dependent creep equation and a radius dependent temperature distribution. The problem was then one of the creep expansion of the shell under the internal pressure.

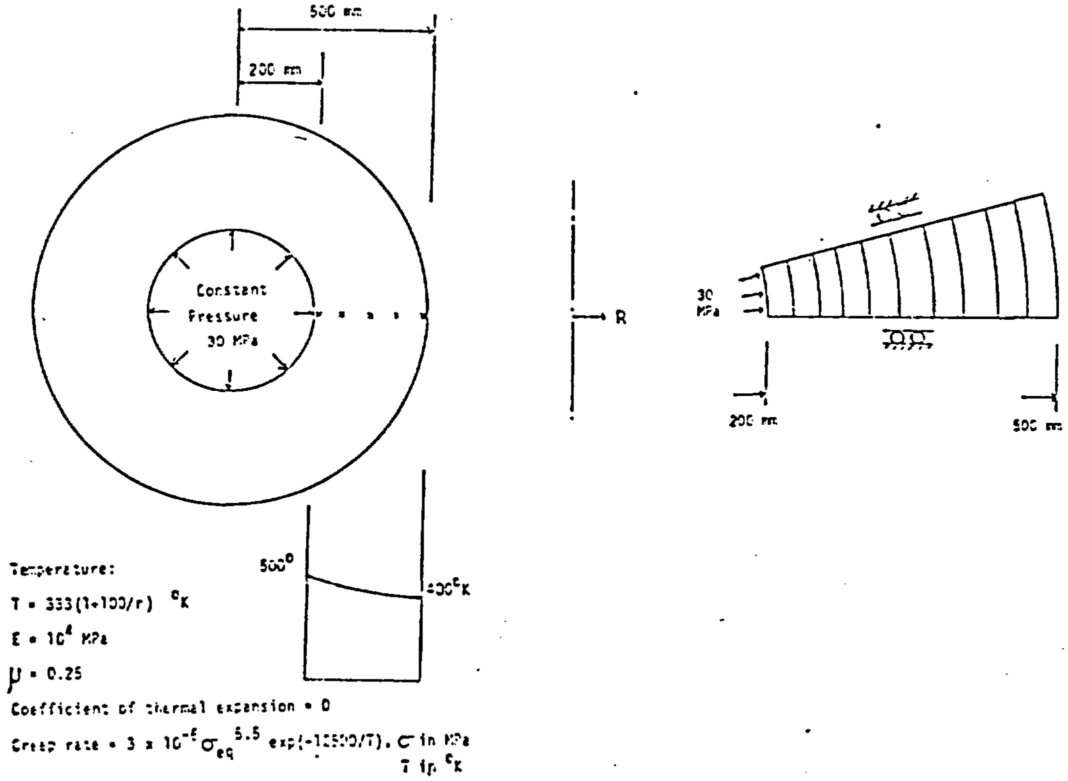
500 mm
200 mm
Constant Pressure 30 MPa
R
30 MPa
200 mm
500 mm
500°
400°K
Temperature:
T = 333(1+100/r) °K
E = 10⁴ MPa
μ = 0.25
Coefficient of thermal expansion = 0
Creep rate = 3 x 10⁻⁵ σeq^5.5 exp(-12500/T), σ in MPa
T in °K

Figure 1 First Benchmark Problem and Typical Finite Element Mesh

Displacement and stress histories up to a time of 10^{10} seconds were required. The problem parameters were chosen to ensure that a marked stress redistribution takes places during this time and a tendency towards a steady stress state is demonstrated at the end of the required solution. The definition was therefore chosen to be numerically useful, albeit not necessarily representative of real life.

Participants were asked to provide solutions at particular points in time as well as precise physical locations. Otherwise there were no restrictions applied to mesh selection or timestep control.

3.2 Solutions

Table 2 gives a summary of statistics associated with the solutions. Further details of the comparative behaviour of the codes is given in (3).

Organisation	Code	No. of Elements	Element Type	Time Integration Type	Timestep Control	Auto Control Criteria	No.of Steps	Computer	ccp Cpu time (Secs)+	No. of ccp for Benchmark
CEA	INCA	14	8 Node ISO	Implicit	MANUAL	-	1500	CRAY XMP	20	14.
ECN	GULIA-RK	40	3 Node CST	4th Order Explicit	AUTO	$\frac{\text{Stress incr.}}{\text{Stress}}$, $\frac{\text{Creep strain incr.}}{\text{Elastic strain}}$	291	CYBER 855	123	0.3
	GULIA-RKM	40	3 Node CST	5th Order Explicit	AUTO		296			0.4
	MARC	10	8 Node ISO	Explicit	AUTO		630#			10.#
	ANSYS	10	8 Node ISO	Explicit	AUTO	$\frac{\text{Creep strain increment}}{\text{Elastic strain}}$	930#			14.#
EMP	VIPLEF	35	9 Node ISO	Explicit	AUTO	Creep strain increment	2239	VAX 11/780	497	11.
	CYSIF	0		Explicit	AUTO	Creep strain increment	2239			
FURAKY	CREEP	30	4 Node ISO	Explicit	AUTO	$\frac{\text{Stress increment}}{\text{Stress}}$	1299	HP 1000	7857	2.1
GSF	ANSALT	16	8 Node ISO	Implicit	AUTO + MANUAL	Creep strain increment	195	CYBER	397	3.4
ISMES	GAMBLE*	17	8 Node ISO	Explicit +Implicit	AUTO	$\frac{\text{Creep strain increment,}}{\text{Elastic strain}}$ Creep Rate increment	193	VAX 8600	56	11.
KfK	ADINA	22	8 Node ISO	Implicit	MANUAL	-	90	SIEMENS 7890	45	6.7
LMS	ASTREA	864	3 Node CST	4th order explicit	AUTO	Maximum displacement	1979	NAS 9080	59	90.
RISO	ADINA	13	8 Node ISO	Implicit	MANUAL	-	350	BURROUGHS B7800	258	19.
RWTH	MAUS	10	8 Node ISO	Implicit	AUTO	Creep strain increment	38	2xCYBER 175	49	0.4

* General purpose commercial code
# Estimated values
+ For MT = 1000

Notes: (1) ISO = Isoparametric
(2) CST = Constant strain triangle

Table 2 Summary of Run Statistics

Typical of the results are the histories of maximum and minimum stress at various radii (Figure 3) and of displacement (Figure 4).

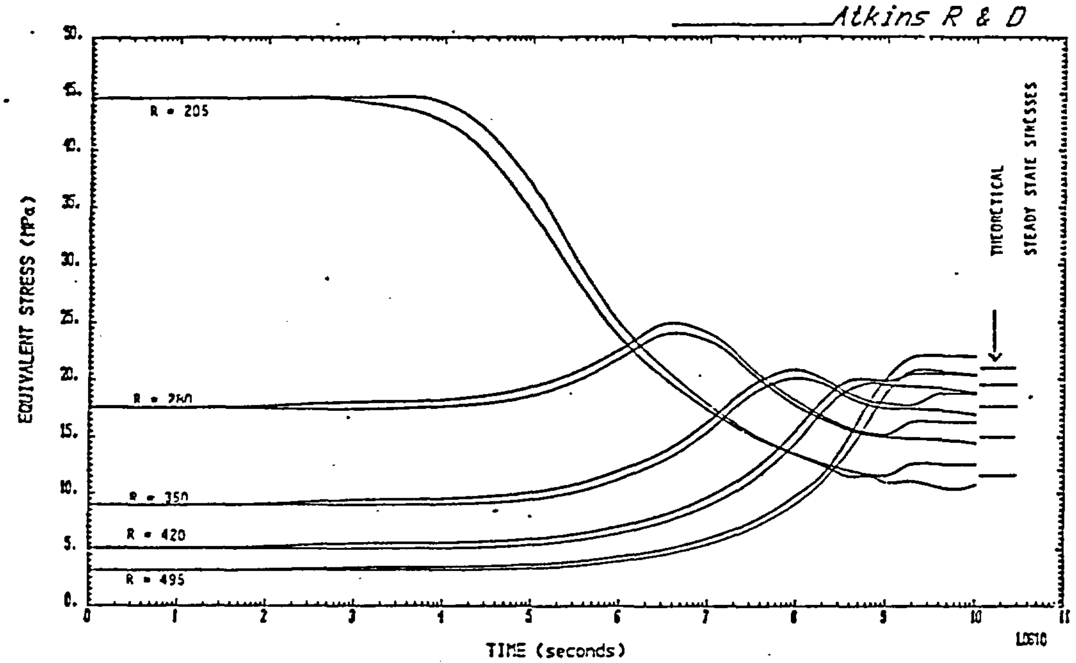

Figure 3 Maximum and Minimum Stresses at Various Radii

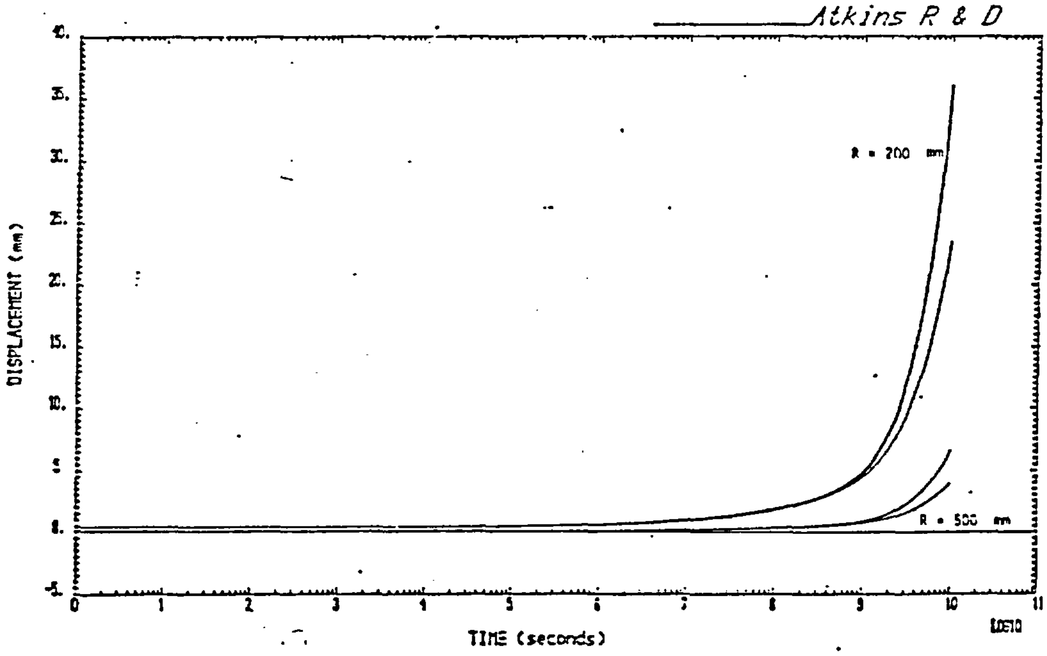

Figure 4 Displacement Bounds for Inner and Outer Radii

There was wide variation in element mesh density. However, two codes provided additional solutions with mesh variations, and on this evidence the problem is not particularly sensitive to the spatial discretisation.

There is some evidence that the results of the codes which use an explicit method to integrate the creep rate equation are sensitive to time step size. In contrast, the results from the implicit codes appear to be relatively insensitive. The implicit and high-order explicit codes, as expected, appear to be more efficient (on a ccp basis) than the single step explicit codes. Indeed the problem is particularly challenging to the latter at late times when accuracy considerations appear to impose unrealisatically short time steps relative to the time scale of the problem.

Codes with manual timestep control generally were more difficult to use on this problem and appear to be less efficient than those with automatic timestepping.

On the evidence of this problem all codes were capable of reproducing the thermo-mechanical behaviour of a creeping solid, to satisfactory accuracy, albeit with some variations in computational efficiency. In terms of overall reliability of the predictions, many factors have to be considered and it is inappropriate to place undue weight on any single aspect. Nevertheless in terms of computational practice a clear preference has emerged for the use of high order (quadratic) spatial discretisation and either implicit or high order explicit time integration operators in conjunction with an automatic selection of time step.

4. BENCHMARK 2

4.1 Experimental Details

The small-scale test which provided the basis of Benchmark 2 was conducted in the Mining Department of the Technical University of Delft, Holland. It consisted of a salt cube, subjected to triaxial compression and heated internally by a heater placed in cylindrical axial hole. The salt was sampled from the "Na_2" seam at the Asse mine in West Germany which has been the subject of considerable rheological study for several years and as such was familiar to most participants. The test duration was 13.5 hours. Figure 5 show a quarter symmetric view of the cube with the data measurement and reference positions.

Temperatures were monitored by thermocouples placed as indicated in Figure 5 and convergence of the borehole was measured using an optical system sighted along the borehole axis. External deformations of the cube were also recorded.

The loading history is illustrated in Figure 6.

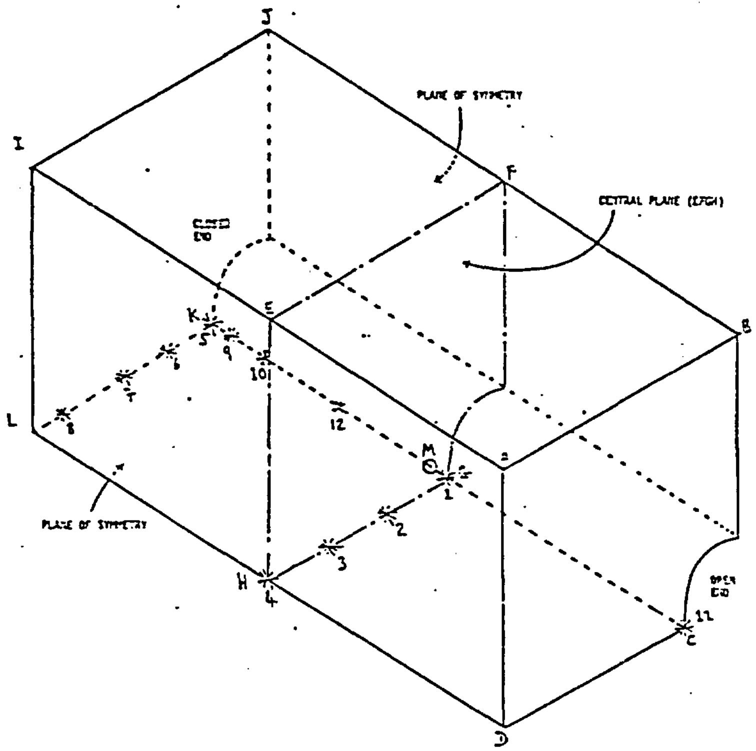
J
I
PLANE OF SYMMETRY
F
CENTRAL PLANE (EFGH)
CLOSED END
E
K
B
5
9
6
7
10
L
8
12
M
G
1
2
PLANE OF SYMMETRY
3
H
4
OPEN END
11
C
D

Figure 5 Schematic View of 1/4 cube

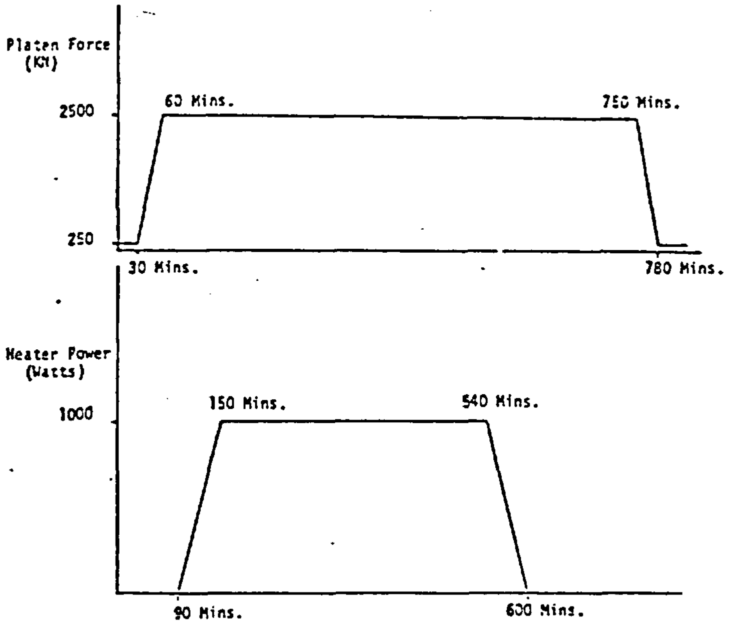

Figure 6 Loading History

Participants modelled the experiment in two parts. First, the transient temperature distributions were calculated up to the full time of 810 minutes. Predictions were compared with experimental measurements and then, satisfied that the thermal behaviour was represented adequately, creep calculations were conducted up to 600 minutes.

An axisymmetric representation was chosen. This was necessary because several codes could not model generalised plane strain (i.e. the condition that the strain normal to the plane is uniform), which was the other possible 2-D representation (3-D models were not actively considered on grounds of cost).

4.2 Thermal Analysis

For the thermal analysis, the loading platens were modelled as an equivalent disc and concentric cylinder respectively with their thicknesses adjusted to give the correct heat capacity. Figure 7 shows a typical finite element mesh of salt and platens.

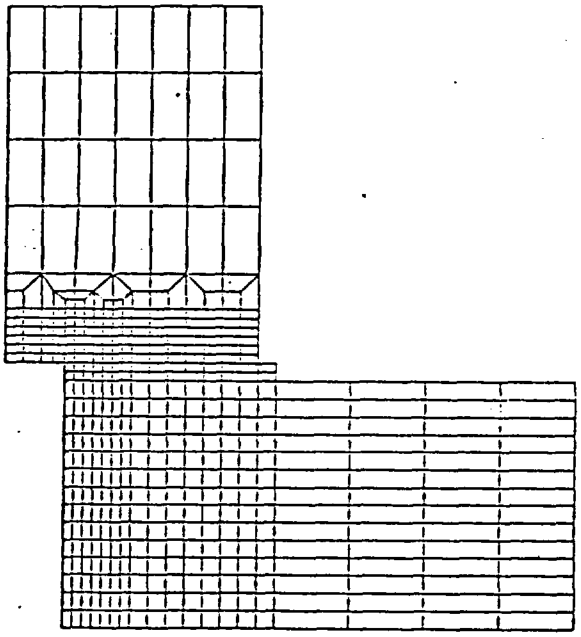

Figure 7 Typical Finite Element Mesh

The thermal boundary conditions are complex because of the shape, mass and forced cooling of the testing machine and unknown details of the heater. The heat input was approximated by a heat flux history applied uniformly over the borehole surface. Temperature histories at the outside boundaries of the platens were prescribed using the measured temperatures.

Salt Properties

Density = 2187 Kg/m^3

Coefficient of thermal conductivity = $a_0 + a_1{}^T + a_{2T}{}^2 + a_{3T}{}^3$ $W/(^ocm)$

Where $a_0 = 5.734$, $a_1 = -1.838 \times 10^{-2}$

$a_2 = 2.86 \times 10^{-5}$ and $a_3 = -1.51 \times 10^{-8}$

T is temperature in ^oC.

Specific heat capacity = $b_0 + b_1{}^T$ $J/(^ocm^3)$

Where $b_0 = 1.8705 \times 10^6$ and $b_1 = 3.8772 \times 10^2$

T is temperature in ^oC.

Young's modulus = 24000 MPa

Poisson's ratio = 0.27

Coefficient of thermal expansion - $4.2 \times 10^{-5}\ /^{oC}$

Steel Properties

Density = 7830 Kg/m^3

Coefficient of thermal conductivity = 60.0 $W/(^ocm)$

Specific heat capacity = 3.758×10^6 $J/(^ocm^3)$

Young's modulus = 210 000 MPa

Poisson's ratio = 0.3

Coefficient of thermal expansion = $1.6 \times 10^{-5}\ /^oC$

Table 3 Second Benchmark Material Properties

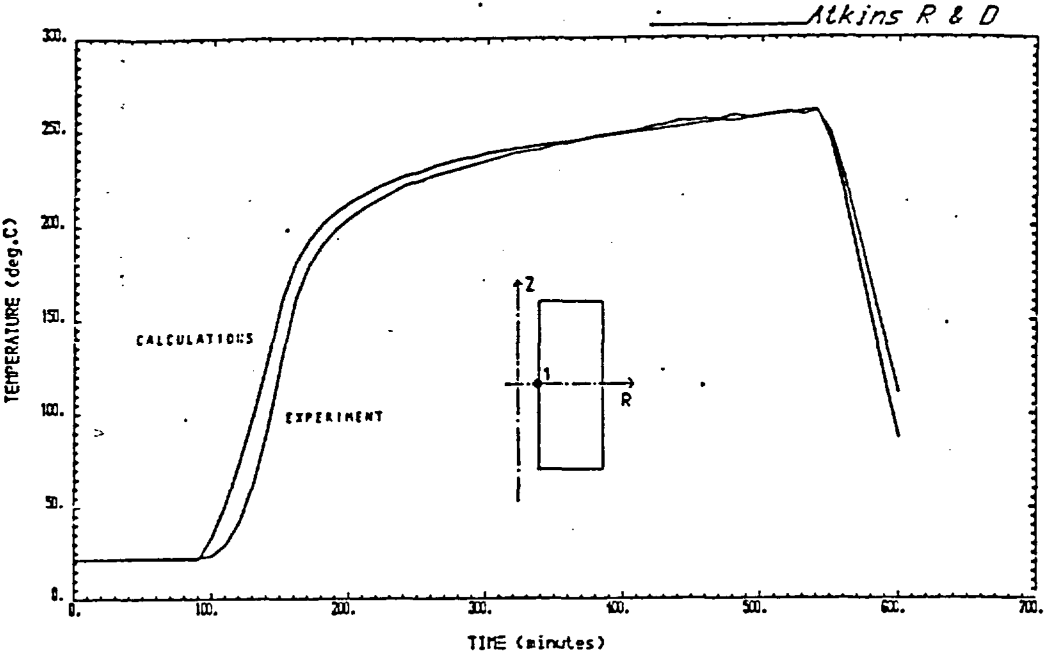

Figure 8 Temperature at Borehole Surface

Solution of the creep part of the benchmark was more difficult and generally required considerably more computing resources than had been anticipated. The number of timesteps used ranged from 43 to 2700 with a corresponding range of time integration schemes.

Displacement results for ten solutions are illustrated in Figure 9 showing the borehole convergence at position M near the central plane. Similarly wide variations were evident in the predictions of displacement at the other positions and also in stresses.

Detailed examination showed that 'user errors' and in one case a "code discrepancy" account for many of the differences. Subsequently a number of corrected analyses were performed and far better agreement between the individual solution was obtained, as shown in Figure 10.

No escriba [illegible]

4.3 Creep Analysis

For the creep model the side platen was removed. This was necessary because of its unrealistic circumferential stiffness. Participants otherwise kept the same meshes as had been used for their thermal models, using appropriate structural elements. Most participants used eight-noded isoparametric quadrilateral elements but nine-noded isoparametric quadrilaterals, six-noded isoparametric triangles and four-noded isoparametric quadrilaterals were also used.

At the central plane, symmetry boundary conditions were applied and at the end-plane frictionless sliding between the salt and the loading platen was allowed. Ideally the cylindrical outer surface of the salt would have been constrained to remain flat but this was not possible in all of the codes and so it was left as a free surface. The platen forces were represented by pressures applied axially to the outside boundary of the end platen and radially to the free cylindrical surface of the salt.

The basic mechanical properties of salt (see Table 3) were obtained from previous research at Asse in the form of primary and secondary creep equations. Only primary (transient) creep was considered for the short duration of the test and this was described by

$$\dot{\varepsilon}_{cr} = mB \exp(-mt)\, \sigma^{n} \exp(-Q/RT)$$

$$\text{with } m = 0.35 \text{ day}^{-1},\ B = 0.21,\ n = 5,\ Q = 44.8 \times 10^{3} \text{ J}$$

However, some codes could handle only secondary type creep laws and the primary creep equation was therefore approximated to a time-independent form by setting m=0.

4.4 Results

Solution of the thermal part of this benchmark proved to be reasonably straightforward and there was generally close agreement between codes. Predicted temperatures also agreed acceptably with the experimental measurements, particularly at the central (symmetry) plane. Figure 8 shows a typical temperature history prediction together with measured values at the borehole wall on the central plane.

NOMBRE DEL AUTOR

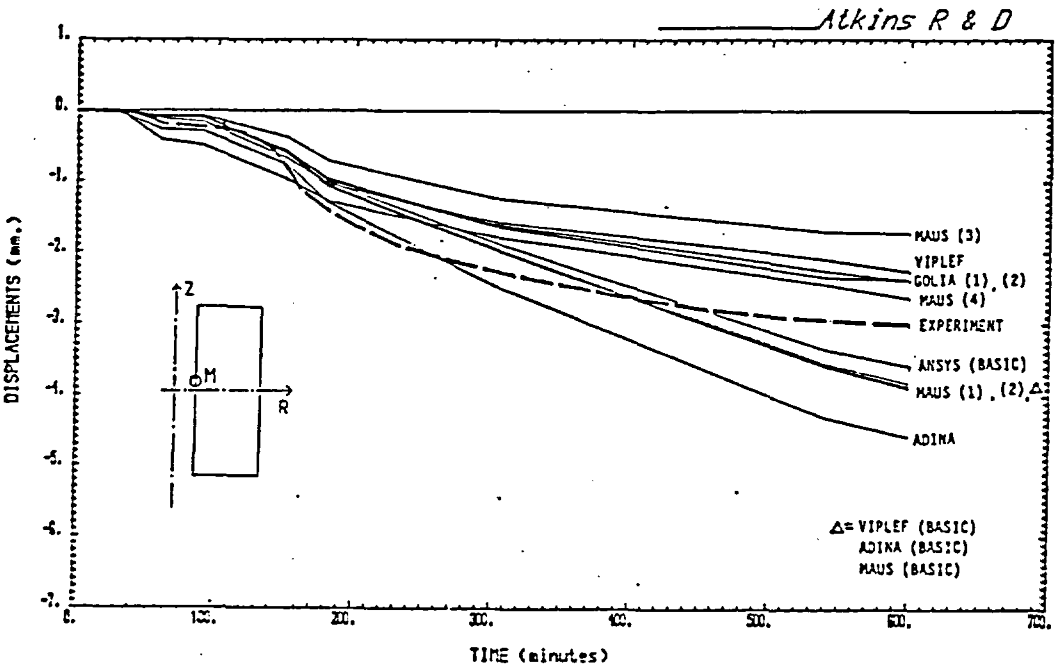

Figure 9 Radial Movement at Borehole Surface (Position M) - Initial Results

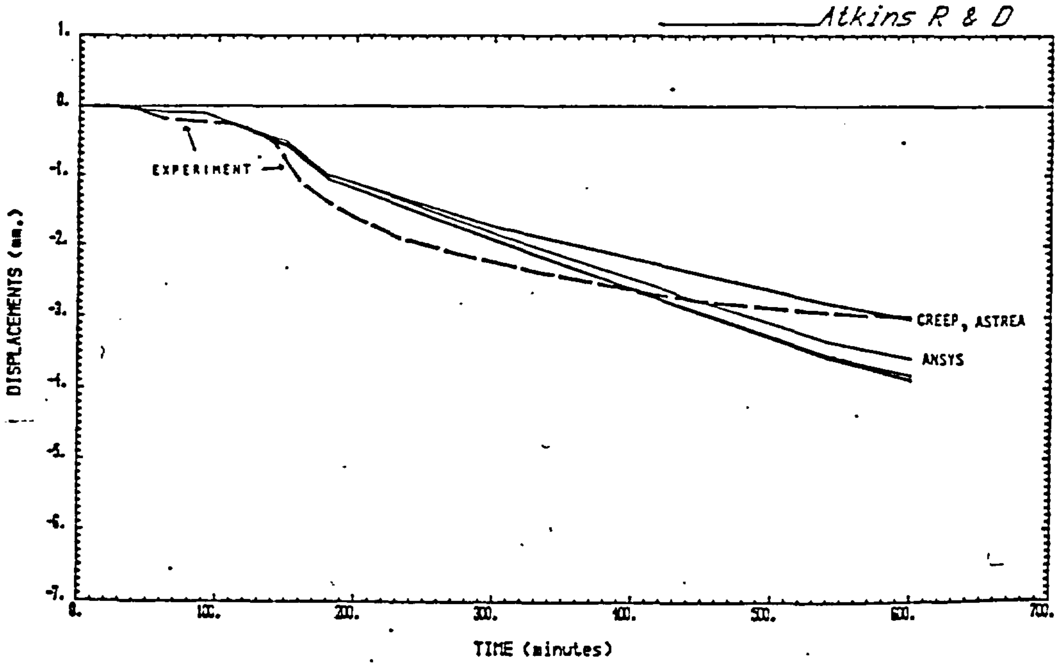

Figure 10 Radial Movement at Borehole Surface (Position M) - Revised Results

4.5 Creep Analysis - Variants

A number of variants to the 'basic' solution described in 4.4 were subsequently obtained and provide a limited 'sensitivity analysis'. The results of these variant calculations are illustrated in Figure 11.

Four variants dealt with salt vheology

(i) EMP fitted a Lemaitre strain hardening model to the results of new creep tests they carried out on the same salt as the test block. This was described in the VIPLEF code by the equation :

$$\dot{\varepsilon}_{ev} = \frac{\alpha\left[(\sigma/K)^{\beta}\exp(-A/T)\right]^{1/\alpha}}{\varepsilon_{ev}^{(1-\alpha)/\alpha}}$$

with = 0.463, β = 3.57, K = 0.166, A = 2540

The results are labelled 'VIPLEF' in Figure 11.

(ii) RWTH used an alternative time independent (secondary) creep law ("MAUS (3)" in Figure 11) of the form :

$$\dot{\varepsilon}_{ev} = 4.85\times10^{6}\,\sigma^{5}\exp(-6520/T)$$

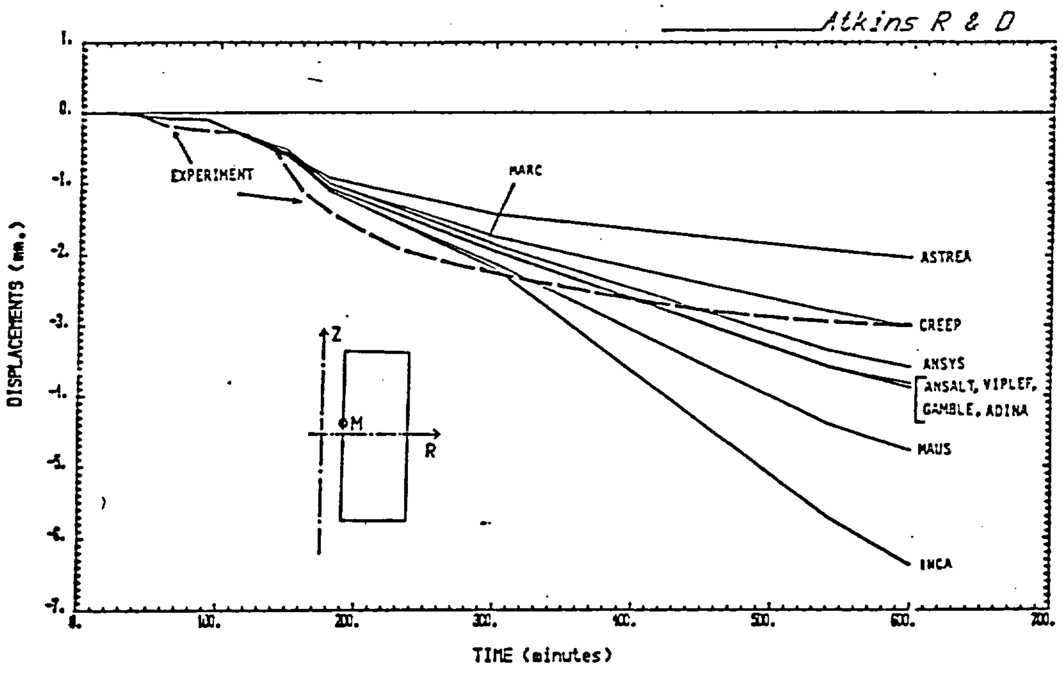

Figure 11 Radial Movement at Bore-Hole Surface - Variants

No escriba por debajo de esta linea

(iii) RWTH also tried a strain hardening primary creep model ("MAUS (4)"

$$\dot{\varepsilon}_{c} = 4.85\times10^{6} \langle(\sigma-\sigma_0)\rangle^{n} \exp(-6880/T)$$

where $\langle\sigma-\sigma_0\rangle = \begin{cases} (\sigma-\sigma_0) & \text{iff} \geq 0 \\ 0 & \text{iff} < 0 \end{cases}$

and $\sigma_0 = K\left[\int_{t_0}^{t} \dot{\varepsilon}_{eff}\, dt\right]^{0.36}$ with $K = 100$ MPa

(iv) KfK supplied results ("ADINA") for a value of Youngs modulus of 7 GPa rather than 24 MPa for the base case.

5 variants dealt with the idealisation of the experiment.

(v) Curve "GOLIA (1)" was obtained assuming that there was no sliding between the steel platens and the salt.

(vi) Curve "GOLIA (2)" corresponds to the case where the lateral pressure is applied directly to the salt (i.e. no steel platen).

(vii) Variant "MAUS(1)" was obtained with 64 time steps (cf.133).

(viii) Variant "MAUS(2)" was obtained with 47 time steps.

(ix) A plane strain axisymmetric analysis (ie. one-dimensional) analysis of the mid-plane was carried out by KfK with ADINA. Borehole convergence was very similar to the base case.

5. CONCLUDING DISCUSSION

Given the protracted timescales involved, estimates of repository behaviour necessarily rely on computer predictions. The measure of confidence in long term predictions can only be based on comparisons with short term experiments and the degree of consistency between alternative computer calculations. The reliability of calculations for the short term is therefore clearly of great importance in the context of nuclear waste disposal.

Benchmark 1 showed that all codes were capable of reproducing satisfactory results for simple hypothetical problems. However the same cannot be said about prediction of more complex realistic situations.

It was clear from the outset that the simplifying assumptions required to model Benchmark 2 would preclude the successful prediction of the experimental results. Three sources of difficulty were identified. Firstly the need to represent a complex 3-D problem by a 2-D model. Secondly the short term of the experiment for which reliable rheological data for salt were not available (and certainly not in a form amenable for computation). Thirdly the need to create a model which would be solved by all codes. The departure of the computational predictions from the experimental results shown in Figures 9 and 10 is therefore to be expected. As expected for better agreement was achieved by those variants which addressed the short term creep behaviour directly (Figure 11).

Of greater significance is the wide variation in the computational results as initially reported (closure rates vary by a factor of 6). Several participants produced results which are broadly similar and there is an implication that this 'common' solution is the correct one for the specified model. Note however that despite wide variations in the results, all solutions are plausible in isolation. By implication it appears that independent assessment by several teams will be required of complex non-linear phenomena.

Project COSA is continuing with a third problem which is based on an in-situ experiment. In this phase participants will have increased latitude to model the problem according to the dictates of their experience and capabilities of their codes. It will be interesting to observe how this increased freedom affects the degree of agreement in their predictions.

REFERENCES :

1. BROYD T W, KNOWLES N C, et al - 'A Directory of Computer Programs for Assessment of Radioactive Waste Disposal in Geological Formations', CEC, EUR Report 8669 EN 1985.

2. COME B, ed 'Computer Modelling of Stresses in Rock', CEC, EUR Report 9355 EN 1985.

3. LOWE M J S, and KNOWLES N C, 'Project COSA - An Intercomparison Exercise of Geotechnical Computer Codes for Salt', CEC to be published as a EUR Report 1986.

4. MORGAN H S, KRIEG R D and MATALUCCI R V - 'Comparative Analysis of Nine Structural Codes used in the Second WIPP Benchmark Problem', SAND81-1389, Sandia National Labs, New Mexico 1981.

The Derivation of Simple Models and Data Sets using Detailed Deterministic Models of Radioactive Waste Transport

By T.W. Broyd
Atkins Research and Development
Epsom
Surrey
England

Introduction

Within the United Kingdom, the disposal of both low level radioactive wastes (ILW) and intermediate level radioactive wastes (ILW) is the responsibility of UK Nirex Ltd (Nirex), a body whose directorate is formed of personnel from the major waste producers. High level (or heat generating) wastes are due to be stored for several decades pending final disposal, by which time much of the heat and radioactivity will have decayed. The work of Nirex is regulated by a number of government bodies, but it is the Department of Environment (DOE) who act as the licensing authority for disposal sites.

The DOE published a set of disposal site assessment principles towards the end of 1984 (Ref 1) in which there is a stated requirement for Nirex to base the radiological assessment of any proposed disposal site on objectives not of dose, but of risk to the individual, with risk being defined as the probability that a given dose will be received multiplied by the probability that such a dose will result in a fatal cancer. The assessment principles in effect contain the following:

i) The appropriate target applicable to a single repository at any time is a risk to an individual in a year equivalent to that associated with a dose of 0.1mSv; about 1 chance in a million.

ii) Radiation exposures resulting from the disposal of radioactive wastes must be shown to be as low as reasonably achievable, taking into account economic and social factors (ALARA)

In order properly to assess any proposals submitted by Nirex, the DOE has been deriving an independent radiological assessment methodology over the past few years, with much of the work carried out by organisations within the private sector.

Requirements of Predictive Models

Present considerations are for the disposal of LLW in near surface repositories situated in low permeability clays, and ILW in deeper (100 - 200m) low permeability clays. Thus both types of disposal options would seek to utilise the natural geosphere barrier properties of low ground water flow and high sorption provided by such geological media.

The various types of radionuclide release scenarios and subsequent exposure routes may be categorised as follows:

Natural	- groundwater transport
	- occurrence of faults
	- glacial action
	- biotic transfer
Repository induced	- gas generation and movement
	- mechanical/thermal/chemical/biological disturbance
Human induced	- transfer of contaminated material by
	- repository construction
	- resource exploitation
	- pumped water abstraction

Thus the long-term prediction of risk to mankind from buried radioactive waste requires the modelling and interaction of many different transport processes. The pathways travelled by radionuclides are generally split into the categories of vault, geosphere and biosphere, but this can mask the fact that many of the processes affecting waste transport are common to each category. For example, knowledge of groundwater flow is essential in each component, and the interaction of waste and ground water chemistry may be handled by similar methods throughout the transport path. As far as the prediction of risk is concerned, it is perhaps better to separate the types of model used into the categories of:

- research models
- process models
- simple models

Research models include those areas for which single mechanisms are addressed, e.g. corrosion. Process models include those areas involving multiple interacting processes modelling overall systems, e.g. groundwater flow and associated radionuclide transport. In order to establish a figure of risk from a proposed disposal facility, it is necessary to carry out and combine the results of many individual calculations to ensure that uncertainties in data and inaccuracies in models are taken into consideration. This generally requires a probabilistic approach involving simplified, often one-dimensional models.

Validity of Models

In theory, all models used in the prediction of radiological risk should be rigorously validated. In practise, however, this is not possible due in part to the very long time periods required, and in part to the measurement errors, sampling errors and process interactions which will cloud the validation attempt.

Because of the general impracticality of rigorous validation, much use is currently being made of comparison, or benchmark studies of predictive models, whereby a number of different computer programs are used to 'solve' a set of well defined test cases. Table 1 lists a number of recent and current examples of such studies. Whilst being no substitute for full validation (where this is possible), such studies serve to highlight areas of current agreement and disagreement, and help to maximise research effort by providing an environment for the exchange of work and ideas.

Derivation of models and data

The prediction of radiological risk requires that both models and data be derived from given repository/site combinations. Whilst most if not all modelling attempts will be site specific, there are a number of steps which will be common to all sites, as follows:

* site characterisation

  - establish conceptual model(s) of groundwater flow and radionuclide transport, using all available recorded data and all realistic radionuclide transport routes to the biosphere.
  - carry out process modelling of groundwater flow and radionuclide transport, using 2D/3D models as appropriate. From this modelling derive a set of simple models which account for all main transport processes.
  - make use of the derived simple models within a sampling framework to undertake a full PRA of the repository/site combination.

Note that, whilst the majority of simple models will be one dimensional, it is necessary to take account of all significant transport processes. Thus, whereby it may be possible to discount lateral dispersion effects for advection dominated transport in clay (Ref 2) it is possible to include such affects for transport in a confined aquifer by appropriate use of simple post-processors to a 1-D solution (Ref 3). Similarly, the effects of pumped well abstraction may be included within a 1-D geosphere model provided that it is previously shown that the abstracted water contains all significant activity (Ref 3).

In addition to site characterisaction studies, it is necessary also to carry out studies on proposed repository/site combinations, as follows:

- repository/site characterisation
  - establish conceptual model(s) of the physical and chemical environments
  - carry out process modelling of the effect of the repository on the water flow through the host stratum
  - carrying out process modelling of the chemical effect of the repository/host water combination, to provide relevant solubility limits and sorption characteristics for use in the simple modelling required for a PRA.

Whilst some types of data required for a PRA may be acquired from judicious use of sensitivity studies of process models and experimentation, the use of formalised and repeatable procedures for eliciting subjective probability distributions from 'experts' have also shown promise (Ref 4).

Case Study

In order to demonstrate how a PRA of an underground radioactive waste disposal facility might be undertaken, a single groundwater release scenario from a hypothetical repository for ILW situated in a clay layer at a depth of about 150m under Harwell has recently been studied (Ref 5). The assessment procedure adopted was fairly complex, but contained the following general stages:

1. Selection of scenarios
2. Characterisation studies, using process models
3. Sensitivity studies, using process models
4. PRA, using simple models
5. Reconsideration of high risks, using process models
6. Decision on site/respository/inventory combinations.

Point 5 is of importance since the experience of this and other work suggests that the PRA runs giving the higher doses contribute most to risk even though their probabilities are small. Consequently, the conditions sampled may be very different from those assumed earlier in the process modelling of stages 2 and 3. It is necessary, therefore, to check that the simple PRA models are satisfactory by comparision with more precise process model calculations under these extreme circumstances.

Figure 1 - 5 show, respectively, a plan of the Harwell region together with the model section chosen, groundwater streamlines predicted using a 2-D groundwater flow model, the conceptual transport models derived from the 2-D flow modelling, the contribution of individual nuclide chains to the overall variation of risk with time, and the comparision of PRA prediction of I-129 flux out of the repository host clay layer with results of a 2-D calculation (giving an example of Stage 5, above). The PRA code used was SYVAC A/C (Ref 6)

Current Developments

Work on the Harwell case study highlighted a number of issues in need of further consideration, and the UK Department of Environment are currently funding development in the following general areas:

- combination of risk estimates arising from different exposure route scenarios
- simple regional network hydrogeology models
- time dependency in PRA models
- coupling of groundwater flow and chemistry effects within a single model
- use of a site evolution prediction model
- improved methods of sensitivity analysis
- methods of accounting for human-induced effects

Acknowledgement

The majority of studies reported in this paper have been funded by the UK Department of the Environment, and the author is indebted to Dr. B.G.J. Thompson of the DOE and Drs. S.K. Liew and R.W. Paige of Atkins R & D, for their continued enthusiastic support and guidance in this work.

References

1. Department of the Environment, "Disposal Facilities on Land for Low and Intermediate - Level Radioactive Wastes: Principles for the Protection of the Human Environment", 1984.

2. Paige, RW, Stephens, JL and Broyd, TW, "Evaluation and Use of Geosphere Flow and Migration Computer Programs for Land 1/2 Type Disposal Facilities", DOE Disposal Assessments Report TR-WSA-15, ED1, 1986.

3. Liew, SK, Krol, AA & Broyd TW "Improvement to the Geosphere Models Used within SYVAC A/C", DOE SYVAC report TR-WSA-16, ED1, 1986.

4. Dalrymple, GJ, Johnson, KB and Phillips, LD. "Final Report on the Acquisition of Data for Use in the Probabilistic Risk Assessment of Underground Disposal of Radioactive Wastes", DOE SYVAC report TR-STH-19, ED 2, 1986.

5. Thompson, BGJ and Broyd, TW "DRY RUN 1: An Initial Examination of a Procedure for Post-Closure Radiological Risk Assessment of an Underground Disposal Facility for Radioactive Waste", DOE Disposal Assessments Report TR-DOE-4, Ed 1, 1986.

6. Lane, GD, Hall, PA, "SYVAC 'A/C' User Guide", DOE SYVAC User Document UD-SCE-2, Ed1, 1985.

Table 1 - Benchmark Studies

Project	Area	Type	Test
INTRACOIN	Geos (mig)	P,S	Ve, Va
MIRAGE	Geos (mig)	P,S	Ve
MIRAGE	Chem	P	Ve
HYDROCOIN	Geos (flow)	P	Ve, Va, A
BOIMOVS	Bios	P	Ve(?)
SYVACOIN	PRA	S	Ve, A
PACOMA	All	P,S	Ve, A
INTRAVAL	Geos (mig)	P	Va
COSA	Geomech	P	Ve, Va
NAWG	Geos, Chem	P	Ve(?), A(?)
CHEMVAL	Geos, Chem, Data aq.	P	Ve, Va, A

P = Process S = Simple
Ve = Verification Va = Validation A = Application

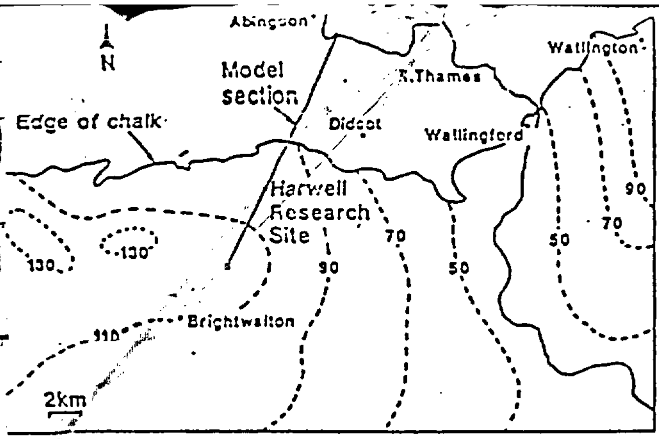
Abingdon
N
Model section
R.Thames
Wallington
Edge of chalk
Didcot
Wallingford
Harwell Research Site
130
130
70
90
50
50
70
90
110
Brightwalton
2km

FIGURE 1 : GROUNDWATER CONTOURS IN CHALK

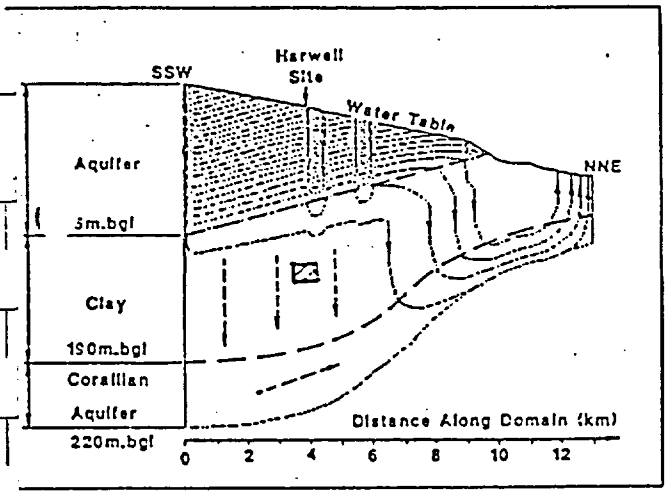
SSW
Harwell Site
Water Table
NNE
Aquifer
5m.bgl
Clay
150m.bgl
Corallian Aquifer
220m.bgl
Distance Along Domain (km)
0
2
4
6
8
10
12

IGURE 2: GROUNDWATER STREAMLINES USING GEOHYDROFLOW

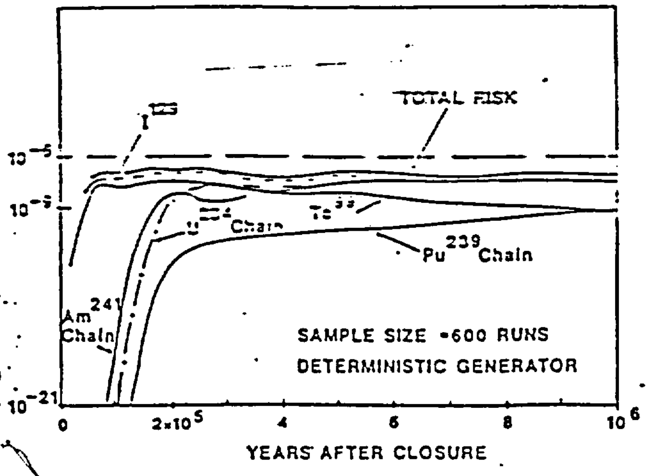

RE 4 : CONTRIBUTION OF INDIVIDUAL NUCLIDE CHAINS TO THE OVERALL VARIATION OF RISK WITH TIME

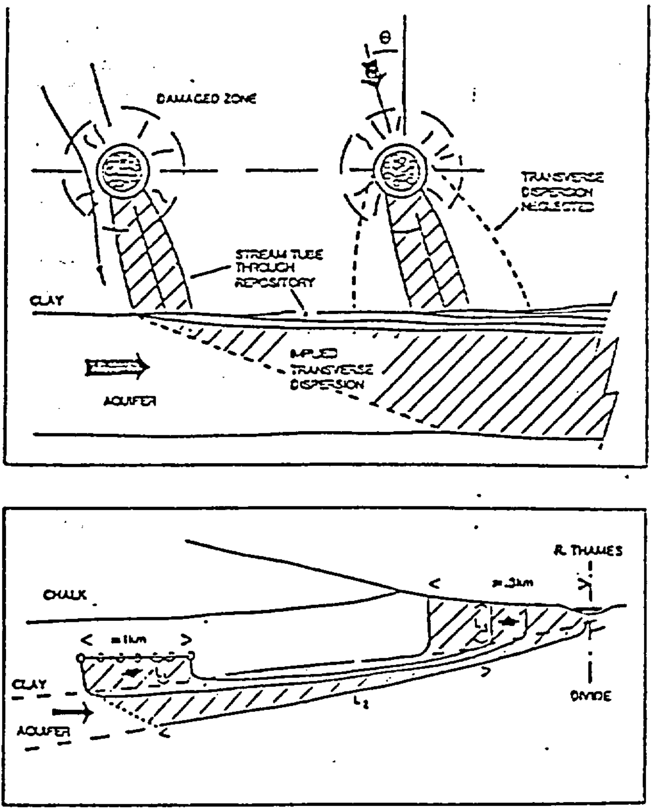
θ
DAMAGED ZONE
TRANSVERSE DISPERSION NEGLECTED
STREAM TUBE THROUGH REPOSITORY
CLAY
IMPLIED TRANSVERSE DISPERSION
AQUIFER
R. THAMES
CHALK
≈3km
≈1km
L1
L2
CLAY
AQUIFER
DIVIDE

FIGURE 3 : GROUNDWATER FLOW AND NUCLIDE TRANSPORT MODEL USED IN SYVAC 'A/C' FOR HARWELL SITE

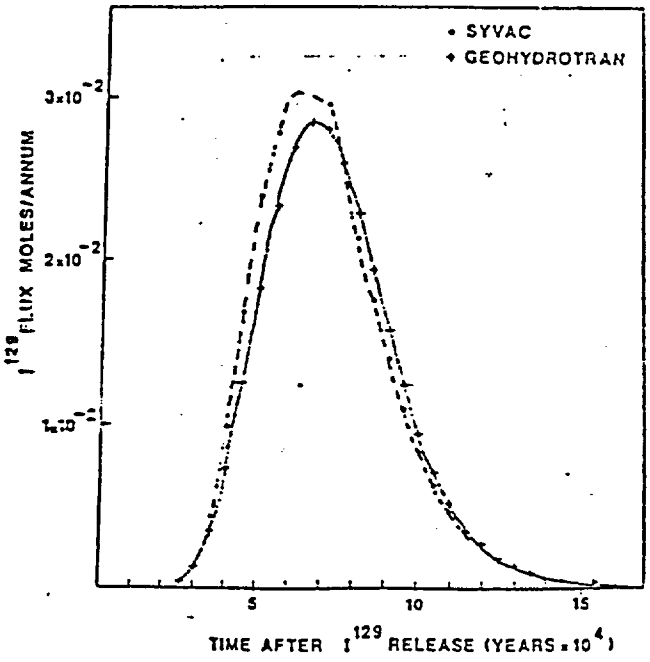

FIGURE 5: COMPARISON OF SYVAC PREDICTION FOR I^{129} FLUX OUT OF THE CLAY LAYER INTO THE AQUIFER, WITH RESULTS OF A DETAILED TWO-DIMENSIONAL CALCULATION